ZAKLJUČNO POROČILO
O REZULTATIH OPRAVLJENEGA RAZISKOVALNEGA DELA NA PROJEKTU V OKVIRU CILJNEGA RAZISKOVALNEGA PROGRAMA (CRP) »KONKURENČNOST SLOVENIJE 2006 – 2013«

I. Predstavitev osnovnih podatkov raziskovalnega projekta

1. Naziv težišča v okviru CRP:

5.8.1. Varnostna vprašanja tehnologij jedrskih in sevalnih objektov

2. Šifra projekta:

V2-0553

3. Naslov projekta:

Razvoj potrebnih znanj za spremljanje, ovrednotenje in nadzor obvladovanja staranja jedrskih objektov

3. Naslov projekta

3.1. Naslov projekta v slovenskem jeziku:

Razvoj potrebnih znanj za spremljanje, ovrednotenje in nadzor obvladovanja staranja jedrskih objektov

3.2. Naslov projekta v angleškem jeziku:

Development of knowledge, indispensable for evaluation, assessment and surveillance of ageing management in nuclear facilities

4. Ključne besede projekta

4.1. Ključne besede projekta v slovenskem jeziku:

upravljanje z znanji, obvladovanje staranja, jedrski objekti, jedrska varnost

4.2. Ključne besede projekta v angleškem jeziku:

Knowledge management, ageing management, nuclear facilities, nuclear dafety

5. Naziv nosilne raziskovalne organizacije:

Institut "Jožef Stefan"

5.1. Seznam sodelujočih raziskovalnih organizacij (RO):

6. Sofinancer/sofinancerji:

MOP, Uprava za jedrsko varnost Republike Slovenije

7. Šifra ter ime in priimek vodje projekta:

07025	prof. dr. Leon Cizelj

Datum: 15.9.2010

Podpis vodje projekta:

prof. dr. Leon Cizelj

Podpis in žig izvajalca:

prof.dr.Jadran Lenarčič
direktor

II. Vsebinska struktura zaključnega poročila o rezultatih raziskovalnega projekta v okviru CRP

1. Cilji projekta:

1.1. Ali so bili cilji projekta doseženi?

☒ a) v celoti
☐ b) delno
☐ c) ne

Če b) in c), je potrebna utemeljitev.

Cilji projekta so v celoti doseženi. Štejemo, da so preseženi, še posebej na področju upravljanja z znanjem. V času projekta smo namreč pripravili monografijo in dve poglavji v monografijah pri priznanih mednarodnih založbah (več v tč 6 tega poročila)..

1.2. Ali so se cilji projekta med raziskavo spremenili?

☐ a) da
☒ b) ne

Če so se, je potrebna utemeljitev:

2. Vsebinsko poročilo o realizaciji predloženega programa dela[1]:

1. sklop: Znanja za obvladovanje staranja

Pomembnost prehodnih pojavov za utrujanje smo ocenjevali na primeru razslojenega toka v prelivnem vodu tlačnika. Razslojeni tok sodi med najpomembnejše prispevke k utrujanju tlačne meje reaktorskega hladila. Na konkretnih primerih smo s pomočjo realističnih podatkov ocenili pomembnost, potrebno natančnost in pogostost meritev temperatur na zunanji površini prizadetega cevovoda. Pomembnost, potrebno natančnost in potrebno pogostost meritev smo ocenili s pomočjo analitičnih rešitev in numeričnih simulacij z metodo končnih elementov. Podrobni opisi in zaključki so zbrani v treh delovnih poročilih ([COBISS.SI-ID 22545191], [COBISS.SI-ID 22545447], in[COBISS.SI-ID 22545703]), dveh konferenčnih prispevkih ([COBISS.SI-ID 23179047], [COBISS.SI-ID 23660839]) in članku v SCI reviji [COBISS.SI-ID 23572007].

Okrepljeno sodelovanje v mednarodnih projektih s področja staranja jedrskih objektov na kratko opisujemo v nadaljevanju.

NULIFE
V evropski mreži odličnosti NULIFE (6. Okvirni program EURATOM) so zbrani pomembnejši industrijski in raziskovalni akterji na področju obvladovanja staranja jedrskih objektov. IJS koordinira izmenjavo doktorskih študentov med partnerji, kar sodi med pomembnejše aktivnosti mreže. Neposredno smo sodelovali pri naslednjih izmenjavah: mag. Mitja Uršič iz IJS v IRSN, David Gonzalez iz Materials Performance Centre Univerze v Manchestru v IJS in Stefan Heussner iz Areva v IJS. Posredno pa smo sodelovali pri organizaciji približno 10 izmenjav.

Mreža odličnosti NULIFE prerašča v neprofitno združenje, pri čemer z več kot 50 partnerji mreže aktivno sodelujemo.

ICONE
International Conference on Nuclear Engineering (ICONE) sodi med v industriji najodmevnejše mednarodne konference na področju jedrske tehnike. Soorganizirajo jo ameriško (ASME) in japonsko (JSME) združenje strojnih inženirjev in kitajsko jedrsko združenje (CNS). Pri organizaciji kot kot »track co-chair«, torej so-predsedujoča tematskim sklopom konference že nekaj let sodelujeva L. Cizelj »Structural integrity« in I. Kljenak »Advanced Reactor Designs«. V obdobju tega projekta smo izpeljali konferenci ICONE 17 (Bruselj, julij 2009, več kot 800 udeležencev iz vseh kontinentov) in ICONE 18 (Xi'An, Kitajska, maj 2010, več kot 1000 udeležencev). Trenutno pa so v teku priprave za ICONE 19 (maj 2011, Makuhari, Japonska).

Vzporedno s konferenco nastajajo tudi strokovni odbori ASME na področju jedrskega inženirstva, ki jih »track co-chairs« organiziramo in jim tudi sopredsedujemo.

[1] Potrebno je napisati vsebinsko raziskovalno poročilo, kjer mora biti na kratko predstavljen program dela z raziskovalno hipotezo in metodološko-teoretičen opis raziskovanja pri njenem preverjanju ali zavračanju vključno s pridobljenimi rezultati projekta.

ENEN
Združenje ENEN (European Nuclear Education Network) je združenje, ki evropske univerze in inštitute z jedrskim program povezuje med sabo in z jedrskimi deležniki. Združenje predvsem pospešuje mednarodno sodelovanje pri magistrskem študiju jedrske tehnike. Podeljuje tudi naziv »evropski magister jedrske tehnike«, ki ga ima že več kot 40 diplomantov. V upravnem odboru združenja aktivno deluje L. Cizelj. Med 4. in 6.03.2010 smo v v Ljubljani izpeljali sestanek upravnega odbora in skupščino združenja. Del dogodkov v sklopu skupščine je bila tudi okrogla miza z naslovom »Strategija izobraževanja in usposabljanja za potrebe povečane proizvodnje jedrske energije«, na kateri so sodelovali prof. dr. Joseph Safieh, European Nuclear Engineering Network, Pariz, Francija, dr. Keiko Hanamitsu, International Atomic Energy Agency, Dunaj, Avstrija, dr. FranckWastin, Skupni raziskovalni center Evropske komisije, Bruselj, Belgija, dr. David Gilchrist, Ente Nazionale per l'Energia eLettrica, Rim, Italija, dr. Andrej Stritar, Uprava Republike Slovenije za jedrsko varnost, Ljubljana, Slovenija in dr. Georges Van Goethem, Direktorat za raziskave Evropske komisije, Bruselj, Belgija

OECD/NEA
Udeležili smo se delavnice »Commendable Practices for the Safe, Long Term Operation of Nuclear Reactors - OECD/NEA Stress Corrosion Cracking and Cable Ageing Project (SCAP)« in srečanja »International symposium on ageing management of the NPP (ISAG2010)« (Tokia, Japonska, maj 2010). Na srečanjih so bili predstavljeni rezultati mednarodnih raziskovalnih projektov, ki jih je na področju staranja opreme in kablov jedrskih elektrarn financirala japonska uprava za jedrsko varnost (NISA), izpeljal pa jih je mednarodni konzorcij pod pokroviteljstvom OECD/NEA.

Organizirali in izpeljali smo mednarodno konferenco Nuclear Energy for New Europe 2009 (Bled, Slovenija, september 2009)z več kot 200 registriranimi udeleženci iz 30 držav.

2. sklop: Varnostna vprašanja

Razvijali smo uporabo metod za modeliranje staranja v verjetnostnih varnostnih analizah. Pri tem nas je zanimala predvsem primerjava vključitve modelov staranja v začetne dogodke dreves odpovedi z vključitvijo modelov staranja v najkrajše poti odpovedi, ki so rezultati analize dreves odpovedi. Razvijali smo nadgradnjo modelov staranja v okviru verjetnostnih analiz z mislimi na optimizacije preizkušanja in vzdrževanja. Sodelovali smo z Institute for Energy iz Pettna na Nizozemskem. Delo smo predstavili na mednarodnih konferencah ter ga objavili v njihovih zbornikih in v reviji s SCI faktorjem. Rezultat dela je članek o staranju in verjetnostnih varnostnih analizah v reviji s faktorjem vpliva, ki vključuje razvoj metode za upoštevanje staranja v verjetnostnih analizah (M. Čepin, A. Volkanovski, Consideration of ageing within probabilistic safety assessment models and results, Kerntechnik (1987), vol. 74, no. 3, pp. 140-149, 2009. [COBISS.SI-ID 22601767]. Vključuje tudi način in vpliv vključitve zanesljivosti pasivnih komponent in sistemov v verjetnostne varnostne analize. Proučevali smo vpliv staranja, ki lahko spremeni zanemarljivo majhnost prispevka zanesljivosti pasivnih komponent in sistemov k rezultatom verjetnostnih varnostnih analiz. Najpomembnejša ugotovite glede vključitve pasivnih sistemov je ta, da glede prispevka k frekvenci poškodbe sredice ne prispevajo veliko ali pa skoraj nič, lahko pa imajo pasivni sistemi visoke faktorje povečanja tveganja, kar pomeni, da niso tako zanemarljivi, kot na prvi pogled kaže le merilo tveganja: frekvenca poškodbe sredice.

Razvijali smo metodo za izboljšano modeliranje varnostnih sistemov, kjer je s kombiniranimi modeli možno modelirati več konfiguracij istih sistemov, več funkcij teh sistemov in več obratovalnih stanj elektrarne. Delo smo podkrepili realnimi analizami za jedrsko elektrarno v Krškem, s katero smo sodelovali pri modifikaciji verjetnostnih varnostnih analiz. Rezultat dela je referat o opisu metode namenjene združitvi obravnavanja načinov delovanja elektrarne (M. Čepin, R. Prosen, Probabilistic safety assessment for other modes than power operation, V: Safety, reliability and risk analysis: theory, methods and applications : proceedings of the European Safety and Reliability Conference, ESREL 2008, and 17th SRA-Europe, Valencia, Spain, September 22-25, 2008, Sebastián Martorell, ur., C. Guedes Soares, ur., Julie Barnett, ur., Boca Raton ... [etc.], CRC Press, 2009, zv. 4, pp. 2883-2889. [COBISS.SI-ID 22036007]. Rezultati kažejo, da so merila tveganja večinoma nižja za stanje obratovanja na nizki moči, za stanje v pripravljenosti in za stanje v vroči zaustavitvi, če jih primerjamo z merili tveganja s stanjem na moči. Poleg tega smo analizirali posebej vpliv človeških akcij v okviru primerjav verjetnostnih varnostnih analiz za različna stanja elektrarne. Rezultati dela so objavljeni v referatu na mednarodni konferenci (M. Čepin, Human reliability analysis within probabilistic safety assessment for other modes than power operation, V: Challenges to PSA during the nuclear renaissance, PSA 2008, International Topical Meeting on Probabilistic Safety Assessment & Analysis September 7 - 11, 2008 Knoxville, Tennessee, TN, [S. l.], American Nuclear Society, 2008, 8 pp. [COBISS.SI-ID 22034727]. Glavna ugotovitev je ta, da je prispevek človeških akcij k tveganju večji za ostala omenjena stanja elektrarne: stanje obratovanja na nizki moči, stanje v pripravljenosti in stanje v vroči zaustavitvi, v primerjavi s stanjem obratovanja na moči.

Analizirali smo izboljšano izračunavanje prispevka človeškega faktorja v kompleksnih sistemov k tveganju. Osredotočili smo se na vplive medsebojnih odvisnosti med človeškimi akcijami in na napredovanje negotovosti od deterministčnih analiz do verjetnostnih varnostnih analiz. Obravnavanje medsebojne odvisnosti je izjemno subjektivno in njegovo ocenjevanje je povezano z velikimi negotovostmi. Napredovanje negotovosti od deterministčnih do verjetnostnih varnostnih analiz smo preverili na izbranih človeških akcijah v zvezi z izbranimi scenariji varnostnih analiz jedrske elektrarne. Del aktivnosti je potekal v sodelovanju z Nuclear Regulatory Commission iz ZDA.

Rezultat dela so članki v tuji reviji in v mednarodni reviji s faktorjem vpliva, kjer članki vključujejo opis razvoja in primerjave metod za vključevanje obnašanja človeka v PSA. Opis metode je v članku v tuji reviji (M. Čepin, IJS-HRA - a method for human reliability analysis, Asigurarea Calitatii, vol. 15, no. 57, pp. 21-27, 2009. [COBISS.SI-ID 23174183].

Razvito metodo smo analizirali in pri pregledu rezultatov in napredovanja vplivov podatkov skozi metodo do rezultatov ugotovili, da je pomembnost le majhnega števila človeških akcij velika. Pomembnost velikega števila človeških akcij je majhna, kar pomeni, da se je dobro osredotočiti le na nekaj najpomembnejših. Hkrati je prikazan pomen specifičnih parametrov človeških akcij, kjer se prav tako izkaže, da je le nekaj parametrov, ki po pomembnosti odstopajo. Rezultati dela so v mednarodni reviji s faktorjem vpliva (M. Čepin, Importance of human contribution within the human reliability analysis (IJS-HRA), Journal of Loss Prevention in the Process Industries, vol. 21, no. 3, pp. 268-276, 2008, [COBISS.SI-ID 20884775].

Primerjava metod za analizo človeškega faktorja je v objavljenem referatu na mednarodni konferenci (M. Čepin, Risk comparison of methods for dependency determination within human reliability analisys, V: Proceedings : an IAPSAM conference, PSAM 9, International Conference on Probabilistic Safety Assessment & Management, 18-23 May 2008, Hong Kong, China, Tsu-Mu Kao, ur., Enrico Zio, ur., Vincent Ho, ur., Hong Kong, Edge Publication Group Limited, 2008, 8 pp. [COBISS.SI-ID 21796135]. Glavna ugotovitev je v tem, da zaradi velikih subjektivnosti, ki so vključene v metode za analizo zanesljivosti človeka in v medsebojne odvisnosti med človeškimi akcijami, rezultati različnih metod dajejo za enake človeške akcije precej različne vrednosti verjetnosti človeških napak.

Med izvajanjem projekta smo dobili še pametne ideje, ki jih je bilo vredno raziskati (to ni bilo čisto predvideno v projektu, pa dodajamo, ker je pomemben prispevek na področju). Raziskovali smo vpliv negotovosti na rezultate verjetnostnih varnostnih analiz. To pomeni proučevati zadevo, ki je izjemno kompleksna. Vpliv negotovosti na rezultate verjetnostnih varnostnih analiz smo prikazali na primerih povezave deterministčnih in verjetnostnih varnostnih analiz, za kar je bilo tudi v tujini kar nekaj zanimanja (A. Prošek, M. Čepin, Success criteria time windows of operator actions using RELAP5/MOD3.3 within human reliability analysis, Journal of Loss Prevention in the Process Industries, vol. 21, no. 3, pp. 260-267, 2008. [COBISS.SI-ID 21594151].

ESREL
International conference on Safety and Reliability sodi med najbolj industrijsko znanstveno povezane konference s področja varnosti in zanesljivosti. Organizira jo združenje ESRA (European safety and Reliability Association), kjer M. Čepin vodi področje Kvantitativne analize tveganja (Quantitative Risk Analysis). Pri organizaciji konferenc in pri njihovi izpeljavi aktivno sodelujemo pri izbiri referatov in pripravi programa ter pri vodenju sekcij. Primer ESREL 2008: M. Čepin (Koordinator tehničnega področaj - Technical Area Coordinator). Primer ESREL 2009: M. Čepin (Odgovorna oseba tehničnega področja - technical area responsible), A. Volkanovski (član programskega odbora - Technical Programme Committee). Primer ESREL 2010: A. Volkanovski (član programskega odbora - Technical Programme Committee).

3. Izkoriščanje dobljenih rezultatov:

3.1. Kakšen je potencialni pomen[2] rezultatov vašega raziskovalnega projekta za:

☐ a) odkritje novih znanstvenih spoznanj;
☐ b) izpopolnitev oziroma razširitev metodološkega instrumentarija;
☒ c) razvoj svojega temeljnega raziskovanja;
☐ d) razvoj drugih temeljnih znanosti;
☒ e) razvoj novih tehnologij in drugih razvojnih raziskav.

3.2. Označite s katerimi družbeno-ekonomskimi cilji (po metodologiji OECD-ja) sovpadajo rezultati vašega raziskovalnega projekta:

☐ a) razvoj kmetijstva, gozdarstva in ribolova - Vključuje RR, ki je v osnovi namenjen razvoju in podpori teh dejavnosti;

☒ b) pospeševanje industrijskega razvoja - vključuje RR, ki v osnovi podpira razvoj industrije, vključno s proizvodnjo, gradbeništvom, prodajo na debelo in drobno, restavracijami in hoteli, bančništvom, zavarovalnicami in drugimi gospodarskimi dejavnostmi;

☒ c) proizvodnja in racionalna izraba energije - vključuje RR-dejavnosti, ki so v funkciji dobave, proizvodnje, hranjenja in distribucije vseh oblik energije. V to skupino je treba vključiti tudi RR vodnih virov in nuklearne energije;

☐ d) razvoj infrastrukture - Ta skupina vključuje dve podskupini:

- transport in telekomunikacije - Vključen je RR, ki je usmerjen v izboljšavo in povečanje varnosti prometnih sistemov, vključno z varnostjo v prometu;
- prostorsko planiranje mest in podeželja - Vključen je RR, ki se nanaša na skupno načrtovanje mest in podeželja, boljše pogoje bivanja in izboljšave v okolju;

☒ e) nadzor in skrb za okolje - Vključuje RR, ki je usmerjen v ohranjevanje fizičnega okolja. Zajema onesnaževanje zraka, voda, zemlje in spodnjih slojev, onesnaženje zaradi hrupa, odlaganja trdnih odpadkov in sevanja. Razdeljen je v dve skupini:

☐ f) zdravstveno varstvo (z izjemo onesnaževanja) - Vključuje RR - programe, ki so usmerjeni v varstvo in izboljšanje človekovega zdravja;

☐ g) družbeni razvoj in storitve - Vključuje RR, ki se nanaša na družbene in kulturne probleme;

☒ h) splošni napredek znanja - Ta skupina zajema RR, ki prispeva k splošnemu napredku znanja in ga ne moremo pripisati določenim ciljem;

☐ i) obramba - Vključuje RR, ki se v osnovi izvaja v vojaške namene, ne glede na njegovo vsebino, ali na možnost posredne civilne uporabe. Vključuje tudi varstvo (obrambo) pred naravnimi nesrečami.

[2] Označite lahko več odgovorov.

3.3. Kateri so **neposredni rezultati** vašega raziskovalnega projekta glede na zgoraj označen potencialni pomen in razvojne cilje?

Okrepljena kadrovska struktura
Okrepljene mednarodne raziskovalne in poslovne povezave

3.4. Kakšni so lahko **dolgoročni rezultati** vašega raziskovalnega projekta glede na zgoraj označen potencialni pomen in razvojne cilje?

Ohranjena in okrepljena odličnost raziskovanja
Odlična strokovna podpora industriji in upravnim organom doma in v tujini

3.5. Kje obstaja verjetnost, da bodo vaša znanstvena spoznanja deležna zaznavnega odziva?

☒ a) v domačih znanstvenih krogih;
☒ b) v mednarodnih znanstvenih krogih;
☒ c) pri domačih uporabnikih;
☒ d) pri mednarodnih uporabnikih.

3.6. Kdo (poleg sofinancerjev) že izraža interes po vaših spoznanjih oziroma rezultatih?

Industrijski člani mreže odličnosti NULIFE
Člani združenja ENEN

3.7. Število diplomantov, magistrov in doktorjev, ki so zaključili študij z vključenostjo v raziskovalni projekt?

1 magisterij
1 diploma

4. Sodelovanje z tujimi partnerji:

4.1. Navedite število in obliko formalnega raziskovalnega sodelovanja s tujimi raziskovalnimi inštitucijami.

Mreža odličnosti NULIFE (Nuclear Plant Life Management, 6. okvirni program EURATOM), polnopravni član mreže

Združenje ENEN (European Nuclear Education Network), član mreže, L. Cizelj član upravnega odbora

APSA European Network, Use of PSA for evaluation of ageing effects to the safety of energy facilities, M. Čepin

4.2. Kakšni so rezultati tovrstnega sodelovanja?

Okrepljena kadrovska struktura
Okrepljene mednarodne raziskovalne in poslovne povezave
Ohranjena in okrepljena odličnost raziskovanja
Odlična strokovna podpora industriji in upravnim organom doma in v tujin

5. Bibliografski rezultati[3] :

Za vodjo projekta in ostale raziskovalce v projektni skupini priložite bibliografske izpise za obdobje zadnjih treh let iz COBISS-a) oz. za medicinske vede iz Inštituta za biomedicinsko informatiko. Na bibliografskih izpisih označite tista dela, ki so nastala v okviru pričujočega projekta.

[3] Bibliografijo raziskovalcev si lahko natisnete sami iz spletne strani:http:/www.izum.si/

6. Druge reference[4] vodje projekta in ostalih raziskovalcev, ki izhajajo iz raziskovalnega projekta:

Monografija:
L. Cizelj, I. Simonovski, Microstructurally Short Cracks in Polycrystalls Described by Crystal Plasticity, Nova Science Publishers, ZDA, ISBN 978-1-61668-811-0
https://www.novapublishers.com/catalog/product_info.php?products_id=14542

Poglavje v knjigi:
L. Cizelj, G. Roussel, Reliability of Steam Generator Tubes, in Steam Generator Systems, ISBN 978-953-7619-X-X, Intechweb.org

Poglavje v knjigi:
M. Čepin, Probabilistic Safety Assessment and Risk-Informed Decision-Making, Nuclear Power", ISBN 978-953-7619-X-X, Sciyo

Urejanje posebne številne revije Nuclear Engineering and Design
B. Mavko, L. Cizelj, Y. Hassan: posebna številka revije Nuclear Engineering and Design, s 40 izbranimi in razširjenimi prispevki s konference Nuclear Energy for New Europe 2009.

Članstvo v uredniškem odboru znanstvene revije Reliability Engineering and System Safety (M. Čepin)

[4] Navedite tudi druge raziskovalne rezultate iz obdobja financiranja vašega projekta, ki niso zajeti v bibliografske izpise, zlasti pa tiste, ki se nanašajo na prenos znanja in tehnologije.
Navedite tudi podatke o vseh javnih in drugih predstavitvah projekta in njegovih rezultatov vključno s predstavitvami, ki so bile organizirane izključno za naročnika/naročnike projekta.

IJS Delovno Poročilo
IJS Report
IJS-DP-10077

Izdaja 1, marec 2009
Revision 1, March 2009

Baza prehodnih pojavov v jedrski elektrarni Krško

Data Base of Transients in Nuclear Power Plant Krško

B. Zafošnik, L. Cizelj

Ljubljana, marec 2009

Institut »Jožef Stefan«, Ljubljana, Slovenija

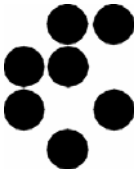

Institut »Jožef Stefan«, Ljubljana, Slovenija

Naročnik: Ordered by:	Javna agencija za raziskovalno dejavnost Republike Slovenije Tivolska c. 30, Ljubljana Nuklearna elektrarna Krško d.o.o., Vrbina 12, 8270 Krško
Izvajalec: Prepared by:	Institut »Jožef Stefan« 1000 Ljubljana Jamova 39 Slovenija Odsek za reaktorsko tehniko (Reactor Engineering Division)
Pogodba štev.: Contract Number:	Z2-9488-0106-06 (IJS in ARRS) U1-BL-R4-3/03 (IJS in NEK)
Nosilec naloge: Responsible Person:	dr. Boštjan Zafošnik, univ. dipl. inž. str.
Naslov poročila: Report Title:	Baza prehodnih pojavov v jedrski elektrarni Krško Data Base of Transients in Nuclear Power Plant Krško
Avtorji poročila: Authors:	Dr. Boštjan Zafošnik, univ.dipl.inž.str. Prof. dr. Leon Cizelj, univ.dipl.inž.str.
Štev. delovnega poročila: Report Number: Konto: Account Number:	IJS-DP-10077 Izdaja 1 V2-0375-C
Kopije: Distribution:	➢ Naročnik (3) ➢ Knjižnica/Library (1x) ➢ Nosilec naloge/Responsible Person (1x) ➢ Avtorji/Authors (1x) ➢ Arhiv OR4/Archive (1x + original)

Ljubljana, marec 2009

POVZETEK

V poročilu smo zbrali najpomembnejše vire informacij o projektnih in dejanskih prehodnih pojavih reaktorskega hladilnega sistema jedrske elektrarne v Krškem. Mednje sodijo projekt elektrarne z vsemi spremembami, procesni informacijski sistem elektrarne in lokalne meritve temperatur na zunanji površini nekaterih cevovodov. Opravili smo preliminarno analizo celovitosti in uporabnosti dostopnih podatkov o prehodnih pojavih za analize utrujanja komponent ter preliminarno primerjavo med izbranimi izmerjenimi in projektnimi prehodnimi pojavi. Izbrani izmerjeni prehodni pojavi so bili s stališča utrujanja ugodnejši od projektnih.

Opredelimo najpogostejše težave pri interpretaciji podatkov, še posebej v primerih, ko o temperaturah hladila sklepamo na podlagi meritev na zunanji površini cevi. Nakazujemo tudi nekatere prijeme, s katerimi bi bilo mogoče manjkajoče podatke rekonstruirati.

Poročilo predstavlja del rezultatov projekta »**Zasnova metode za spremljanje izrabe komponent jedrskih elektrarn**«, ki sta ga sofinancirala Javna agencija za raziskovalno dejavnost Republike Slovenije (pogodba št. 1000-07-219488) in Nuklearna elektrarna Krško d.o.o. (pogodba št. POG-3408).

ABSTRACT

The most relevant sources of information on design and actual transients of the reactor coolant system in Krško nuclear power plant are identified in the report. These include design documentation of the plant including all relevant design changes, plant process information system and local measurements of temperatures at the outer surface pf pipes. A preliminary analysis of consistency and applicability of the available transient data to the fatigue analyses has been performed, followed by a preliminary comparison of selected design and actual transients. Selected actual transients confirmed conservativity of design transients from the fatigue viewpoint.

The most probable difficulties with interpretation of transient data in fatigue analyses have been identified with special emphasis on coolant temperatures deduced form the measured temperatures at the tube outside surface. Some approaches facilitating the reconstruction of the missing data are also highlighted.

This report contains a part of the results of the project »**Conception of a method for monitoring of the usage of nuclear power plant components**«, cosponsored by the Slovene research Agency (grant No. 1000-07-219488) and Nuklearna elektrarna Krško d.o.o. (grant No. POG-3408).

KAZALO

POVZETEK II

ABSTRACT III

KAZALO IV

SEZNAM SLIK VI

SEZNAM TABEL VII

1 UVOD 1

1.1 Namen poročila 1

1.2 Ozadje 1

1.3 Organizacija poročila 1

2 PROJEKTNI PREHODNI POJAVI V JE KRŠKO 2

2.1 Obratovalne obremenitve 2
2.1.1 Normalno obratovanje 2
2.1.2 Moteno obratovanje 2
2.1.3 Zasilno obratovanje 2
2.1.4 Nezgoda 3

2.2 Preizkusi 3

2.3 Projektni prehodni pojavi za primarni krog jedrske elektrarne Krško 3

2.4 Viri informacij o projektnih prehodnih pojavih jedrske elektrarne Krško 3

3 IZMERJENI PREHODNI POJAVI V JE KRŠKO 5

3.1 Globalno merjenje tlaka in temperature reaktorskega hladila 5
3.1.1 Ogrevanje elektrarne 6
3.1.2 Ohlajanje elektrarne 8
3.1.3 Ustavitev reaktorja s polne moči 10

3.2 Lokalno merjenje temperature reaktorskega hladila 11
3.2.1 Turbulentna penetracija 11
3.2.2 Toplotno razslojeni tokovi 12
3.2.3 Meritve temperatur na zunanji površini stene cevi 13
3.2.4 Osnovne omejitve meritev na zunanji steni cevi 15
3.2.5 Vpliv prestopa toplote iz tekočine na cev 18

3.3 Rekonstrukcija manjkajočih podatkov 18

3.4 Prehodni pojavi, ki so se zgodili v NEK 19

4 ZAKLJUČKI 20

5 VIRI 21

SEZNAM SLIK

Slika 1 Primer izmerjenega poteka temperatur med ogrevanjem elektrarne 6
Slika 2 Primer izmerjenega poteka tlaka v primarnem krogu med ogrevanjem elektrarne 7
Slika 3 Primerjava tlaka v primarnem krogu in tlaka nasičenja v tlačniku 7
Slika 4 Primer izmerjenega poteka temperatur med ohlajanjem elektrarne 8
Slika 5 Primer izmerjenega poteka tlaka v primarnem krogu med ohlajanjem elektrarne 9
Slika 6 Primer izmerjenega poteka temperatur med ustavitvijo reaktorja s polne moči 9
Slika 7 Primer izmerjenega poteka tlaka v primarnem krogu med ustavitvijo reaktorja s polne moči 10
Slika 8 Turbulentna penetracija iz glavnega cevovoda v stanski cevovod [9] 11
Slika 9 Razslojeni tok v horizontalni cevi 12
Slika 10 Značilne razporeditve merilnih elementov na zunanji površini cevi 13
Slika 11 Razporeditev senzorjev pri cevovodu za nadzor toplotnega šoka in stratifikacije cevi [10] 14
Slika 12 Primer izmerjenih temperature na zunanji površini prelivnega voda med zagonom elektrarne [10] 14
Slika 13 Stopničasta sprememba temperature iz 0 na 1 in nazaj na 0: a) enkratna in b) periodična 15
Slika 14 Maksimalna temperatura na zunanji površini kot funkcija debeline stene cevi a in normaliziranega časa trajanja Δt temperaturne spremembe na notranji površini cevi 16
Slika 15 Zakasnitev Δt_{max} med koncem temperaturne spremembe in pojavom maksimalne temperature T_{max} na zunanji površini 17
Slika 16 Amplituda temperaturne spremembe na zunanji strani cevi glede na različne debeline cevi a in frekvenco spremembe temperature na notranji strani 17

SEZNAM TABEL

Tabela 1 Projektni prehodni pojavi jedrske elektrarne Krško [13] **4**
Tabela 2 Prehodni pojavi, ki so se zgodili v NEK **18**

1 UVOD

1.1 Namen poročila

V poročilu predstavljamo del rezultatov projekta »**Zasnova metode za spremljanje izrabe komponent jedrskih elektrarn**«, ki sta ga sofinancirala Javna agencija za raziskovalno dejavnost Republike Slovenije (pogodba št. 1000-07-219488) in Nuklearna elektrarna Krško d.o.o. (pogodba št. POG-3408).

Preostali rezultati projekta so predstavljeni v spremljajočih poročilih:

- Zasnova metode za spremljanje izrabe komponent jedrskih elektrarn [1] in
- Pilotni primeri izračuna faktorja utrujenostne izrabe [2].

1.2 Ozadje

Projektna trajnostna doba jedrskih elektrarn temelji na zbirki predpostavljenih projektnih dogodkov. Vsak izmed projektnih dogodkov v sistemih in komponentah elektrarne povzroči prehodne pojave s spremembami temperatur, tlakov in včasih tudi drugih obratovalnih parametrov. Prehodni pojavi torej povzročajo tudi spremembe napetosti v cevovodih in tlačnih posodah in s tem potencialno prispevajo k njihovemu utrujanju.

Za natančno določevanje faktorjev izrabe posameznih komponent je torej natančno poznavanje prehodnih pojavov ključno. Pri tem imamo v mislih tako predpostavljene projektne prehodne pojave kot tudi izmerjene dejanske prehodne pojave. Hkrati je pomembno upoštevati tudi dejstvo, da ločljivost podatkov v projektu in v zapisih izmerjenih prehodnih pojavov praviloma zadoščata za popis večine enostavnejših stanj v sistemih in njihovih komponentah.

V primeru nekaterih kompleksnejših pojavov, kot so npr. toplotno razslojeni tokovi, turbulentna penetracija v priključni cevovod s pretežno mirujočo tekočino in toplotni šok ([3], [4], [5], [6], [7], [8], [9]), so za pravilno karakterizacijo dogajanj in s tem obremenitev v cevovodih nujno potrebne podrobnejše lokalne meritve [3], [10]. Zanesljiva interpretacija lokalnih meritev ponavadi zahteva tudi razmeroma zahtevne analize izmerjenih vrednosti, še posebej v primerih, ko na temperaturo tekočine v cevi sklepamo na osnovi meritev temperatur na zunanji površini cevi [11].

Osnovni cilj pričujočega poročila sta identifikacija in preliminarna analiza celovitosti in uporabnosti dostopnih podatkov o prehodnih pojavih za analize utrujanja komponent. Nakazujemo tudi nekatere prijeme, s katerimi bi bilo mogoče manjkajoče podatke rekonstruirati. Pri tem se omejujemo na komponente reaktorskega hladilnega sistema.

1.3 Organizacija poročila

V poglavju 2 opisujemo projektne prehodne pojave v reaktorskem hladilnem sistemu jedrske elektrarne Krško. Poglavje 3 predstavlja prehodne pojave, ki so jih v jedrski elektrarni Krško izmerili in so zabeleženi v procesno informacijskem sistemu. Opredelimo najpogostejše težave pri interpretaciji podatkov in nakažemo nekatere prijeme, s katerimi bi bilo mogoče manjkajoče podatke rekonstruirati. Poročilo se konča z zaključki v poglavju 4 in viri v poglavju 5.

2 PROJEKTNI PREHODNI POJAVI V JE KRŠKO

Jedrske elektrarne so po ASME B&PV Code [12] projektirane za projektne, obratovalne in preizkusne obremenitve. Prehodni pojavi s spremembami obremenitev, predvsem temperature in tlaka, so sestavni delo obratovalnih in preizkusnih obremenitev, ki so podrobneje opredeljene v nadaljevanju.

Projektne obremenitve so statične in kot takšne na utrujanje nimajo vpliva.

2.1 Obratovalne obremenitve

V skladu z ASME B&PV Code [12] obratovalne obremenitve s spremljajočimi prehodnimi pojavi razdelimo v štiri skupine in sicer:

- normalno obratovanje,
- moteno obratovanje,
- zasilno obratovanje in
- nezgode.

V nadaljevanju podrobneje opišemo vse štiri skupine. Tabela 1 podaja tudi vsa v projektu predvidene obratovalne dogodke skupaj z njihovim projektno predvidenim številom.

Kontrola na utrujanje po ASME B&PV Code [12] izrecno zajema normalno in moteno obratovanje. Zasilno obratovanje pa je v kontrolo utrujanja vključeno le posredno in sicer z omejitvijo skupnega števila vseh obremenitvenih ciklov z amplitudo napetosti večjo od amplitude napetosti pri 10^6 obremenitvenih ciklih (Wöhlerjeva krivulja) na največ 25.

2.1.1 Normalno obratovanje

Normalno obratovanje zajema vsa stanja pri zagonu, obratovanju v predvidenem območju moči, vročo zaustavitev in zaustavljanje elektrarne, ki ne sodijo v moteno ali zasilno obratovanje ali med nezgode.

2.1.2 Moteno obratovanje

Moteno obratovanje zajema vsa stanja, ki odstopajo od normalnega obratovanja in se lahko zgodijo dovolj pogosto, da jih je elektrarna sposobna vzdržati brez kakršnihkoli poškodb. V moteno obratovanje sodijo predvsem tisti prehodni pojavi, ki so posledica enojne odpovedi opreme ali enojne napake operaterjev.

Vzroke za moteno obratovanje je praviloma mogoče odpraviti brez zaustavitve elektrarne. V redkih primerih, ko je zaustavitev potrebna, pa zaradi posledic motenega obratovanja ne bo potrebno odpravljati poškodb na opremi.

2.1.3 Zasilno obratovanje

Zasilno obratovanje je odstopanje od normalnega obratovanja, ki ga je mogoče odpraviti z zaustavitvijo elektrarne in zamenjavo oz. popravilom poškodovane opreme. Projektiranje opreme na tovrstne dogodke zagotavlja, da naključne okvare opreme ne bodo povzročile poškodb tlačne meje reaktorskega hladila. Skupno število predvidenih tovrstnih dogodkov v trajnostni dobi elektrarne naj bi povzročilo kvečjemu 25 obremenitvenih ciklov z amplitudo napetosti večjo od amplitude napetosti pri 10^6 obremenitvenih ciklih (Wöhlerjeva krivulja).

2.1.4 Nezgode

Nezgode so kombinacije dogodkov izjemno nizkih verjetnosti, ki bi lahko ogrozile obratovalno sposobnost elektrarne, vodile do trajnih poškodb opreme in v izjemnih primerih vplivale tudi na varnost in zdravje okoliškega prebivalstva. Pri tovrstnih dogodkih je ključni cilj projekta varna ustavitev elektrarne, možnost morebitnega ponovnega zagona pa je prepuščena prihodnjim analizam in odločitvam upravnih organov.

2.2 Preizkusi

V skladu z ASME B&PV Code [12] je opredeljenih več vrst preizkusov, ki dokazujejo predvsem celovitost tlačnih mej primarnega in sekundarnega hladilnega kroga ter obratovalno sposobnost turbine. Tabela 1 podaja vse v projektu predvidene prizkuse skupaj z njihovim projektno predvidenim številom.

Kontrola na utrujanje po ASME B&PV Code [12] izrecno zajema obremenitve zaradi preizkusov.

2.3 Projektni prehodni pojavi za primarni krog jedrske elektrarne Krško

Projektni dogodki oz. prehodni pojavi, ki jih je za 40 letno trajnostno dobo predvidel projekt jedrske elektrarne Krško, so skupaj s projektno predvidenim številom dogodkov zbrani v Tabeli 5.2-1 v [13] (Tabela 1 jih povzema).

2.4 Viri informacij o projektnih prehodnih pojavih jedrske elektrarne Krško

Podrobnejši potek projektnih prehodnih pojavov opisujejo tudi dokumenti [13], [14], [15], [16], [17] in v njih citirani dokumenti. Pomembne informacije je mogoče dobiti tudi v projektnih specifikacijah in poročilih. V precejšnji meri so omenjeni v dokumentu [18].

Projektni prehodni pojavi so se v času obratovanja elektrarne nekajkrat spremenili. Kot največja mejnika sprememb omenjamo projektne analize, ki so omogočale obratovanje z začepljenimi uparjalniki [14] in projektne analize ob zamenjavi uparjalnikov in hkratnem povečanju moči elektrarne [15], [16], [17]. Mogoče je torej pričakovati, da se bodo spreminjali tudi v bodočnosti.

Pomembno je poudariti, da zbrani podatki podajajo dobro globalno sliko o predvidenem dogajanju v sistemih jedrske elektrarne. Praviloma pa so bili obratovalni prehodni pojavi in njihovo število v fazi projekta ocenjeni dokaj konzervativno in so opredeljeni do te mere, da je mogoče izpolniti projektne zahteve. Hkrati pa praviloma niso dovolj podrobni za natančno oceno lokalnih razmer v posameznih komponentah. Pogost primer tovrstne situacije je mešanje tekočin v spojih cevi. Že zmerne razlike v temperaturah in pretokih lahko vodijo v spremembe lokalnih napetosti, ki so s stališča utrujanja pomembne. V takšnem primeru lahko kompleksne termo-hidravlične robne pogoje določimo oz. rekonstruiramo s pomočjo računalniških programov za dinamiko tekočin. Začetne in robne pogoje za tovrstne simulacije lahko dobimo iz projektnih opisov prehodnih pojavov, podatkov iz procesnega informacijskega sistema in neposrednih meritev.

Sodobna orodja praviloma omogočajo predvsem simulacijo povprečnih hitrosti fluidov in temperatur pri turbulentnih tokovih. V nekaterih primerih je mogoča tudi neposredna simulacija turbulentnih tokov; omejitev so predvsem izjemno dolgi računski časi.

Prehodni pojav	Število v projektu predvidenih dogodkov
NORMALNO OBRATOVANJE	
Ogrevanje s 100°F (55.6 K) na uro	200
Ohlajanje s 100°F (55.6 K) na uro	200
Zvezno povečevanje moči s hitrostjo 5% polne moči na minuto	13200
Zvezno zmanjševanje moči s hitrostjo 5% polne moči na minuto	13200
Koračno povečanje moči za 10% polne moči	2000
Koračno zmanjšanje moči za 10% polne moč	2000
Veliko koračno zmanjšanje moči z dušenjem pare skozi turbinski obvod	200
Nihanja temperature in tlaka reaktorskega hladila (± 1.67°C, ± 0.17 MPa)	$1.5 \cdot 10^5$
Nihanja temperature in tlaka reaktorskega hladila (± 0.28°C, ± 0.041 MPa)	$1.5 \cdot 10^6$
Vbrizgavanje mrzle napajalne vode v uparjalnika v stanju vroče zaustavitve	2000
Obremenjevanje med 0% in 15% celotne moči	500
Razbremenjevanje med 0% in 15% celotne moči	500
Izenačevanje koncentracije borove kisline	26400
Menjava goriva	80
MOTENO OBRATOVANJE	
Izpad električnega bremena brez takojšnje zaustavitve reaktorja	80
Izpad zunanjega napajanja (z naravno cirkulacijo v reaktorskem hladilnem sistemu)	40
Delna izguba pretoka reaktorskega hladila zaradi izpada ene črpalke	80
Ustavitev reaktorja s polne moči	
brez ohlajanja	230
z ohlajanjem, brez varnostnega vbrizgavanja	160
z ohlajanjem, z varnostnega vbrizgavanjem	10
Nenamerno zmanjšanje tlaka reaktorskega hladila	20
Padec regulacijske palice	80
Nenamerna vključitev sistema za zasilno hlajenje sredice	60
Potres ob obratovanju (OBE, 20 potresov s po 10 cikli)	200
Prekomeren pretok napajalne vode	30
ZASILNO OBRATOVANJE	
Mala izlivna nezgoda	5
Mali zlom parovoda	5
Popolni izpad pretoka reaktorskega hladila	5
NEZGODA	
Velika izlivna nezgoda	1
Zlom glavnega parovoda	1
Zlom glavnega napajalnega cevovoda	1
Blokada rotorja črpalke reaktorskega hladila	1
Izmet regulacijske palice	1
Zlom cevi uparjalnika	
Potres ob varni ustravitvi (SSE)	1
PREIZKUSI	
Preizkus turbine	20
Tlačni preizkus primarnega sistema	10
Tlačni preizkus sekundarnega sistema	10
Preizkus netesnosti primarnega sistema	200
Preizkus netesnosti sekundarnega sistema	80
Preizkus netesnosti cevi uparjalnikov	800

Tabela 1 Projektni prehodni pojavi jedrske elektrarne Krško [13]

3 IZMERJENI PREHODNI POJAVI V JE KRŠKO

3.1 Globalno merjenje tlaka in temperature reaktorskega hladila

V nadaljevanju na kratko opišemo meritve temperature in tlaka, ki jih opravlja originalna instrumentacija elektrarne predvsem v podporo varnemu obratovanju. Rezultate teh meritev zajema in hrani tudi procesni informacijski sistem v jedrski elektrarni Krško. Tovrstni podatki so posredno uporabni tudi pri analizah utrujenosti sistemov in komponent.

Tlak reaktorskega hladila v jedrski elektrarni Krško merijo v vroči in hladni veji ter v tlačniku z induktivnimi tlačnimi tipali.

Za merjenje temperature reaktorskega hladila uporabljajo uporovne merilne naprave RTD (Resistant Temperature Detectors), ki so nameščene v posebni zaščiti (angl. thermowell), ki ščiti merilno napravo, hkrati pa zmanjšuje možnost puščanja reaktorskega hladila. Merilno območje RTD naprav je med 0 in 400°C. Takšno območje merjenja je potrebno za merjenje temperature pri prehodnih pojavih in za izvajanje postopkov zaganjanja in zaustavitev elektrarne.

Glede na posredovane podatke iz NEK, se bomo v nadaljevanju omejili na merjenje temperature hladila v vroči in hladni veji ter v prelivnem vodu in tlačniku.

Temperaturo reaktorskega hladila merijo v obeh vročih in hladnih vejah [13]. V obeh vročih vejah reaktorsko hladilo zajamejo na približno polovici dolžine skozi po tri odjemna mesta, nameščena po obodu v razmiku 120° (TE-413 in TE-423). Cevi iz treh odjemnih mest se združijo in vodijo reaktorsko hladilo iz vsake izmed obeh vročih vej posebej skozi merilce temperature [13].

V obeh hladnih vejah hladilo zajamejo za črpalkama (TE-414 in TE-424, [13]). V prelivnem vodu merijo temperaturo hladila približno na polovici dolžine med vročo vejo in tlačnikom s potopljenim termometrom [13]. V tlačniku merijo temperaturo kapljevine (TE-608, v bližini grelcev) in temperaturo pare (TE-607) s potopljenima termometroma [13].

Posredne meritve v vroči in hladni veji zagotavljajo natančne meritve temperature hladila v vseh razmerah, kjer so spremembe temperature razmeroma počasne. Neposredno merjenje temperature (prelivni vod, tlačnik) pa zagotavlja razmeroma natančne meritve tudi v primeru hitrih sprememb v temperaturi hladila.

Za zanesljivo oceno porazdelitve temperatur po notranji steni cevi, ki pri ocenah utrujanja predstavlja vhodni podatek, tovrstne meritve zadoščajo le v primeru velikih pretokov, torej v področjih hitrih in turbulentnih tokov. V vseh ostalih primerih je kompleksne termo-hidravlične robne pogoje smiselno določiti s pomočjo računalniških programov za dinamiko tekočin. Začetne in robne pogoje za tovrstne simulacije pa lahko dobimo iz izmerjenih vrednosti.

Nekaj podatkov o spremembah temperature in tlaka pri obratovalnih dogodkih v jedrski elektrarni Krško, ki so bili zabeleženi s procesno informacijskim sistemom, prestavljamo v nadaljevanju [19].

3.1.1 Ogrevanje elektrarne

Ogrevanje elektrarne spada med normalne obratovalna stanja elektrarne. Med ogrevanjemje hitrost spremembe temperature reaktorskega hladila omejena na 55.6 °C/h [13].

Iz rezultatov meritev (Slika 1) je razvidno, da je hitrost spremembe temperature reaktorskega hladila manjša od dovoljenih 55.6 °C/h. Poleg tega je razvidno, da ogrevanje ne poteka enakomerno s konstantno hitrostjo, kakor je bilo predvideno v projektu [15]. Krivulje ogrevanja prikazujejo, da se pri času 324 min spremeni temperatura reaktorskega hladila v vroči in hladni veji ter v tlačniku. V tlačniku je hitrost spremembe temperature reaktorskega hladila precej višja (14,7 °C/h), medtem ko je v vroči in hladni veji ~1.5 °C/h. Višja hitrost spremembe temperature reaktorskega hladila v tlačniku je pričakovana in je posledica delovanja grelcev.

Podatki o temperaturi so podani do temperature 292°C v vroči in hladni veji primarnega kroga, ki je značilna za vročo zaustavitev reaktorja.

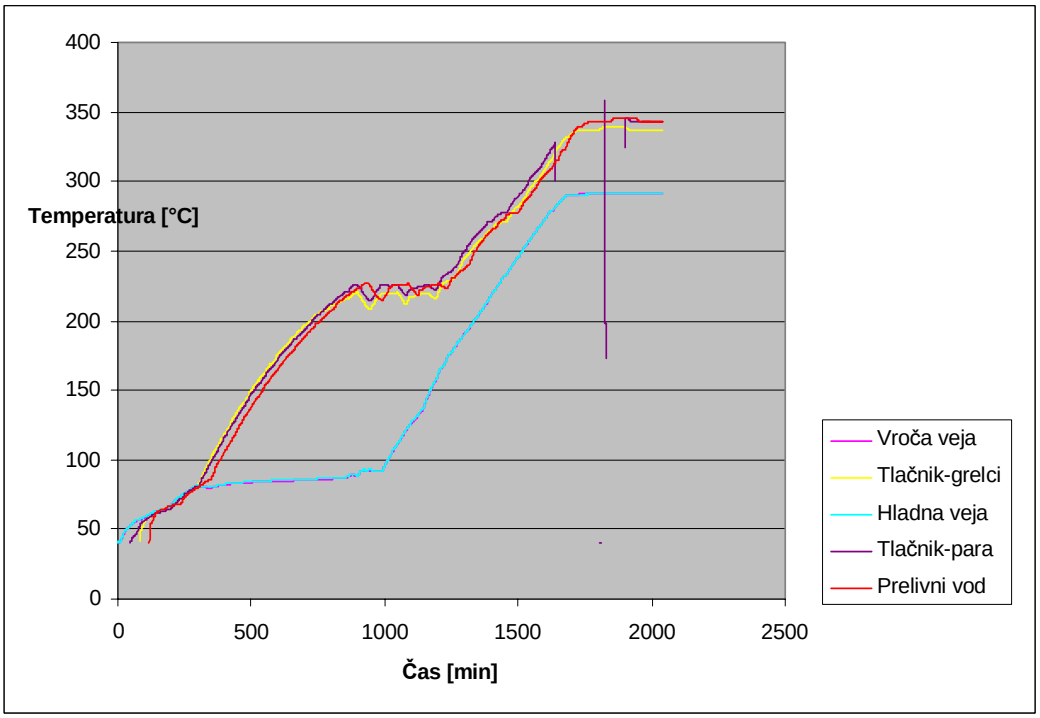

Slika 1 Primer izmerjenega poteka temperatur med ogrevanjem elektrarne

Primerjava izmerjenih in projektne hitrosti ogrevanja pokaže, da je bilo ogrevanje mnogo bolj počasno, kot je predvideno v projektu. Praviloma to pomeni manj utrujanja in manjši faktor izrabe.

Rezultati tudi prikazujejo, da je temperatura v tlačniku nekaj časa nižja od temperature v prelivnem vodu, od časa 805 minut po zagonu elektrarne pa termometer kaže približno enako temperaturo v prelivnem vodu in temperaturo pare v tlačniku.

Tlak v primarnem krogu, merjen v vroči veji, je po zagonu 2.5 MPa (Slika 2). Ta tlak vzpostavijo drugi sistemi v elektrarni (npr. sistem za odvajanje zaostale toplote). Pri tem tlaku lahko parni mehur v tlačniku nastane šele pri 223.9 °C [20].

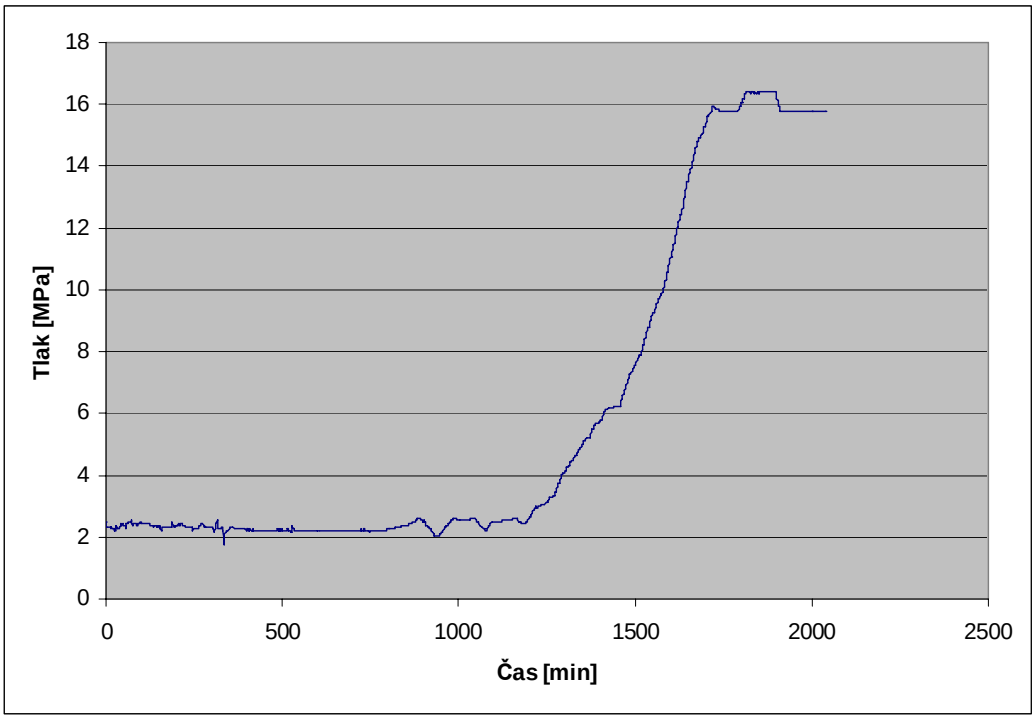

Slika 2 Primer izmerjenega poteka tlaka v primarnem krogu med ogrevanjem elektrarne

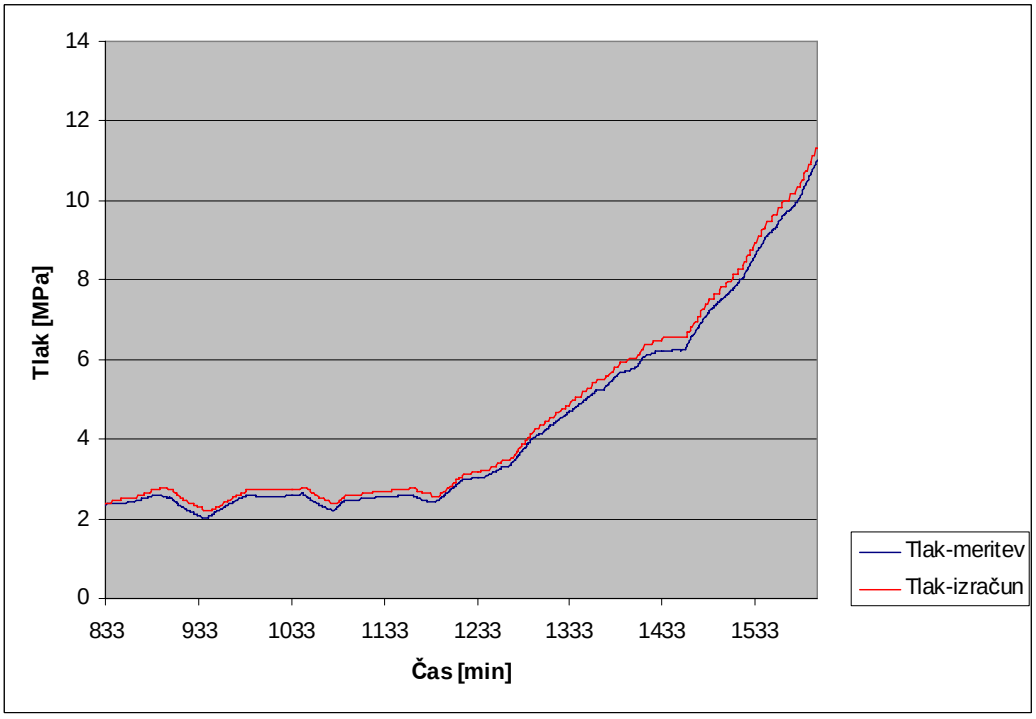

Slika 3 Primerjava tlaka v primarnem krogu in tlaka nasičenja v tlačniku

Časovni potek tlaka (Slika 2) je skoraj brez večjih oscilacij, ki bi lahko dodatno utrujale komponente in vplivale na faktor izrabe.

V tlačniku je reaktorsko hladilo večino časa hkrati v plinati in kapljeviti fazi. Zato lahko na osnovi temperature pare v tlačniku določimo tlak v sistemu (Slika 3). Primerjava med izmerjenim tlakom v vroči veji (Slika 2) in tlakom nasičene vodne pare [20] iz tlačnika ob upoštevanju višinskih razlik in hitrosti hladila kaže dobro ujemanje (Slika 3).

3.1.2 Ohlajanje elektrarne

Slika 4 prikazuje spremembe temperatur pri spremembi moči reaktorja iz 100% na 0%. Temperatura v vroči veji se znižuje iz 325°C na 292°C, ko je reaktor v stanju vroče zaustavite. Po tem se temperaturi v vroči in hladni veji enakomerno znižujeta z največjo hitrostjo ohlajanja 41.1°C/h do temperature hladne zaustavitve. Dovoljena hitrost ohlajanja je 55.6 °C/h. Opazimo lahko spremembo temperature v prelivnem vodu pri času 1262 min. Sklepati je mogoče, da je v tlačniku prišlo do znižanja temperature pare, zaradi česar je prišlo do znižanja tlaka. Zaradi višjega tlaka v preostalem delu sistema je prišlo do vdora hladila iz vroče veje v prelivni vod. Ko so z grelci začeli ogrevati hladilo v tlačniku, se je tlak začel višati in je toplejše hladilo iz tlačnika potisnilo hladnejše hladilo proti vroči veji, s čemer se je višala temperatura v okolici termometra v prelivnem vodu.

Primerjava izmerjenih in projektne hitrosti ogrevanja pokaže, da je bilo ohlajanje mnogo bolj počasno, kot je predvideno v projektu. Praviloma to pomeni manj utrujanja in manjši faktor izrabe.

Časovni potek tlaka (Slika 5) je skoraj brez večjih oscilacij, ki bi lahko dodatno utrujale komponente in vplivale na faktor izrabe.

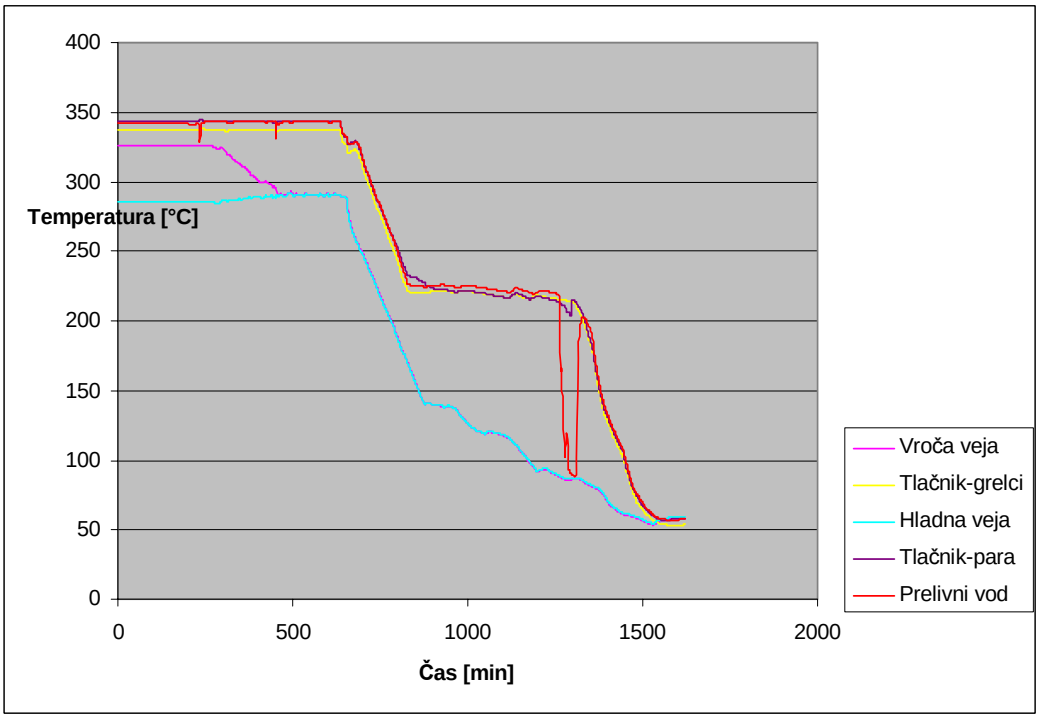

Slika 4 Primer izmerjenega poteka temperatur med ohlajanjem elektrarne

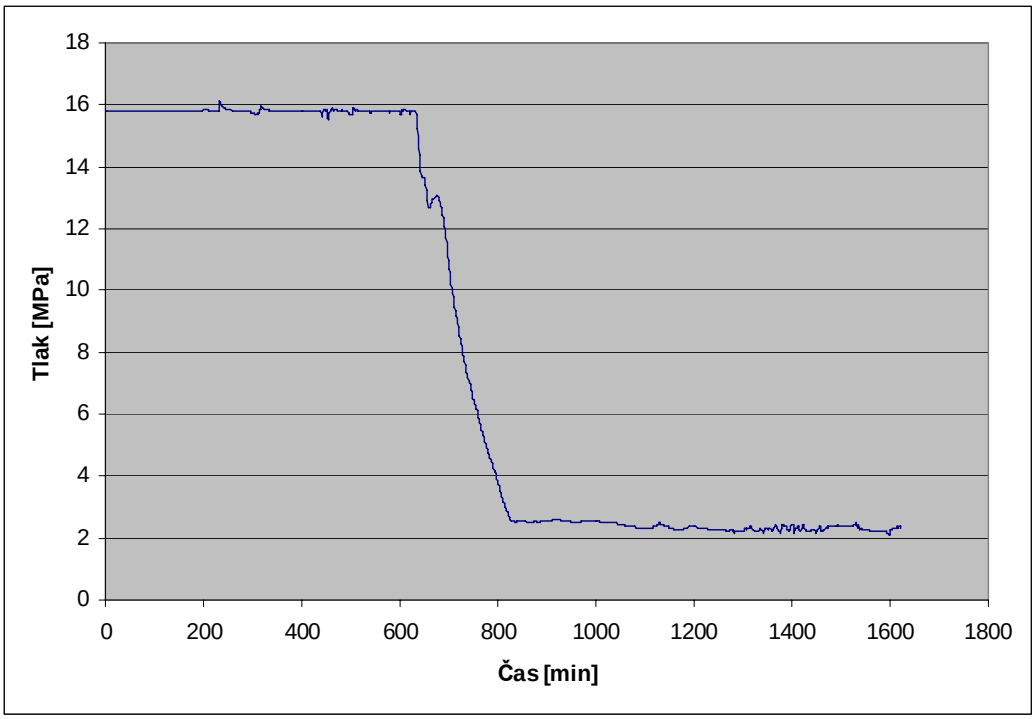

Slika 5 Primer izmerjenega poteka tlaka v primarnem krogu med ohlajanjem elektrarne

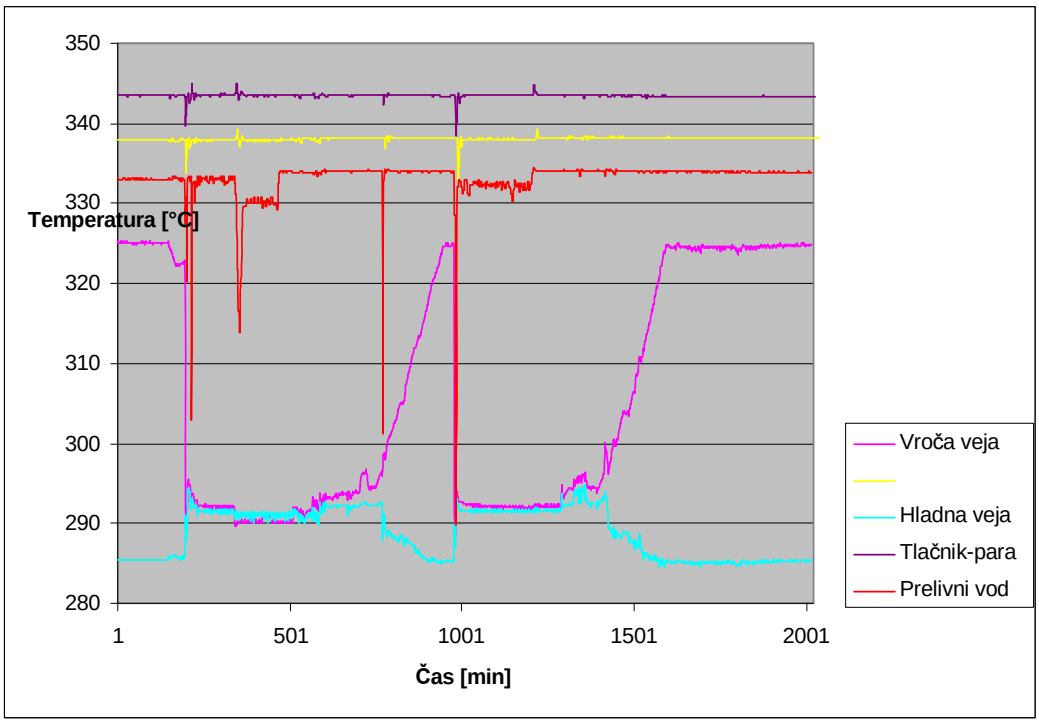

Slika 6 Primer izmerjenega poteka temperatur med ustavitvijo reaktorja s polne moči

3.1.3 Ustavitev reaktorja s polne moči

Slika 6 prikazuje ustavitev reaktorja s polne moči, pri čemer je bila začetna temperatura reaktorskega hladila v vroči veji 325°C. Temperature reaktorskega hladila se spreminjajo v vroči veji, v prelivnem vodu in v tlačniku. Ko je prišlo do ustavitve reaktorja, se je znižala temperatura v vroči veji, hkrati pa sta se znižala tudi temperatura v tlačniku in tlak v sistemu.

Opazimo lahko tudi vdor hladila iz vroče veje v prelivni vod, kar je povzročilo nihanje temperature v prelivnem vodu. Z dvigom temperature v tlačniku se je dvignila tudi tlak v sistemu, zaradi česar je hladilo iz prelivnega voda potisnilo v vročo vejo in dvignilo temperaturo v okolici merilca v prelivnem vodu. Če primerjamo dejanski in projektni prehodni pojav lahko vidimo, da je hitrost spremembe temperature v prelivnem vodu 0.04508 °C/s, medtem ko je projektna hitrost spremembe temperature 1.4 °C/s.

Primerjava izmerjenih in projektne hitrosti ogrevanja pokaže, da so spremembe počasnejše, kot je predvideno v projektu. Praviloma to pomeni manj utrujanja in manjši faktor izrabe.

Časovni potek tlaka (Slika 7) nakazuje padca tlaka na 0 MPa, ko je reaktor še obratoval na polni moči. Do takšnih anomalij prihaja velikokrat zato, ker sistem v tistem trenutku ni zabeležil podatka o tlaku. Na anomalijo pri teh rezultatih je mogoče sklepati tudi s primerjavo med izmerjenimi temperaturami (Slika 6) in spremembami tlaka (Slika 7). Če zanemarimo padce na 0 MPa, so največje spremembe tlaka pri tem prehodnem pojavu nekaj manj kot 10% začetnega. Iz projektnih prehodnih pojavov pa izhaja sprememba, ki je nekaj večja kot 10% začetnega tlaka [15].

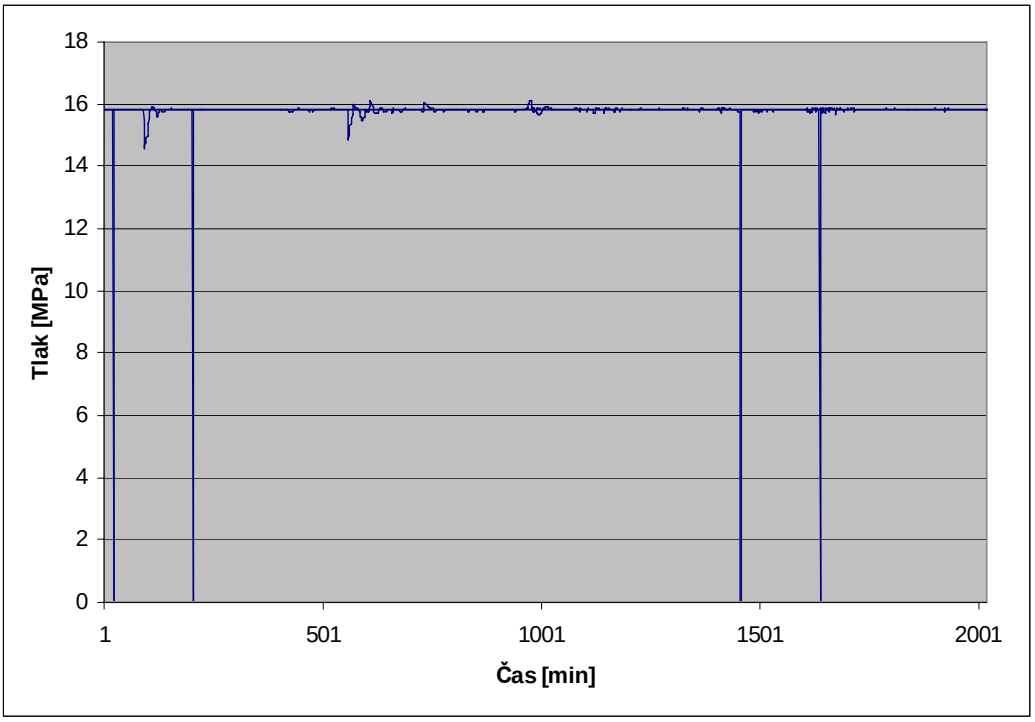

Slika 7 Primer izmerjenega poteka tlaka v primarnem krogu med ustavitvijo reaktorja s polne moči

3.2 Lokalno merjenje temperature reaktorskega hladila

V področjih laminarnih tokov ali skoraj mirujočega hladila lahko zaradi različnih temperatur prihaja do toplotnega razslojevanja. Tovrstni pojavi v originalnem projektu jedrske elektrarne niso bili upoštevani. V zadnjem času pa je znano, da se lahko pojavijo in da lahko imajo razmeroma močan vpliv na napetostno stanje v prizadetih cevovodih, s tem pa tudi na utrujenost materiala cevovoda.

V takih okoliščinah je za zanesljivo oceno napetostnega polja potrebno poznati porazdelitev temperatur po notranji površini cevi. Za takšno meritev bi potrebovali večje število potopljenimi termometrov: rezultate meritev z enim samim potopljenim termometrom lahko namreč uporabimo samo kot dopolnilo k ostalim meritvam. Vgradnja več potopljenih merilcev temperature pa je lahko zapletena ali celo onemogočena, saj gre za neposreden poseg v tlačno mejo hladila. Zato podatke o razmerah znotraj cevovoda najpogosteje dobimo posredno z namestitvijo merilnih elementov na zunanji površini cevi. Za zanesljivo interpretacijo rezultatov takih meritev pa je praviloma potrebno izvesti posebne analize.

V nadaljevanju povzemamo najpomembnejše procese v hladilu znotraj cevi, osnovne načine merjenja temperatur na zunanji steni cevi in osnovne rezultate analitičnih prijemov, ki so lahko v veliko pomoč pri interpretaciji izmerjenih temperatur.

V zahtevnejših primerih je potrebno uporabiti računalniške simulacije s pomočjo orodij za računalniško dinamiko tekočin. Tako dobljene rezultate lahko z analizo pretvorimo v temperaturo na notranji strani cevi.

3.2.1 Turbulentna penetracija

Turbulentna penetracija tekočine iz večje cevi v manjšo je pomemben pojav pri spoju dveh cevi, v katerih sta tekočini različnih temperatur in hitrosti (Slika 8). Globine turbulentne penetracije navadno ni mogoče enostavno določiti. Znano je, da se intenzivnost turbulentne penetracije zmanjšuje eksponentno z razdaljo, pri čemer je temperatura tekočine približno konstantna na dolžini nekaj premerov cevovoda, kasneje pa se zmanjšuje [9].

Dolžina turbulentne penetracije je večja pri večjih hitrostih tekočine v večjem cevovodu. Odvisna je tudi od oblike manjšega cevovoda. Za tlačnovodne reaktorje, kakršen je tudi v NEK, je značilna dolžina turbulentne penetracije v stransko vejo z mirujočo tekočino v območju od 15 do 25 notranjih premerov stranske veje. Pri tem lahko turbulentna penetracija med drugim povzroča mešanje tekočin v cevovodih, toplotno razslojenost ali vzdolžno gibanje meje med vročo in hladno tekočino oz. toplotni šok.

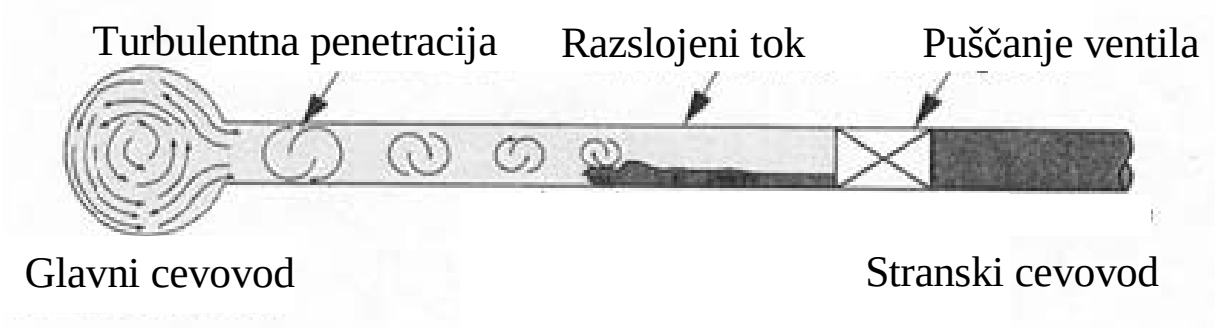

Slika 8 Turbulentna penetracija iz glavnega cevovoda v stanski cevovod [9]

3.2.2 Toplotno razslojeni tokovi

Toplotno razslojevanje tokov praviloma nastane kot posledica različnih gostot oz. temperatur medija. Pojav oz. njegove posledice so v prelivnih vodih jedrskih elektrarn opazili konec 80 let prejšnjega stoletja [21], [22]. Vroč medij se bo zaradi nižje gostote zbiral na vrhu posode ali cevovoda, hladen pa spodaj (Slika 9). Pojav je izrazitejši pri neizoliranih komponentah z majhnim pretokom ali celo brez pretoka, kjer so temperaturne razlike lahko tudi več 10 °C [23]. Pojav toplotnega razslojevanja lahko v ravnih delih cevovoda povzroči po prerezu spremenljive toplotne napetosti oz. deformacije. Meja med hladnim in vročim medijem se lahko spreminja.

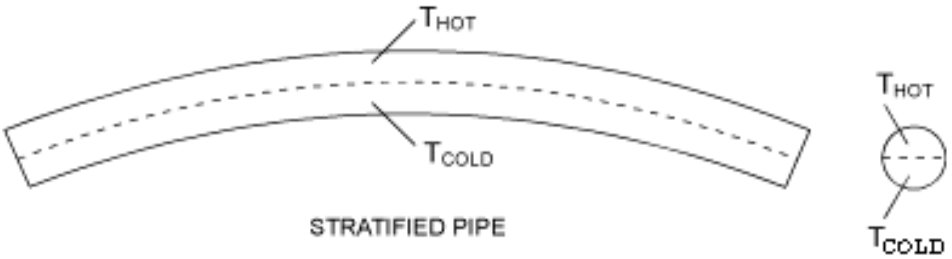

Upogibanje cevi zaradi toplotnega razslojevania

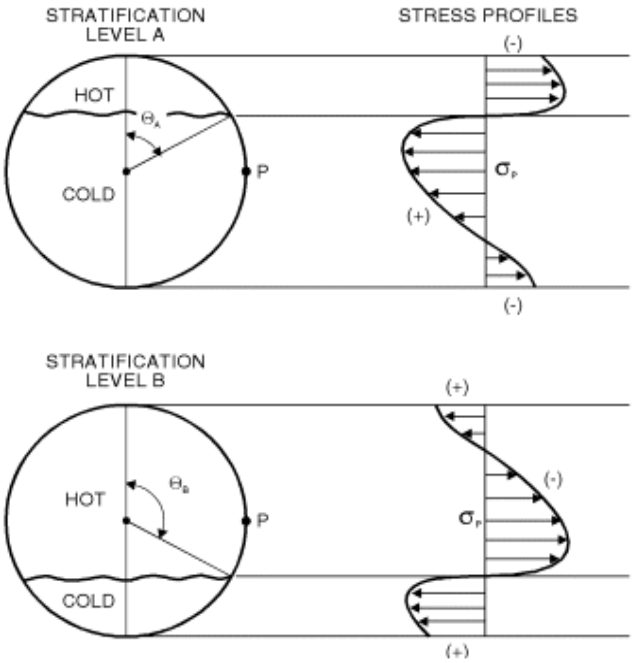

Napetosti po prerezu cevi zaradi toplotnega razslojevanja

Slika 9 Razslojeni tok v horizontalni cevi

3.2.3 Meritve temperatur na zunanji površini stene cevi

Da bi dobili čimbolj natančno informacijo o dogajanju v notranjosti cevovoda, je potrebno merilne elemente namestiti smiselno tako, da dobimo čim več informacij o dogajanju na zunanjem obodu cevi [3], [10]. Slika 10 prikazuje značilne razporeditve merilcev na zunanji površini cevi.

Toplotni šok lahko zaznamo že z dvema merilnima elementoma, ki sta nameščena na zgornji in spodnji površini cevovoda (Slika 10a, Slika 11a). Ta konfiguracija načeloma zadošča tudi za zaznavo toplotnega razslojevanja tekočine. Opredelitev meje med toplotno razslojenima tekočinama praviloma zahteva podrobnejše informacije. V primeru horizontalnega cevovoda ali cevovoda z majhnim nagibom navadno zadošča namestitev nekaj merilnih elementov po polovici oboda cevi (Slika 10b in Slika 11b).

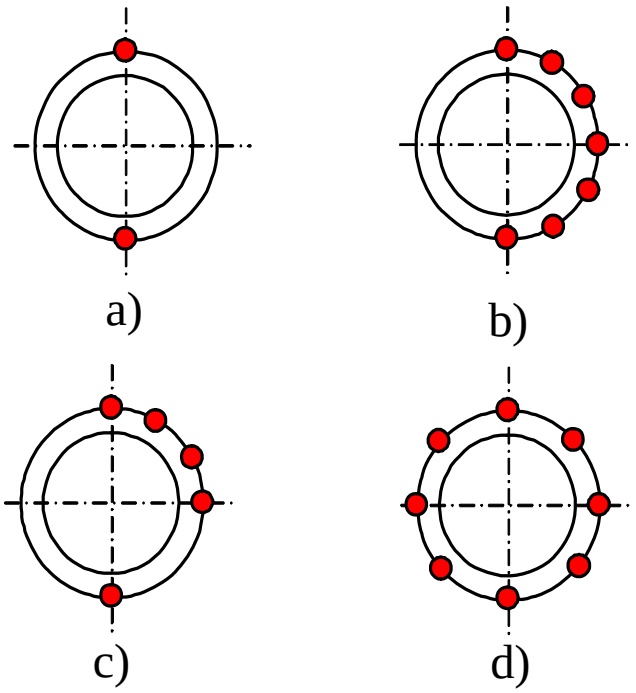

Slika 10 Značilne razporeditve merilnih elementov na zunanji površini cevi

Če želimo opredeliti razmere pri turbulentnem mešanju v bližini spojev dveh cevi ali tokovne razmere v navpični cevi, je smiselno merilne elementi namestiti po celem obodu (Slika 10d) [1]. V primerih določevanja temperature tekočine pred in za spojem vroče veje in prelivnega voda v praksi merijo temperaturo na zunanji strani cevovoda kot prikazuje Slika 10c [3].

Do velikih temperaturnih sprememb navadno prihaja v prelivnem vodu, kjer lahko prihaja tudi do toplotnega razslojevanja in toplotnih šokov [10]. Slika 12 prikazuje primer temperatur, izmerjenih na zunanji površini prelivnega voda.

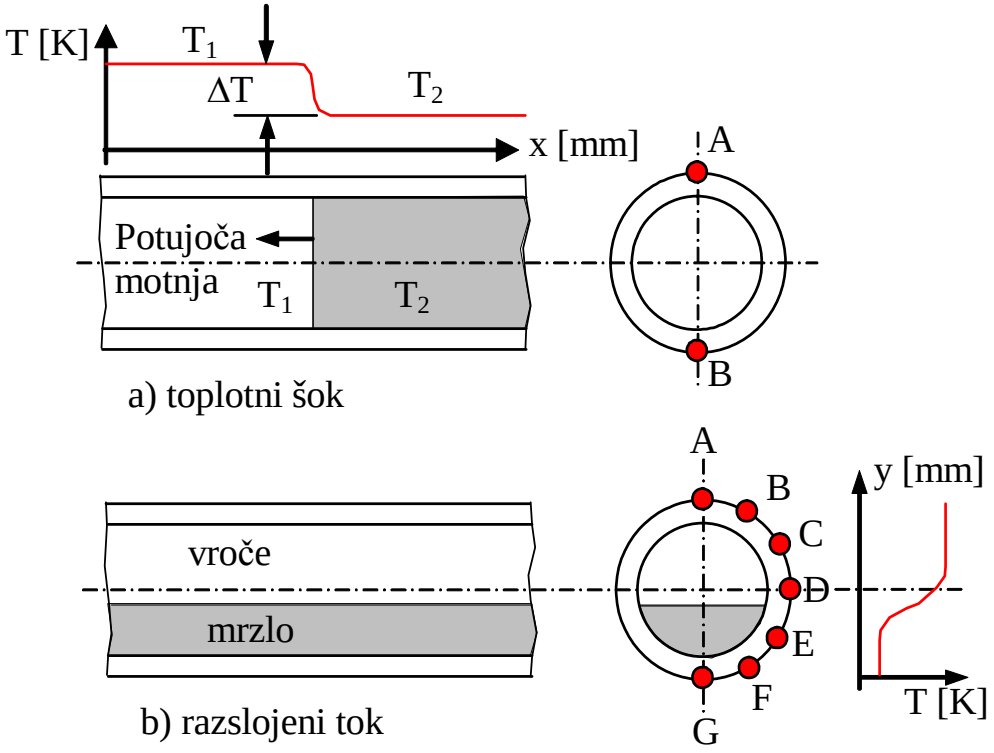

Slika 11 Razporeditev senzorjev pri cevovodu za nadzor toplotnega šoka in stratifikacije cevi [10]

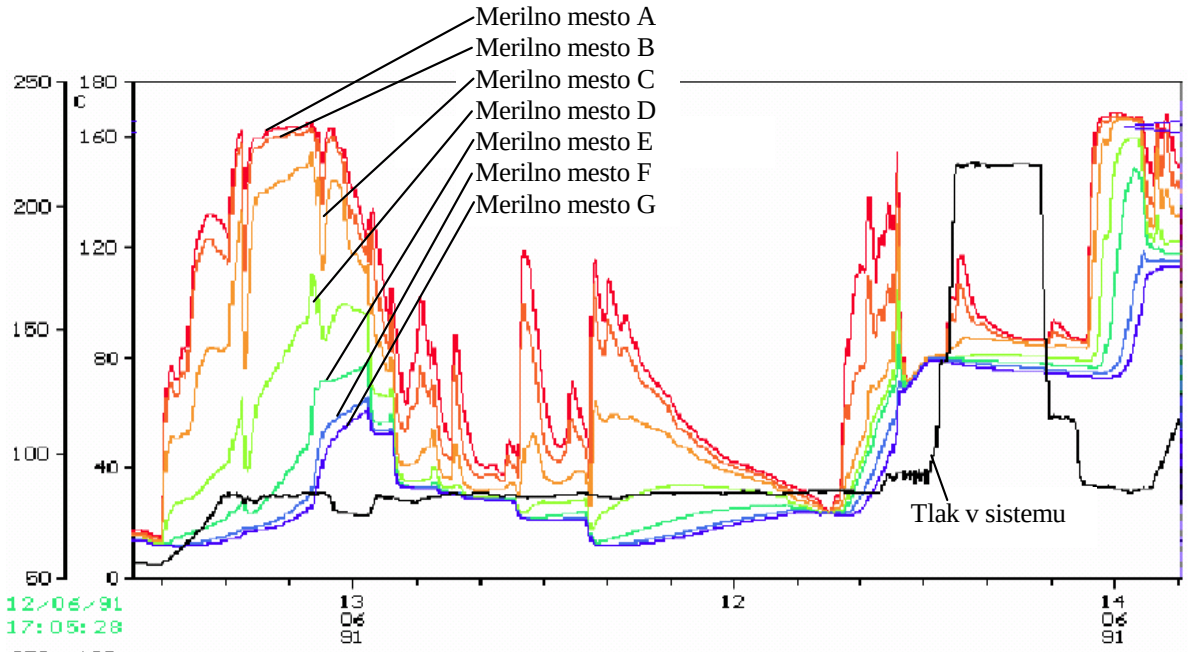

Slika 12 Primer izmerjenih temperature na zunanji površini prelivnega voda med zagonom elektrarne [10]

3.2.4 Osnovne omejitve meritev na zunanji steni cevi

Iz temperatur, izmerjenih na zunanji površini cevi (Slika 12), je mogoče sklepati tudi na temperature notranje površine cevi, ki jih potrebujemo pri analizah utrujanja [1]. Prevajanje toplote skozi steno cevi namreč povzroči zakasnitve in večinoma tudi zmanjšanje temperaturnih sprememb. Dogajanje v dolgi, na zunanji strani izolirani cevi s predpisano temperaturo na notranji površini lahko popišemo z analitičnimi rešitvami [1].

Predpostavimo, da spremembe temperature na notranji površini cevi sledijo stopničasti funkciji (Slika 13), kjer se temperatura hipoma spremeni od 0 na 1. Ker imamo opravka z linearnim sistemom, lahko rešitve pri drugačnih spremembah temperature enostavno dobimo kar s skaliranjem. Poleg tega stopničasta sprememba temperature povzroča največje temperaturne gradiente in je zato med vsemi mogočimi spremembami temperature tudi najbolj konzervativna.

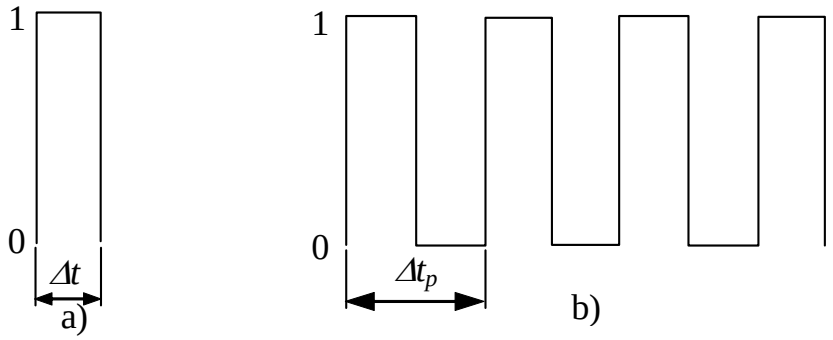

Slika 13 Stopničasta sprememba temperature iz 0 na 1 in nazaj na 0: a) enkratna in b) periodična

Spremembe temperature na zunanji steni cevovoda pri stopničasti spremembi temperature na notranji steni cevovoda so prikazane na primeru cevi iz primarnega kroga jedrske elektrarne. Debeline cevi v primarnem krogu jedrske elektrarne značilno v področju med 5 in 15% polmera cevi. Iz tega sledi področje razmerij med notranjim in zunanjim polmerom med a = 0.85 in a = 0.95. Rezultati (Slika 14) so v skladu s poglavjem 5.2.2. v [1] predstavljeni za tri značilna razmerja a: 0.85, 0.9 in 0.95. Snovne lastnosti, uporabljene v analizi, so značilne za nerjavna jekla, ki se uporabljajo v jedrski tehnologiji, in zajemajo toplotno prevodnost $\lambda = 20$ W / m K, gostoto ρ = 7880 kg / m^3, specifično toploto c_p = 502 J / kg K, modul elastičnosti E = 206.842 GPa, linearni toplotni razteznostni koeficient $\alpha = 1.87 \cdot 10^{-5}$ K^{-1}. Čas t_0 je izražen z R_2^2 / χ, kjer je toplotna difuzivnost $\chi = 5.056\ 10^{-6}$ m^2 / s.

Za prelivni vod tlačnika z zunanjim radijem R_2.= 0,1619 m torej velja t_0 = 5184 s. Pri slikah v nadaljevanju bi v primeru prelivnega voda tlačnika odčitali:

- Čas 0,005 [t_0] kot 25,9 s in
- Frekvenco 200 [1/t_0] kot 0,039 Hz.

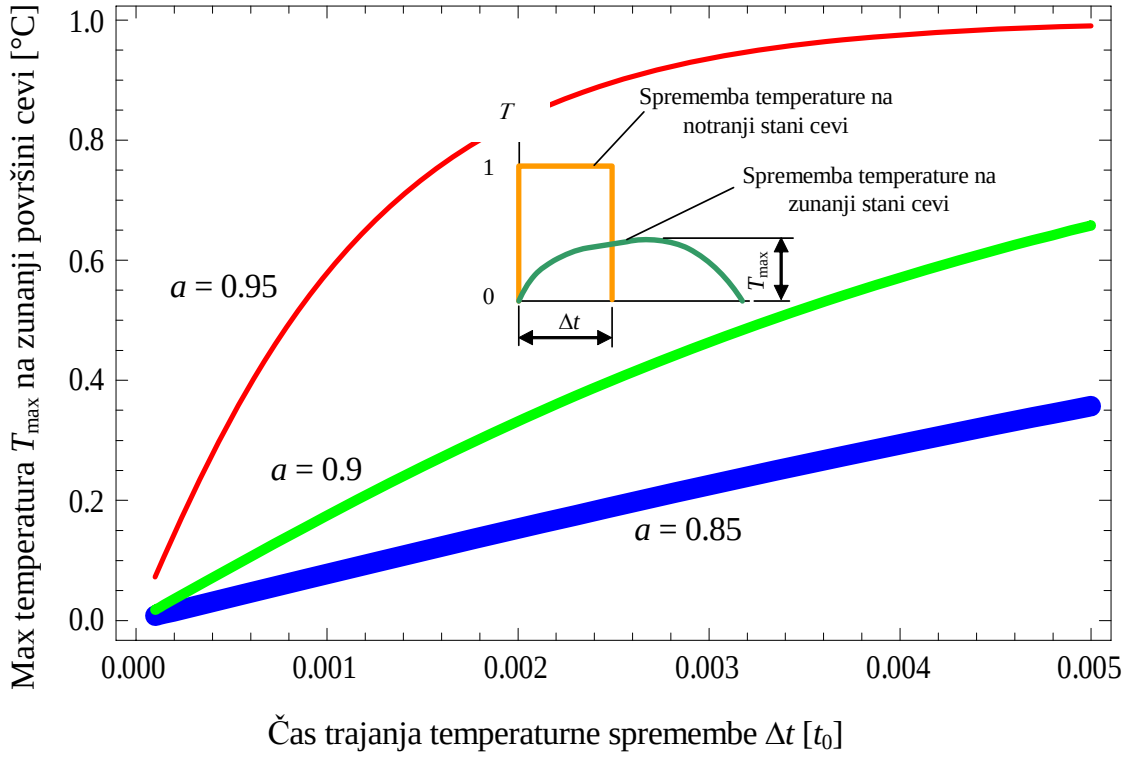

Slika 14 Maksimalna temperatura na zunanji površini kot funkcija debeline stene cevi *a* in normaliziranega časa trajanja Δ*t* temperaturne spremembe na notranji površini cevi

Temperaturne spremembe na notranji površini cevi, ki jih lahko zaznamo na zunanji površini cevi, so močno odvisne od amplitude temperature in trajanja temperaturne spremembe Δ*t*, debeline stene cevi in materiala (Slika 14). Rezultati so predstavljeni za enojno stopničasto spremembo temperature iz 0 na 1 za čas Δ*t* (Slika 13a).

Rezultati (Slika 14) so lahko zelo uporabni pri določevanju temperaturne spremembe skozi steno valja in določevanju najmanjše temperaturne spremembe na notranji površini, ki jo še lahko zaznamo z merilno napravo na zunanji površini.

Pri meritvah je dostikrat pomembno, da poznamo zakasnitev temperaturne motnje skozi steno cevi do merilne naprave. Za primer spremembe temperature na sliki 5a se največja temperatura pojavi na zunanji strani proti koncu prehodnega pojava na notranji površini (Slika 15).

Slika 16 prikazuje največjo temperaturo, ki jo lahko zaznamo na zunanji površini v primeru, da se temperatura na notranji strani spreminja periodično (Slika 13b) z velikostjo amplitude 1 in s frekvenco $1/t_0$ [1]. Pri nizkih frekvencah se amplituda temperature na zunanji strani cevi približuje amplitudi na notranji strani cevi. Povečevanje frekvence na notranji strani in debeline stene cevi znižujeta amplitudo, ki jo zaznamo na zunanji površini.

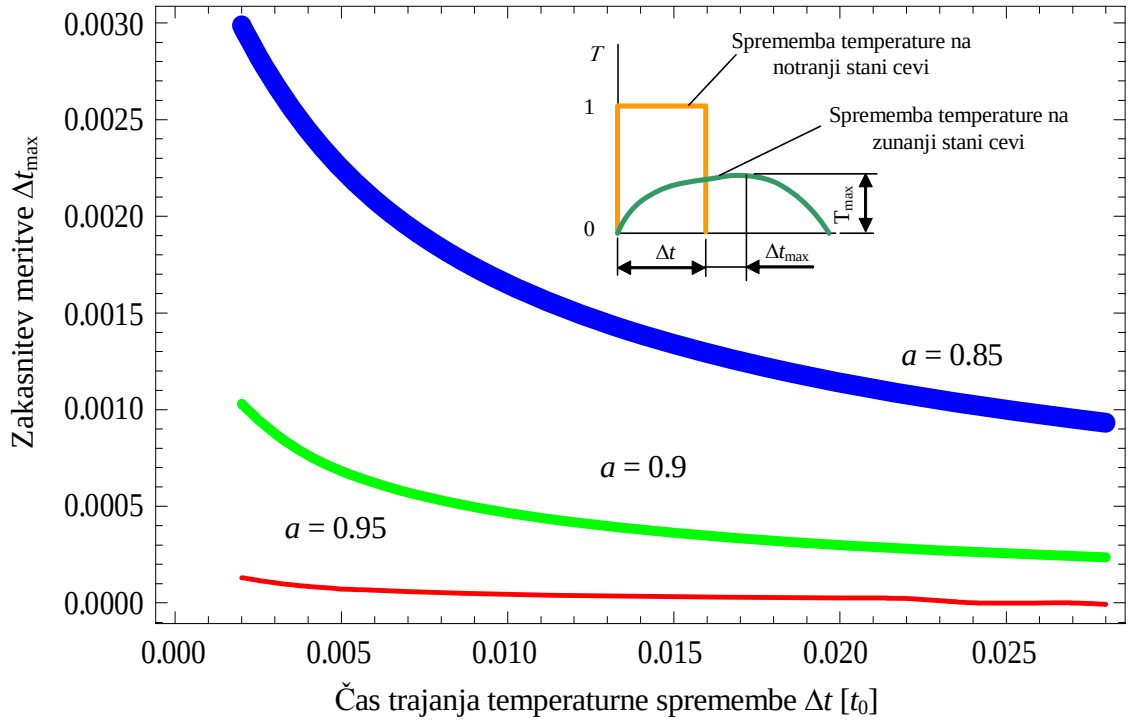

Slika 15 Zakasnitev Δt_{max} med koncem temperaturne spremembe in pojavom maksimalne temperature T_{max} na zunanji površini

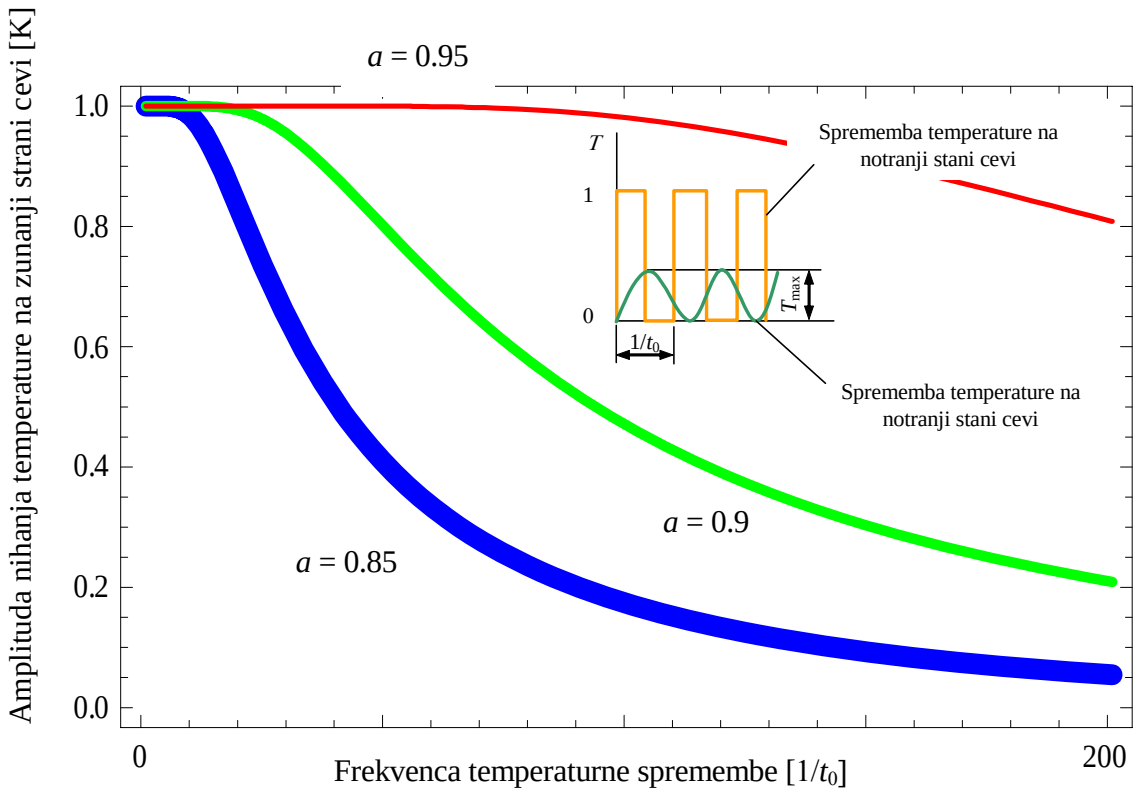

Slika 16 Amplituda temperaturne spremembe na zunanji strani cevi glede na različne debeline cevi a in frekvenco spremembe temperature na notranji strani

3.2.5 Vpliv prestopa toplote iz tekočine na cev

V dosedanji razpravi smo predpostavili, da sta temperatura tekočine in notranje stene cevi enaki. S tem predpostavimo neskončni koeficient prestopa toplote, kar zagotavlja nahjvečje temperaturne gradiente in s tem tudi največje napetosti v cevi in je razumno pri visokih hitrostih tokov, npr. v vroči in hladni veji. Značilne vrednosti koeficienta prestopa toplote tam znašajo tudi več 10 kW/m^2K [24]. Za razslojene tokove pa so značilni laminarni tokovi z nizkimi hitrostmi in več velikostnih razredov nižji koeficienti prestopa toplote v višini nekaj 10 W/m^2K [20].

3.3 Rekonstrukcija manjkajočih podatkov

Določevanje temperaturnih porazdelitev v notranjosti cevovoda je tudi z razmeroma kompleksnimi merskimi rezultati lahko dokaj zapleten proces. Velikokrat lahko za določevanje porazdelitve temperature po obodu in vzdolž notranje površine cevovoda uporabimo numerična orodja, še posebej orodja za modeliranje dinamike tekočin (npr. programski paket CFX). S temi orodji lahko izračunamo porazdelitev temperature v cevovodih (npr. prelivni vod) za primere laminarnih in turbulentnih tokov [5]. Prav tako lahko z orodji za modeliranje dinamike tekočin modeliramo turbulentno penetracijo [8].

Problem pri takšnih modelih je predpisovanje ustreznih robnih in začetnih pogojev (npr. tlak, temperatura in hitrost tekočine). Včasih lahko manjkajoče podatke pomagamo rekonstruirati tudi parametričnimi študijami [5]. Meritve temperatur na zunanji površini cevovoda so pri tem lahko v veliko pomoč.

Ko so znane temperaturne porazdelitve na notranji strani, lahko v skladu z veljavnimi standardi (npr. ASME [12]) razmeroma enostavno opredelimo pripadajoče amplitude napetosti in faktorje utrujenostne izrabe [1].

Prehodni pojav	Zabeleženi v prvi polovici trajnostne dobe	Predvideni v celotni trajnostni dobi
NORMALNO OBRATOVANJE		
Ogrevanje	56	200
Ohlajanje	56	200
MOTENO OBRATOVANJE		
Izpad električnega bremena brez takojšnje zaustavitve reaktorja	5	40
Izpad zunanjega napajanja	3	40
Delna izguba pretoka reaktorskega hladila	2	80
Ustavitev reaktorja s polne moči		
brez ohlajanja	73	230
z ohlajanjem, brez varnostnega vbrizgavanja	62	160
z ohlajanjem, z varnostnega vbrizgavanjem	2	10
Nenamerno zmanjšanje tlaka reaktorskega hladila	3	20
Padec regulacijske palice	2	80
PREIZKUSI		
Tlačni preizkus primarnega sistema	1	20
Tlačni preizkus sekundarnega sistema	1	10
Preizkus netesnosti primarnega sistema	1	10
Preizkus netesnosti primarnega sistema	< 56	200

Tabela 2 Prehodni pojavi, ki so se zgodili v NEK

3.4 Prehodni pojavi, ki so se zgodili v NEK

Prehodne pojave, ki so se zgodili v primarnem krogu jedrske elektrarne Krško v prvi polovici njene projektno predvidene trajnostne dobe 40 let, smo povzeli po [25] (Tabela 2).

Iz primerjave med dejanskimi in projektnimi prehodnimi pojavi (Tabela 2) je razvidno, da je število prehodnih pojavov, ki so se zgodili majhno. Iz te primerjave je mogoče sklepati, da je v izrabi komponente še velika rezerva. Za bolj natančen odgovor o izrabi komponent pa je potrebno najprej določiti dejanske obremenitve in nato izračunati faktor izrabe [1].

4 ZAKLJUČKI

Projektna trajnostna doba jedrskih elektrarn temelji na zbirki predpostavljenih projektnih dogodkov. Vsak izmed projektnih dogodkov v sistemih in komponentah elektrarne povzroči prehodne pojave s spremembami temperatur, tlakov in včasih tudi drugih obratovalnih parametrov. Prehodni pojavi torej povzročajo tudi spremembe napetosti v cevovodih in tlačnih posodah in s tem potencialno prispevajo k njihovemu utrujanju.

Za natančno določevanje faktorjev izrabe posameznih komponent je torej ključno natančno poznavanje prehodnih pojavov. Pri tem imamo v mislih tako predpostavljene projektne prehodne pojave kot tudi izmerjene dejanske prehodne pojave.

V poročilu smo zbrali najpomembnejše vire informacij o projektnih in dejanskih prehodnih pojavih reaktorskega hladilnega sistema jedrske elektrarne v Krškem. Mednje sodijo projekt elektrarne z vsemi spremembami, procesni informacijski sistem elektrarne in lokalne meritve temperatur na zunanji površini nekaterih cevovodov. Opravili smo preliminarno analizo celovitosti in uporabnosti dostopnih podatkov o prehodnih pojavih za analize utrujanja komponent ter preliminarno primerjavo med izbranimi izmerjenimi in projektnimi prehodnimi pojavi. Izbrani izmerjeni prehodni pojavi so bili s stališča utrujanja ugodnejši od projektnih.

Opredelimo najpogostejše težave pri interpretaciji podatkov, še posebej v primerih, ko o temperaturah hladila sklepamo na podlagi meritev na zunanji površini cevi. Nakazujemo tudi nekatere prijeme, s katerimi bi bilo mogoče manjkajoče podatke rekonstruirati.

5 VIRI

[1] Zafošnik, B., Cizelj, L.: Zasnova metode za spremljanje izrabe komponent jedrskih elektrarn, IJS delovno poročilo, IJS-DP-10078, 2009.

[2] Zafošnik, B., Cizelj, L.: Pilotni primeri za izračun faktorja utujenostne izrabe, IJS delovno poročilo, IJS-DP-10076, 2009.

[3] Bartonicek, J., Schoeckle, F.: Monitoring of unspecified loads as a tool for ageing management, ASME PVP Conference, Seattle, 2000.

[4] Pöckl, C., Kleinoeder, W.: Developing and Implementation of a Fatigue Monitoring System for the new European Pressurized Water Reactor EPR, International Conference Nuclear energy for New Europe 2008, Portorož, 10. - 13. september 2007.

[5] Boros, I., Aszódi, A.: Analysis of thermal stratification in the primary circuit of a VVER-440 reactor with the CFX code, *Nucl. Eng. Des.*, 238, 2008, str. 453-459.

[6] Bieniussa, K. W., Reck, H.: Piping specific analysis of stresses due to thermal stratification, *Nucl. Eng. Des.*, 190, 1999, str. 239-249.

[7] Ensel, C., Colas, A., Barthez, M.: Stress analysis of a 900 MW pressurizer surge line including stratification effects, *Nucl. Eng. Des.*, 153, 1995, str. 197-203.

[8] Frank, T., Adlakha M., Adlakha, C., Lifante, H.-M., Prasser, F. Menter: Simulation of Turbulent and Thermal Mixing in T-Junctions Using URANS and Scale-Resolving Turbulenc Models in ANSYS CFX, XCFD4NRS - Experiments and CFD Codes Application to Nuclear Reactor Safety, OECD/NEA & International Atomic Agency (IAEA) Workshop, 10.-12. September 2008, Grenoble, France, str. 23.

[9] Assessment and management of ageing of major nuclear power plant components important to safety, Primary piping in PWRs, IAEA-TECDOC-1361,http://www-pub.iaea.org/MTCD/publications/PDF/te_1361_web.pdf, prenešeno 12. 12. 2008.

[10] Kleinöder, W., Golembiewski, H.-J.: Monitoring for fatigue – examples for unexpected component loading, SMiRT 16, Washington DC, August 2001.

[11] Zafošnik, B., Cizelj, L.: Safe Fatigue Life of Nuclear Piping exposed to Temperature and Pressure Fluctuations, International Conference Nuclear energy for New Europe 2008, Portorož, 8. - 11. september 2008.

[12] ASME Boiler and Pressure Vessel Code, 1986.

[13] NEK, Updated Safety Analysis Report, Rev. 14.

[14] Westinghouse, Krško 18% Steam Generator Tube Plugging Margin Analysis, , WENX 89/06 (1989).

[15] Westinghouse, Design Transients Specification, SSR-NEK-5.1, Revison 3, November 1999, Final

[16] Westinghouse, Balance of Design Transients Specification, SSR-NEK-5.2, Revison 1, November 1999, Final

[17] Westinghouse, Hydraulic Forcing Functions, SSR-NEK-5.3, Revison 2, July 1999, Final

[18] Westinghouse, Mechanical Review, SSR-NEK-12, Rev. 1. Feb. 2000, Final.

[19] Nuklearna elektrarna Krško Thermal Stratification Monitoring, 382-RC-L-ESD-TR-04/06, 2006.

[20] Krautov strojniški priročnik, Tehniška založba Slovenije, 1998.

[21] US NRC Bulletin No. 88-11: Pressurizer Surge Line Thermal Stratification, Dec. 20, 1988.

[22] US NRC Information Notice No. 88-80: Unexpected Piping Movement Attributed To Thermal Stratification, Oct. 7, 1988.

[23] Kleinöder, W., Golembiewski, H.-J.: Monitoring for fatigue – examples for unexpected component loading, SMiRT 16, Washington DC, August 2001.

[24] KWU NDM5/98/E1214, Stress and Fatigue Analysis for the Primary Nozzles of the Replacement Steam Generators, Rev. A, 1998.

[25] Review and Categorization of NPP Krško Transients of Operational Cycles, ESD-TR-08/02, Revison 2, Nuklearna elektrarna Krško, 2008

IJS Delovno Poročilo
IJS Report
IJS-DP-10076

Izdaja 1, marec 2009
Revision 1, March 2009

Pilotni primeri izračuna faktorja utrujenostne izrabe

Pilot cases for the calculation of fatigue usage factor

B. Zafošnik, L. Cizelj

Ljubljana, marec 2009

Institut »Jožef Stefan«, Ljubljana, Slovenija

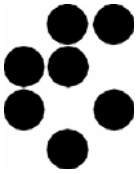

Institut »Jožef Stefan«, Ljubljana, Slovenija

Naročnik: Ordered by:	Javna agencija za raziskovalno dejavnost Republike Slovenije Tivolska c. 30, Ljubljana Nuklearna elektrarna Krško d.o.o., Vrbina 12, 8270 Krško
Izvajalec: Prepared by:	Institut »Jožef Stefan« 1000 Ljubljana Jamova 39 Slovenija Odsek za reaktorsko tehniko (Reactor Engineering Division)
Pogodba štev.: Contract Number:	Z2-9488-0106-06 (IJS in ARRS) U1-BL-R4-3/03 (IJS in NEK)
Nosilec naloge: Responsible Person:	dr. Boštjan Zafošnik, univ. dipl. inž. str.
Naslov poročila: Report Title:	Pilotni primeri izračuna faktorja utrujenostne izrabe Pilot cases for the calculation of fatigue usage factor
Avtorji poročila: Authors:	Dr. Boštjan Zafošnik, univ.dipl.inž.str. Prof. dr. Leon Cizelj, univ.dipl.inž.str.
Štev. delovnega poročila: Report Number:	IJS-DP-10076 Izdaja 1
Konto: Account Number:	V2-0375-C
Kopije: Distribution:	➢ Naročnik (3) ➢ Knjižnica/Library (1x) ➢ Nosilec naloge/Responsible Person (1x) ➢ Avtorji/Authors (1x) ➢ Arhiv OR4/Archive (1x + original)

Ljubljana, marec 2009

POVZETEK

V poročilu demonstriramo uporabo metode za izračun faktorja izrabe v izbranih komponentah na dveh pilotnih primerih: izstopni šobi reaktorske tlačne posode (proti vroči veji) in prelivnem vodu tlačnika. Izbor pilotnih primerov zagotavlja tudi širok spekter obremenitvenih primerov.

Z modelom izstopne šobe reaktorske tlačne posode smo ocenili faktor izrabe za projektne in dejanske prehodne pojave v jedrski elektrarni Krško: ogrevanje in ohlajanje elektrarne ter ustavitev reaktorja s polne moči brez ohlajanja. Primerjava izračunanih faktorjev izrabe je pokazala, da je dejanska izraba obravnavanih komponent za obravnavane prehodne pojave manjša od predvidene v projektu.

Pokazali smo tudi mogoče vplive toplotnega razslojevanja in termičnega šoka na utrujenostno izrabo prelivnega voda tlačnika. Pri tem smo posebno pozornost posvetili temperaturam, ki bi jih v obravnavanih hipotetičnih prehodnih pojavih prikazovali merilci temperatur na zunanjem obodu prelivnega voda.

Poročilo predstavlja del rezultatov projekta »**Zasnova metode za spremljanje izrabe komponent jedrskih elektrarn**«, ki sta ga sofinancirala Javna agencija za raziskovalno dejavnost Republike Slovenije (pogodba št. 1000-07-219488) in Nuklearna elektrarna Krško d.o.o. (pogodba št. POG-3408).

ABSTRACT

The implementation of the method for monitoring the usage of nuclear power plant is demonstrated with two pilot cases: the reactor pressure vessel outlet nozzle and pressurizer surge line. The selection of pilot cases facilitates wide spectra of applied loads.

The model of the reactor pressure vessel outlet nozzle was used to estimate the partial fatigue usage factors during the design and actual transients in Krško nuclear power plant: heatup and cooldown and reactor trip from full power without cooldown. Comparison of calculated partial fatigue usage factors confirms the conservativity of plant design.

Possible consequences of stratified flows and thermal shocks on the fatigue usage of the pressurizer surge line were also demonstrated. Special attention has been devoted to the simulated output of potential termocouples placed at the outer surface of the surge line.

This report contains a part of the results of the project » **Conception of a method for monitoring of the usage of nuclear power plant components** «, cosponsored by the Slovene Research Agency (grant No. 1000-07-219488) and Nuklearna elektrarna Krško d.o.o. (grant No. POG-3408).

KAZALO

POVZETEK II

ABSTRACT III

KAZALO IV

SEZNAM SLIK VI

SEZNAM TABEL VIII

1 UVOD 1

1.1 Namen poročila 1

1.2 Ozadje 1

1.3 Organizacija poročila 1

2 MODELIRANJE TEMPERATURNIH IN NAPETOSTNIH SPREMEMB 2

2.1 Numerično modeliranje temperaturnega polja 2
2.1.1 Vpliv števila končnih elementov po debelini cevi 2
2.1.2 Vpliv koeficienta prestopa toplote s hladila na cev 3

2.2 Numerično modeliranje napetostnega polja 5
2.2.1 Linearizacija napetosti 6

3 IZSTOPNA ŠOBE REAKTORSKE TLAČNE POSODE 8

3.1 Geometrija modela 8
3.1.1 Poenostavitve 8

3.2 Snovne lastnosti 8

3.3 Obremenitve 10
3.3.1 Temperaturne obremenitve 10
3.3.2 Tlačne obremenitve 11

3.4 Robni pogoji 12

3.5 Rezultati 13
3.5.1 Ogrevanje in ohlajanje reaktorja 14
3.5.2 Ustavitev reaktorja s polne moči brez ohlajanja 15

4 MODEL PRELIVNEGA VODA TLAČNIKA 18

4.1 Geometrija modela 18
4.1.1 Poenostavitve 18

4.2 Snovne lastnosti 20

4.3 Obremenitve 20
4.3.1 Toplotno razslojeni tok 20
4.3.2 Toplotni šok 20

4.4 Robni pogoji in predpostavke 21
4.4.1 Toplotna analiza 21
4.4.2 Napetostna analiza 22

4.5 Rezultati 22
4.5.1 Toplotno razslojeni tok 22
4.5.2 Toplotni šok 35

5 ZAKLJUČKI 42

6 VIRI 43

SEZNAM SLIK

Slika 1 Primerjava analitične in numerične porazdelitev temperature po debelini stene cevi pri stopničasti spremembi temperature na notranji površini cevi za 20 °C in 8.1 s (trije končni elementi) 2
Slika 2 Primerjava analitične in numerične porazdelitev temperature po debelini stene cevi pri stopničasti spremembi temperature na notranji površini cevi za 20 °C in 12 s (dva končna elementa) 3
Slika 3 Porazdelitev stacionarnih temperatur po preseku cevi glede na višino meje med vročim in hladnim slojem hladila pri h = 50 W/m^{2}K 4
Slika 4 Primer poti za linearizacijo napetosti 7
Slika 5 Prostorski model izstopne šobe z delom reaktorske posode in vroče veje 9
Slika 6 Kinematični robni pogoji v modelu izstopne šobe 13
Slika 7 Največja Trescova ekvivalnentna napetost med projektnim prehodnim pojavom ogrevanja in ohlajanja reaktorja 14
Slika 8 Močno pretirana deformacija izstopne šobe zaradi obremenitve z notranjim tlakom in pripadajoča Trescova ekvivalentna napetost 15
Slika 9 Največja Trescova ekvivalentna napetost med izmerjenim ogrevanjem in ohlajanjem 16
Slika 10 Največja Trescova ekvivalnentna napetost med projektnim prehodnim pojavom ustavitve reaktorja s polne moči brez ohlajanja 17
Slika 11 Največja Trescova ekvivalnentna napetost med izmerjenim prehodnim pojavom ustavitve reaktorja s polne moči brez ohlajevanja 17
Slika 12 Prostorski model prelivnega voda tlačnika 19
Slika 13 Predpostavljena merilna mesta M1 do M4 na prelivnem vodu tlačnika 19
Slika 14 Kinematični robni pogoji modela prelivnega voda tlačnika 21
Slika 15 Porazdelitev temperature pri spremembi lege gladine iz spodnje do zgornje in nazaj do spodnje z vmesnim stacionarnim stanjem v zgornji legi 23
Slika 16 Porazdelitev temperature v notranji (M4-A-N) in zunanji (M4-A-Z) točki pri spremembi lege gladine z vmesnim stacionarnim stanjem 24
Slika 17 Porazdelitev temperature v notranjih in zunanjih točkah na merilnem mestu M1 v času do 1000 s 24
Slika 18 Porazdelitev temperature v notranjih in zunanjih točkah na merilnem mestu M2 v času do 1000 s 25
Slika 19 Porazdelitev temperature v notranjih in zunanjih točkah na merilnem mestu M3 v času do 1000 s 25
Slika 20 Porazdelitev temperature v notranjih in zunanjih točkah na merilnem mestu M4 v času trajanja cikla do 1000 s 27
Slika 21 Porazdelitev temperature v notranjih in zunanjih točkah na merilnem mestu M1 v času trajanja cikla med 40000 s in 60000 s 27
Slika 22 Porazdelitev temperature v notranjih in zunanjih točkah na merilnem mestu M2 v času trajanja cikla med 40000 s in 60000 s 28
Slika 23 Porazdelitev temperature v notranjih in zunanjih točkah na merilnem mestu M3 v času trajanja cikla med 40000 s in 60000 s 28
Slika 24 Porazdelitev temperature v notranjih in zunanjih točkah na merilnem mestu M4 v času trajanja cikla med 40000 s in 60000 s 29
Slika 25 Največja Trescova ekvivalentna napetost pri enem ciklu z vmesnih stacionarnim stanjem 29
Slika 26 Vpliv tlaka 2,5 MPa na Tresca ekvivalentno napetost v prelivnem vodu 30
Slika 27 Porazdelitev temperature pri spremembi lege gladine iz spodnje do zgornje in nazaj do spodnje brez vmesnega stacionarnega stanja v zgornji legi 31
Slika 28 Porazdelitev temperature v notranji (M4-A-N) in zunanji (M4-A-Z) točki pri spremembi lege gladine (en cikel) brez vmesnega stacionarnega stanja 32
Slika 29 Porazdelitev temperature v notranjih in zunanjih točkah na merilnem mestu M1 v času trajanja cikla do 1000 s 32
Slika 30 Porazdelitev temperature v notranjih in zunanjih točkah na merilnem mestu M2 v času trajanja cikla do 1000 s 33
Slika 31 Porazdelitev temperature v notranjih in zunanjih točkah na merilnem mestu M3 v času trajanja cikla do 1000 s 34
Slika 32 Porazdelitev temperature v notranjih in zunanjih točkah na merilnem mestu M4 v času trajanja cikla do 1000 s 34

Slika 33 Največja Trescova ekvivalentna napetost pri enem ciklu brez vmesnega stacionarnega stanja 35
Slika 34 Porazdelitev temperature pri spremembi lege gladine v vzdolžni smeri cevovoda z vmesnim stacionarnim stanjem v skrajni vzdolžni legi 36
Slika 35 Porazdelitev temperature v notranji (M2-A-N) in zunanji (M2-A-Z) točki pri potovanju motnje preko tega merilnega mesta z vmesnim stacionarnim stanjem (en cikel) 37
Slika 36 Porazdelitev temperature v notranji (M2-A-N) in zunanji (M2-A-Z) točki pri potovanju motnje preko tega merilnega mesta za čas do 40 s 37
Slika 37 Porazdelitev temperature v notranji (M2-A-N) in zunanji (M2-A-Z) točki pri potovanju motnje preko tega merilnega mesta za čas od 4000 do 7000 s 38
Slika 38 Največja Trescova ekvivalentna napetost pri ciklu z vmesnim stacionarnim stanjem 39
Slika 40 Porazdelitev temperature v notranji in zunanji točki na merilnem mestu M2 pri ciklu spremembe lege gladine hladila brez vmesnega stacionarnega stanja 39
Slika 39 Porazdelitev temperature pri spremembi lege gladine v vzdolžni smeri cevovoda brez vmesnega stacionarnega stanja v skrajni vzdolžni legi 40
Slika 41 Največja Tresca ekvivalentna napetost pri enem ciklu brez vmesnega stacionarnega stanja 41

SEZNAM TABEL

Tabela 1 Največja (T_{max}) in najmanjša (T_{min}) temperatura v steni cevi v odvisnosti od koeficienta prestopa toplote in meje med vročim in hladnim slojem (Slika 3) 5
Tabela 2 Primerjava analitičnih in numeričnih ocen Trescove ekvivalentne napetosti pri stopničasti hipni spremembi temperature s časom trajanja 8.1s 5
Tabela 3 Vpliv števila elementov na radialno (σ_r), obročno (σ_ϕ) in vzdolžno (σ_z) komponento napetosti pri stopničasti spremembi temperature dolžine 8.1s (analitično: σ_r = 0 MPa, σ_ϕ = 73.85 MPa in σ_z = 22.16 MPa) 6
Tabela 4 Vpliv števila elementov na radialno (σ_r), obročno (σ_ϕ) in vzdolžno (σ_z) komponento napetosti pri stopničasti spremembi temperature dolžine 60s (analitično: σ_r = 0 MPa, σ_ϕ = 44.55 MPa in σ_z = 13.37 MPa) 6
Tabela 5 Primerjava lineariziranih in neposredno odčitanih Trescovih ekvivalentnih napetosti 6
Tabela 6 Pregled materialov v modelu izstopne šobe 9
Tabela 7 Temperaturni cikel ogrevanja in ohlajanja reaktorja za projektni prehodni pojav 11
Tabela 8 Temperaturni cikel ogrevanja in ohlajanja reaktorja za dejanski prehodni pojav 11
Tabela 9 Temperaturni cikel ustavitve reaktorja s polne moči brez ohlajanja za projektni prehodni pojav 12
Tabela 10 Temperaturni cikel ustavitve reaktorja s polne moči brez ohlajanja za dejanski prehodni pojav 12
Tabela 11 Tlačni cikel ogrevanja in ohlajanja reaktorja za projektni prehodni pojav 12
Tabela 12 Tlačni cikel ogrevanja in ohlajanja reaktorja za dejanski prehodni pojav 13

1 UVOD

1.1 Namen poročila

V poročilu predstavljamo del rezultatov projekta »**Zasnova metode za spremljanje izrabe komponent jedrskih elektrarn**«, ki sta ga sofinancirala Javna agencija za raziskovalno dejavnost Republike Slovenije (pogodba št. 1000-07-219488) in Nuklearna elektrarna Krško d.o.o. (pogodba št. POG-3408).

Preostali rezultati projekta so predstavljeni v spremljajočih poročilih:

- Zasnova metode za spremljanje izrabe komponent jedrskih elektrarn [1] in
- Baza prehodnih pojavov v Nuklearni elektrarni Krško [2].

1.2 Ozadje

Za podaljševanje obratovalne dobe jedrskih elektrarn je zelo pomembno čimbolj natančno določevanje faktorja izrabe komponent. V ta namen smo zasnovali metodo za spremljanje izrabe komponent jedrskih elektrarn [1] in bazo dejanskih prehodnih pojavov [2]. Uporabo metode za izračun faktorja izrabe v izbranih komponentah v poročilu demonstriramo na dveh pilotnih primerih: izstopni šobi reaktorske tlačne posode (proti vroči veji) in prelivnem vodu tlačnika.

Reaktorska tlačna posoda, vroča veja in prelivni vod tlačnika so del tlačne meje reaktorskega hladila v tlačnovodni jedrski elektrarni (varnostni razred 1). Skrbi za dobro projektiranje tlačne meje reaktorskega hladila med obratovanjem elektrarne sledi skrb za njeno varnost in strukturno celovitost. Izbor pilotnih primerov zagotavlja tudi širok spekter obremenitvenih primerov: za prelivni vod tlačnika je znano, da je lahko obremenjen tudi s toplotnim razslojevanje in toplotnimi šoki [3], [4], [5], [6].

1.3 Organizacija poročila

V poglavju 2 je opisano modeliranje temperaturnega in napetostnega polja z metodo končnih elementov, s poudarkom na diskretizaciji modela po debelini stene cevi. V poglavju 3 je predstavljen model spoja izstopne šobe reaktorske tlačne posode ter izračun faktorja izrabe za dejanske prehodne pojave, dobljene iz NEK. V poglavju 4 je na modelu prelivnega voda tlačnika prikazan potencialni vpliv toplotnega razslojevanja in toplotnega šoka na spremembe temperature na hipotetičnih merilnih mestih na zunanjem obodu cevovoda in na delni faktor izrabe. Poročilo se konča z zaključki v poglavju 5 in napisanimi viri v poglavju 6.

2 MODELIRANJE TEMPERATURNIH IN NAPETOSTNIH SPREMEMB

V tem poglavju opišemo najpomembnejše vplive, ki jih je potrebno upoštevati pri modeliranju temperaturnih in napetostnih polj zaradi sprememb temperature in tlaka na notranji strani votle valjaste geometrije.

Vse numerične rešitve, opisane v tem poročilu, so dobljene z metodo končnih elementov in računalniškim programom ABAQUS [7].

2.1 Numerično modeliranje temperaturnega polja

2.1.1 Vpliv števila končnih elementov po debelini cevi

Natančnost numerične ocene nestacionarne porazdelitve temperatur skozi steno cevi je odvisna predvsem od števila končnih elementov po debelini stene. Numerično natančnost najlaže ocenimo tako, da numerične rezultate primerjamo z analitičnimi rešitvami [1].

Kot primer si oglejmo cev z značilnostmi prelivnega voda (notranji polmer R_1 = 128,6 mm, zunanji polmer R_2 = 161,9 mm). Potrebujemo še snovne lastnosti, značeilne za austenitno nerjavno jeklo: toplotna prevodnost materiala λ = 20 W/mK, gostota ρ = 7850 kg/m^3 in specifična toplota c_p = 502 J/kg K.

Na notranji površini stene cevi smo predpostavili hipno stopničasto spremembo temperature za 20°C, ki traja 8.1 sek. Nato opazujemo temperaturno porazdelitev skozi steno cevi (Slika 1). Izkaže se, da trije parabolični končni elementi vzdolž debeline cevi zadoščajo za najmanj 5% natančnost numerične rešitve.

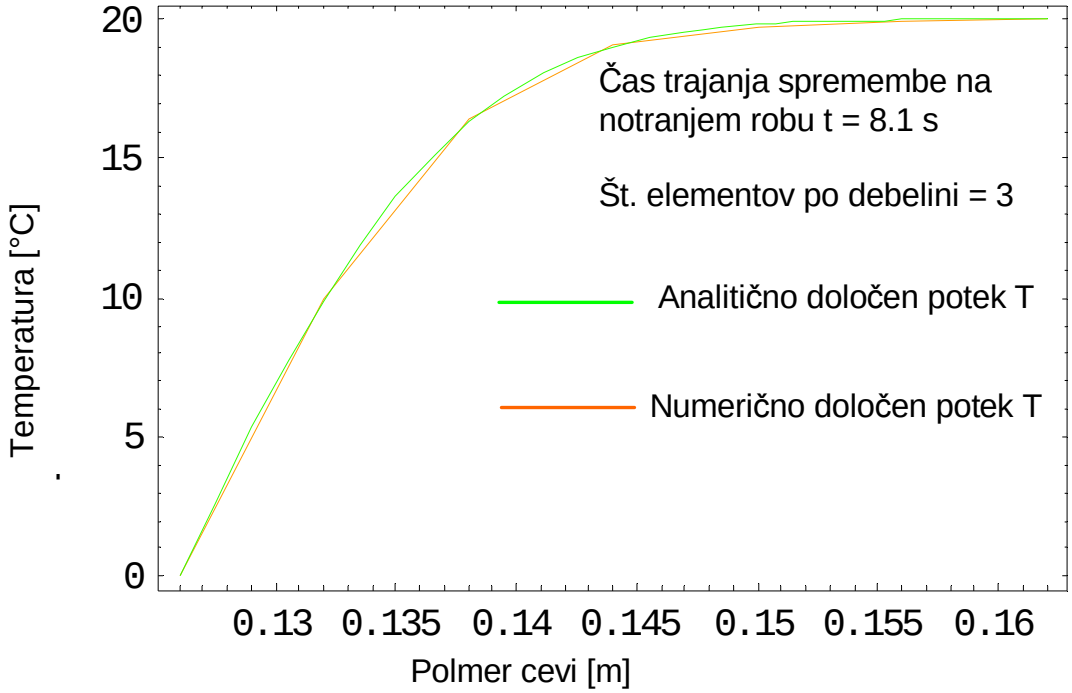

Slika 1 Primerjava analitične in numerične porazdelitev temperature po debelini stene cevi pri stopničasti spremembi temperature na notranji površini cevi za 20 °C in 8.1 s (trije končni elementi)

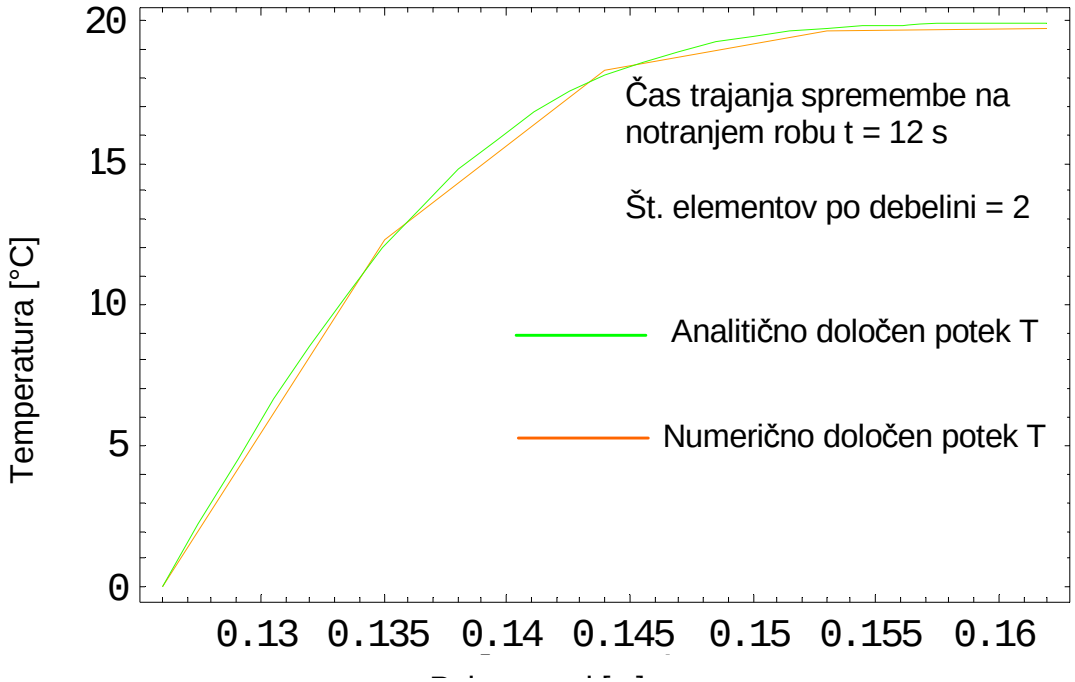

Slika 2 Primerjava analitične in numerične porazdelitve temperature po debelini stene cevi pri stopničasti spremembi temperature na notranji površini cevi za 20 °C in 12 s (dva končna elementa)

Slika 2 prikazuje primerjavo med numerično in analitično porazdelitvijo temperature vzdolž debeline stene cevi pri motnji, ki traja 12 s in z uporabo dveh paraboličnih končnih elementov po debelini valjaste cevi. Tudi tokrat je razlika med numerično in analitično oceno največ 5%. Zaključimo lahko, da lahko z dvema končnima elementoma z zadostno natančnostjo ujamemo posledice stopničastih motenj dolžine 12 s, s tremi končnimi elementi pa 8 s.

2.1.2 Vpliv koeficienta prestopa toplote s hladila na cev

V dosedanji razpravi smo predpostavili, da sta temperatura tekočine in notranje stene cevi enaki. S tem predpostavimo neskončni koeficient prestopa toplote, kar zagotavlja največje temperaturne gradiente in s tem tudi največje napetosti v cevi in je razumno pri visokih hitrostih tokov, npr. v vroči in hladni veji. Značilne vrednosti koeficienta prestopa toplote tam znašajo tudi več 10 kW/m^{2}K [8]. Za razslojene tokove pa so značilni laminarni tokovi z nizkimi hitrostmi in več velikostnih razredov nižji koeficienti prestopa toplote v višini nekaj 10 W/m^{2}K [9].

Pričakujemo, da bo vpliv izbire koeficienta prestopa toplote največji pri modeliranju razslojenih tokov. Tudi tokrat uporabimo cev z značilnostmi prelivnega voda (poglavje 2.1.1). Za vroče hladilo predpostavimo temperaturo T_h = 223°C in T_c = 96 °C za hladno hladilo. Ti dve temperaturi sta značilni za prelivni vod tlačnika med ogrevanjem reaktorja [2].

Koeficiente prestopa toplote izberemo kot h = 50, 500 in 1000 W/m^{2}K. To so značilne vrednosti, ki se lahko pojavijo v prelivnem vodu med obratovanjem jedrske elektrarne in so odvisne predvsem od hitrosti hladila. Zanima pa nas stacionarna porazdelitev temperatur po preseku cevi zaradi razslojenega toka z različnimi višinami meje med obema slojema.

Uporabimo ravninski model (Slika 3), v katerem spreminjamo višino meje med slojema hladila: cev napolnjena z vročim hladilom, meja med toplim in hladnim slojem na polovici

notranjega premera cevi in meja med toplim in hladnim slojem na osmini notranjega premera cevi. Koeficient prestopa toplote smo postavili na h = 50 W/m^{2}K.

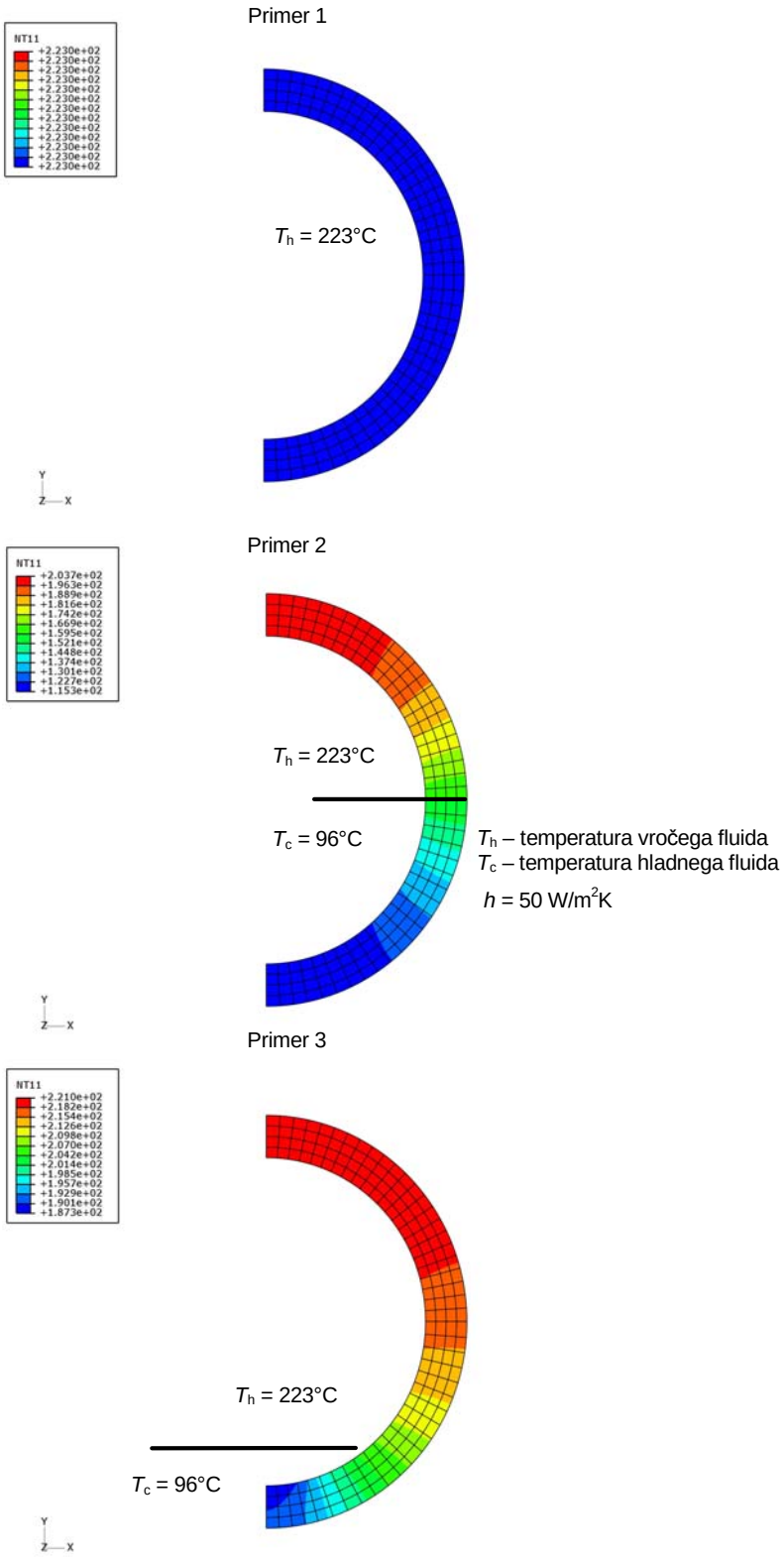

Slika 3 Porazdelitev stacionarnih temperatur po preseku cevi glede na višino meje med vročim in hladnim slojem hladila pri h = 50 W/m^{2}K

V primeru, da je koeficient prestopa toplote enak h = 500 W/m^{2}K h oz. h = 1000 W/m^{2}K, so najvišje (T_{max}) in najnižje (T_{min}) temperature, ki se pojavijo v steni cevi prikazane v Tabeli 1.

Iz rezultatov je razvidno, da imata koeficient prestopa toplote in položaj meje med vročim in hladnim slojem hladila velik vpliv na velikost in porazdelitev temperature po preseku cevi. Pri manjši vrednosti koeficienta prestopa toplote so tudi temperaturni gradienti v steni cevi manjši, kar ugodno vpliva na napetostno stanje v cevi.

Koef. prestopa toplote [W/m^{2}K]	Primer 1	Primer 2	Primer 3
500	T_{max} = 223 °C	T_{max} = 222,5 °C T_{min} = 96,5 °C	T_{max} = 223 °C T_{min} = 138 °C
1000	T_{max} = 223 °C	T_{max} = 222,9 °C T_{min} = 96,1 °C	T_{max} = 223 °C T_{min} = 122,9 °C

Tabela 1 Najvišja (T_{max}) in najnižja (T_{min}) temperatura v steni cevi v odvisnosti od koeficienta prestopa toplote in meje med vročim in hladnim slojem (Slika 3)

2.2 Numerično modeliranje napetostnega polja

V poglavju 2.1 smo ugotovili, da lahko spremembe temperature zadovoljivo opišemo s tremi elementi, če sprememba temperature traja najmanj 8 s. Tabela 2 primerja numerične in analitične vrednosti Trescove ekvivalentne napetosti na notranji površini stene cevi , ki jih povzroči stopničasta sprememba temperature velikosti 20°C v trajanju 8.1s.

Število končnih elementov	σ_p^T [MPa] numerično	σ_p^T [MPa] analitično	Odstopanje [%]
3	66.22	73.85	-10.33
4	69.92	73.85	-5.32
5	71.61	73.85	-3.03

Tabela 2 Primerjava analitičnih in numeričnih ocen Trescove ekvivalentne napetosti pri stopničasti hipni spremembi temperature s časom trajanja 8.1s

V primeru, da traja stopničasta sprememba temperature za 20°C na notranji površini 60s, je za tri elemente po debelini stene cevi razlika med numerično in analitično ocenjeno napetostjo -4.05%, kar je primerljivo s pričakovano natančnostjo metode končnih elementov.

Največji vpliv na natančnost izračuna Trescove ekvivalentne napetosti ima radialna komponenta napetosti, ki je najbolj občutljiva na kvaliteto mreže in čas trajanja prehodnega pojava. Tabela 3 prikazuje rezultate za čas trajanja prehodnega pojava 8.1s in odstopanje od analitično izračunanih vrednosti za radialno (σ_r), obročno (σ_ϕ) in vzdolžno (σ_z) napetost.

Število končnih elementov	σ_r [MPa]		σ_ϕ [MPa]		σ_z [MPa]	
	MKE [MPa]	Δ [%]	MKE [MPa]	Δ [%]	MKE [MPa]	Δ [%]
3	4.13	-	70.33	-4.77	18.59	-16.08
4	2.04	-	71.44	20.32	-3.26	-8.29
5	1.19	-	72.13	21.01	-2.33	-5.18

Tabela 3 Vpliv števila elementov na radialno (σ_r), obročno (σ_ϕ) in vzdolžno (σ_z) komponento napetosti pri stopničasti spremembi temperature dolžine 8.1s (analitično: σ_r = 0 MPa, σ_ϕ = 73.85 MPa in σ_z = 22.16 MPa)

Pri dolžini stopničaste spremembe 60 s pa je odstopanje že pri treh končnih elementih v velikostnem razredu 1% (Tabela 4).

σ_r [MPa]		σ_ϕ [MPa]		σ_z [MPa]	
MKE [MPa]	Δ [%]	MKE [MPa]	Δ [%]	MKE [MPa]	Δ [%]
2.21	-	44.95	0.89	13.71	2.55

Tabela 4 Vpliv števila elementov na radialno (σ_r), obročno (σ_ϕ) in vzdolžno (σ_z) komponento napetosti pri stopničasti spremembi temperature dolžine 60s (analitično: σ_r = 0 MPa, σ_ϕ = 44.55 MPa in σ_z = 13.37 MPa)

2.2.1 Linearizacija napetosti

Glede na navodila standarda ASME se glavne napetosti iz rezultatov MKE računajo z upoštevanjem komponent napetosti, ki se dobijo z linearizacijo napetosti [10]. Pri linearizaciji pa nastopi nevarnost doseganja netočnih rezultatov, na kar vpliva izbira poti, po kateri linearizirамо in število segmentov na katere razdelimo pot. Določanje poti je predvsem zahtevno pri spojih šob in cevovoda ali reaktorske posode.

Število elementov	σ_p^T [MPa] – 7 točk-linearizacija σ_p^T [MPa] – 31 točk-linearizacija	σ_p^T [MPa] direktno iz rezultatov	Odstopanje [%]
3	52.45	51.28	-2.24
	51.76		-0.92
4	53.58	52.29	-2.42
	52.99		-1.32

Tabela 5 Primerjava lineariziranih in neposredno odčitanih Trescovih ekvivalentnih napetosti

Slika 4 Primer poti za linearizacijo napetosti

Analiza na modelu cevi (Slika 4) s programskim paketom Abaqus [7] je pokazala, da je razlika med Trescovo ekvivalentno napetostjo določeno na osnovi linearizacije in direktno odčitano Trescovo ekvivalentno napetostjo na notranji površini stene cevi praktično zanemarljiva. V takem primeru je za določevanje faktorja izrabe smiselno rezultate numerične analize uporabiti neposredno (Tabela 5) in se postopku linearizacije napetosti izogniti.

3 IZSTOPNA ŠOBE REAKTORSKE TLAČNE POSODE

V tem poglavju predstavimo izračun delnega faktorja izrabe za projektne in dejanske prehodne pojave a) ogrevanje in ohlajanje reaktorja in b) ustavitve reaktorja s polne moči brez ohlajanja.

3.1 Geometrija modela

Vsi modeli geometrije posode in izstopne šobe so izdelani po delavniških risbah serije E-19273.

3.1.1 Poenostavitve

Modeliranje z metodo končnih elementov zahteva določeno poenostavljanje geometrije in mej materialov.

1. ***Zanemarjanje drobnih geometrijskih detajlov.*** Modeliranje velikih kosov opreme, kakršna je tlačna posoda reaktorja, s pomočjo končnih elementov praviloma zahteva določene poenostavitve oz. zanemarjanje nekaterih detajlov. Predvsem pri tem mislimo na detajle, kot so npr. predori za instrumentacijo sredice, ki ne vplivajo bistveno na odziv celotne posode. V primeru potrebe pa lahko pozneje iz rezultatov velikega modela dobimo robne pogoje za mikro analizo posameznega detajla.
2. ***Spoji materialov.*** Spoj dveh materialov je praviloma izveden z varjenjem. Za celovito analizo razmer v varjenih spojih (kot npr. spoj posode in vstopne šobe) je potrebno natančno poznati postopek izdelave. Potem je mogoče oceniti zaostale napetosti in kolikor toliko natančno geometrijo spoja. Takih informacij nimamo. Po drugi strani pa je za zvare značilno, da so meje med različnimi materiali in s tem snovnimi lastnostmi v njih in njihovi bližini zabrisane. Ostra meja med snovnimi lastnostmi pa sama po sebi povzroči lokalne koncentracije napetosti, kar je konzervativno. Zato je zvar modeliran kot idealen spoj dveh materialov.
3. ***Oplata posode.*** Oplati posode ni potrebno pripisati nosilnosti, kadar analiziramo odpornost posode na ciklične obremenitve (ASME III NB 3122.3), če je debelina oplate 10% ali manj celotne debeline komponente.

Pri izdelavi prostorskega modela (Slika 5) smo se držali smernic glede uporabe končnih elementov, ki so opisane v [1]. V modelu smo uporabili 6824 paraboličnih končnih elementov. Po debelini posamezne komponente smo uporabili najmanj tri končne elemente. Gostota mreže je primerna glede na spremembe hitrosti temperature v obravnavanih prehodnih pojavih.

3.2 Snovne lastnosti

Posamezni deli tlačne posode in cevovoda vroče veje so izdelani iz različnih materialov (Tabela 6). Snovne lastnosti, ki jih potrebujemo pri analizi so:

- modul elastičnosti E [MPa]
- linearna temperaturna razteznost α [1/K]
- toplotna prevodnost λ [W/mK] in
- specifična toplota c_p [J/kg K]

Snovske lastnosti so definirane za posamezne skupine materialov, kot so npr. ogljikovo jeklo, nerjavno jeklo, itd., v ASME B&PV Code, Section III. (Apendix I) [10] in so temperaturno odvisne.

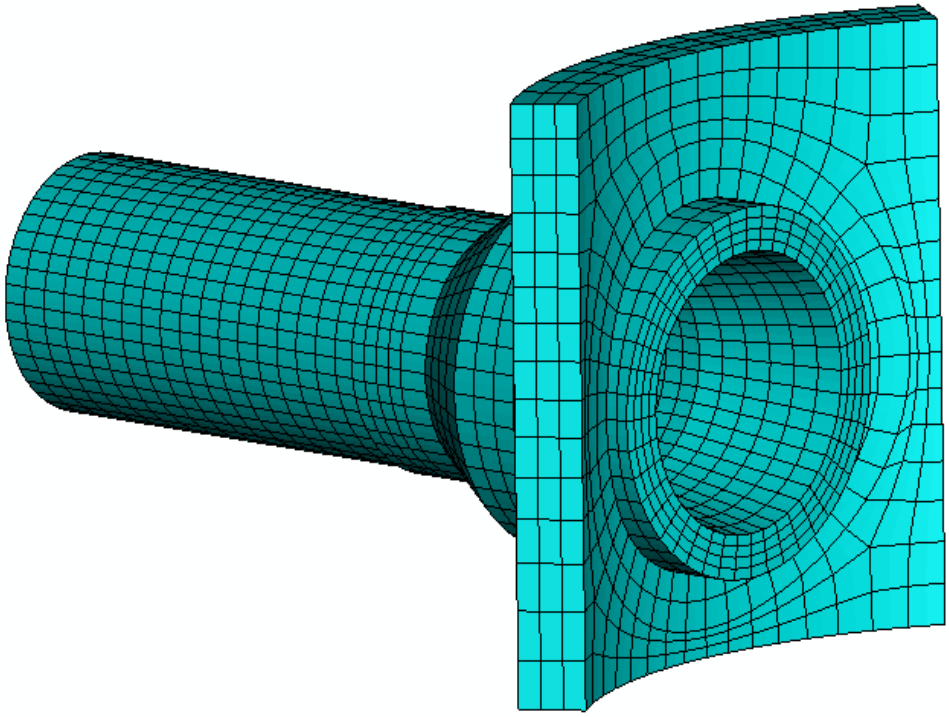

Slika 5 Prostorski model izstopne šobe z delom reaktorske posode in vroče veje

Del komponente	Vrsta materiala	Oznaka	Referenca
Telo posode	Nizko legirano jeklo (Mn-1/2 Mo-1/2 Ni)	SA 533 Gr B, Class I	[10]
Šoba posode	Ogljikovo jeklo (3/4 Ni-1/2 Mo- 1/3 Cr- V)	SA 508, Class II	[10]
Zaključek šobe (safe end)	Avstenitno nerjavno jeklo (16 Cr-12 Ni - 2 Mo)	SA 182 Gr F 316	[10]
Cevovod vroče veje	Avstenitno nerjavno jeklo (16 Cr-8 Ni)	SA-351 Gr CF8A	[10]

Tabela 6 Pregled materialov v modelu izstopne šobe

Moduli elastičnosti s temperaturo padajo približno linearno, pri čemer ima nerjavno jeklo pri sobni temperaturi nekaj nižji modul elastičnosti kot ogljikova in nizko legirana jekla. Približno pri obratovalni temperaturi razlika postane zanemarljiva in se pri 400°C praktično izgubi. Razlika v elastičnih modulih je pomembna zato, ker povzroča lokalne napetosti v bližini spoja materialov.

Linearna temperaturna razteznost s temperaturo narašča pri vseh štirih vrstah materialov. Nerjavno jeklo se pod vplivom toplote širi najbolj. Razlike v linearni temperaturni razteznosti, podobno kot pri modulih elastičnosti, povzročajo lokalne napetosti v bližini spojev različnih materialov.

Toplotna prevodnost skupaj s specifično toploto določa hitrost prodiranja toplote v telo. Nerjavno jeklo ima nižjo toplotno prevodnost kot konstrukcijski jekli za telo posode in šobo posode, medtem ko je razlika njihovih specifičnih toplot pri obratovalni temperaturi povsem zanemarljiva.

Upoštevanje temperaturne odvisnosti snovskih lastnosti povzroči nelinearnost problema temperaturnega polja, kar podraži numerično reševanje. Neupoštevanje temperaturnih odvisnosti snovskih lastnosti po drugi strani bistveno oteži analizo napetosti na spojih različnih materialov. Zato smo se odločili za modeliranje temperaturno odvisnih snovskih lastnosti.

3.3 Obremenitve

Opazujemo samo obremenitve, ki se s časom spreminjajo in kot take povzročajo ciklične spremembe napetosti v obravnavanih komponentah. Take obremenitve povzročajo tlačni in temperaturni prehodni pojavi reaktorskega hladila.

Prehodni pojavi v reaktorskem hladilu na stene primarnega kroga vplivajo neposredno, kar pomeni, da povzročajo napetosti, ki so popisane v [1]. Poleg tega je posledica temperaturnih prehodnih pojavov raztezanje oz. krčenje primarnega kroga, kar povzroča dodatne obremenitve cevovodov in s tem tudi šob. Poseben problem je realistično modeliranje drsenja podpor reaktorske posode v radialni smeri. V pričujoči analizi smo upore proti drsenju podpor zanemarili.

V poročilu obravnavamo samo neposredne efekte prehodnih pojavov. Vpliv različnega raztezanja vroče in hladne veje, ki bi preko vroče veje lahko povzročalo dodatne obremenitve šobe, smo zanemarili.

Obravnavali smo dva tlačno temperaturna prehodna pojava reaktorskega hladila, za katere smo dobili podatke iz NEK [2]:

1. ogrevanje in ohlajanje reaktorja
2. ustavitev reaktorja s polne moči brez ohlajanja.

3.3.1 Temperaturne obremenitve

Na osnovi standarda ASME smo ocenili, da lahko temperaturne (pod)cikle, manjše od 11.7°C, zanemarimo. Pri tem smo upoštevali snovne lastnosti za zaključke šob, ki imajo od obravnavanih materialov najnižje mehanske lastnosti (S_m = 114,5 MPa in S_a (pri 10^6 ciklih) = 86 MPa) [11].

Temperaturne obremenitve za prehodni pojav ogrevanja in ohlajanja reaktorja so zbrane v tabeli 7 (projekt) in v tabeli 8 (izmerjeno). Pri tem so podatki pri ogrevanju reaktorja, ki smo jih dobili iz NEK, zabeleženi in upoštevani le do temperature 292 °C [1], ko je toplotna moč reaktorje enaka nič. Glede na projektne podatke ogrevanje reaktorja s stanja vroče ugasnitve do polne moči časovno poteka s približno enako hitrostjo spremembo temperature kot ohlajanje s temperature pri polni moči reaktorja do stanja vroče ugasnitve, smo hitrost segrevanja pri dejanskem prehodnem pojavu določili na osnovi znane hitrosti ohlajanja s polne moči [2].

Pri zasilni ustavitvi reaktorja s polne moči brez ohlajanja so razpoložljivi podatki, ki smo jih dobili iz NEK takšni, da ne prikazujejo celotnega cikla. Zato smo manjkajoče podatke predpostavili. Iz rezultatov meritve temperature je razvidno, da je bil reaktor v vroči ugasnitvi več kot 20 ur. Ogrevanje na polno moč poteka mnogo počasneje, kot je bila sprememba

temperature pri ustavitvi reaktorja s polne moči brez ohlajanja. Hitrost ogrevanja v praksi poteka s hitrostjo približno 5°C/h. Zato smo to vrednost upoštevali tudi v naši analizi. Čas, ko je bil reaktor v vroči ustavitvi pa smo aproksimirali s časom, pri katerem v obravnavanih pogojih temperatura v komponenti doseže stacionarno stanje (pribl. 11,1 ure oz. 40000 s).

Čas [h]	T[°C]
0	49
4,4	292
5,3	292
5,5	321,5
17,2	321,5
17,5	292
18,0	292
22,4	49

Tabela 7 Temperaturni cikel ogrevanja in ohlajanja reaktorja za projektni prehodni pojav

Čas [h]	T[°C]
0	44
5,5	84
16,7	96
28,3	290
34	290
34,6	325
45.7	325
48,3	290
51,4	282
55,3	141
66,2	44

Tabela 8 Temperaturni cikel ogrevanja in ohlajanja reaktorja za dejanski prehodni pojav

3.3.2 Tlačne obremenitve

Na osnovi standarda ASME smo ocenili, da lahko tlačne (pod)cikle, manjše od 3,96 MPa, zanemarimo.

Tlačne spremembe v obravnavanih komponentah pri ogrevanju in ohlajanju reaktorja, ki smo jih upoštevali v analizi, prikazujeta tabeli 11 in 12.

Iz tabele 12 izhaja, da smo pri času 51,1 ure upoštevali tudi spremembo tlaka v sistemu, ki je bila manjša od 3,96 MPa in torej po ASME zanemarljiva. To smo naredili zato, ker se je v času 50. ure pojavila največja Trescova ekvivalentna napetost in smo s tem natančnejše simulirali dogajanje v komponenti.

Čas [s]	T [°C]
0	321,5
25	290,5
75	287,4
40075	287,4
64458	321,5

Tabela 9 Temperaturni cikel ustavitve reaktorja s polne moči brez ohlajanja za projektni prehodni pojav

Čas [s]	T [°C]
0	325
720	288
1920	292
41920	292
65680	325

Tabela 10 Temperaturni cikel ustavitve reaktorja s polne moči brez ohlajanja za dejanski prehodni pojav

Čas [h]	p [MPa]
0	3,32
2,3	3,32
4,4	16,08
18,0	16,08
19,1	3,32
22,4	3,32

Tabela 11 Tlačni cikel ogrevanja in ohlajanja reaktorja za projektni prehodni pojav

Pri ustavitvi reaktorja s polne moči brez ohlajanja so vse tlačne spremembe manjše od 3.96 MPa. Zato smo v analizi upoštevali stacionarni tlak 16,08 MPa za projektni prehodni pojav in 15,81 MPa za dejanski prehodni pojav, s čemer smo zagotovili konservativnost rezultatov.

3.4 Robni pogoji

V analizi smo obravnavali izsek iz reaktorske posode z izstopno šobo in del cevovoda vroče veje. Upoštevali smo takšne robne pogoje, s katerimi simuliramo vpliv okoliških komponent na obravnavan model.

Čas [h]	*p* [MPa]
0	2,5
20,0	2,83
28,9	13,97
30,6	16,39
32,1	15,77
34,6	15,77
51,1	15,6
54,5	2,5
66,2	2,5

Tabela 12 Tlačni cikel ogrevanja in ohlajanja reaktorja za dejanski prehodni pojav

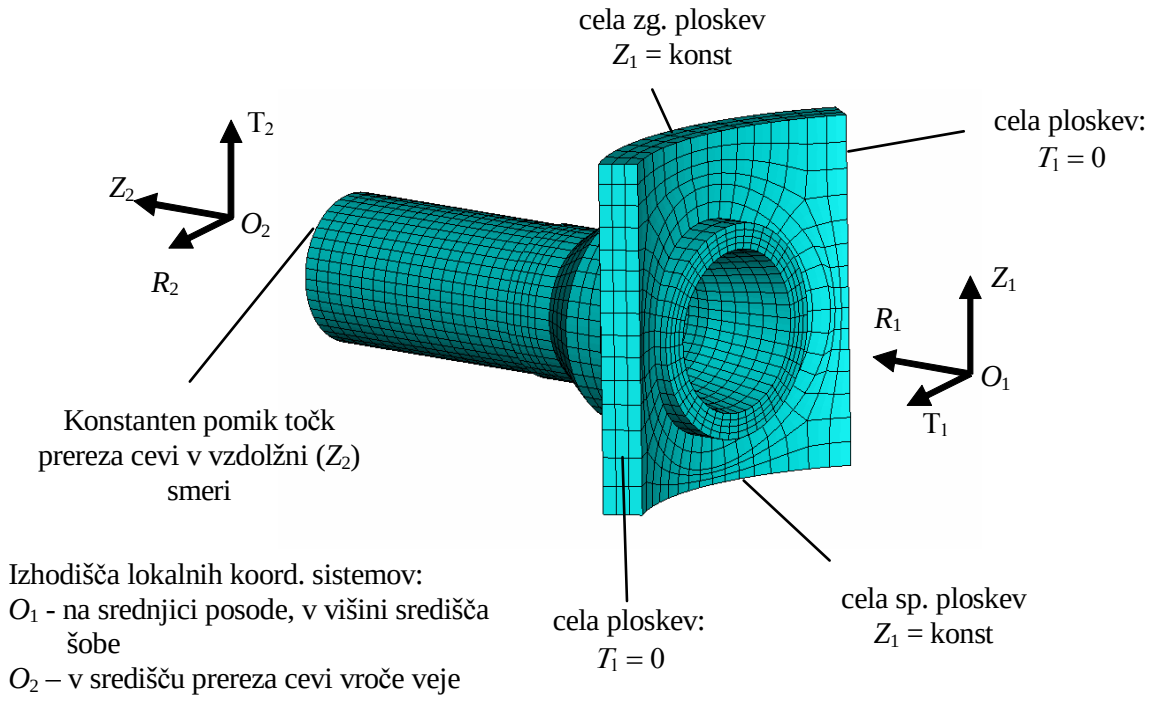

Slika 6 Kinematični robni pogoji v modelu izstopne šobe

3.5 Rezultati

Kot rezultate analize predstavljamo največje Trescove ekvivalentne napetosti med obremenitvenimi cikli , ki so definirani v 3.3.1 in 3.3.2. Vrednosti predstavljajo vsoto termičnih in tlačnih napetosti . Na osnovi Trescove ekvivalentne napetosti izračunamo amplitudo nihanja napetosti S_a in nato delni faktor izrabe.

Pri tem smo izračunali faktor izrabe, tako za projektne prehodne pojave, kot za dejanske prehodne pojave.

3.5.1 Ogrevanje in ohlajanje reaktorja

V projektnem prehodnem pojavu se največja Trescova ekvivalentna napetost 360,4 MPa pojavi v času 17,5 ur (ohlajanje reaktorja) na notranji površini izstopne šobe (Slika 7), ko je dosežena temperatura 292°C. Po 18 h urah se v sistemu začne zmanjševati tlak, kar zmanjšuje napetosti kljub temu, da je gradient temperature velik. Dopustna napetost za ciklično obremenjeno šobo znaša $3S_m$ = 552,3 MPa [10], kar pomeni, da je šoba obremenjena v dopustnih mejah.

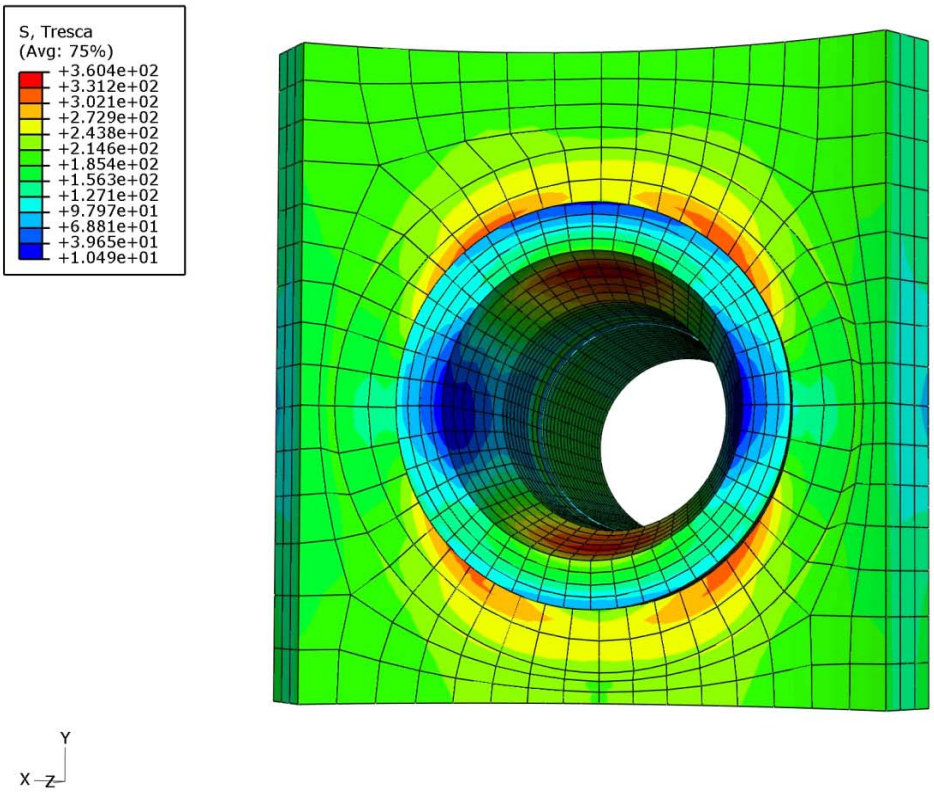

Slika 7 Največja Trescova ekvivalnentna napetost med projektnim prehodnim pojavom ogrevanja in ohlajanja reaktorja

Amplituda nihanja napetosti S_a = 180,2 MPa se izračuna kot polovica Trescove ekvivalentne napetosti [1]. Na osnovi S_a določimo dopustno število obremenitev N = 34153 iz ustrezne Wöhlerjeve krivulje (krivulja za materiale z natezno trdnostjo manjšo od 551,6 MPa [10]). Delni faktor izrabe za eno ponovitev prehodnega pojava je tako $u_1 = 2{,}93 \cdot 10^{-5}$ oz. $u_{56} = 1{,}64 \cdot 10^{-3}$ za 56 ponovitev prehodnega pojava, kolikor se jih je glede na dostavljene podatke zgodilo do sedaj v NEK [2].

V času 17,5 ure je bil reaktor v fazi ohlajanja. Razlog za največje napetosti pri zniževanju temperature je razviden iz slike 9, ki prikazuje močno pretirano deformacijo izstopne šobe in Trescovo ekvivalentno napetost izstopne šobe zaradi obremenitve s tlakom 16,08 MPa in brez toplotnih obremenitev.

Primerjava napetosti (slika 7 in slika 8) pokaže, da imajo napetosti zaradi tlačne obremenitve večji vpliv na največje napetosti v šobi kot temperaturne spremembe za obravnavane prehodne pojave.

Pri analizi izmerjenega prehodnega pojava se največja Trescova ekvivalentna napetost 338,3 MPa pojavi v času 50 ur (ohlajanje reaktorja) na notranji površini šobe (Slika 9). V tem času se

v sistemu že delno znižuje tlak, kar znižuje napetosti. Ker se v tem času znižuje tudi temperatura, ki povečuje napetosti, je v času 50 ur dosežena najbolj neugodna kombinacija vpliva tlaka in temperature. Dopustna napetost za ciklično obremenjeno šobo znaša $3S_m$ = 552,3 MPa [10], kar pomeni, da je šoba obremenjena v dopustnih mejah.

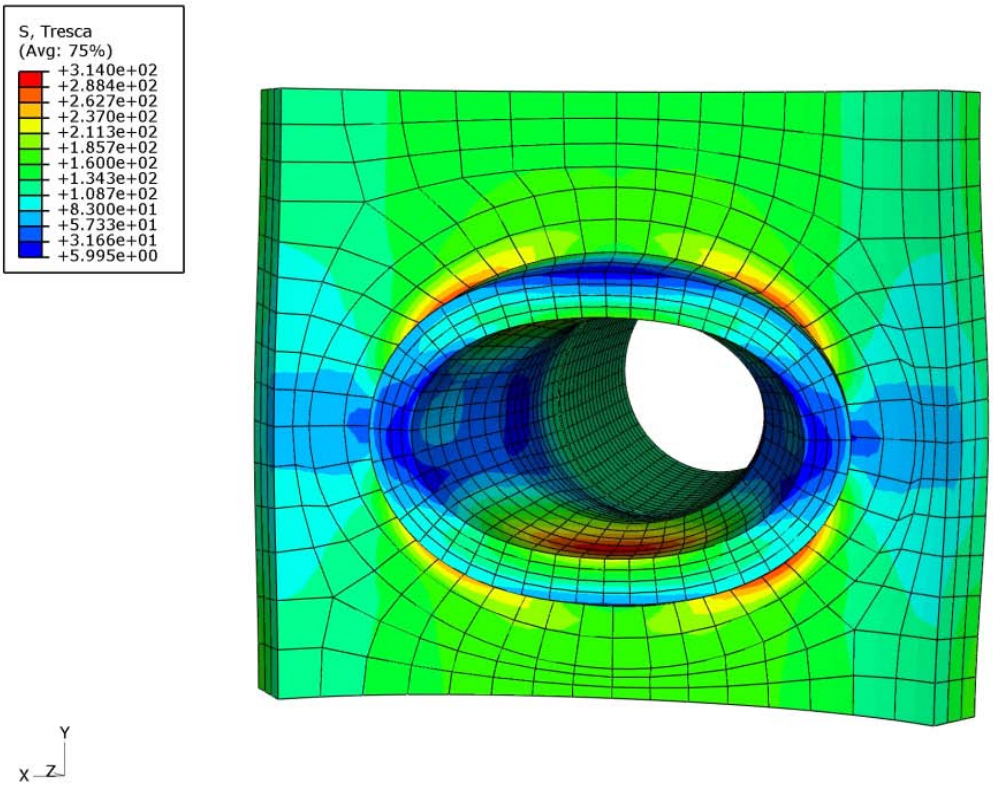

Slika 8 Močno pretirana deformacija izstopne šobe zaradi obremenitve z notranjim tlakom in pripadajoča Trescova ekvivalentna napetost

Amplituda nihanja napetosti S_a = 169,2 MPa se izračuna kot polovica Trescove ekvivalentne napetosti [1]. Na osnovi S_a določimo dopustno število obremenitev N = 40765 iz ustrezne Wöhlerjeve krivulje (krivulja za materiale z natezno trdnostjo manjšo od 551,6 MPa). Delni faktor izrabe za eno ponovitev prehodnega pojava je tako $u_1 = 2{,}45 \cdot 10^{-5}$. Ob nekoliko nerealni predpostavki, da so bila vsa dosedanja ogrevanja in ohlajanja reaktorja enaki obravnavanemu, bi faktor izrabe za 56 ponovitev prehodnega pojava, kolikor se jih je glede na dostavljene podatke zgodilo do sedaj v NEK, znašal $u_{56} = 1{,}37 \cdot 10^{-3}$.

Primerjava rezultatov pokaže, da ima izmerjeni prehodni pojav manjši vpliv na utrujanje obravnavanih komponent kot projektni, kar kaže v tem primeru na konzervativnost projektiranja elektrarne.

3.5.2 Ustavitev reaktorja s polne moči brez ohlajanja

Prii analizi projektne ustavitve reaktorja s polne moči brez ohlajevanja se največja Trescova ekvivalentna napetost 381,2 MPa pojavi v času 25 s (ohlajanje reaktorja) na notranji površini izstopne šobe (Slika 10), ko je dosežena temperatura 290,5°C. V nadaljevanju se sicer temperatura še znižuje do 287,4 °C, vendar je hitrost zniževanja temperature mnogo manjša in zato ne vpliva na povečanje napetosti. Dopustna napetost za ciklično obremenjeno šobo znaša $3S_m$ = 552,3 MPa [10], kar pomeni, da je šoba obremenjena v dopustnih mejah.

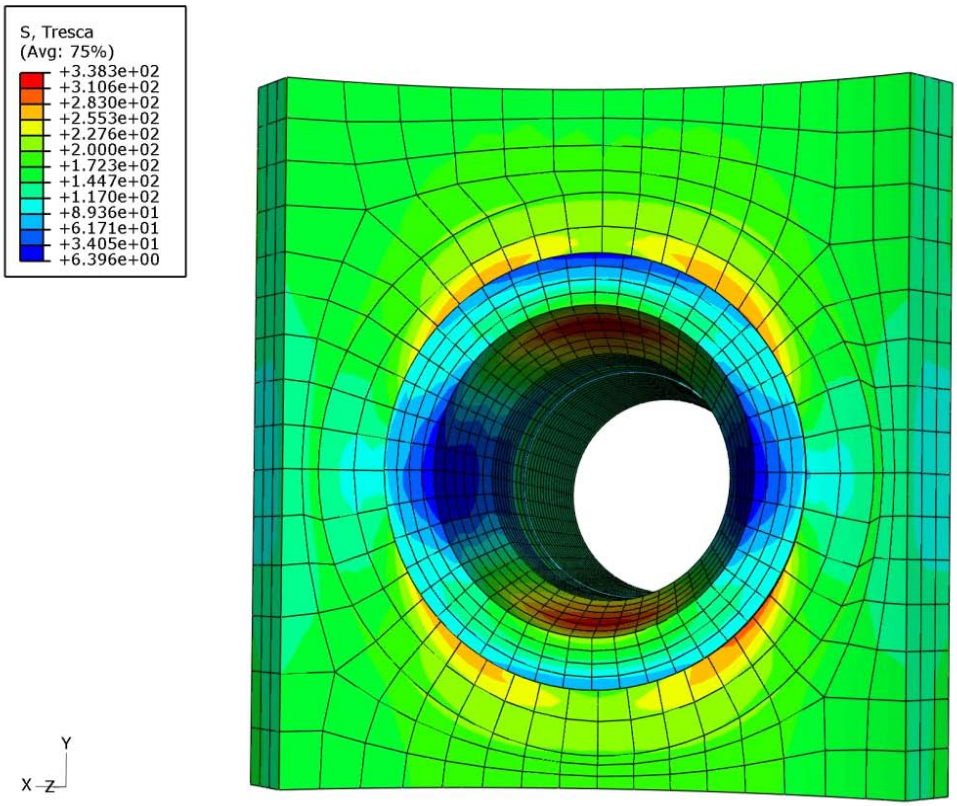

Slika 9 Največja Trescova ekvivalentna napetost med izmerjenim ogrevanjem in ohlajanjem

Amplituda nihanja napetosti S_a = 190,6 MPa se izračuna kot polovica Trescove ekvivalentne napetosti [1]. Na osnovi S_a določimo dopustno število obremenitev N = 29194 iz ustrezne Wöhlerjeve krivulje (krivulja za materiale z natezno trdnostjo manjšo od 551,6 MPa). Delni faktor izrabe za eno poonvitev prehodnega pojava je tako $u_1 = 3{,}43 \cdot 10^{-5}$ oz. $u_{73} = 2{,}5 \cdot 10^{-3}$ za 73 ponovitev prehodnih pojavov, kolikor se jih je glede na dostavljene podatke zgodilo do sedaj v NEK.

Analiza izmerjenega prehodnega pojava pokaže največjo Trescovo ekvivalentno napetost 354,9 MPa pojavi v času 720 s (ohlajanje reaktorja) na notranji površini izstopne šobe (Slika 11), ko je dosežena temperatura 288 °C. Dopustna napetost za ciklično obremenjeno šobo znaša $3S_m$ = 552,3 MPa [10], kar pomeni, da je šoba obremenjena v dopustnih mejah-

Amplituda nihanja napetosti S_a = 181,2 MPa se izračuna kot polovica Tresca ekvivalentne napetosti [1]. Na osnovi S_a določimo dopustno število obremenitev N = 33629 iz ustrezne Wöhlerjeve krivulje (krivulja za materiale z natezno trdnostjo manjšo od 551,6 MPa). Delni faktor izrabe za eno ponovitev prehodnega pojava je tako $u_1 = 2{,}97 \cdot 10^{-5}$. Ob nekoliko nerealni predpostavki, da so bila vsa dosedanja ogrevanja in ohlajanja reaktorja enaki obravnavanemu, bi faktor izrabe za 73 prehodnih pojavov, kolikor se jih je glede na dostavljene podatke zgodilo do sedaj v NEK, znašal $u_{73} = 2{,}17 \cdot 10^{-3}$.

Primerjava rezultatov pokaže, da ima obravnavani izmerjeni prehodni pojav ustavitve reaktorja s polne moči brez ohlajevanja manjši vpliv na utrujanje obravnavanih komponent kot projektni, kar kaže v tem primeru na konzervativnost projektiranja elektrarne.

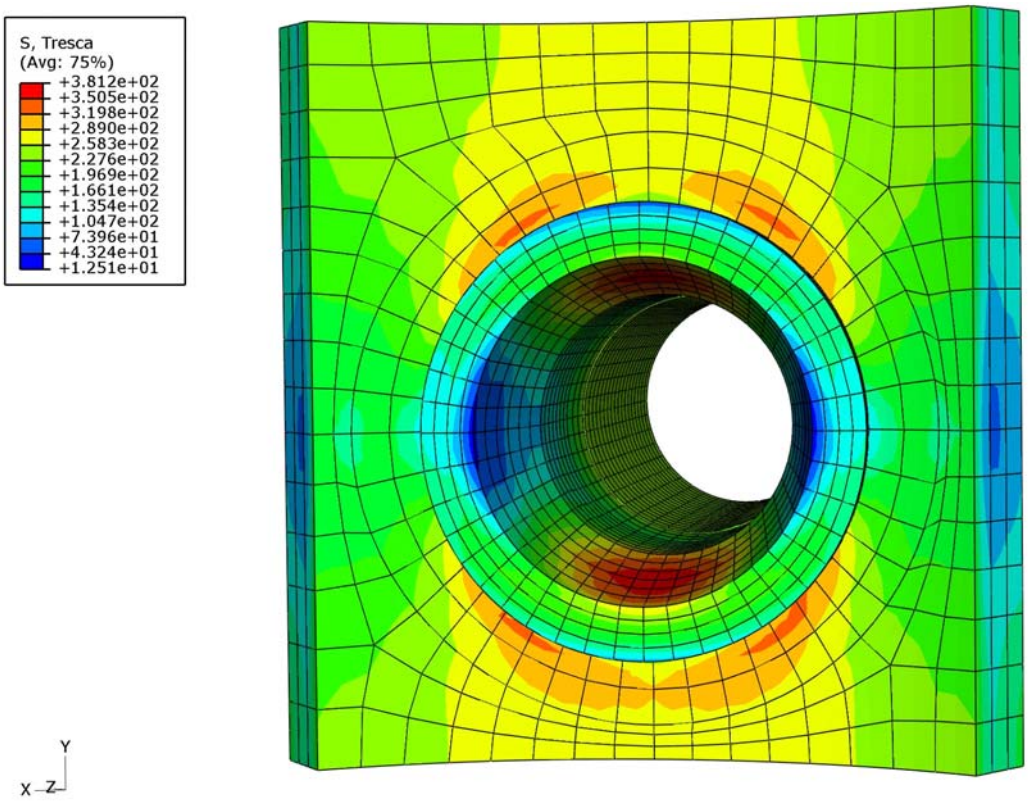

Slika 10 Največja Trescova ekvivalnentna napetost med projektnim prehodnim pojavom ustavitve reaktorja s polne moči brez ohlajanja

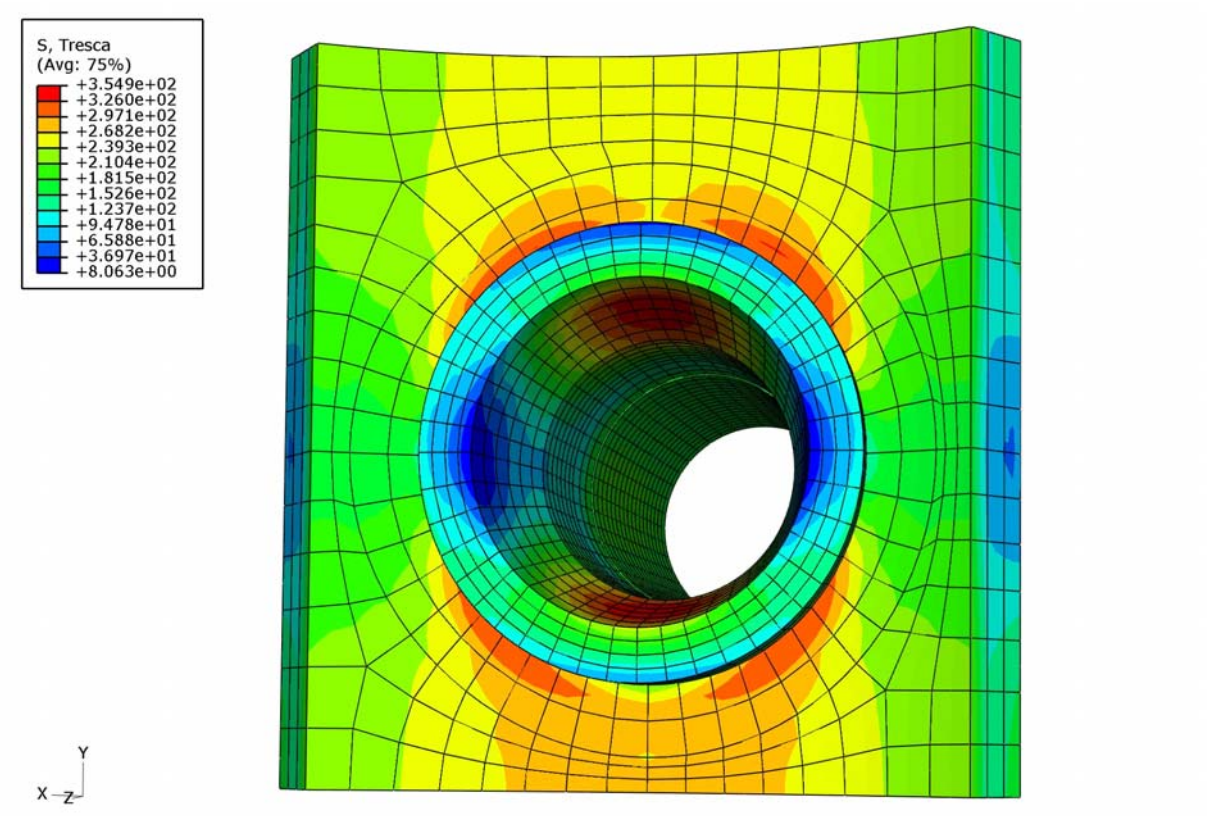

Slika 11 Največja Trescova ekvivalnentna napetost med izmerjenim prehodnim pojavom ustavitve reaktorja s polne moči brez ohlajevanja

4 MODEL PRELIVNEGA VODA TLAČNIKA

V tem poglavju predstavimo izračun temperatur, napetosti in delnih faktorjev izrabe v prelivnem vodu tlačnika med dvema hipotetičnima prehodnima pojavoma toplotnega razslojevanja hladila in potovanja toplotnega šoka po prelivnem vodu. Pri tem opazujemo tudi časovne poteke temperatur na hipotetično zamišljenih položajih temperaturnih tipal na zunanji površini prelivnega voda.

4.1 Geometrija modela

Vsi modeli geometrije prelivnega voda in šobe med prelivnim vodom in vročo vejo so izdelani po risbah C-318-601 in 1209E72.

4.1.1 Poenostavitve

Modeliranje z metodo končnih elementov zahteva določeno poenostavljanje geometrije in mej materialov.

1. ***Zanemarjanje drobnih geometrijskih detajlov.*** Podobno kot v primeru izstopne šobe reaktorske tlačne posodein smo tudi v modelu prelivnega voda tlačnika zanemarili nekatere detajle. Predvsem pri tem mislimo na detajle, kot so npr. a) predori za merjenje temperature v prelivnem vodu s potopljenim termometrom, b) obešala za prelivni vod , ki ne vplivajo bistveno na odziv celotnega sistema v predstavljenih analizah. V primeru potrebe pa lahko pozneje iz rezultatov modela dobimo robne pogoje za mikro analizo posameznega detajla.
2. *Modeliran del cevi vroče veje* v okolici spoja s prelivnim vodom, ki služi predvsem kot podpora prelivnemu vodu, saj je praktično gledano prelivni vod dvostransko trdno pritrjen cevovod.
3. ***Spoji materialov.*** Spoj dveh materialov je praviloma izveden z varjenjem. Za celovito analizo razmer v varjenih spojih (kot npr. spoj šobe in prelivnega voda) je potrebno natančno poznati postopek izdelave. Potem je mogoče oceniti zaostale napetosti in kolikor toliko natančno geometrijo spoja. Takih informacij nimamo. Po drugi strani pa je za zvare značilno, da so meje med različnimi materiali in s tem snovnimi lastnostmi v njih in njihovi bližini zabrisane. Zato je zvar modeliran kot idealen spoj prelivnega voda in šobe.

Pri izdelavi prostorskega modela smo se držali smernic glede uporabe končnih elementov, ki so opisane v [1]. Prostorski model prelivnega voda je modeliran v celotni dolžini od spoja s šobo pri vroči veji do reducirke pred vstopno šobo tlačnika. Gostota mreže je primerna glede na hitrost spremembe temperatur.

Temperaturno porazdelitev smo določili z modelom, v katerem smo uporabili 34049 paraboličnih končnih elementov za simulacijo prenosa toplote. Za trdnostno analizo pa smo model diskretizirali z enako mrežo, pri čemer smo uporabili končne elemente, ki omogočajo izračun napetostno-deformacijskega polja. V obeh analizah smo po debelini uporabili tri končne elemente, s čemer lahko glede na uporabljene vhodne podatke z zadostno natančnostjo modeliramo temperaturna in napetostno deformacijska polja.

V prelivnem vodu tlačnika smo predpostavili štiri hipotetična merilna mesta za merjenje temperatur na zunanji površini cevi (M1 do M4 na sliki 13). Izračunane časovne poteke

temperatur smo v nadaljevanju poleg v v petih točkah (A do E) na zunanji površini cevovoda prikazali tudi v pripadajočih petih točkah na notranji površini cevovoda.

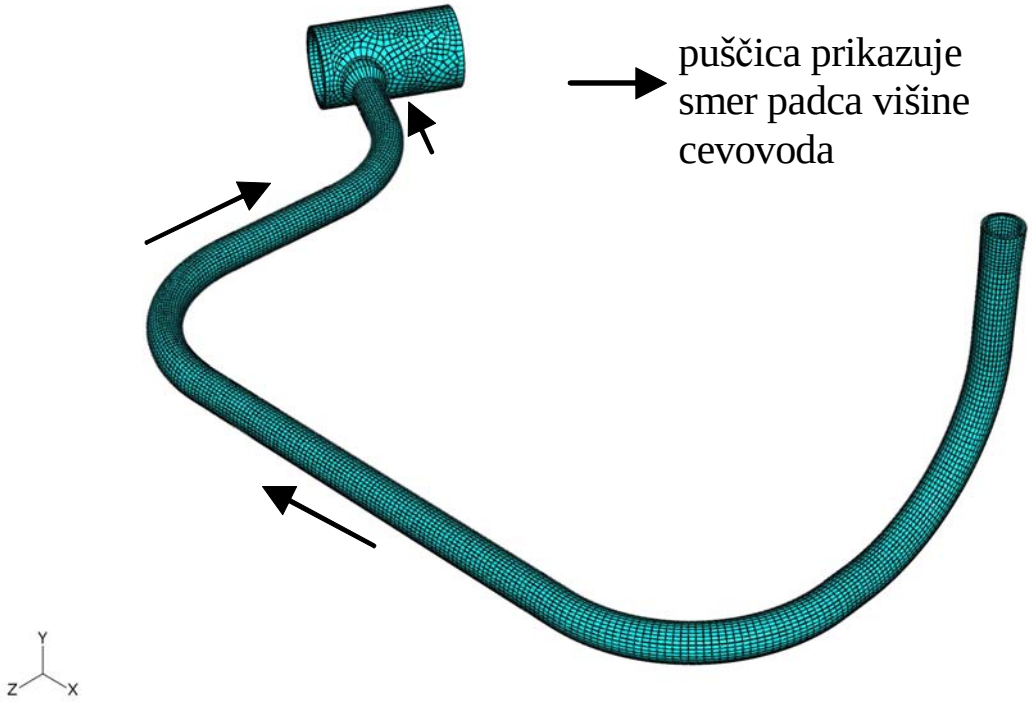

Slika 12 Prostorski model prelivnega voda tlačnika

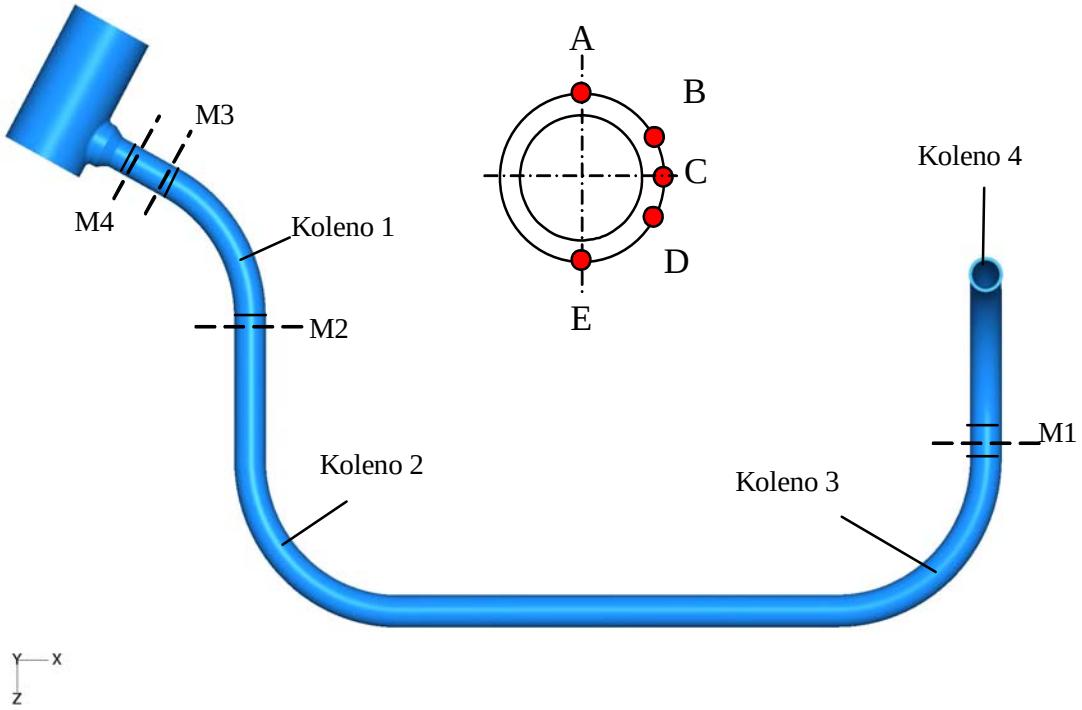

Slika 13 Predpostavljena merilna mesta M1 do M4 na prelivnem vodu tlačnika

4.2 Snovne lastnosti

Cevovod in šoba prelivnega voda sta izdelani iz materiala SA376 Type 316, za katerega so snovske lastnosti definirane v ASME B&PV Code, Section III. (Apendix I) [10] in so temperaturno odvisne.
Snovne lastnosti, ki jih potrebujemo pri analizi so:

- modul elastičnosti E [MPa]
- linearna temperaturna razteznost α [1/K]
- toplotna prevodnost λ [W/mK] in
- specifična toplota c_p [J/kg K]
- koeficient prestopa toplote h [W/m^{2}K]

4.3 Obremenitve

Izbrane obremenitve so hipotetične in so namenjene demonstraciji možnosti, ki jih zasnovana metoda ponuja pri analizi odziva prelivnega voda na toplotne šoke in toplotno razslojene tokove s spremenljivo mejo med toplim in hladnim slojem. Obremenitve so izbrane z ozirom na zmogljivosti sistemov v jedrski elektrarni Krško [2] tako, da se po naši oceni lahko pojavijo tudi v praksi. Namen tega dela analize torej ni podati prispevka prehodnega pojava k utrujenosti komponente, ampak demonstracija možnosti zasnovane metode.

Kot temperaturi hladnega in toplega sloja hladila privzamemo največjo temperaturno razliko med hladilom v vroči veji in v tlačniku med ogrevanja in ohlajanja reaktorja: T_c = 96 °C in T_h = 223 °C [2]. Upoštevamo tudi tlak p = 2,5 MPa [2].

4.3.1 Toplotno razslojeni tok

Toplo hladilo je v tlačniku, hladno v vroči veji. Med njima je idealna vodoravna meja. Na začetku analize predpostavimo mejo med obema hladiloma blizu spodnje površine cevovoda na mestu, kjer se začne drugo koleno (Slika 13), gledano iz smeri vroče veje proti tlačniku. Na začetku prehodnega pojava predpostavimo, da je toplotno polje v stacionarnem stanju.

Mejo med hladiloma nato v prehodnem pojavu dvigamo in spuščamo. V prvem primeru v najvišji točki počakamo na stacionarno stanje, nato gladino z enako hitrostjo spustimo v izhodišče. V drugem primeru gladina nemudoma zapusti najvišjo točko in se z enako hitrostjo vrne v izhodišče.

Hitrost dviganja in spuščanja gladine smo ocenili na 2,57 mm/s. Ocena upošteva značilno hitrost potovanja hladila po prelivnem vodu, pri katerem se razslojeni tekočini ne pomešata in znaša v literaturi okoli 50 mm/s [6]. Koeficient prestopa toplote pri taki hitrosti ocenimo na h = 50 W/m^{2}K.

4.3.2 Toplotni šok

Toplo hladilo je v tlačniku, hladno v vroči veji. Med njima je idealna meja, ki je pravokotna glede na os prelivnega voda tlačnika. Meja med hladnim in vročim hladilom potujena razdalji 2,1 m po prelivnem vodu tlačnika s hitrostjo 0,4 m/s, ki smo jo ocenili na osnovi moči grelcev v tlačniku [12]. Pri takšni hitrosti hladila sledi koeficient prestopa toplote h = 2100 W/m^{2}K. Pred začetkom premikanja meje predpostavimo, da je toplotno polje v stacionarnem stanju.

Analizirali smo dve značilni gibanji meje med hladiloma. V prvem primeru prepotuje 2,1 m s hitrostjo 0,4 m/s. V novem položaju meja miruje vse dotlej, da se ponovno vzpostavi stacionarno stanje. Nato se z enako hitrostjo vrne v izhodišče. V drugem primeru prepotuje 2,1 m s hitrostjo 0,4 m/s in se nato nemudoma obrne in z enako hitrostjo vrne v izhodišče.

Izhodiščni položaj meje med hladiloma je od merilnega mesta M2 dovolj oddaljen v smeri proti vroči veji, da merilno mesto ob začetku prehodnega pojava ne zazna vpliva različnih temperatur hladil.

4.4 Robni pogoji in predpostavke

V analizi smo obravnavali prelivni vod tlačnika od spoja s šobo na vroči veji do reducirke pri vstopni šobi v tlačnik. Upoštevali smo takšne robne pogoje, s katerimi simuliramo vpliv okoliških komponent na obravnavan model.

4.4.1 Toplotna analiza

Glavni predpostavki pri toplotni analizi sta:

- zunanje površine primarnega kroga so popolnoma izolirane. Pri ohlajanju sistema zato vso toploto odvedemo iz stene s pomočjo reaktorskega hladila, kar zagotavlja največje temperaturne gradiente in s tem konzervativnost analize.
- v prelivnem vodu upoštevamo prestop toplote s hladila na trdnino in obratno preko koeficienta prestopa toplote *h*. Kot je že bilo poudarjeno, je porazdelitev temperature po preseku cevi zelo odvisna od koeficienta prestopa toplote s tekočine na trdnino. Pri višjem koeficientu prestopa toplote (višje hitrosti tekočine) se temperatura trdnine hitreje izenači s temperaturo tekočine. Nižji koeficienti prestopa toplote torej praviloma pomenijo nižje razlike temperatur v trdnini in posledično tudi nižje napetosti.

Snovske lastnosti z izjemo koeficienta prestopa toplote so modelirane kot temperaturno odvisne veličine, zato je analiza temperaturnega polja nelinearna.

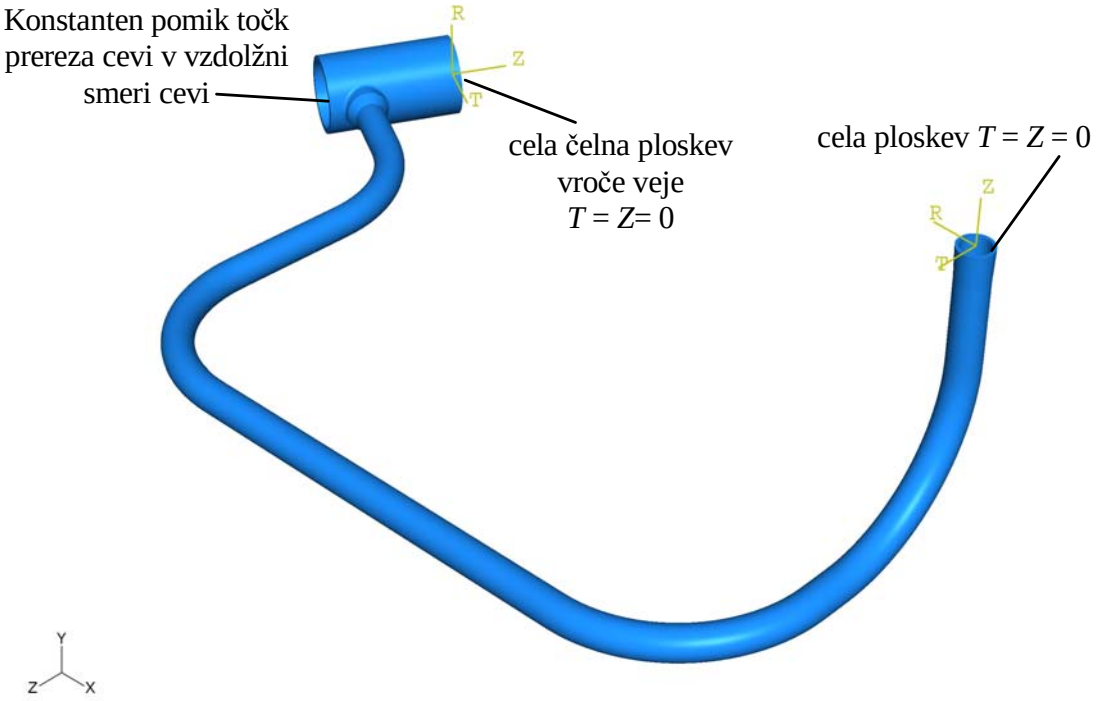

Slika 14 Kinematični robni pogoji modela prelivnega voda tlačnika

4.4.2 Napetostna analiza

Robne pogoje pri napetostni analizi predstavljajo časovno odvisna temperaturna polja. Slika 14 prikazuje kinematične robne pogoje. Premike vroče veje zaradi toplotnega raztezanja smo v analizi zanemarili.

V primeru toplotnega razslojevanja se lahko v šobi med vročo vejo in prelivnim vodom med prehodnim pojavom spreminjajo smeri glavnih napetosti. To v skladu s pravili kontrole na utrujanje po ASME B&PV Code zahteva posebno obravnavo, ki pa jo na tem mestu nismo izvedli, ker so ocenjeni delni faktorji izrabe le hipotetični.

4.5 Rezultati

V analizi smo obravnavali dva značilna primera, ki se lahko pojavita v prelivnem vodu:

1. toplotno razslojeni tok in
2. toplotni šok.

4.5.1 Toplotno razslojeni tok

Kot rezultat analize predstavljamo:

1. časovno odvisno porazdelitev temperature na notranji in zunanji steni cevovoda na mestih, kjer smo predpostavili merilce temperature po zunanjem obodu cevovoda (Slika 13).
2. največjo vrednost Trescove ekvivalentne napetosti in faktor izrabe.
3.

Obravnavali smo dva primera:

1. gladina se dvigne iz spodnje lege v zgornjo lego in tam obstane dokler se ne vzpostavi stacionarno stanje. Po tem se gladina vrne nazaj v izhodiščno lego.
2. gladina se dvigne iz spodnje lege v zgornjo lego in takoj nazaj v izhodiščno lego.

Za spremembo gladine iz spodnje lege v zgornjo lego cevovoda, kjer stoji toliko časa, da se vzpostavi stacionarno stanje in šele po tem vrne v izhodiščno lego, prikazuje slika 16 temperaturne porazdelitve v vmesnih stanjih.

V primeru, da se gladina dvigne od spodnjega do zgornjega roba cevovoda in tam obstane dokler se ne vzpostavi stacionarno stanje (Slika 15) in se šele nato vrne v izhodiščno lego, se temperatura za cel cikel na merilnem mestu M4-A spreminja kot prikazuje slika 16.

Zaradi lažje predstavitve rezultatov bomo prikazali porazdelitev temperature za čas:

- od 0 do 1000 s, ko se je gladina dvigovala iz začetne lege na tem intervalu in
- od 40000 do 60000 s, kar zajema čas preden je v zgornji legi doseženo stacionarno stanje in čas ko se je gladina spustila v izhodiščno lego

Slika 17 prikazuje spremembo temperature na merilnem mestu M1.

Iz rezultatov na sliki 17 je razvidno, da je po celem obodu in skozi debelino stene cevi dosežena konstantna temperatura 223°C in da obravnavana sprememba gladine med vročim in hladnim fluidom ne vpliva na temperaturne spremembe na tem mestu.

Slika 18 prikazuje spremembo temperature na merilnem mestu M2.

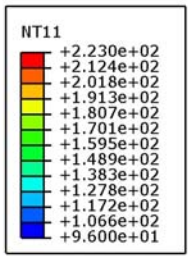

Spodnja lega gladine

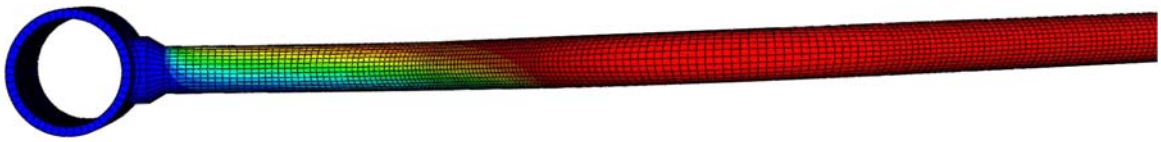

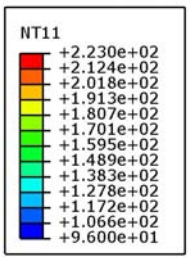

Zgornja lega gladine v stacionarnem stanju

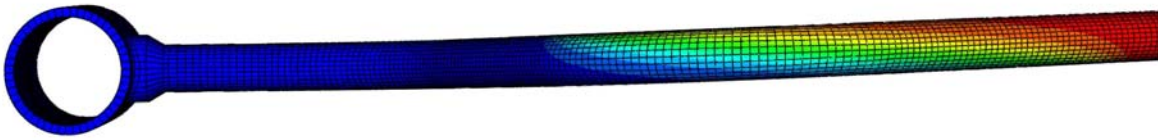

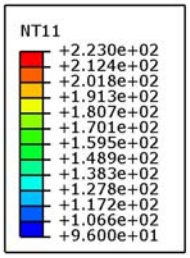

Spodnja lega gladine

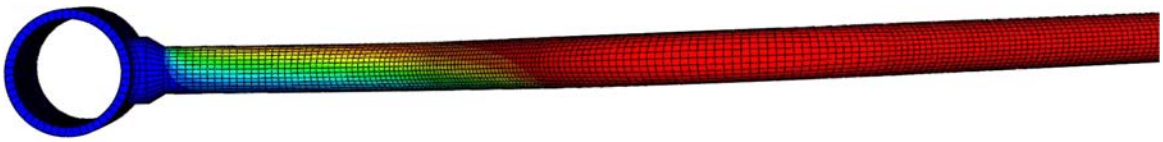

Slika 15 Porazdelitev temperature pri spremembi lege gladine iz spodnje do zgornje in nazaj do spodnje z vmesnim stacionarnim stanjem v zgornji legi

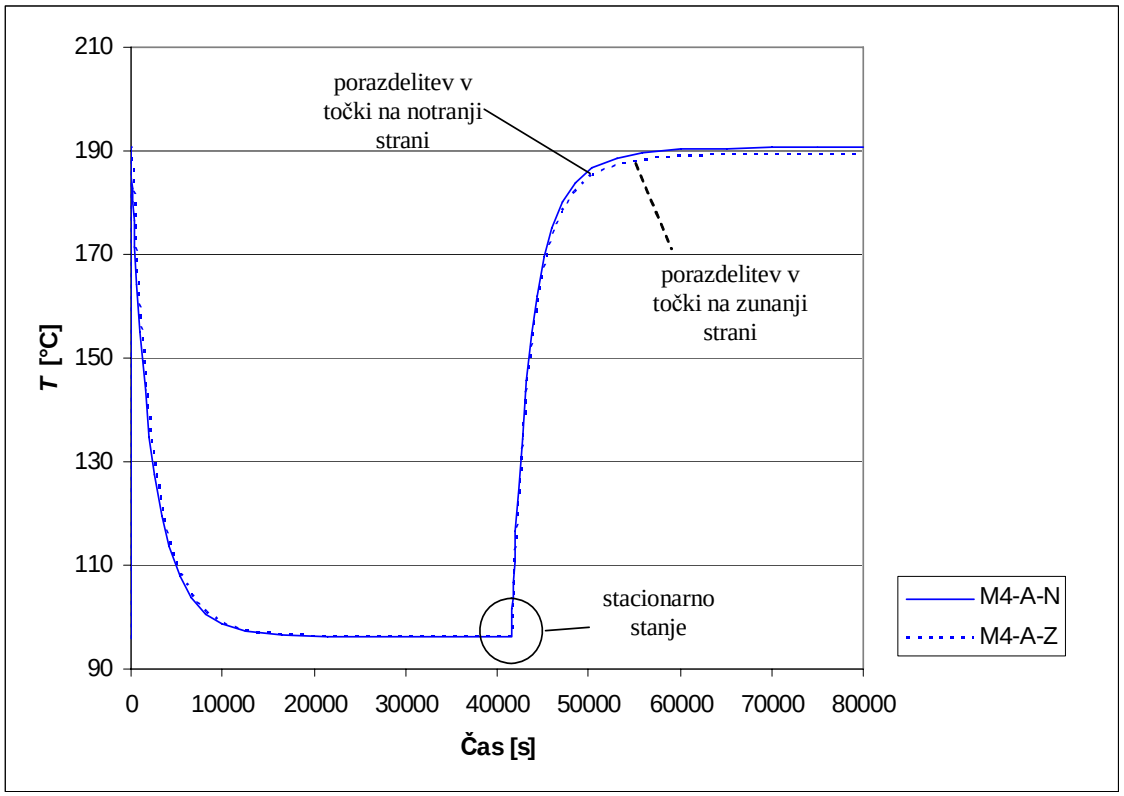

Slika 16 Porazdelitev temperature v notranji (M4-A-N) in zunanji (M4-A-Z) točki pri spremembi lege gladine z vmesnim stacionarnim stanjem

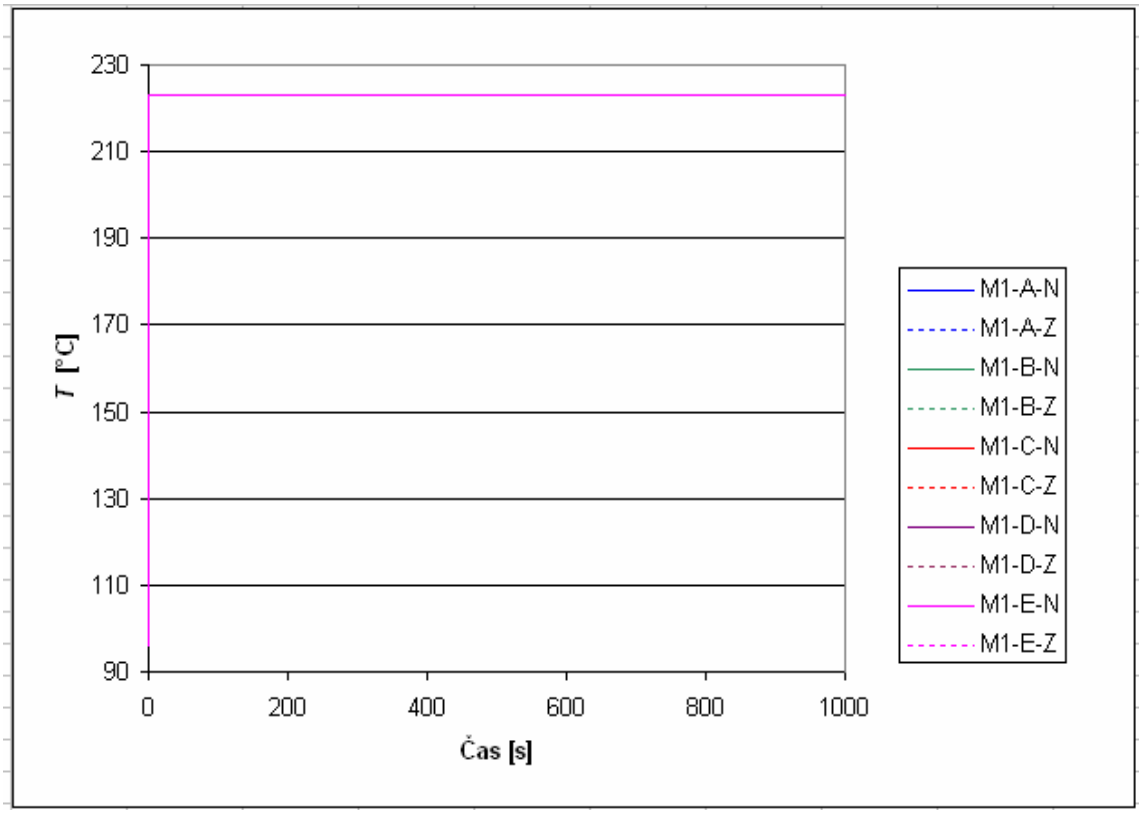

Slika 17 Porazdelitev temperature v notranjih in zunanjih točkah na merilnem mestu M1 v času do 1000 s

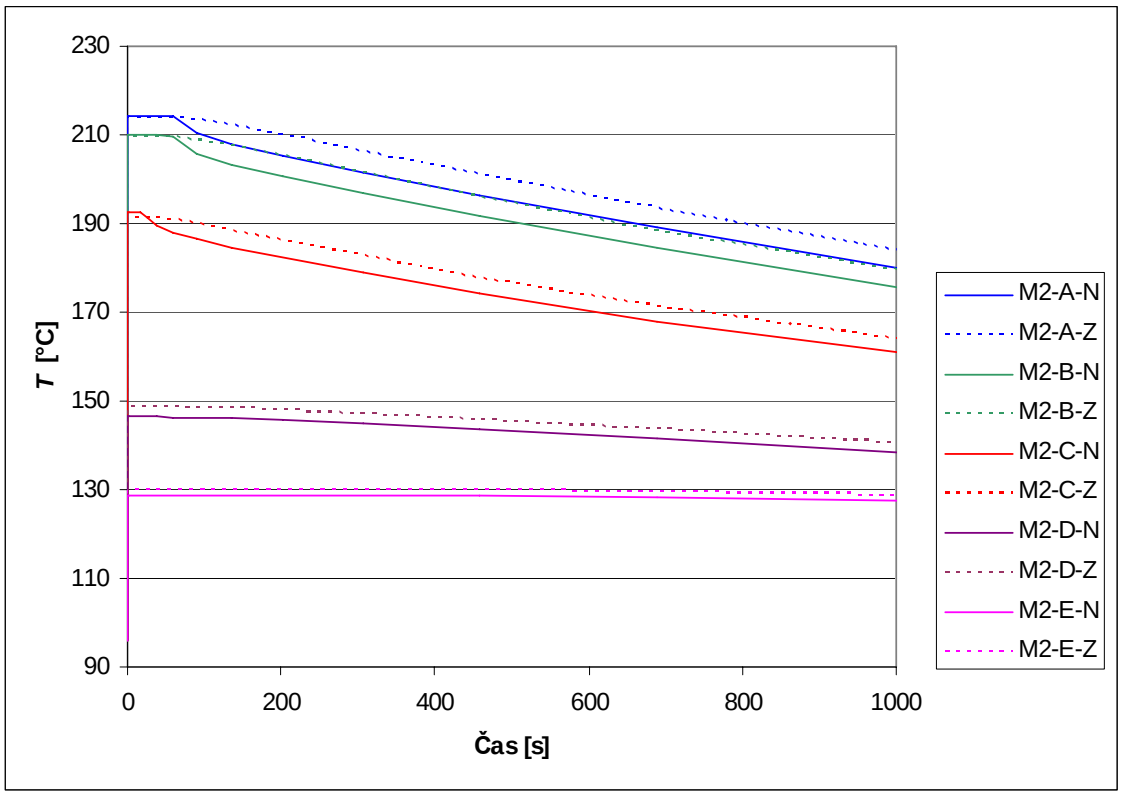

Slika 18 Porazdelitev temperature v notranjih in zunanjih točkah na merilnem mestu M2 v času do 1000 s

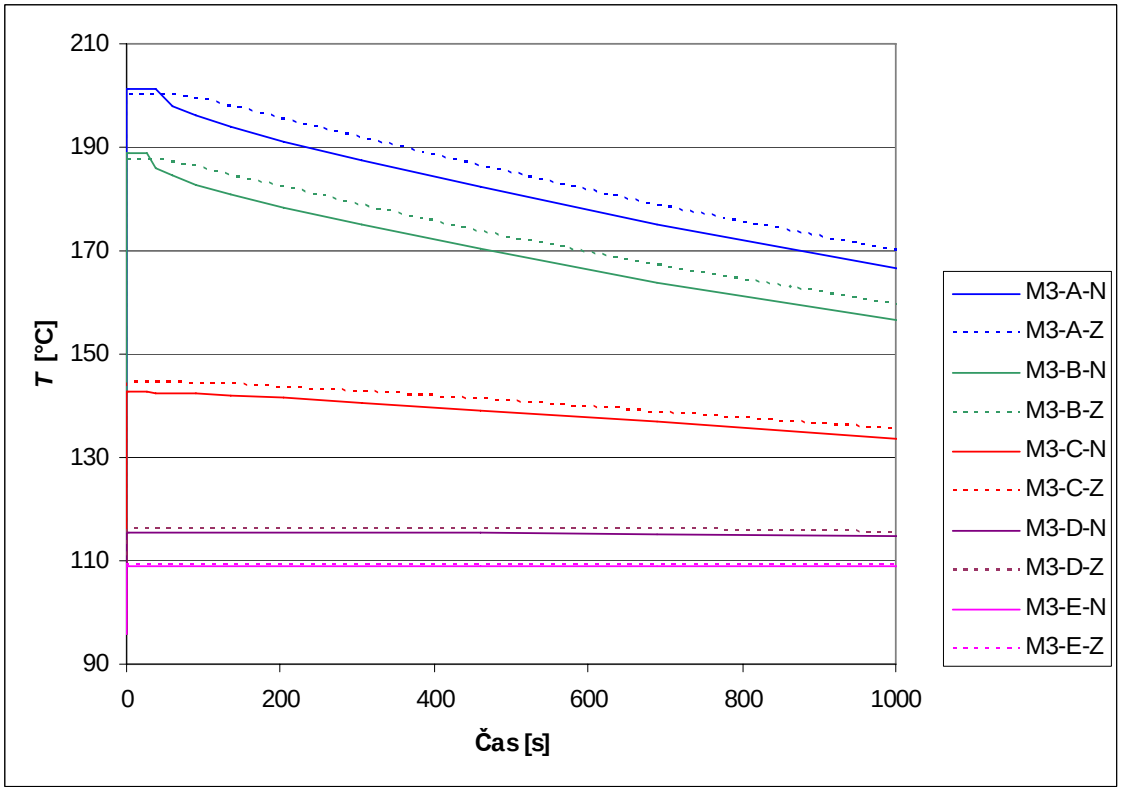

Slika 19 Porazdelitev temperature v notranjih in zunanjih točkah na merilnem mestu M3 v času do 1000 s

Iz rezultatov na sliki 18 je razvidno, da so razlike med notranjimi in zunanjimi temperaturami pri dvigovanju gladine večje v zgornjem delu cevovoda, kjer so tudi največji temperaturni gradienti. Iz diagrama je tudi razvidno, da se je začela temperatura na merilnem mestu M2-A-N spreminjati najkasneje. Temperaturne spremembe v točkah na zunanji površini so bolj gladke, kot na notranji strani. Temperature na zunanji strani so po nižanju temperature v cevovodu po višini višje kakor na notranji strani, kar je posledica vpliva koeficienta prestopa, koeficienta prevoda toplote in omočenosti z vročo in hladno vodo (poglavje 2.1.2).

Slika 19 prikazuje spremembo temperature na merilnem mestu M3.

V primerjavi z rezultati na sliki 18 se pri dvigu gladine temperatura na mestu M3-A-N začne spreminjati prej kot na mestu M2-A-N, saj je mesto M3-A-N nižje po višini kot M2-A-N (Slika 14), zaradi česar do tega mesta prej pride hladen fluid. Pri nižjih merilnih merilnih mestih (M3-D in M3-E) spremembe temperature praktično ni zaznati.

Slika 20 prikazuje spremembo temperature na merilnem mestu M4.

Rezultati kažejo podobno spreminjanje temperature kot pri merilnem mestu M3.

Slika 17 prikazuje spremembo temperature na merilnem mestu M1 v času med 40000 in 60000 s.
Rezultati na sliki 21 kažejo, da je skozi debelino dosežena konstantna temperatura 223°C, kar pomeni, da sprememba gladine med vročim in hladnim hladilom za obravnavani primer ne vpliva na temperaturne spremembe na tem mestu.

Slika 22 prikazuje spremembo temperature na merilnem mestu M2 v času med 40000 s in 60000 s.

Iz rezultatov na sliki 22 je razvidno, da je po gibanju gladine navzdol za merilno mesto M2 temperatura na zunanjih točkah D in E višja od notranje temperature, medtem, ko je v točkah A do C temperatura na notranji strani višja. Do tega pride zaradi interakcije temperatur pri prestopu toplote s tekočine na trdnino in pri prevodu skozi po steni cevi.

Slika 23 prikazuje spremembo temperature na merilnem mestu M3 v času med 40000 s in 60000 s.

Iz rezultatov na sliki 23 je razvidno, da je hitrost spreminjanja temperature manjša kot na merilnem mestu M2.

Slika 24 prikazuje spremembo temperature na merilnem mestu M4 v času med 40000 s in 60000 s.

Primerjava rezultatov z merilnim mestom M2 in M3 pokaže, da je tukaj hitrost spreminjanja temperature najmanjša, ko se gladina na začetku drugega kolena spušča iz zgornje površine proti spodnji površini.

Slika 25 prikazuje največjo Trescovo ekvivalentno napetost med spremembo gladine od spodnje lege do zgornje lege in nazaj. Največja napetost se pojavi v začetnem oz. končnem stacionarnem stanju, torej, ko je gladina v spodnji legi.

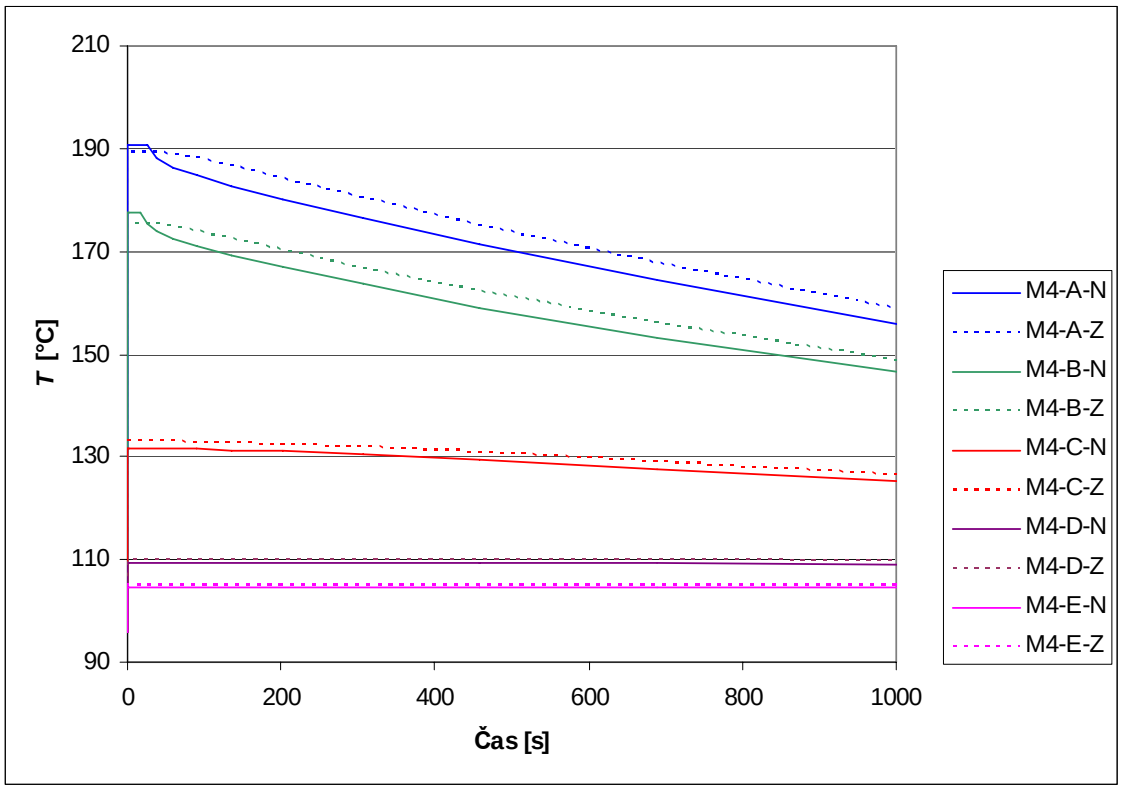

Slika 20 Porazdelitev temperature v notranjih in zunanjih točkah na merilnem mestu M4 v času trajanja cikla do 1000 s

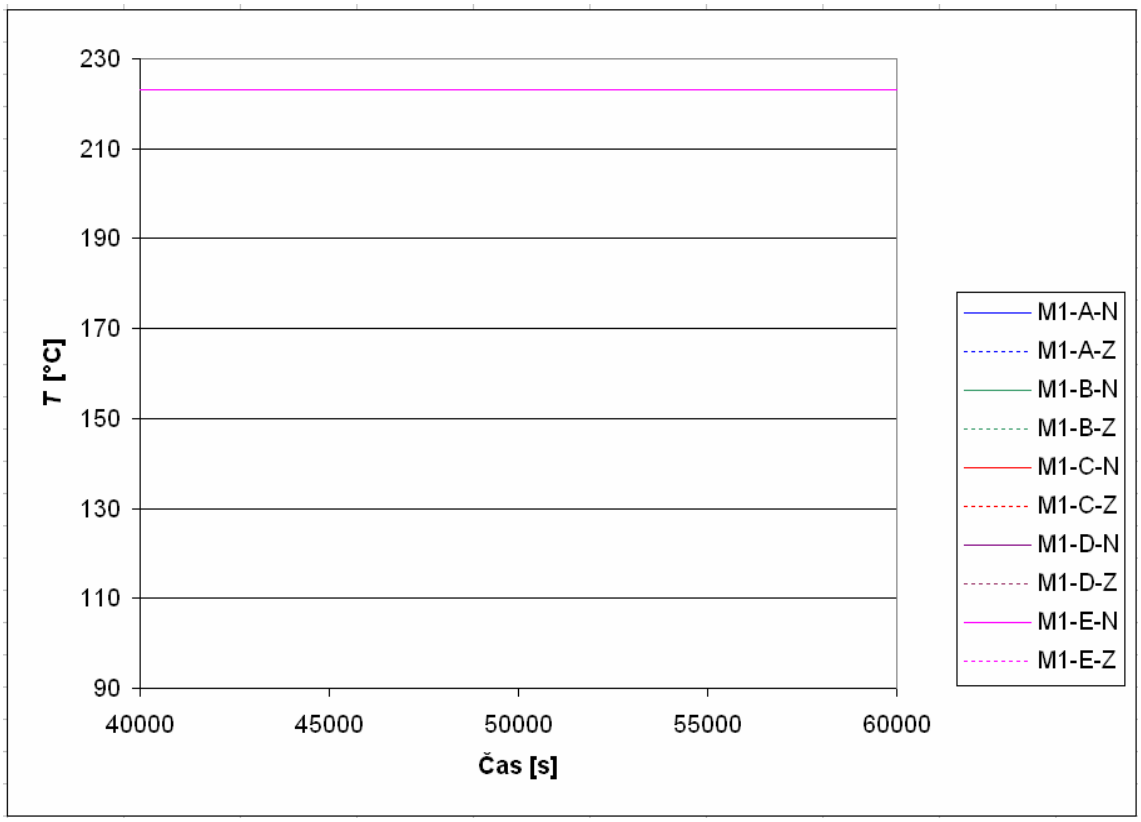

Slika 21 Porazdelitev temperature v notranjih in zunanjih točkah na merilnem mestu M1 v času trajanja cikla med 40000 s in 60000 s

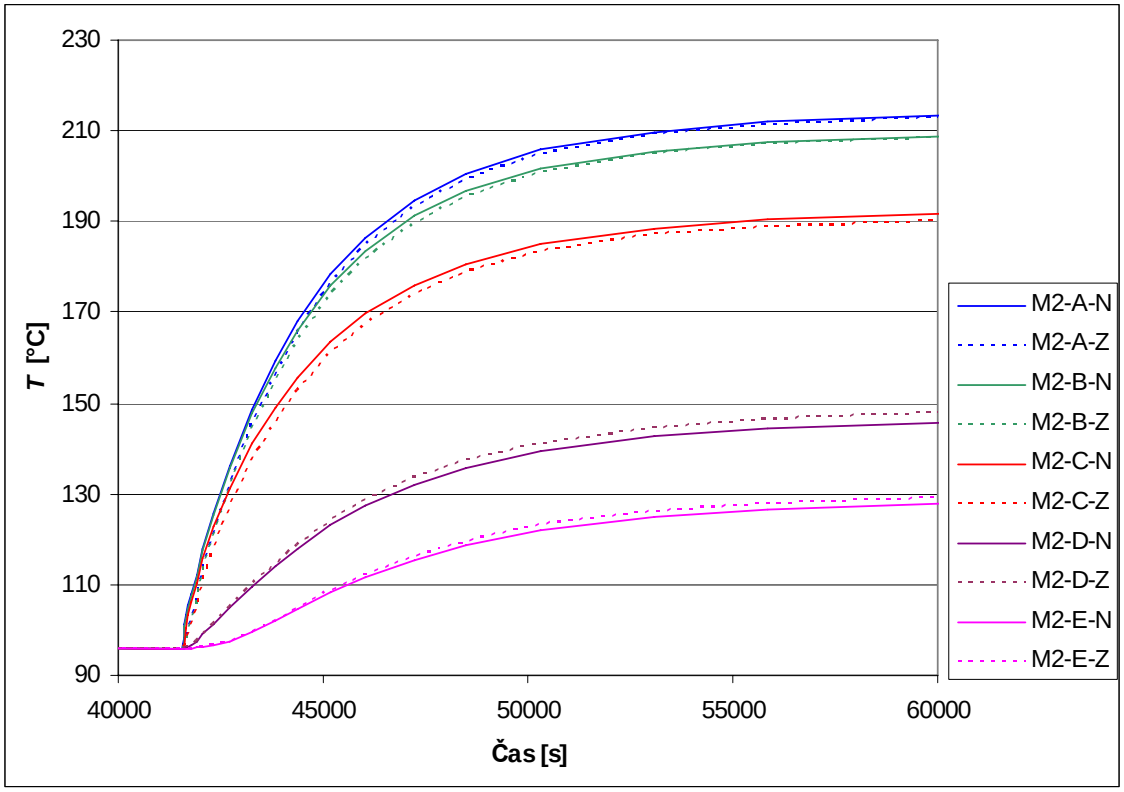

Slika 22 Porazdelitev temperature v notranjih in zunanjih točkah na merilnem mestu M2 v času trajanja cikla med 40000 s in 60000 s

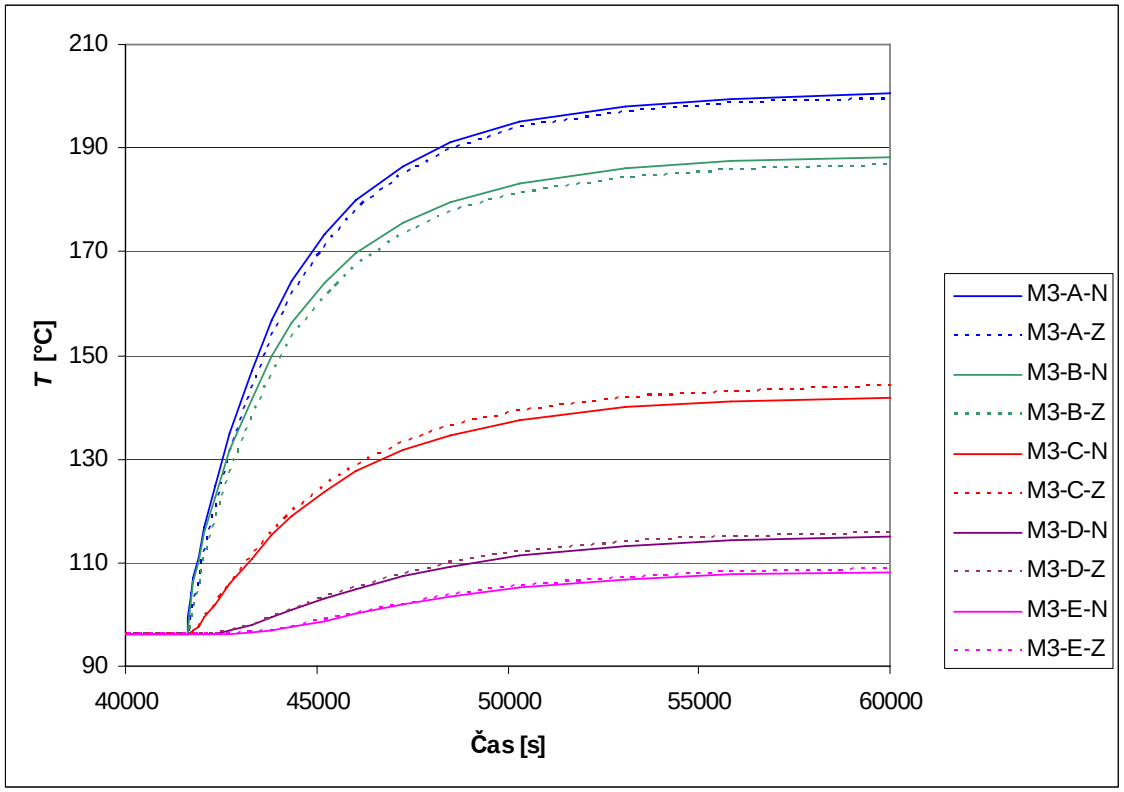

Slika 23 Porazdelitev temperature v notranjih in zunanjih točkah na merilnem mestu M3 v času trajanja cikla med 40000 s in 60000 s

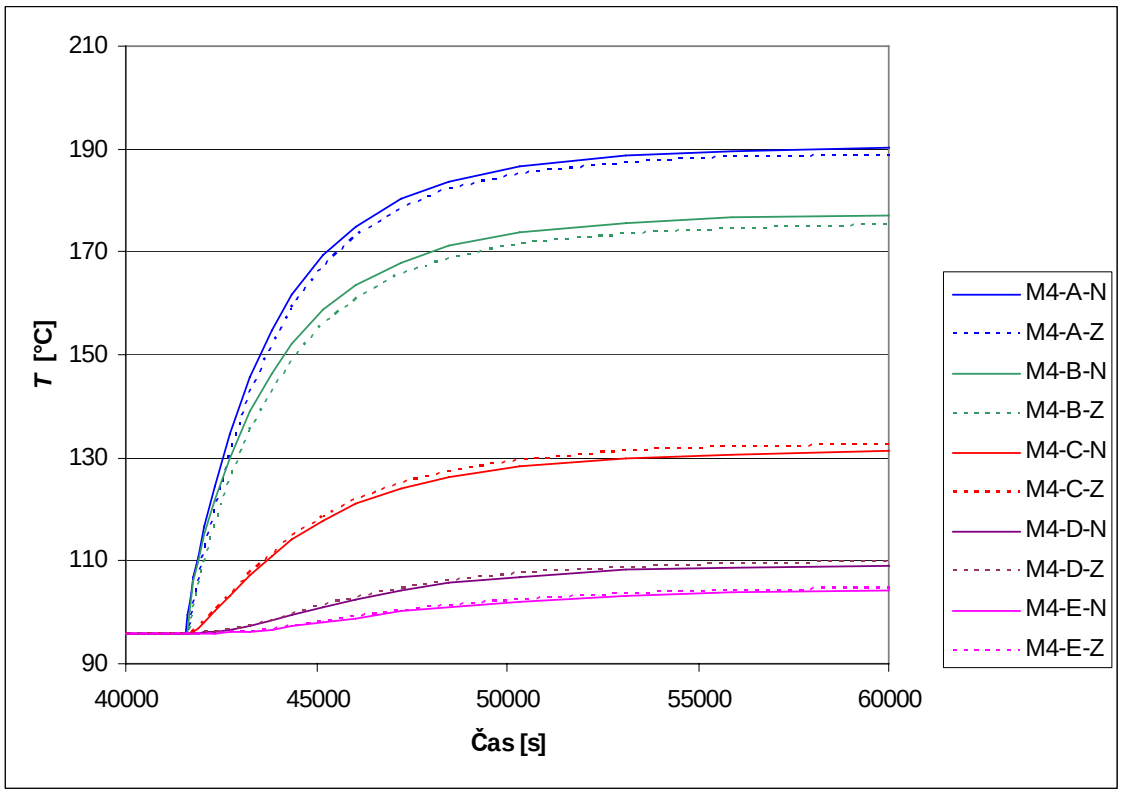

Slika 24 Porazdelitev temperature v notranjih in zunanjih točkah na merilnem mestu M4 v času trajanja cikla med 40000 s in 60000 s

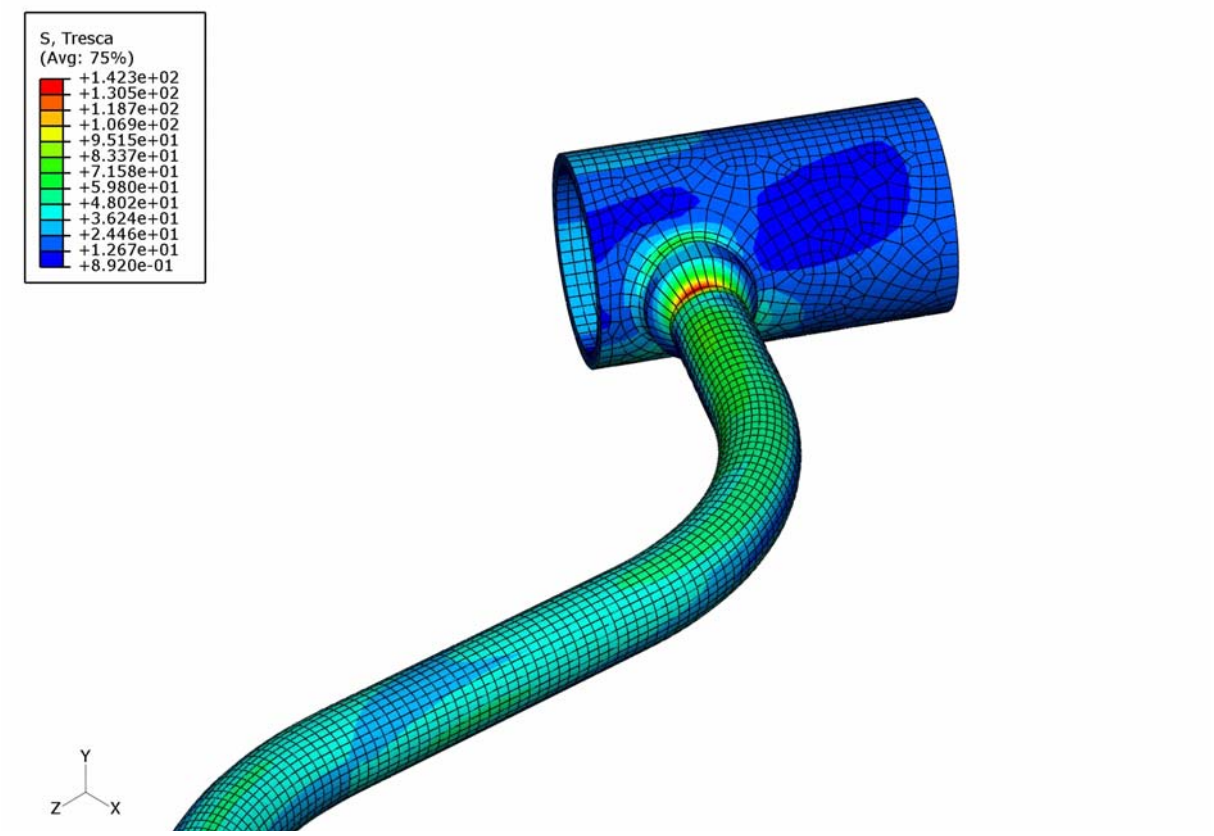

Slika 25 Največja Trescova ekvivalentna napetost pri enem ciklu z vmesnih stacionarnim stanjem

Amplituda nihanja napetosti S_a = 71,2 MPa se izračuna kot polovica Tresca ekvivalentne napetosti [1]. Na osnovi S_a določimo dopustno število obremenitev N = $3{,}18 \cdot 10^8$ iz ustrezne Wöhlerjeve krivulje (krivulja za avstenitne materiale z S_a < 198,6 MPa). Delni faktor izrabe za eno ponovitev prehodnega pojava je tako $u_1 = 3{,}15 \cdot 10^{-9}$.

Pri analizi spoja izstopne šobe iz reaktorske posode smo ugotovili, da ima tlak večji vpliv na napetosti kot temperaturne spremembe. V prelivnem vodu povzroča tlak 2,5 MPa največjo Trescovo ekvivalentno napetost v velikosti 15,7 MPa, kar je mnogo manj kot jo povzroča toplotno razslojevanje. Zato je v primeru prelivnega voda potrebno posebno pozornost posvetiti temperaturnim obremenitvam.

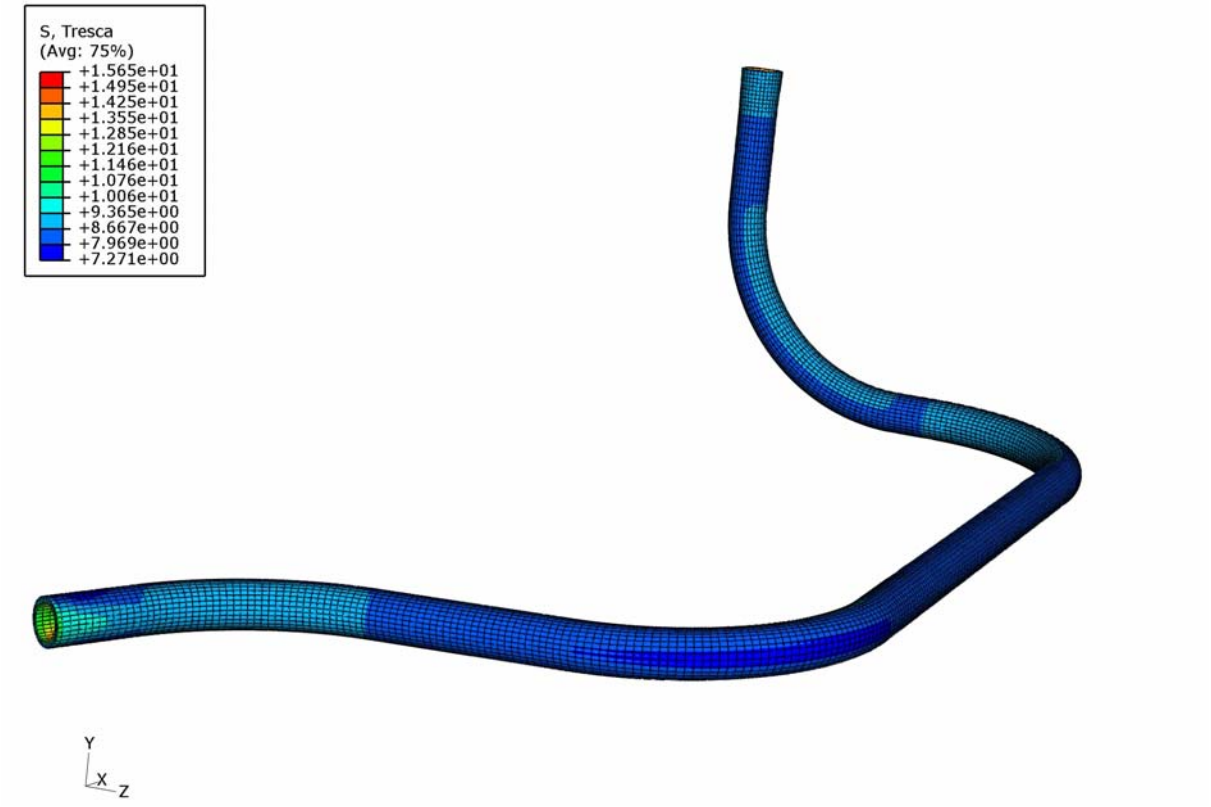

Slika 26 Vpliv tlaka 2,5 MPa na Tresca ekvivalentno napetost v prelivnem vodu

V primeru, da se gladina dvigne od spodnje površine do zgornje površine cevovoda in nato takoj nazaj v izhodiščno lego, prikazuje slika 27 porazdelitev temperature v vmesnih stanjih.

Iz rezultatov na sliki 27 je razvidno, da je sprememba temperature na zunanji površini mnogo manj izrazita, kot je v primeru, če gladina v zgornji legi stoji toliko časa, da se vzpostavi stacionarno stanje (Slika 15).

V primeru, da se gladina dvigne od spodnjega robu do zgornjega robu cevovoda in takoj nazaj v izhodiščno lego, se temperatura za cel cikel na merilnem mestu M4-A spreminja kot prikazuje slika 27.

Slika 29 prikazuje spremembo temperature na merilnem mestu M1.

Iz rezultatov na sliki 28 je razvidno, da je po celem obodu in skozi debelino dosežena konstantna temperatura 223°C in da obravnavana sprememba gladine med vročim in hladnim fluidom ne vpliva na temperaturne spremembe na tem mestu.

Slika 30 prikazuje spremembo temperature na merilnem mestu M2.

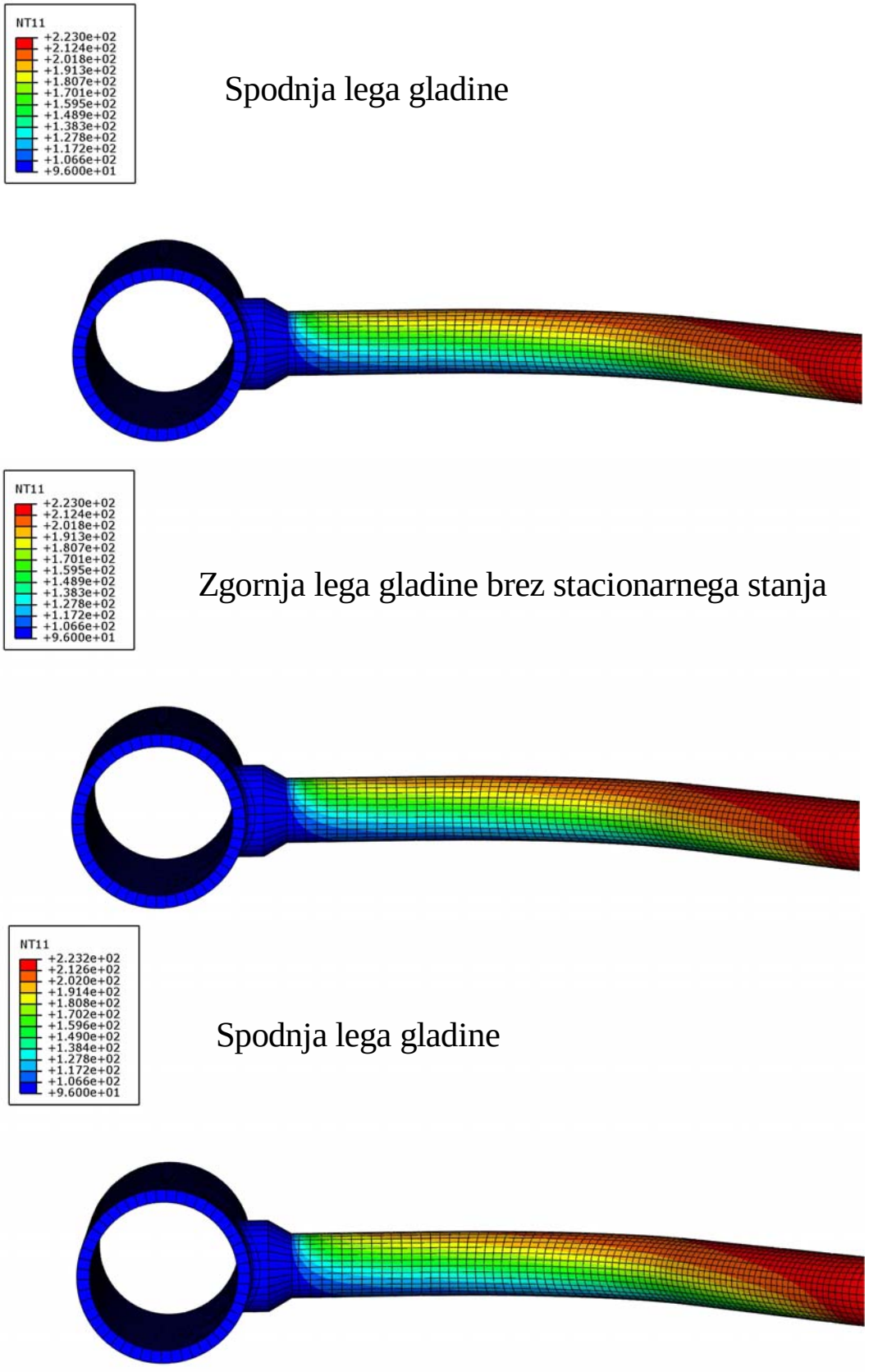

Slika 27 Porazdelitev temperature pri spremembi lege gladine iz spodnje do zgornje in nazaj do spodnje brez vmesnega stacionarnega stanja v zgornji legi

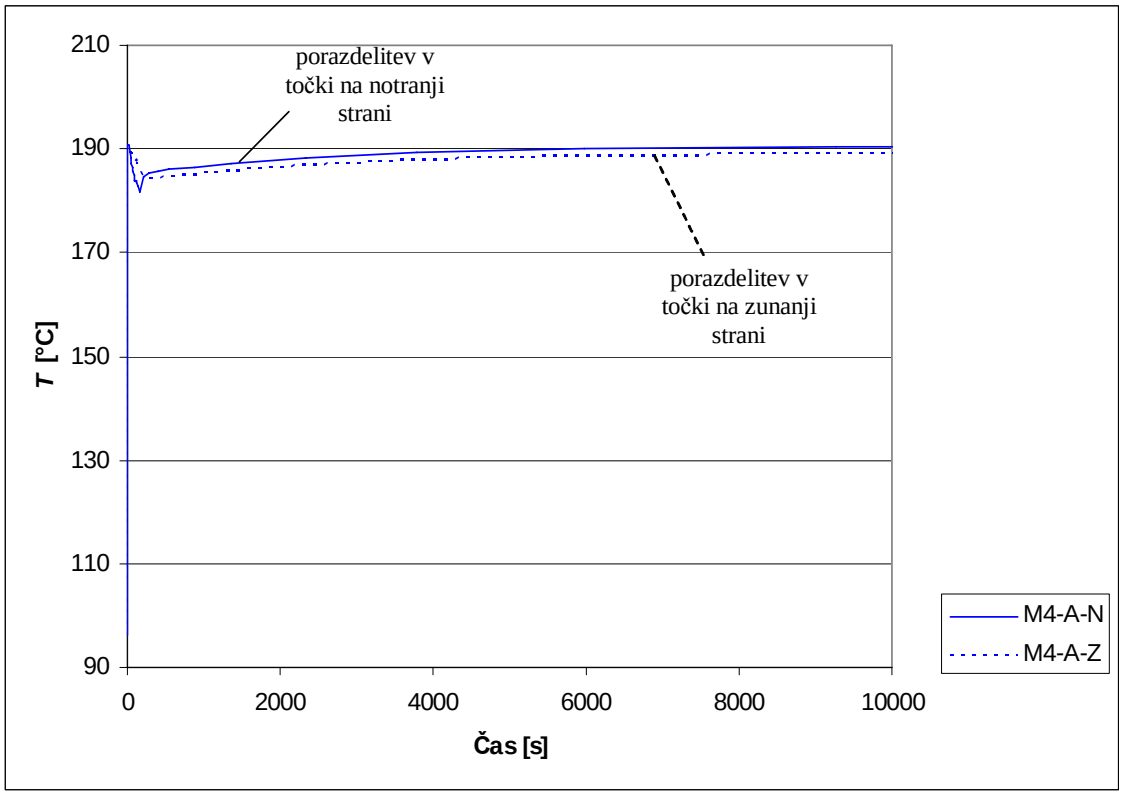

Slika 28 Porazdelitev temperature v notranji (M4-A-N) in zunanji (M4-A-Z) točki pri spremembi lege gladine (en cikel) brez vmesnega stacionarnega stanja

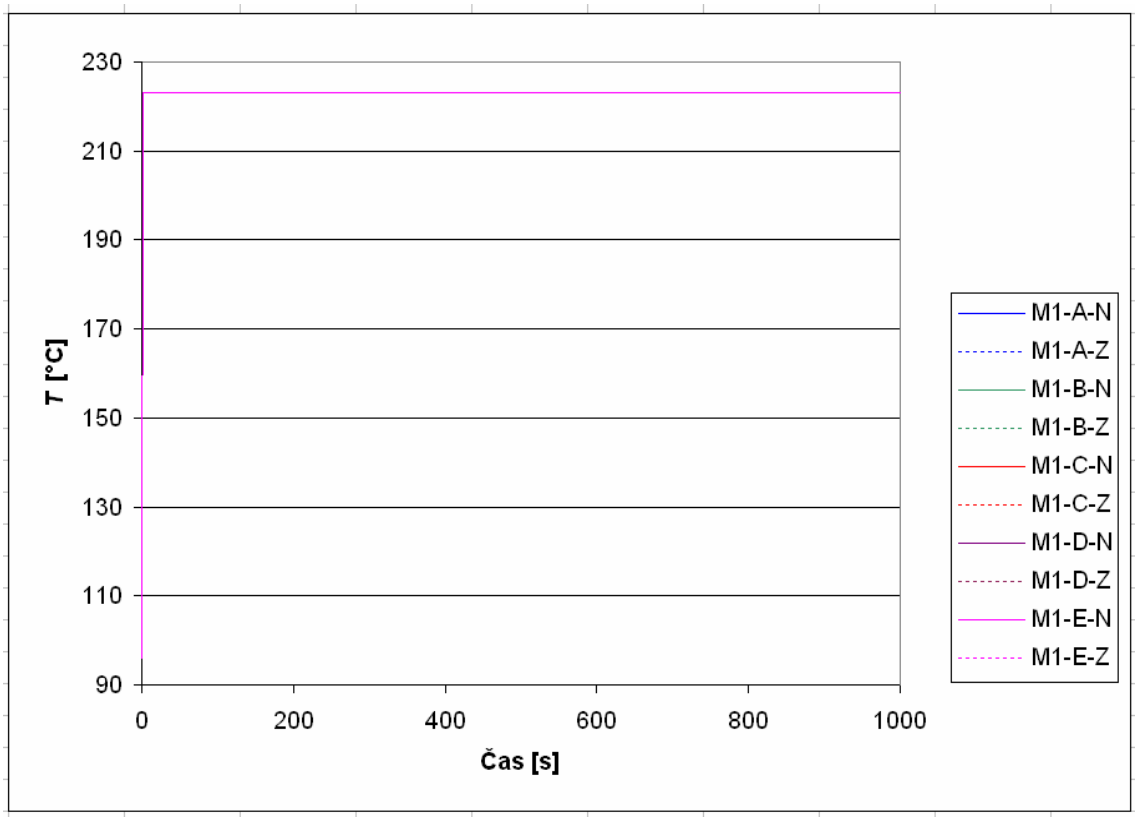

Slika 29 Porazdelitev temperature v notranjih in zunanjih točkah na merilnem mestu M1 v času trajanja cikla do 1000 s

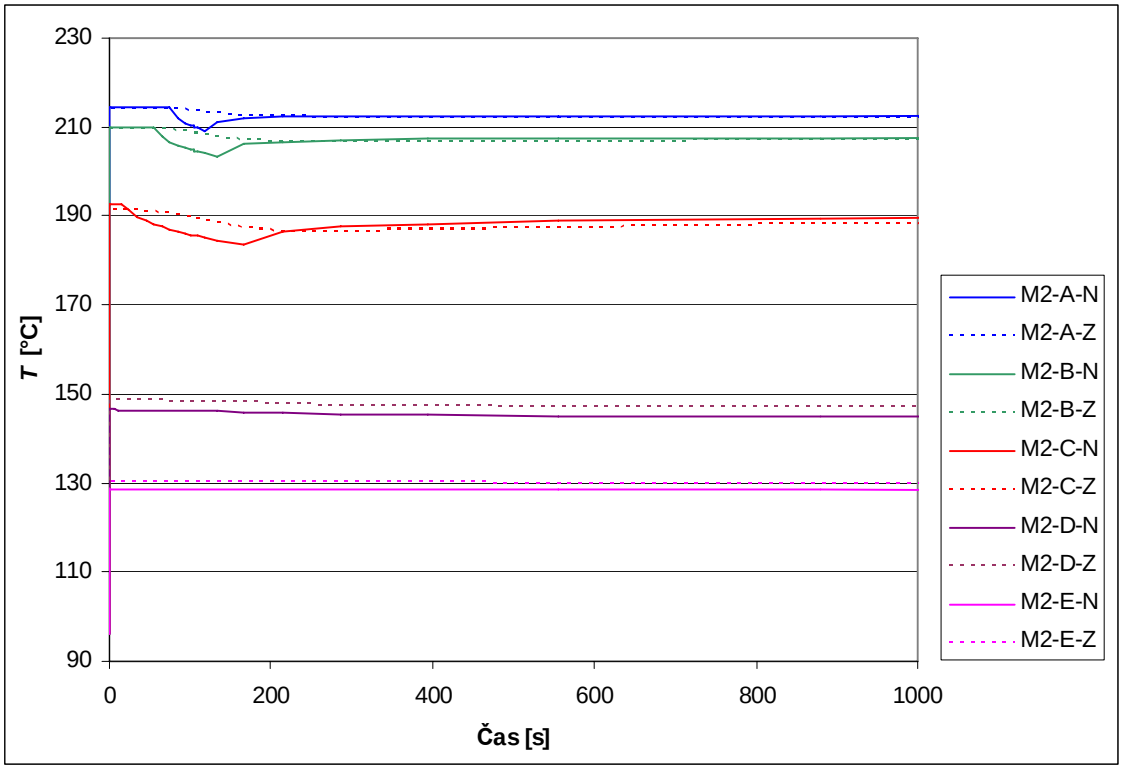

Slika 30 Porazdelitev temperature v notranjih in zunanjih točkah na merilnem mestu M2 v času trajanja cikla do 1000 s

Iz rezultatov na sliki 30 je razviden čas trajanja spremembe temperature na notranji strani cevovoda, pri čemer je na merilnih mestih D in E sprememba temperature najmanj izrazita. Iz rezultatov je tudi razvidno, da se je sprememba na merilnem mestu A začela najkasneje in se je tudi najhitreje končala, kar je skladno z gibanjem gladine. Spremembe v točkah na zunanji površini so gladke in ne pokažejo na način spremembe gibanja gladine v cevovodu.

Slika 31 prikazuje spremembo temperature na merilnem mestu M3. V primerjavi z rezultati na sliki 30 traja temperaturna sprememba na notranji strani dlje časa, vendar tudi tukaj te spremembe na zunanji strani ni zaznati.

Slika 32 prikazuje spremembo temperature na merilnem mestu M4.Temperaturna sprememba na notranji strani je na merilnem mestu M4 trajala najdlje, pri čemer so spremembe na notranji strani praktično opazne samo za točke A in B. Na zunanji strani sprememb temperature na način, kot se spreminja na notranji strani, ni mogoče opaziti.

Slika 33 prikazuje največjo Tresca ekvivalentno napetost med spremembo gladine od spodnje lege do zgornje lege in nazaj brez vmesnega stacionarnega stanja. Največja napetost se pojavi v začetnem oz. končnem stacionarnem stanju, torej, ko je gladina v spodnji legi. Rezultat je enak kot v primeru z vmesnim stacionarnim stanjem, kar pomeni, da v obravnavanem primeru hitrost spremembe gladine iz zgornjega v spodnje stanje nima vpliva na največjo napetost.

Amplituda nihanja napetosti S_a = 71,2 MPa se izračuna kot polovica Trescove ekvivalentne napetosti [1]. Na osnovi S_a določimo dopustno število obremenitev N = $3{,}18 \cdot 10^8$ iz ustrezne Wöhlerjeve krivulje (krivulja za avstenitne materiale z S_a < 198,6 MPa). Delni faktor izrabe za eno ponovitev prehodnega pojava je tako $u_1 = 3{,}15 \cdot 10^{-9}$.

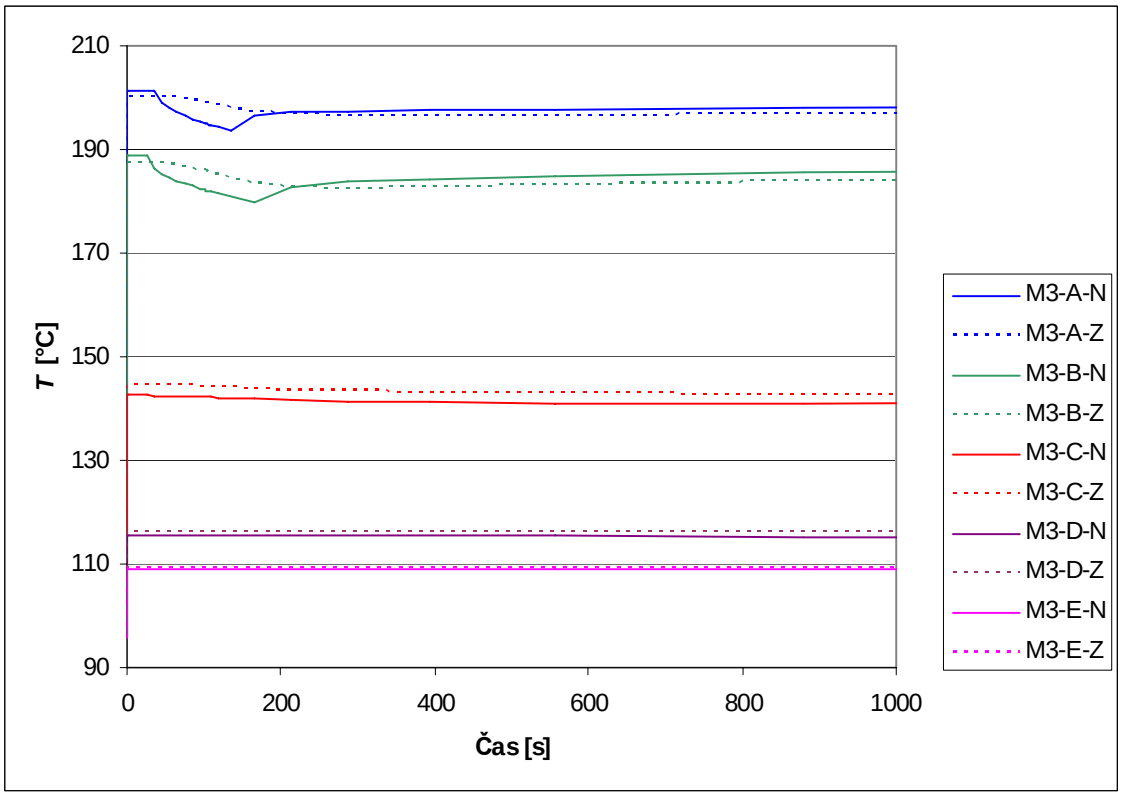

Slika 31 Porazdelitev temperature v notranjih in zunanjih točkah na merilnem mestu M3 v času trajanja cikla do 1000 s

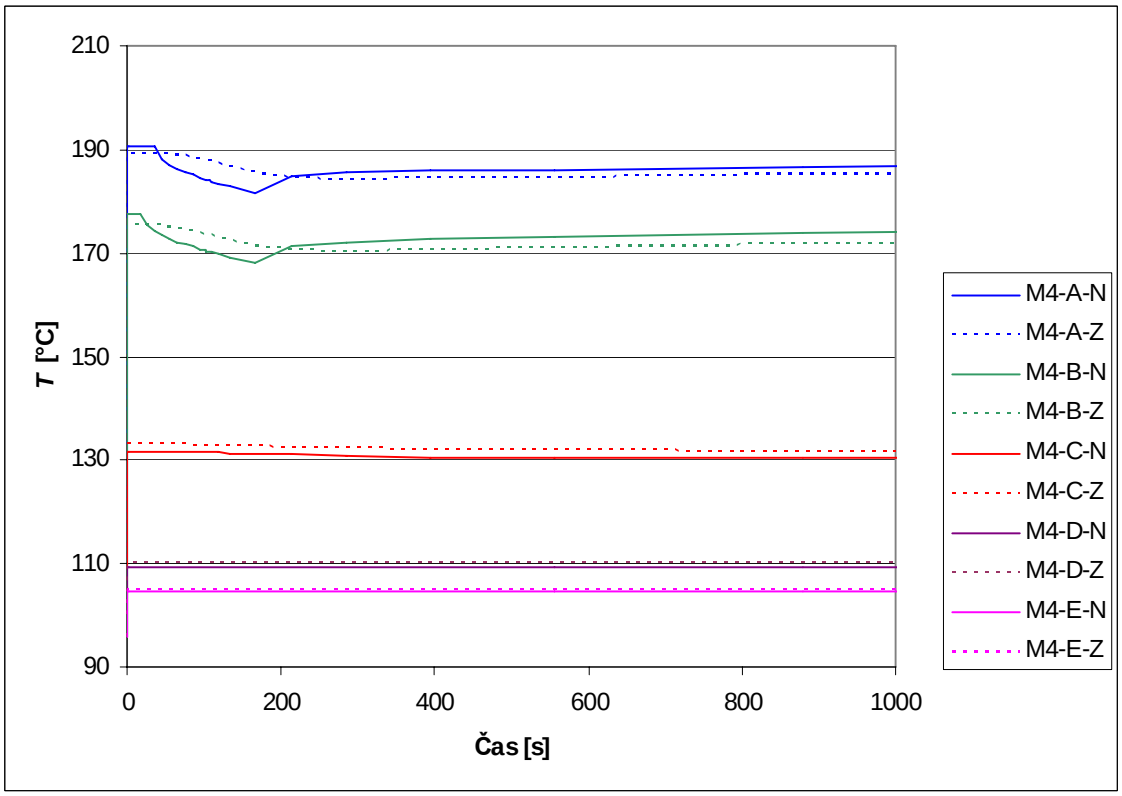

Slika 32 Porazdelitev temperature v notranjih in zunanjih točkah na merilnem mestu M4 v času trajanja cikla do 1000 s

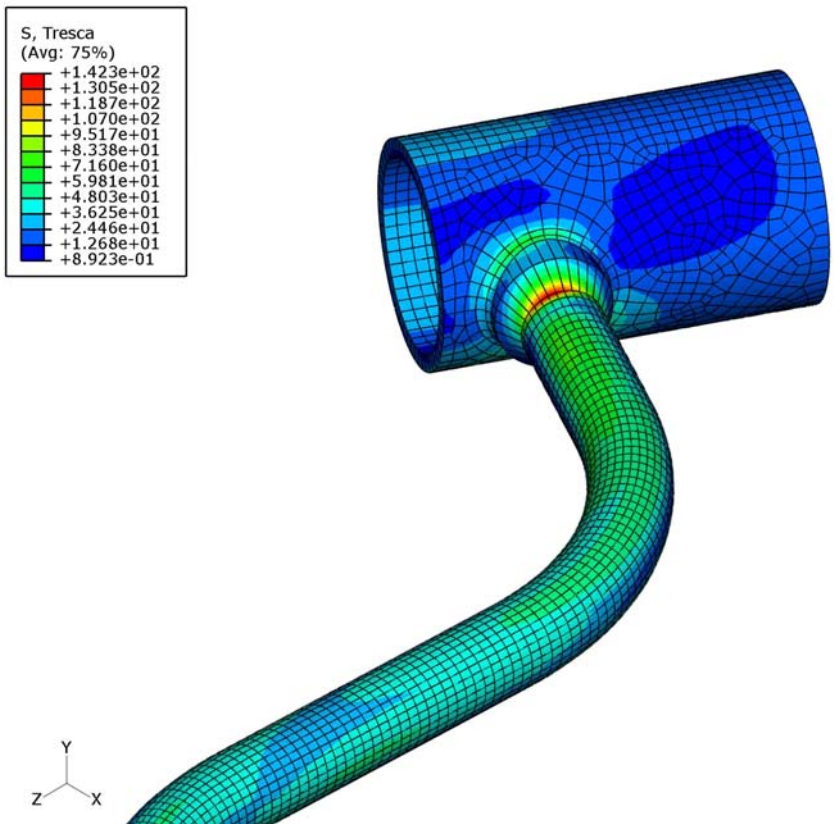

Slika 33 Največja Trescova ekvivalentna napetost pri enem ciklu brez vmesnega stacionarnega stanja

4.5.2 Toplotni šok

Kot rezultat analize predstavljamo:

1. časovno odvisno porazdelitev temperature na notranji in zunanji steni cevovoda na mestu M2, kjer smo hipotetično predpostavili merilec temperature po zunanjem obodu cevovoda (Slika 13).
2. največjo vrednost Trescove ekvivalentne napetosti in faktor izrabe.

Obravnavali smo dva primera:

1. meja med vročim in hladnim hladilom se v končni legi ustavi in stoji, dokler ni vzpostavljeno stacionarno stanje in nato potuje nazaj v izhodiščno lego.
2. meja med vročim in hladnim hladilom se po zaustavitvi v vmesni legi giba takoj nazaj v izhodiščno lego.

Za spremembo lege meje med vročim in hladnim hladilom iz začetne lege v skrajno lego vzdolž cevovoda, kjer meja stoji toliko časa, da se vzpostavi stacionarno stanje in se šele po tem vrne v izhodiščno lego, prikazuje slika 34 temperaturne porazdelitve v izbranih stanjih. Ker se vertikalna meja giba, vsa merilna mesta po obodu cevovoda kažejo enako temperaturo (Slika 35). Zato bomo v nadaljevanju prikazovali rezultate le za točko A merilnega mesta M2.

Zaradi lažje predstavitve rezultatov bomo prikazali porazdelitev temperature za čas:

- od 0 do 40 s, ko se je meja gibala preko merilnega mesta M2 in
- od 4000 do 7000 s, kar zajema čas preden je gladina dosegla stacionarno stanje v skrajni vzdolžni legi, in čas po tem, ko se je meja gibala nazaj v izhodiščno mesto.

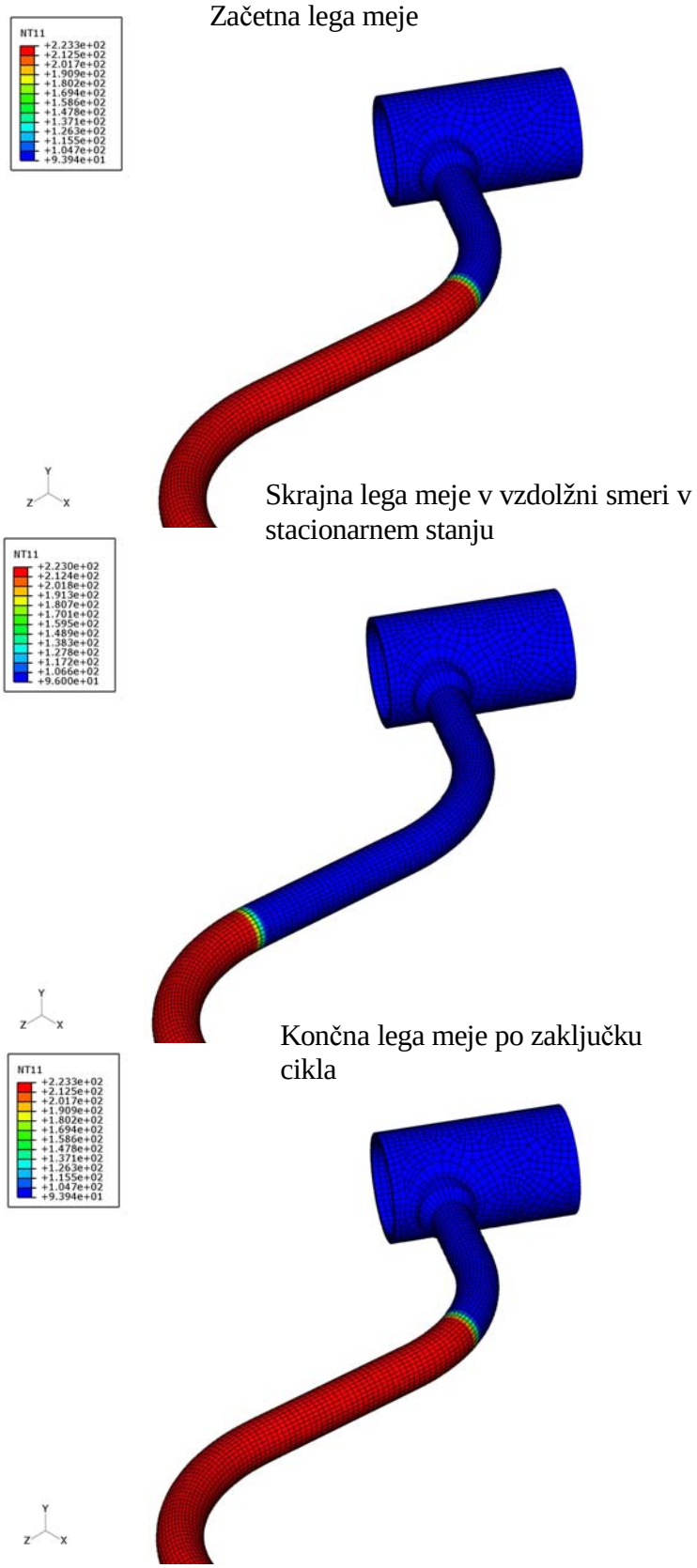

Slika 34 Porazdelitev temperature pri spremembi lege gladine v vzdolžni smeri cevovoda z vmesnim stacionarnim stanjem v skrajni vzdolžni legi

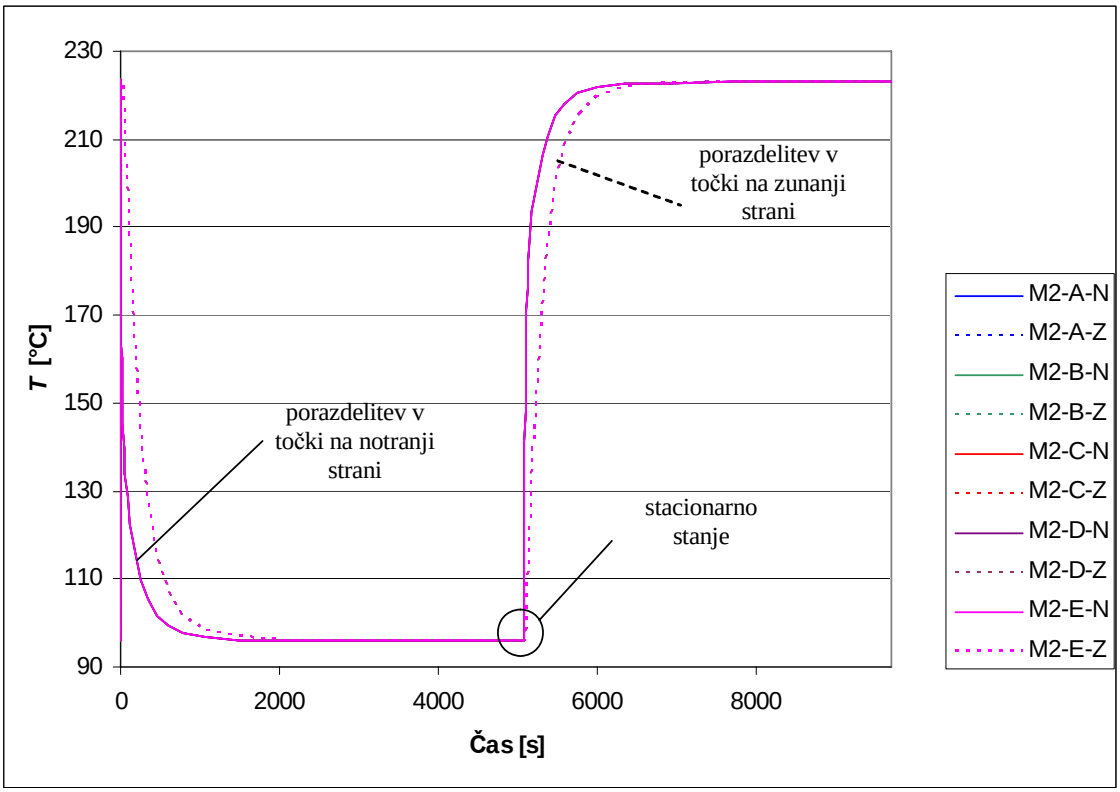

Slika 35 Porazdelitev temperature v notranji (M2-A-N) in zunanji (M2-A-Z) točki pri potovanju motnje preko tega merilnega mesta z vmesnim stacionarnim stanjem (en cikel)

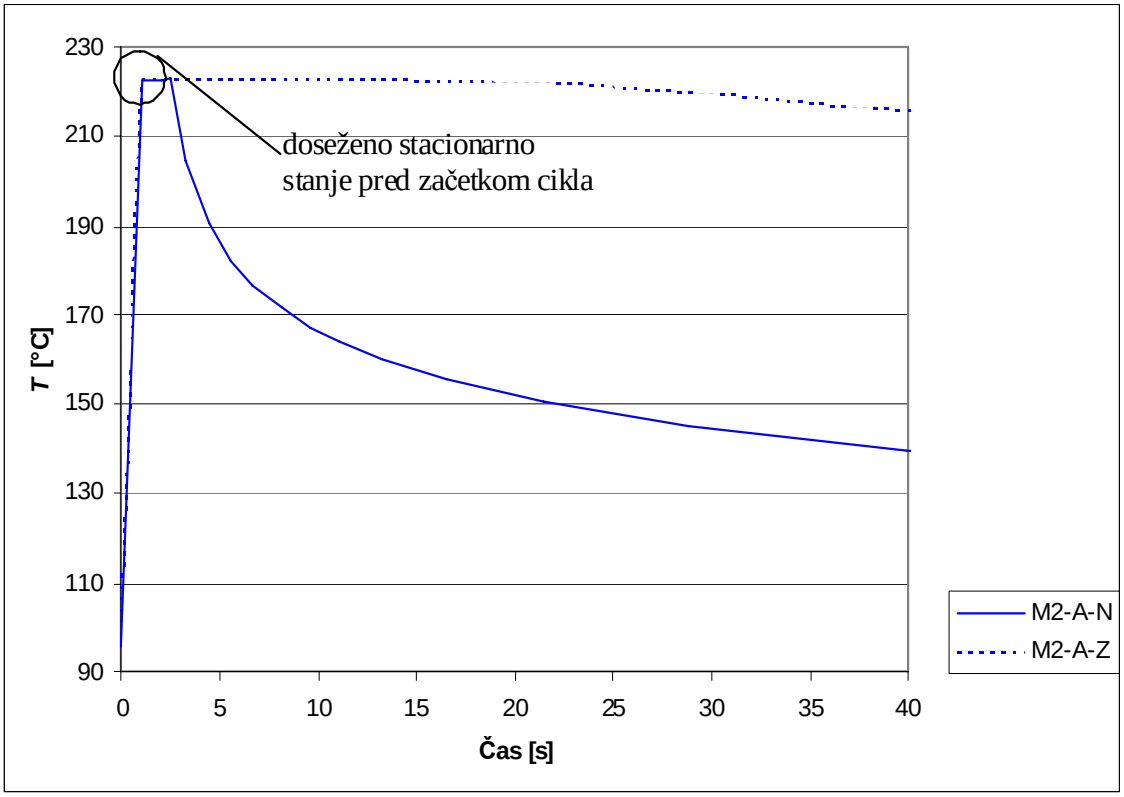

Slika 36 Porazdelitev temperature v notranji (M2-A-N) in zunanji (M2-A-Z) točki pri potovanju motnje preko tega merilnega mesta za čas do 40 s

Iz rezultatov na sliki 36 je razvidna velika razlika med temperaturo na notranji strani in temperaturo na zunanji strani, kar pomeni, da se je gladina gibala tako hitro, da zunaj ni mogoče zaznati te spremembe, ko je gladina dosegla skrajno sprednjo točko po času 5,25 s.

Slika 37 prikazuje spremembo temperature na merilnem mestu M2 za čas od 4000 do 7000 s.

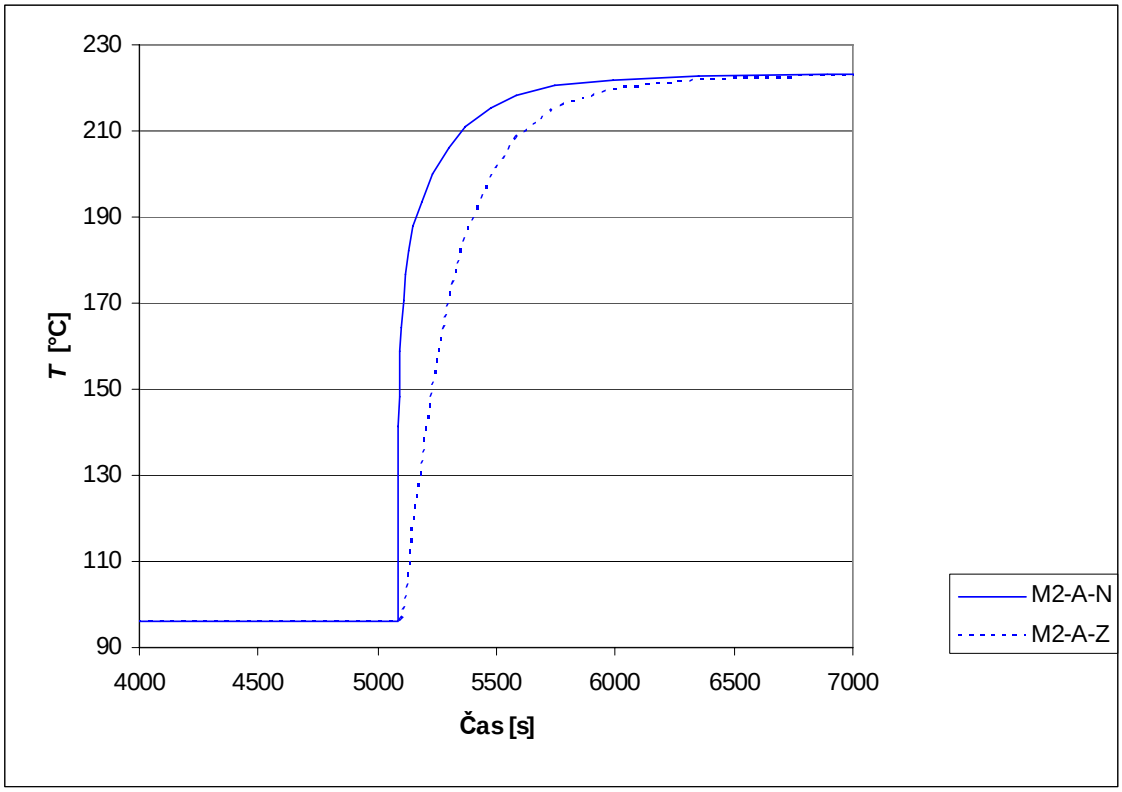

Slika 37 Porazdelitev temperature v notranji (M2-A-N) in zunanji (M2-A-Z) točki pri potovanju motnje preko tega merilnega mesta za čas od 4000 do 7000 s

Iz rezultatov na sliki 37 je razvidno hitro naraščanje temperature namerilnem mestu M2 zaradi velike hitrosti gibanja meje in kasnejše počasno spremembo do stacionarnega stanja.

Slika 38 prikazuje največjo Trescovo ekvivalentno napetost med spremembo meje v vzdolžni smeri iz začetnega stanja naprej do skrajne lege v vzdolžni smeri in nazaj v izhodiščno lego z vmesnim stacionarnim stanjem v skrajni vzdolžni legi (Slika 34). Največja napetost se pojavi v času 38,81 s po začetku gibanja gladine, kar pomeni, da v času, ko je meja med vročim in hladnim hladilom že bila v skrajni vzdolžni legi.

Amplituda nihanja napetosti S_a = 159,7 MPa se izračuna kot polovica Tresca ekvivalentne napetosti [1]. Na osnovi S_a določimo dopustno število obremenitev N = $2{,}02 \cdot 10^6$ iz ustrezne Wöhlerjeve krivulje (krivulja za avstenitne materiale z S_a < 198,6 MPa). Delni faktor izrabe za eno ponovitev prehodnega pojava je tako $u_1 = 4{,}95 \cdot 10^{-7}$.

Za gibanje vertikalne meje med vročim in hladnim hladilom tako, da ni vmesnega stacionarnega stanja, prikazuje temperaturne porazdelitve po obodu cevovoda v skrajnih legah slika 39.

Slika 39 prikazuje spremembo temperature na merilnem mestu M2, ko se meja med vročim in hladnim hladilom giba v vzdolžni smeri proti skrajni legi in nazaj v izhodišče.

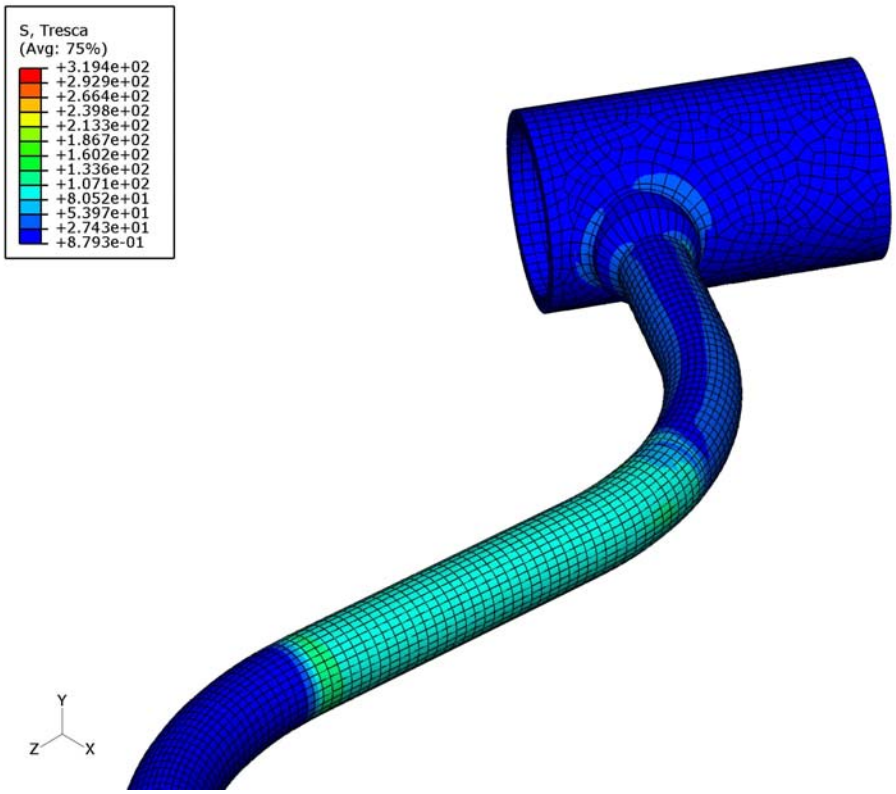

Slika 38 Največja Trescova ekvivalentna napetost pri ciklu z vmesnim stacionarnim stanjem

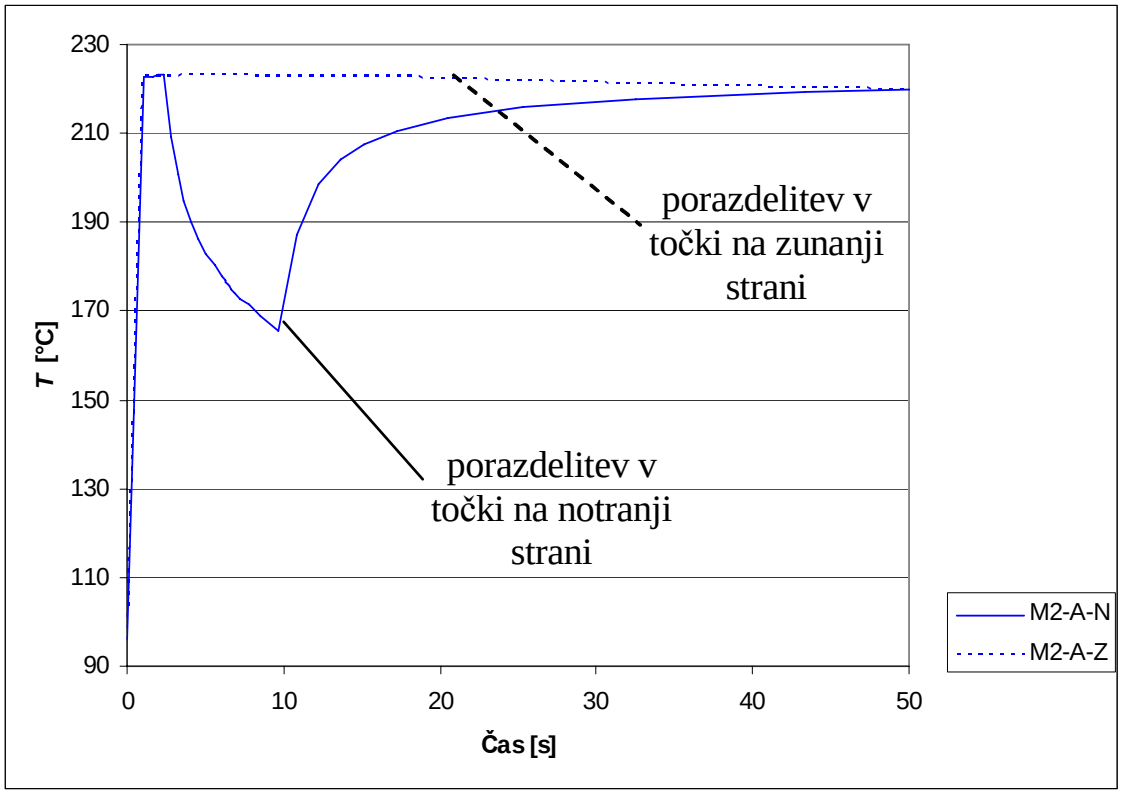

Slika 39 Porazdelitev temperature v notranji in zunanji točki na merilnem mestu M2 pri ciklu spremembe lege gladine hladila brez vmesnega stacionarnega stanja

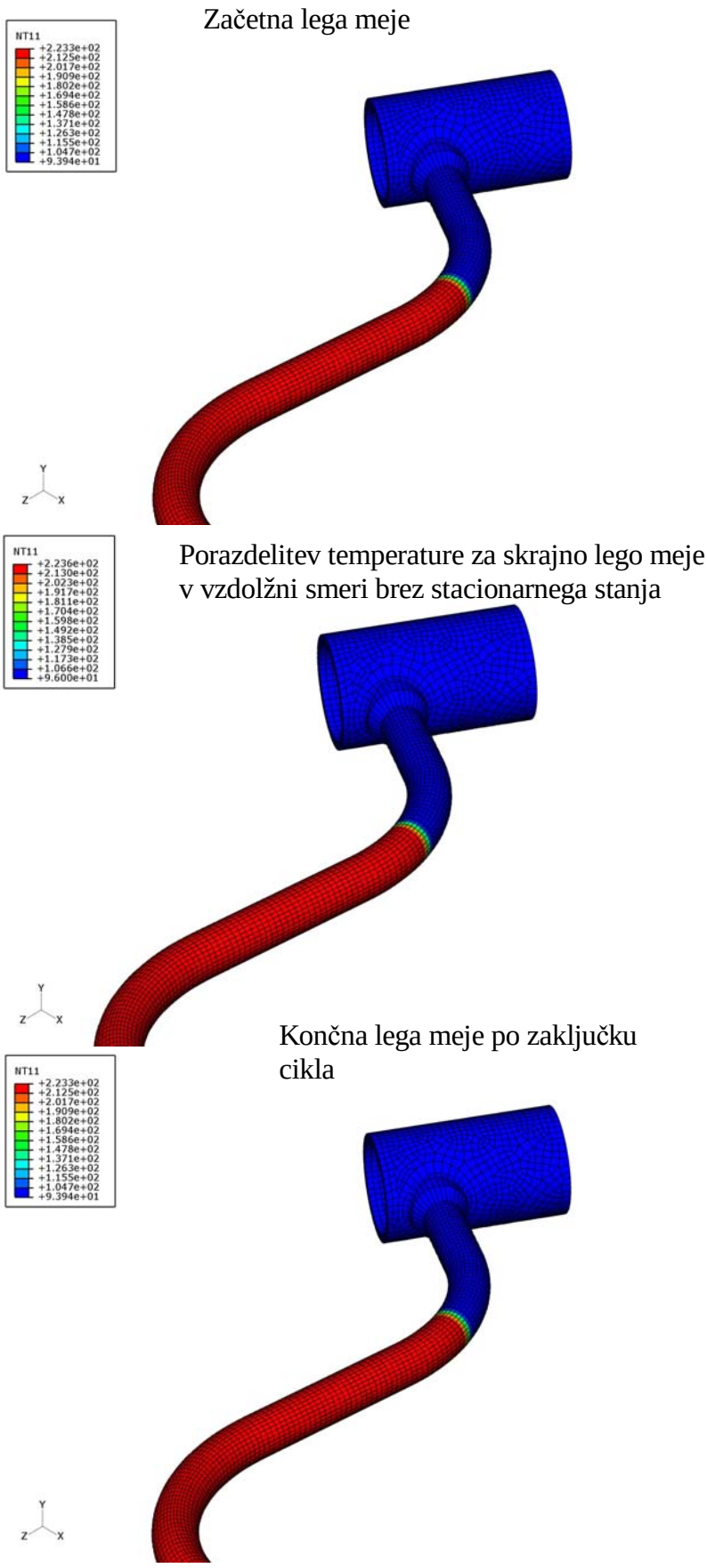

Slika 40 Porazdelitev temperature pri spremembi lege gladine v vzdolžni smeri cevovoda brez vmesnega stacionarnega stanja v skrajni vzdolžni legi

Iz rezultatov na sliki 40 je razvidno, da se je gladina gibala v času približno 10 s nazaj proti izhodiščni legi. Potek temperature na zunanji strani kaže na to, da merilec ne bi mogel zaznati takšne spremembe temperature v cevovodu, saj temperatura pada zelo počasi.

Slika 41 prikazuje največjo Trescovo ekvivalentno napetost med spremembo meje med vročim in hladnim hladilom v vzdolžni smeri naprej in nazaj brez vmesnega stacionarnega stanja. Največja napetost se pojavi v času 5,25 s po začetku gibanja meje, kar pomeni, da v času, ko je meja dosegla skrajno vzdolžno lego.

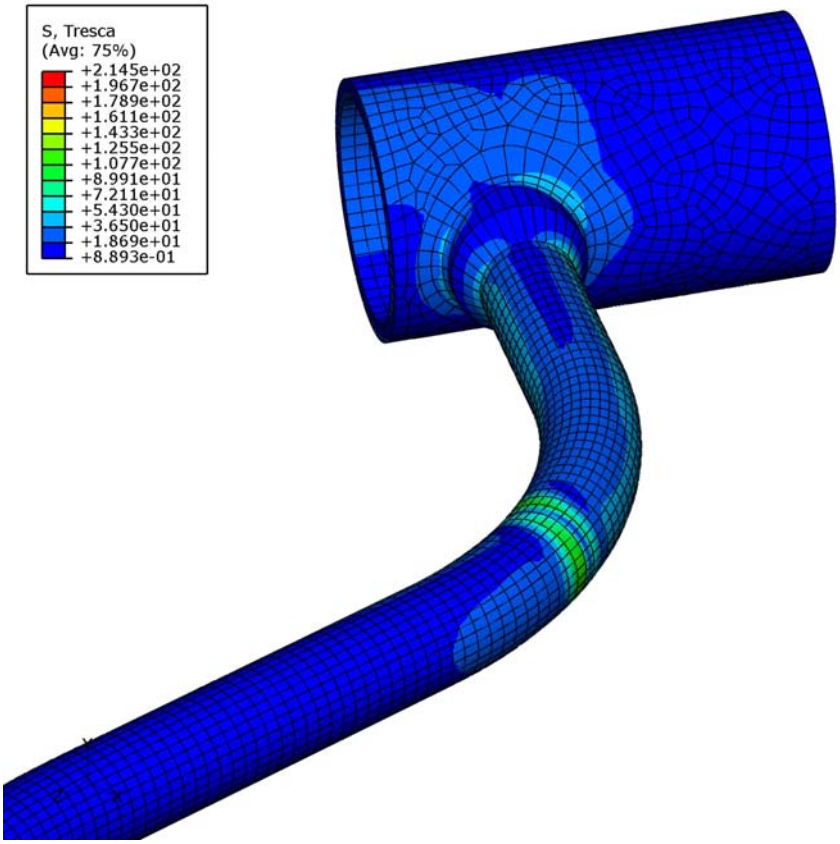

Slika 41 Največja Tresca ekvivalentna napetost pri enem ciklu brez vmesnega stacionarnega stanja

Amplituda nihanja napetosti S_a = 107,3 MPa se izračuna kot polovica Tresca ekvivalentne napetosti [1]. Na osnovi S_a določimo dopustno število obremenitev N = $9{,}14 \cdot 10^6$ iz ustrezne Wöhlerjeve krivulje (krivulja za avstenitne materiale z S_a < 198,6 MPa). Delni faktor izrabe za eno ponovitev prehodnega pojava je tako $u_1 = 1{,}09 \cdot 10^{-7}$.

Primerjava rezultatov z vmesnim stacionarnim stanjem in brez njega pokaže, da slednje bolj ugodno vpliva na napetosti, saj v tem primeru toplota ni imela dovolj časa za prestop na trdnino, s čemer bi temperaturno obremenjevala cevovod.

.

5 ZAKLJUČKI

V poročilu demonstriramo uporabo metode za izračun faktorja izrabe v izbranih komponentah na dveh pilotnih primerih: izstopni šobi reaktorske tlačne posode (proti vroči veji) in prelivnem vodu tlačnika. Izbor pilotnih primerov zagotavlja tudi širok spekter obremenitvenih primerov: za prelivni vod tlačnika je namreč znano, da je lahko obremenjen tudi s toplotnim razslojevanje in toplotnimi šoki.

Z modelom izstopne šobe reaktorske tlačne posode smo ocenili faktor izrabe za projektne in dejanske prehodne pojave v jedrski elektrarni Krško: ogrevanje in ohlajanje elektrarne ter ustavitev reaktorja s polne moči brez ohlajanja. Primerjava izračunanih faktorjev izrabe je pokazala, da je dejanska izraba obravnavanih komponent za obravnavane prehodne pojave manjša od predvidene v projektu. To spoznanje je lahko pomembno tudi s stališča morebitnega podaljševanja obratovalne dobe elektrarne. Seveda pa bi bilo za dokončno odločitev potrebno ovrednotiti vse projektne in dejanske prehodne pojave.

Pokazali smo tudi mogoče vplive toplotnega razslojevanja in termičnega šoka na utrujenostno izrabo prelivnega voda tlačnika. Pri tem smo posebno pozornost posvetili temperaturam, ki bi jih v obravnavanih hipotetičnih prehodnih pojavih prikazovali merilci temperatur na zunanjem obodu prelivnega voda. Model prelivnega voda tlačnika je zastavljen tako, da lahko rezultate tovrstnih meritev v prihodnosti s pridom uporabi.

6 VIRI

[1] Zafošnik, B., Cizelj, L.: Zasnova metode za spremljanje izrabe komponent jedrskih elektrarn, IJS delovno poročilo, IJS-DP-10078, 2008.

[2] Zafošnik, B., Cizelj, L.: Baza prehodnih pojavov v Nuklearni elektrarni Krško, IJS delovno poročilo, IJS-DP-10077, 2008

[3] Kleinöder, W., Golembiewski, H.-J.: Monitoring for fatigue – examples for unexpected component loading, SMiRT 16, Washington DC, August 2001.

[4] Bartonicek, J., Schoeckle, F.: Monitoring of unspecified loads as a tool for ageing management, ASME PVP Conference, Seattle, 2000.

[5] Boros, I., Aszodi, A.: Analysis of thermal stratification in the primary circuit of a VVER-440 reactor with the CFX code, *Nucl. Eng. Des.*, 238, 2008, str. 453-459.

[6] Jong, C. J., Young, H. C. Seok, K. C.: Numerical Analysis of Unsteady Conjugate Heat Transfer and Thermal Stress for a Curved Piping System Subjected to Thermal Stratification, *J. Press. Vess. Tech.*, 125, 2003, str. 467-474.

[7] ABAQUS 6.6-1, 2006.

[8] KWU NDM5/98/E1214, Stress and Fatigue AnalyReplacement Steam Generators, Rev. A, 1998.

[9] Krautov strojniški priročnik, Tehniška založba Slovenije, 1998.

[10] ASME Boiler and Pressure Vessel Code, 1986.

[11] Krško modernization – UPR, Mechanical Review, SSR-NEK-12, Revison 1, February 2000, Final.

[12] USAR (varnostna poročila NEK).

IJS Delovno Poročilo
IJS Report
IJS-DP-10078

Izdaja 1, marec 2009
Revision 1, March 2009

Zasnova metode za spremljanje izrabe komponent jedrskih elektrarn

Design of a method for monitoring the usage of nuclear power plant components

B. Zafošnik, L. Cizelj

Ljubljana, marec 2009

Institut »Jožef Stefan«, Ljubljana, Slovenija

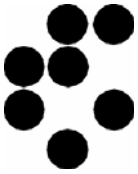

Institut »Jožef Stefan«, Ljubljana, Slovenija

Naročnik: Ordered by:	Javna agencija za raziskovalno dejavnost Republike Slovenije Tivolska c. 30, Ljubljana Nuklearna elektrarna Krško d.o.o., Vrbina 12, 8270 Krško
Izvajalec: Prepared by:	Institut »Jožef Stefan« 1000 Ljubljana Jamova 39 Slovenija Odsek za reaktorsko tehniko (Reactor Engineering Division)
Pogodba štev.: Contract Number:	Z2-9488-0106-06 (IJS in ARRS) U1-BL-R4-3/03 (IJS in NEK)
Nosilec naloge: Responsible Person:	dr. Boštjan Zafošnik, univ. dipl. inž. str.
Naslov poročila: Report Title:	Zasnova metode za spremljanje izrabe komponent jedrskih elektrarn Design of a method for monitoring the usage of nuclear power plant components
Avtorji poročila: Authors:	Dr. Boštjan Zafošnik, univ.dipl.inž.str. Prof. dr. Leon Cizelj, univ.dipl.inž.str.
Štev. delovnega poročila: Report Number:	IJS-DP-10078 Izdaja 1
Konto: Account Number:	V2-0375-C
Kopije: Distribution:	➢ Naročnik (3) ➢ Knjižnica/Library (1x) ➢ Nosilec naloge/Responsible Person (1x) ➢ Avtorji/Authors (1x) ➢ Arhiv OR4/Archive (1x + original)

Ljubljana, marec 2009

POVZETEK

V poročilu smo zasnovali metodo za spremljanje izrabe komponent jedrskih elektrarn. Za zanesljivo oceno dejanske izrabe komponent poleg projektnih in dejansko izmerjenih podatkov o obratovalnih dogodkih in prehodnih pojavih potrebujemo še primerne računske modele.

V poročilu nakazujemo ključne vire podatkov, ki jih lahko v ta namen uporabimo. To so projektna dokumentacija, procesni informacijski sistem, neposredne meritve, simulacije s programi za računalniško dinamiko tekočin in tuje izkušnje. Dostopnost in podrobnost podatkov pa seveda bistveno vplivata na natančnost ocene izrabe.

Zasnovano metodo označujeta primerno uravnotežena dostopnost podatkov in kompleksnost uporabljenih računskih modelov. Nakazujemo tudi nekatere možne poti za rekonstrukcijo manjkajočih podatkov. Metoda je zasnovana v skladu s standardom ASME, po katerem je projektirana in grajena jedrska elektrarna v Krškem. Zato omogoča tudi primerjave z originalnimi projekti.

Metoda je namenjena predvsem podpori pri načrtovanju zamenjave komponent in preventivnega vzdrževanja jedrskih elektrarn. Zelo uporabna bi lahko bila tudi pri neodvisni presoji projektnih izračunov, tudi tistih v podporo podaljšanju obratovalnega dovoljenja. Zasnova pa omogoča tudi morebitno dodelavo in razširitev za izvajanje projektnih izračunov v prihodnosti.

Poročilo predstavlja del rezultatov projekta »**Zasnova metode za spremljanje izrabe komponent jedrskih elektrarn**«, ki sta ga sofinancirala Javna agencija za raziskovalno dejavnost Republike Slovenije (pogodba št. 1000-07-219488) in Nuklearna elektrarna Krško d.o.o. (pogodba št. POG-3408).

ABSTRACT

Design of a method for monitoring of the usage of nuclear power plant components is detailed in the report. Design and operational data are needed in addition to the appropriate computational models to arrive at a reliable estimate of the component usage.

The crucial sources of the data needed in monitoring the usage are identified. These include design documentation, process information system, direct measurements, simulations with computational fluid dynamics software and relevant experience from third parties. The availability and accuracy of data are key factors affecting the accuracy of the estimated usage.

The proposed method is characterized by balanced availability of data and complexity of the computational models utilized. Some possible approaches to reconstruct the missing data are indicated. The method is consistent with the ASME Code, which was utilized during the design of the Krško nuclear power plant. It therefore enables comparisons with the original design.

The method is intended to be used primarily as tool supporting the component replacement schedule and preventive maintenance of nuclear power plants. Another possible use is the independent verification of design analyses supporting the plant life extension. Finally, a possibility of future upgrades toward a tool for design analyses is also assumed in the design.

This report contains a part of the results of the project »**Conception of a method for monitoring of the usage of nuclear power plant components**«, cosponsored by the Slovene research Agency (grant No. 1000-07-219488) and Nuklearna elektrarna Krško d.o.o. (grant No. POG-3408).

KAZALO

POVZETEK III

ABSTRACT IV

KAZALO V

SEZNAM SLIK VII

SEZNAM TABEL VIII

1 UVOD 1

1.1 Namen poročila 1

1.2 Ozadje 1

1.3 Organizacija poročila 2

2 UTRUJANJE KOVINSKIH MATERIALOV 3

2.1 Opis utrujanja 3

2.2 Osnovne metode projektiranja 3
2.2.1 Napetostna metoda 3
2.2.2 Deformacijska metoda 5

2.3 Utrujanje in ASME B&PV Code 5
2.3.1 Ključne predpostavke 5
2.3.2 Upoštevane obremenitve 7
2.3.3 Toplotno razslojeni tokovi 8
2.3.4 Varnostna klasifikacija komponent 8

3 VIRI PODATKOV O OBREMENITVENIH CIKLIH 9

3.1 Originalni projekt 9

3.2 Spremembe originalnega projekta 9

3.3 Procesni informacijski sistem 9

3.4 Neposredne meritve 10

3.5 Simulacije s programi za računalniško dinamiko tekočin 10

4 OCENA UTRUJENOSTNE IZRABE 12

4.1 Obremenitveni cikli 12
4.1.1 Definicija 12
4.1.2 Wöhlerjeva krivulja 12

4.2 Skupni faktor izrabe 13

4.3 Delni faktorji izrabe 13
4.3.1 Napetosti 13
4.3.2 Glavne napetosti 13
4.3.3 Največje strižne napetosti – Trescova ekvivalentna napetost 14
4.3.4 Amplituda nihanja napetosti 14
4.3.5 Delni faktor izrabe 15

5 OCENA CIKLIČNIH NAPETOSTI 16

5.1 Osnovne enačbe 16

5.2 Analitično reševanje 16
5.2.1 Omejitve in predpostavke 16
5.2.2 Napetosti zaradi temperaturnih sprememb 17
5.2.3 Napetosti zaradi notranjega tlaka 22

5.3 Numerično reševanje 23
5.3.1 Metoda končnih elementov 23
5.3.2 Osnovne omejitve, predpostavke in značilna uporaba modelov 23

6 ZAKLJUČKI 25

7 VIRI 26

SEZNAM SLIK

Slika 1	**Sinusna ciklična obremenitev**	**4**
Slika 2	**Potek določitve faktorja izrabe**	**6**
Slika 3	**Razslojeni tok v horizontalni cevi**	**7**
Slika 4	**Meritev temperature po obodu cevi v odvisnosti od lege cevovoda [8]**	**10**
Slika 5	**Simulacija vrtinčnega mešanja tekočin z različnima temperaturama [20]**	**11**
Slika 6	**Določitev dopustnega števila ciklov obremenitve glede na izračunano amplitudo nihanja napetosti S_a**	**12**
Slika 7	**Stopničaste spremembe temperature iz 0 na 1 in nazaj na 0**	**20**
Slika 8	**Vpliv frekvence *f* stopničaste spremembe temperature na notranji površini stene cevi na amplitudo nihanja napetosti S_a**	**21**
Slika 9	**Vpliv brezdimenzijskega polmera R_1/R_2 na brezdimenzijsko amplitudo napetosti S_a**	**23**

SEZNAM TABEL

Tabela 1 Vpliv stopničaste spremembe (Slika 7a) na amplitudo nihanja napetosti S_a za različne debeline stene cevi 21

1 UVOD

1.1 Namen poročila

V poročilu predstavljamo del rezultatov projekta »**Zasnova metode za spremljanje izrabe komponent jedrskih elektrarn**«, ki sta ga sofinancirala Javna agencija za raziskovalno dejavnost Republike Slovenije (pogodba št. 1000-07-219488) in Nuklearna elektrarna Krško d.o.o. (pogodba št. POG-3408).

Preostali rezultati projekta so predstavljeni v spremljajočih poročilih:

- Baza prehodnih pojavov v Nuklearni elektrarni Krško [1] in
- Pilotni primeri izračuna faktorja utrujenostne izrabe [2].

1.2 Ozadje

Med gradnjo NE Krško in vse do uveljavitve ZVISJV [3] 1.10.2002 je bila v Sloveniji v primeru odsotnosti domačih predpisov uzakonjena uporaba predpisov države, ki je jedrsko elektrarno dobavila. Zato je jedrska elektrarna Krško projektirana v skladu s predpisi in prakso v ZDA (ASME Boiler and Pressure Vessel Code, [4], v nadaljevanju ASME B&PV Code) za trajnostno dobo 40 let.

Predvidena trajnostna doba jedrske elektrarne Krško (in podobnih jedrskih elektrarne v ZDA) temelji na ekonomskih razmislekih in je bila opredeljena na 40 let [5]. Opredelitev trajnostne dobe je vplivala na zasnovo in projekte elektrarn. V projektnih predpisih (ASME B&PV Code [4]) je s stališča trajnostne dobe elektrarne velika pozornost posvečena odpornosti na utrujanje. Projekti predvidevajo vnaprej določen nabor hipotetičnih obratovalnih dogodkov in prehodnih pojavov. Za 40 letnemu obratovanju prilagojeno število obratovalnih dogodkov s predpisano varnostno rezervo tudi dokažejo ustrezno odpornost na utrujanje. Obratovalno osebje elektrarne nato izrabo komponent enostavno oceni kar s štetjem obratovalnih dogodkov in prehodnih pojavov, ki ga primerja s projektno predvidenim številom.

Izkušnje z obratovanjem in vzdrževanjem jedrskih elektrarn ter seveda tudi napredek znanosti v zadnjih desetletjih jasno kažejo na možnost podaljšanja trajnostne dobe. Ključni element pri podaljšanju obratovalnega dovoljenja v ZDA predstavlja obvladovanje staranja pasivnih in za varnost pomembnih sistemov, struktur in komponent, ki je opredeljeno v 10 CFR 54 [6].

Med pomembnejše aktivnosti pri obvladovanju staranja pasivnih komponent (npr. cevovodi in tlačne posode) sodi tudi ponovna analiza odpornosti na utrujanje. Tukaj si lahko obratovalno osebje elektrarne v veliki meri pomaga z izmerjenimi parametri obratovalnih dogodkov in prehodnih pojavov. Praviloma so spremembe tlakov, temperatur in pretokov manjše, kot je bilo konzervativno ocenjeno v projektu. Zato je tudi njihov vpliv na trajnostno dobo dostikrat manjši.

Za zanesljivo oceno dejanske izrabe komponent poleg projektnih in dejansko izmerjenih podatkov o obratovalnih dogodkih in prehodnih pojavih potrebujemo še računske modele, s katerimi ocenimo prispevke posameznega prehodnega pojava k skupni izrabi komponent. Skupku medsebojno uravnoteženih podatkov in računskih modelov v literaturi navadno pravijo metoda ali sistem za spremljanje izrabe komponent.

V literaturi najdemo različne metode oziroma sisteme za spremljanje izrabe komponent jedrskih objektov (npr. [7] in [8]). Eden izmed zelo pomembnih korakov pri spremljanju izrabe komponent je določitev temperaturnega in napetostnega odziva v komponentah. Pogosto je uporabljena tehnika Greenovih funkcij [9], [10] ki je v splošnem omejena na analize linearnih odzivov [11]. Zelo pogosto za določevanje temperaturnih in napetostnih odzivov uporabljajo tudi metodo končnih elementov [7], [10], [12], [13], [14]. Metoda je zelo splošna in uporabna tudi v zelo kompleksnih situacijah. Je pa za uporabo potrebno imeti ustrezno usposobljeno osebje ter programsko in strojno opremo.

Zasnova tovrstne metode s primerno uravnoteženo natančnostjo in kompleksnostjo je osnovni cilj projekta, o katerem poročamo v tem poročilu. Metoda je namenjena predvsem podpori pri načrtovanju zamenjave komponent in preventivnega vzdrževanja jedrskih elektrarn. Zelo uporabna bi lahko bila tudi pri neodvisni presoji projektnih izračunov. Zasnova pa omogoča tudi morebitno dodelavo in razširitev za izvajanje projektnih izračunov v prihodnosti.

1.3 Organizacija poročila

V poglavju 2 opisujemo fenomen utrujanja, ki je splošnem posledica spreminjajočih se obremenitev. Osnovne informacije o virih podatkov o obremenitvenih ciklih, ki so potrebni za določanje izrabe komponent, predstavljamo v poglavju 3. Postopek za določitev izrabe komponente na osnovi delnih in skupnega faktorja izrabe opisujemo v poglavju 4. V poglavju 5 so zbrane osnovne enačbe za napetosti, ki so pomembne za določitev izrabe komponente, z izbranimi analitičnimi in numeričnimi rešitvami. Sledijo zaključki v poglavju 6 in viri v poglavju 7.

2 UTRUJANJE KOVINSKIH MATERIALOV

V tem poglavju na kratko orišemo pomembnost spreminjajočih se obremenitev za projektiranje komponent na utrujanje.

2.1 Opis utrujanja

Kovinske mehanske komponente, ki so obremenjene s spreminjajočimi se obremenitvami, lahko odpovedo pri napetostih, ki so bistveno nižje od natezne trdnosti. Odpoved je tudi pri žilavih materialih posledica nastanka in napredovanja kvazi krhkih utrujenostnih razpok. Pred nastankom razpok pa je mogoče opaziti značilne spremembe v mikrostrukturi. Takšen pojav imenujemo utrujanje. V literaturi je bil prvič omenjen že v letu 1838 [15].

Utrujanje praviloma povzročajo spreminjajoče se toplotne ali mehanske obremenitve. Tem se bomo posvetili v pričujočem poročilu. V nekaterih primerih se lahko utrujanje pojavi v kombinaciji z drugimi degradacijskimi procesi. Spreminjajoča se obremenitev pri visokih temperaturah lahko povroči utrujenostno lezenje (angl. creep fatigue), v prisotnosti agresivnega medija pa korozijsko utrujanje (angl. corrosion fatigue, environmentally assissted fatigue).

Značilne faze razvoja utrujenostnih poškod v splošnem zajemajo:
- mikrostukturne spremembe v materialu,
- nastanek mikroskopskih razpok,
- rast in združevanje mikroskopskih razpok, ki oblikujejo t. i. vodilne makrorazpoke,
- stabilna rast vodilnih makrorazpok in končno
- strukturna nestabilnost oz. lom komponente

Celotno trajnostno dobo komponente lahko torej delimo v čas oz. obremenitvene cikle pred nastankom utrujenostnih razpok in čas oz. število ciklov stabilne rasti razpok. V pričujočem poročilu se omejujemo na čas do nastanka utrujenostnih razpok.

2.2 Osnovne metode projektiranja

V literaturi pogosto naletimo na dve značilni vrsti mehanskega in toplotnega utrujanja z značilnima pripadajočima metodama za oceno trajnostne dobe komponente pred nastankom razpok [15], [5]:
- visoko ciklično utrujanje – napetostna (σ - N) metoda in
- nizko ciklično utrujanje – deformacijska (ε - N) metoda.

ASME B&PV Code uporablja pristop, ki je nekoliko bliže (σ - N) metodi. Zato se (σ - N) metodi v nadaljevanju posvečamo nekoliko podrobneje.

2.2.1 Napetostna metoda

Napetostna metoda (σ – N) je najstarejša metoda projektiranja na utrujanje. Temelji na Wöhlerjevi krivulji dinamične trdnosti gradiva (Slika 6). Wöhlerjeva krivulja povezuje amplitudo napetosti σ_A z največjim številom ciklov N, ki še zagotavlja nepoškodovanost komponente. Uporabljamo jo predvsem pri visokocikličnem utrujanju, ko je komponenta praviloma izpostavljena visokemu številu ciklov z razmeroma nizko amplitudo napetosti. Gonilna sila visoko cikličnega utrujanja so praviloma ciklične napetosti.

Slika 1 prikazuje predpostavljeno sinusno ciklično spreminjanje napetosti v odvisnosti od števila ciklov.

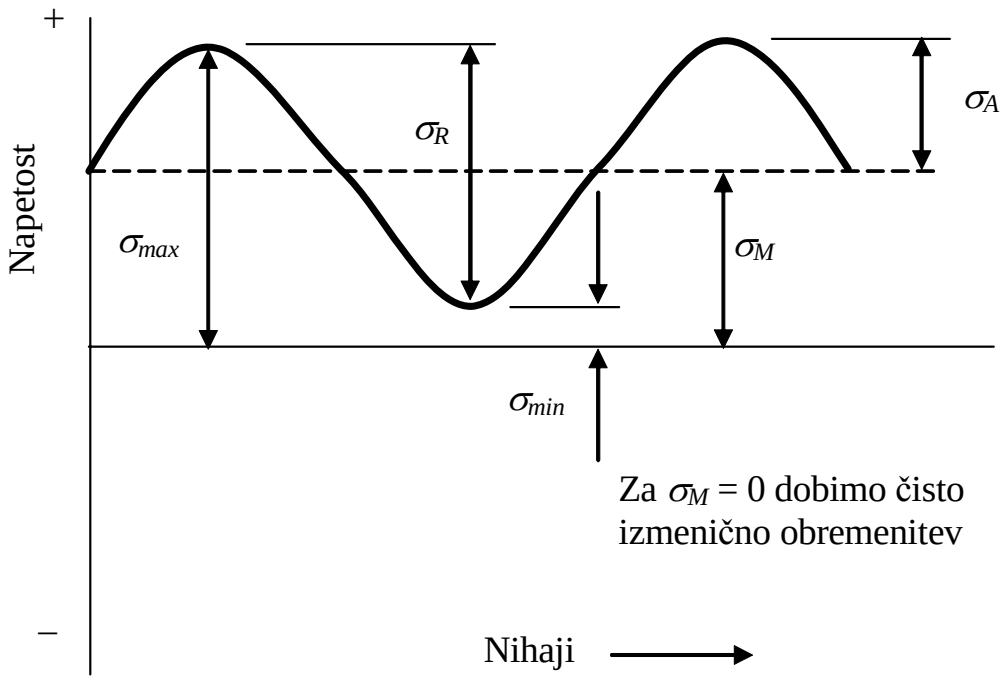

Slika 1 Sinusna ciklična obremenitev

Značilne vrednosti napetosti (Slika 1) so opredeljene z največjo (σ_{max}) in najmanjšo (σ_{min}) napetostjo. Prvi je razpon napetosti σ_R:

$$\sigma_R = \sigma_{\max} - \sigma_{\min}\,, \tag{1}$$

Sledi izmenična napetost oz. amplituda napetosti σ_A, ki je definirana kot polovica razpona napetosti:

$$\sigma_A = \frac{\sigma_R}{2} = \frac{\sigma_{\max} - \sigma_{\min}}{2}\,. \tag{2}$$

Srednja vrednost σ_M je aritmetična sredina največje in najmanjše napetosti:

$$\sigma_M = \frac{\sigma_{\max} + \sigma_{\min}}{2}\,. \tag{3}$$

Definirajmo tudi napetostno razmerje R:

$$R = \frac{\sigma_{\min}}{\sigma_{\max}}\,. \tag{4}$$

Vrednost R znaša pri enosmerni dinamični obremenitvi $0 < R < 1$, pri utripni $R = 0$, pri splošni izmenični $-1 < R < 0$ in pri čisti izmenični $R = -1$ in lahko pomembno vpliva na odpornost materiala, torej na Wöhlerjevo krivuljo.

ASME B&PV Code napetostno razmerje upošteva le posredno in sicer s pomočjo razširjene Goodmanove povezave. Efektivno amplitudo napetosti $\sigma_{A,ef}$ lahko namreč za material z natezno trdnostjo σ_{UT} popišemo kot:

$$\sigma_{A,ef} = \sigma_A \left(1 - \frac{\sigma_M}{\sigma_{UT}} \right) \tag{5}$$

Razmerje med najbolj neugodno srednjo napetostjo σ_M in natezno trdnostjo σ_{UT} je mogoče določiti vnaprej in ga vgraditi kar v Wöhlerjevo krivuljo [5].

2.2.2 Deformacijska metoda

Deformacijska metoda ($\varepsilon - N$) je novejša metoda pri projektiranju dinamično obremenjenih komponent (začetki uporabe segajo v leto 1960). Njena osnovna značilnost je, da upošteva lokalno deformacijsko polje ob koncentracijah napetosti (razni prehodi, zaokrožitve, prebodi itd.), kjer je verjetnost nastanka utrujenostnih razpok zaradi zareznega učinka večja. Deformacijsko metodo uporabljamo predvsem pri nizko cikličnem utrujanju, še posebej kadar je obnašanje gradiva vsaj lokalno v elasto-plastičnem področju. Pogosto je nizko ciklično utrujanje posledica zavrte toplotne razteznosti materiala [16]. Gonilna sila so ciklične deformacije, ki so značilno relativno visoke pri razmeroma nizkem število ciklov. Za oceno trajnostne dobe komponente pred nastankom razpok praviloma uporabljamo deformacijsko metodo (poglavje 2.2.2).

2.3 Utrujanje in ASME B&PV Code

2.3.1 Ključne predpostavke

Kontrola na utrujanje v ASME B&PV Code [4] je enostavna, robustna in temu primerno konzervativna. Ključni namen njenih snovalcev je bil namreč zagotoviti predpisano trajnostno dobo 40 let v delovnih pogojih, ki jih ni bilo mogoče predvideti v vseh podrobnostih [5].

Kontrola na utrujanje, tako kot ostala pravila za dimenzioniranje jedrskih komponent v ASME B&PV Code [4], temelji na Trescovi teoriji največje strižne napetosti in uporablja napetostno metodo ($\sigma - N$). Wöhlerjevo krivuljo (Slika 6) so razvili tako, da upošteva varnostna faktorja 2 na amplitudo napetosti in 20 na število ciklov, hkrati pa še vpliv srednje napetosti. Od projektanta jedrske elektrarne pričakuje, da predvidi in konzervativno oceni parametre obratovalnih dogodkov in prehodnih pojavov ter njihovo število v trajnostni dobi elektrarne. Za vsakega izmed teh dogodkov nato oceni prispevek k utrujanju v obliki delnega faktorja izrabe. Skupni faktor izrabe pa zopet konzervativno oceni s pomočjo linearne Palmgren-Minerjeve hipoteze in ga omeji z najvišjo dovoljeno vrednostjo 1.

ASME B&PV Code [4] v dosedanjih izdajah predpostavlja, da izkazujejo nizkolegirana in avstenitna nerjavna jekla (komponente varnostnih sistemov) trajno dinamično trdnost pri 10^6 ciklih. Zato fluktuacij obremenitev, ki povzročajo amplitude napetosti pod trajno dinamično trdnostjo, ni (bilo) potrebno upoštevati pri kontroli na utrujanje. Novejša spoznanja kažejo, da se trajna dinamična trdnost pokaže pri bistveno večjem številu ciklov (npr. 10^{11}), ali pa sploh ne.

Komponente v jedrski elektrarni, še posebej tlačne posode, so izpostavljene velikim spremembam temperatur. Velik del prispevkov k utrujenostni izrabi bo torej posledica

cikličnih deformacij zaradi zavrte toplotne razteznosti. Uporaba napetostne metode v takem okolju je sicer smiselna, a le pri obremenitvah pod mejo plastičnosti materiala komponente. V ta namen je predvidena kontrola na »ratcheting« oz. »shakedown«.

»Ratcheting« (ratchet = raglja) je nedopusten pojav, pri katerem se plastična oz. trajna deformacija v vsakem novem obremenitvenem ciklu poveča. To seveda lahko vodi v pomembno spremembo oblike komponente in končno v njeno porušitev. Manjše plastične deformacije lahko vseeno dovolimo, kadar se material v prvih nekaj ciklih utrdi do te mere, da so obremenitve v naslednjih ciklih v celoti v elastičnem področju. Tako stanje ASME B&PV Code [4] imenuje »shakedown«.

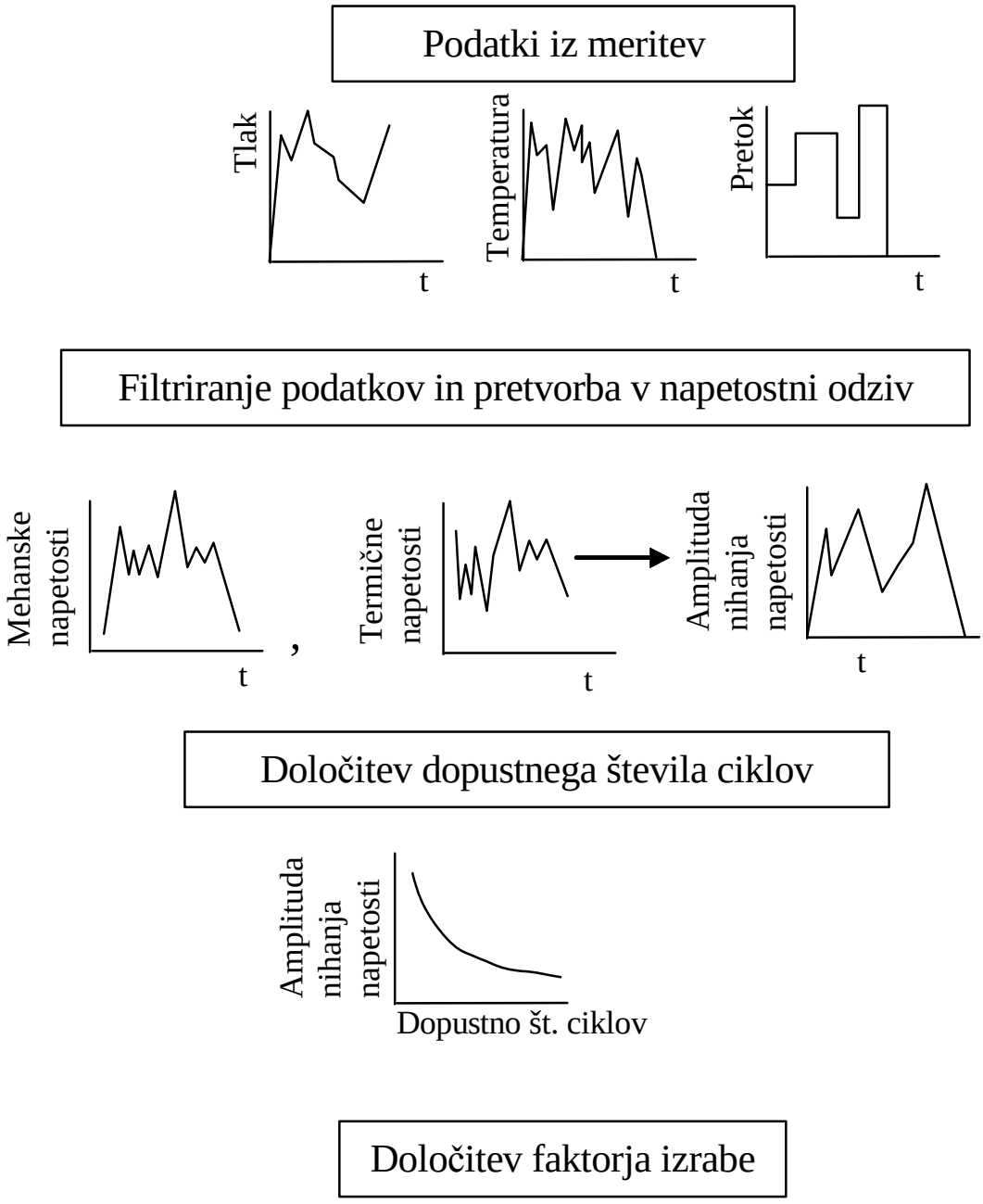

Slika 2 Potek določitve faktorja izrabe

Slika 2 shematsko prikazuje potek kontrole na utrujanje po ASME B&PV Code [4]. Nekatere elemente podrobneje predstavljamo v poglavju 4.

2.3.2 Upoštevane obremenitve

Komponente jedrskih elektrarn so izpostavljene različnim obratovalnim in testnim obremenitvam. V skladu z ASME B&PV Code [4] jih je potrebno razvrstiti v naslednje skupine:

- projektne obremenitve,
- obratovalne obremenitve, ki izvirajo iz:
  - normalnega obratovanja,
  - motenega obratovanja,
  - zasilnega obratovanja in
  - nezgod.
- testne obremenitve.

Pri kontroli utrujanja oz. izrabe komponent je potrebno upoštevati obremenitve pri normalnih in motenih obratovalnih stanjih ter testne obremenitve. Obremenitve iz zasilnega obratovanja in nezgod so sicer praviloma višje kot pri normalnem oz motenem obratovanju ali testiranju. Ni pa predvideno, da bi se v trajnostni dobi elektrarne taka stanja ponavljala, zato ne vplivajo na utrujanje oz. izrabo elektrarne in njenih komponent.

Značilne spremenljive obremenitve, ki so posledica normalnih in motenih obratovalnih stanj ter testiranj, so notranji tlak, temperatura, hidrodinamične obremenitve zaradi spremenjenih pretokov in obratovalni potres (OBE).

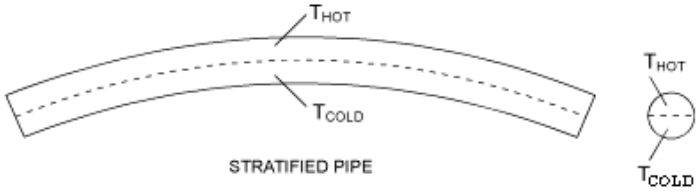

Upogibanje cevi zaradi toplotnega razslojevania

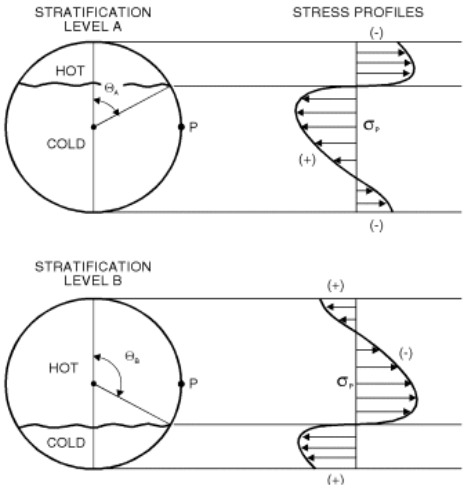

Napetosti po prerezu cevi zaradi toplotnega razslojevanja

Slika 3 Razslojeni tok v horizontalni cevi

2.3.3 Toplotno razslojeni tokovi

Toplotno razslojevanje tokov praviloma nastane kot posledica različnih gostot oz. temperatur medija. Pojav oz. njegove posledice so v prelivnih vodih jedrskih elektrarn opazili konec 80 let prejšnjega stoletja [17], [18]. Vroč medij se bo zaradi nižje gostote zbiral na vrhu posode ali cevovoda, hladen pa spodaj. Pojav je izrazitejši pri neizoliranih komponentah z majhnim pretokom ali celo brez pretoka, kjer so temperaturne razlike lahko tudi več 10 °C [8]. Pojav toplotnega razslojevanja lahko v ravnih delih cevovoda povzroči po prerezu spremenljive toplotne napetosti oz. deformacije. Meja med hladnim in vročim medijem se lahko spreminja. Ciklično ponavljanje tega pojava povzroči toplotno utrujanje, ki v končni fazi lahko pripelje do nastanka razpok.

2.3.4 Varnostna klasifikacija komponent

Komponente jedrskih elektrarn so razvrščene v varnostne razrede. Klasifikacija komponent je odvisna od tipa jedrske elektrarne in se naredi glede na primerne standarde in predpise. Za klasifikacijo komponent tlačnovodne jedrske elektrarne se uporablja standard ANS N-18.2 [19], ki predpisuje določitev razreda glede na kategorizacijo obratovalnega stanja oziroma glede na hipotetično nezgodo.

V **varnostni razred 1** spadajo komponente, katerih odpoved bi lahko povzročila nezgodo III ali IV kategorije (ANS N-18.2 [19]), ki vključuje tudi izgubo reaktorskega hladila. V varnostni razred 1 sodi n.pr. celotna tlačna meja reaktorskega hladila.

V skladu z ASME B&PV Code [4] je za vse komponente varnostnega razreda 1 potrebno dimenzioniranje na utrujanje.

V **varnostni razred 2** spadajo predvsem zadrževani hram, komponente sistemov, kjer se pretaka reaktorsko hladilo, a niso zajete v varnostnem razredu 1 (npr. sistem za odvajanje zaostale toplote, sistem za uravnavanje kemijske sestave in prostornine itd.), in komponente varnostnih sistemov, ki so locirane znotraj zadrževalnega hrama (npr. sistem glavne pare do vključno glavnega izolacijskega ventila, gledano iz smeri uparjalnika itd.).

V skladu z ASME B&PV Code [4] je potrebno za tlačne posode in njihove dele v varnostnem razredu 2 preveriti, ali sploh potrebujejo kontrolo na utrujanje (NC-3210). Če jo, je postopek primerljiv tistemu za komponente varnostnega razreda 1.

V **varnostni razred 3** spadajo komponente, ki podpirajo katerokoli funkcijo varnostnih sistemov in niso zajete v varnostni razred 1 ali 2. Značilni sistemi varnostnega razreda 3 so sistem hladilne vode, sistem dodajalne vode in podobno.

Standard ASME B&PV Code [4] v ND-3649.4 g) zahteva kontrolo na utrujanje za komponente, ki omogočajo dilatacijo cevovodov.

V zasnovi metode obravnavamo komponente iz varnostnega razreda 1, saj s tem konzervativno pokrijemo tudi morebitne zahteve za spremljanje izrabe komponent varnostnih razredov 2 in 3.

3 VIRI PODATKOV O OBREMENITVENIH CIKLIH

Natančnost določanja faktorja izrabe komponent je v največji meri odvisna od natančnosti dostopnih podatkov o relevantnih obratovalnih dogodkih in prehodnih pojavih. Še posebej pomembna postane kakovost dostopnih podatkov pri ocenah, ki vodijo v odločitve o podaljšanju obratovalnega dovoljenja. V takih primerih lahko pomemben del konzervativnosti v projektu predvidenih podatkov o prehodnih pojavih odpravimo z dejansko izmerjenimi.

V nadaljevanju povzemamo ključne informacije o najpomembnejših virih podatkov, iz katerih je mogoče zajeti informacije, pomembne za utrujenostno izrabo komponent jedrske elektrarne v Krškem. Celovit pregled je predstavljen v spremljajočem poročilu [1].

3.1 Originalni projekt

V originalnem projektu in pripadajoči dokumentaciji (projektne specifikacije itd.) lahko najdemo osnovne informacije o značilnostih in predvidenem številu obratovalnih dogodkov in prehodnih pojavov, ki so bili upoštevani pri načrtovanju jedrske elektrarne.

Pomembno je poudariti, da zbrani podatki podajajo zelo dobro globalno sliko o zamišljenem oz. predvidenem dogajanju v sistemih jedrske elektrarne. Praviloma pa so bili obratovalni prehodni pojavi in njihovo število v fazi projekta ocenjeni dokaj konzervativno in zadoščajo za izpolnjevanje projektnih zahtev. Hkrati pa praviloma niso dovolj podrobni za natančno oceno lokalnih razmer v posameznih komponentah v primeru odločanja o podaljšanju obratovalnega dovoljenja.

3.2 Spremembe originalnega projekta

Spremembe v konfiguraciji jedrske elektrarne lahko vplivajo na značilnosti projektnih prehodnih pojavov in s tem tudi na utrujenostno izrabo komponent. Med ključne spremembe konfiguracije jedrske elektrarne v Krškem lahko štejemo veliko začepljenost uparjalnikov v zadnjih letih pred zamenjavo v letu 2000. Tudi zamenjava uparjalnikov v letu 2000 z hkratnim povečanjem moči elektrarne sodi v konfiguracijske spremembe, ki bi lahko imele vpliv na utrujenostno izrabo komponent.

Spremembe značilnosti prehodnih pojavov in morebitne ponovne kontrole izpolnjevanja projektnih predpostavk in zahtev so opredeljene v dokumentaciji v podporo konfiguracijskim spremembam.

3.3 Procesni informacijski sistem

Procesno informacijski sistem spremlja in hrani ključne podatke o delovanju elektrarne. Mednje sodijo predvsem temperature, tlaki, pretoki hladila ipd. v več pomembnih sistemih. V procesno informacijskem sistemu je torej mogoče dobiti vpogled v parametre vseh tistih obratovalnih dogodkov in prehodnih pojavov, ki so se v elektrarni dejansko zgodili.

Ti podatki omogočajo razmeroma zanesljivo oceno konzervativnosti projektnih prehodnih pojavov. Hkrati pa praviloma niso dovolj podrobni za natančno oceno lokalnih razmer v posameznih komponentah v primeru odločanja o podaljšanju obratovalnega dovoljenja.

3.4 Neposredne meritve

V nekaterih posebnih primerih, kot na primer pri razslojenem toku tekočin, je za zanesljivo oceno utrujenostne izrabe smiselno izvesti neposredne meritve. To je dostikrat edini način, da razslojeni tok zaznamo in hkrati tudi razmeroma zanesljivo ocenimo njegove najpomembnejše parametre, kot npr. položaj meje med toplo in hladno tekočino ter temperature obeh tekočin [8]. Slika 4 shematično prikazuje primer neposredne meritve temperatur na zunanji steni cevovoda.

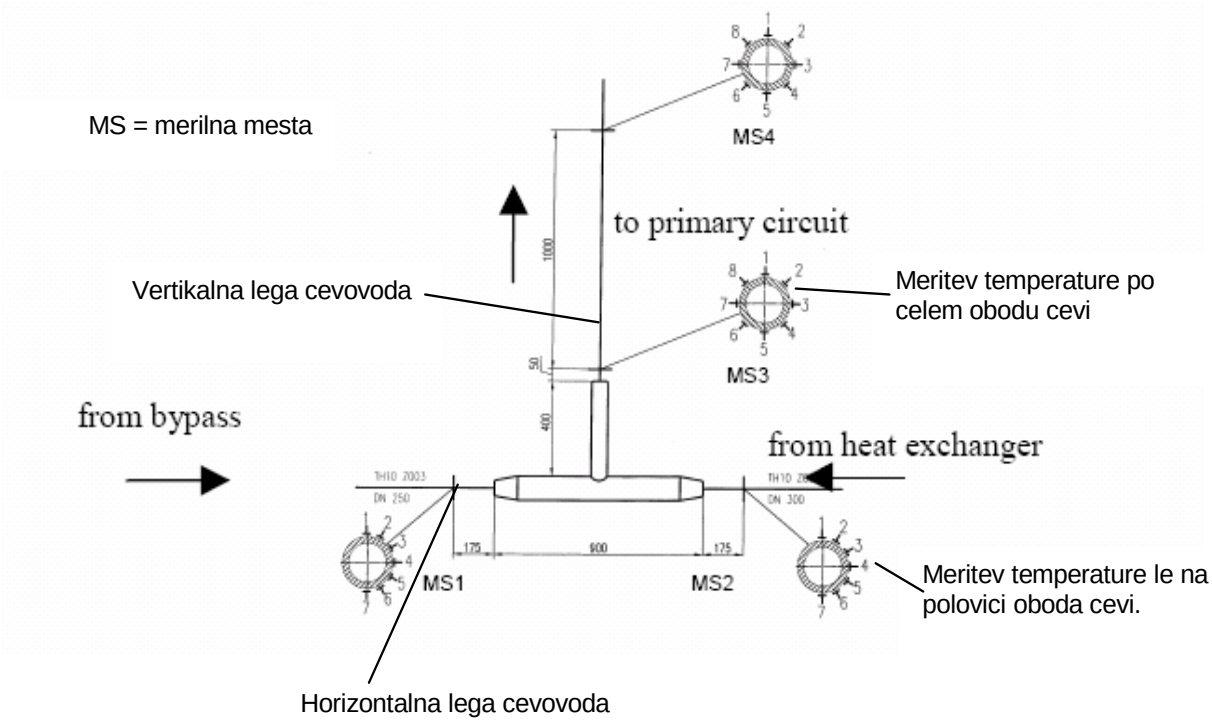

Slika 4 Meritev temperature po obodu cevi v odvisnosti od lege cevovoda [8]

3.5 Simulacije s programi za računalniško dinamiko tekočin

Projektni prehodni pojavi in meritve, zabeležene v procesnem informacijskem sistemu, praviloma podajajo dobro globalno sliko o dogajanju v sistemih jedrske elektrarne. Žal pa praviloma ne zadoščajo za podrobno oceno lokalnih razmer v komponenti, ki so seveda ključne za natančno oceno izrabe komponente.

Pogost primer tovrstne situacije je mešanje tekočin v spojih cevi. Že zmerne razlike v temperaturah in pretokih lahko vodijo v spremembe lokalnih napetosti, ki so s stališča utrujanja pomembne. V takšnem primeru lahko kompleksne termo-hidravlične robne pogoje (Slika 5) določimo oz. rekonstruiramo s pomočjo računalniških programov za dinamiko tekočin.

Sodobna orodja praviloma omogočajo predvsem simulacijo poprečnih hitrosti fluidov in temperatur pri turbulentnih tokovih. V nekaterih primerih je mogoča tudi neposredna simulacija turbulentnih tokov; omejitev so predvsem izjemno dolgi računski časi.

Začetne in robne pogoje za tovrstne simulacije lahko dobimo iz projektnih opisov prehodnih pojavov, podatkov iz procesnega informacijskega sistema in neposrednih meritev.

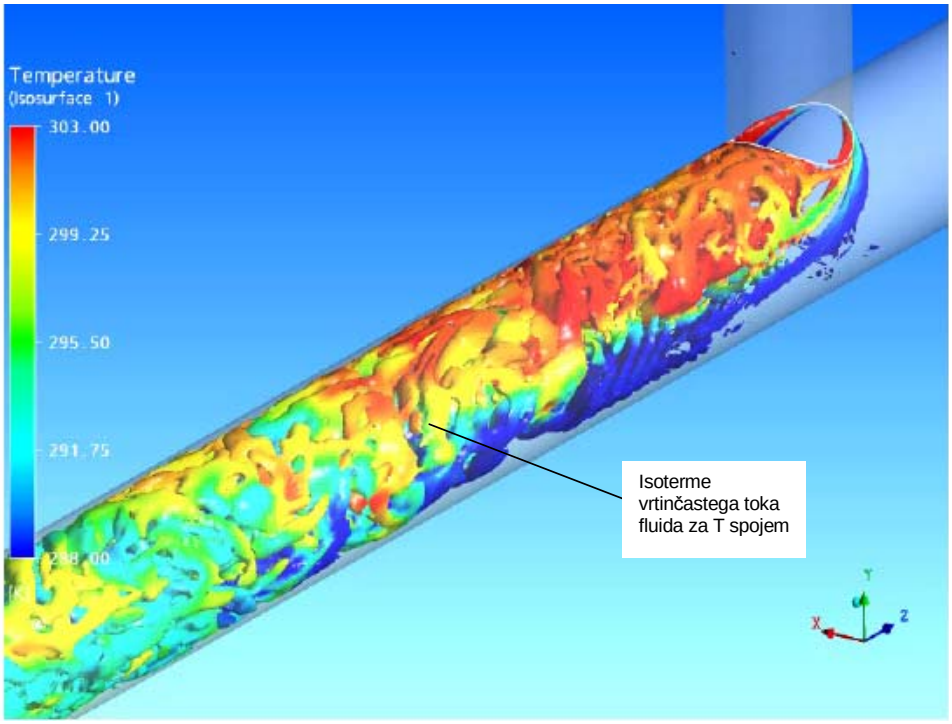

Slika 5 Simulacija vrtinčnega mešanja tekočin z različnima temperaturama [20]

4 OCENA UTRUJENOSTNE IZRABE

Pri oceni preostanka trajnostne dobe komponente je potrebno poznati njeno obratovalno zgodovino in predvideti posledice obratovalnih stanj v prihodnosti. Metoda, ki jo za kontrolo utrujanja uporablja ASME B&PV Code [4], je bila zasnovana za oceno posledic obratovalnih stanj v prihodnosti. Uporabiti jo je mogoče tudi za oceno posledic obratovalne zgodovine, torej za oceno trenutne utrujenostne izrabe. Na ta način dobimo rezultate, ki so neposredno primerljivi z originalnimi projektnimi zahtevami. Uspešnost pa je odvisna predvsem od kvalitete razpoložljivih podatkov o obratovalni zgodovini.

ASME B&PV Code [4] ocenjuje utrujenostno izrabo ocenimo s skupnim faktorjem izrabe (angl. Cumulative Usage factor - CUF), ki je vsota prispevkov vseh prehodnih pojavov, in mora biti manjši od 1. To zagotavlja, da med predvidenimi obratovalnimi dogodki in prehodnimi pojavi ne bodo nastale utrujenostne razpoke.

4.1 Obremenitveni cikli

4.1.1 Definicija

Cikel definiramo kot proces, pri katerem se sistem vrne v začetno stanje. Pri tem je pomembno, da ujamemo stanji z največjo in najmanjšo obremenitvijo.

4.1.2 Wöhlerjeva krivulja

Wöhlerjeve krivulje iz standarda ASME B&PV Code [4] podajajo dopustne vrednosti dinamičnih obremenitev (amplituda nihanja napetosti S_a) v odvisnosti od števila ciklov (N). Pri znani amplitudi nihanja napetosti S_a lahko iz njih odčitamo dovoljeno število ciklov (Slika 6).

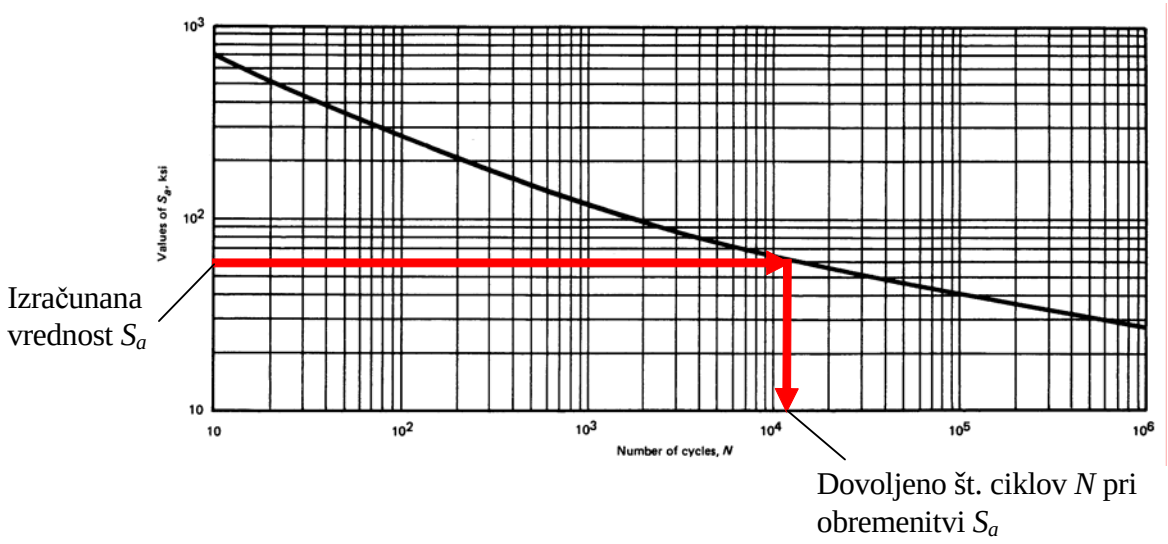

Slika 6 Določitev dopustnega števila ciklov obremenitve glede na izračunano amplitudo nihanja napetosti S_a

Krivulje so konzervativne, saj glede na eksperimentalne rezultate vsebujejo varnostna faktorja 2 na velikost napetosti in 20 na število ciklov, poleg tega tudi morebiten vpliv srednje

napetosti. Krivulje so specifične za skupine značilnih materialov (Slika 6) prikazuje primer za avstenitna jekla), kot so npr. nizko legirana jekla in avstenitna nerjavna jekla. Značilno najvišje število ciklov v krivuljah je med 10^6 in 10^{11}. Pri še višjem številu ciklov je predpostavljeno, da je dosežena trajna dinamična trdnost materiala, pri kateri bo komponenta zdržala poljubno število ciklov.

4.2 Skupni faktor izrabe

Skupni faktor izrabe U določa utrujenostno izrabo komponente v izbrani materialni točki. Izračuna se kot vsota vseh delnih faktorjev izrabe u_i:

$$U = \sum_{i=1}^{m} u_i = \sum_{i=1}^{m} \frac{n_i}{N_i} \tag{6}$$

kjer m pomeni število različnih napetostnih ciklov z delnim faktorjem izrabe u_i in številom ponovitev cikla n_i.

Če je skupni faktor izrabe $U < 1$, potem v analizirani materialni točki glede na ASME [4] ni nevarnosti za pojav utrujenostnih razpok.

4.3 Delni faktorji izrabe

4.3.1 Napetosti

Za določitev utrujenostne izrabe komponent je potrebno poznati napetosti v materialni točki. Ker je večina komponent jedrske elektrarne valjaste oblike, je smiselno komponente tenzorja napetosti zapisati v cilindričnem koordinatnem sistemu:

$$\sigma_{ij} = \begin{bmatrix} \sigma_r & \sigma_{r\phi} & \sigma_{rz} \\ \sigma_{\phi r} & \sigma_{\phi} & \sigma_{\phi z} \\ \sigma_{zr} & \sigma_{z\phi} & \sigma_z \end{bmatrix}. \tag{7}$$

Pri tem so napetosti na glavni diagonali σ_r, σ_ϕ in σ_z normalne napetosti, izven diagonalne komponente napetosti pa predstavljajo strižne napetosti.

4.3.2 Glavne napetosti

Glavne napetosti simetričnega tenzorja so lastne vrednosti, katerih normale imenujemo glavne smeri. Lastne vrednosti in lastne smeri so definirane z izrazom

$$\sigma_{ij}\vec{x} = \sigma\,\vec{x}\,, \tag{8}$$

kjer prostorskemu tenzorju σ_{ij} pripadajo tri realne vrednosti L_1, L_2 in L_3 v ravninah, katere normale kažejo v smereh $\vec{x}_1, \vec{x}_2, \vec{x}_3$, ki so med seboj ortogonalne. Lastne vrednosti dobimo z razrešitvijo pogojne enačbe [21]

$$\text{Det}\left|\sigma_{ij} - \sigma\,\delta_{ij}\right| = 0\,, \tag{9}$$

kjer je δ_{ij} enotski tenzor. Izraz (9) lahko zapišemo tudi kot

$$\mathrm{Det}\begin{bmatrix} \sigma_r-\sigma & \sigma_{r\phi} & \sigma_{rz} \\ \sigma_{\phi r} & \sigma_\phi-\sigma & \sigma_{\phi z} \\ \sigma_{zr} & \sigma_{z\phi} & \sigma_z-\sigma \end{bmatrix}=0\,. \tag{10}$$

Iz izraza (10) dobimo kubično enačbo, katere rešitev so trije realni koreni, ki jih lahko uredimo po velikosti, tako da je $\sigma_1 > \sigma_2 > \sigma_3$, ki predstavljajo glavne napetosti.

4.3.3 Največje strižne napetosti – Trescova ekvivalentna napetost

Napetostni tenzorje v praksi navadno primerjamo s podatki o materialih, ki so bili izmerjeni v razmerah enoosnih obremenitev. V ta namen uvedemo ekvivalentno napetost, ki je nekakšna skalarna mera velikosti napetostnega tenzorja. V inženirski praksi uporabljamo več definicij ekvivalentne napetosti; možnosti je namreč neskončno mnogo. Inženirske definicije praviloma temeljijo na fizikalno smiselnih podmenah.

ASME B&PV Code [4] uporablja Trescovo ekvivalentno napetost, ki temelji na predpostavki, da nastopi porušitev materiala zaradi delovanja največje strižne napetosti τ_{max} [15]. Trescova ekvivalentna napetost sodi med najkonzervativnejše ekvivalentne napetosti v inženirski praksi. Izračunamo jo kot:

$$\sigma_p^{Tr} = 2\tau_{\max} = \max\left(\left|\sigma_1-\sigma_2\right|,\left|\sigma_2-\sigma_3\right|,\left|\sigma_3-\sigma_1\right|\right), \tag{11}$$

kjer predstavljajo σ_1, σ_2 in σ_3 glavne napetosti.

4.3.4 Amplituda nihanja napetosti

Določitev velikosti amplitude nihanja napetosti S_a, s pomočjo katere se določi dovoljeno število ciklov obremenitve, se izvaja po naslednjem postopku:

1. določitev glavnih napetosti za obremenitveni cikel v odvisnosti od časa $\sigma_1(t)$, $\sigma_2(t)$ in $\sigma_3(t)$,
2. določitev absolutne vrednosti razlik glavnih napetosti med potekom cikla

$$\begin{aligned} S_{12}(t) &= \left|\sigma_1(t)-\sigma_2(t)\right| \\ S_{23}(t) &= \left|\sigma_2(t)-\sigma_3(t)\right| \text{ in} \\ S_{31}(t) &= \left|\sigma_3(t)-\sigma_1(t)\right| \end{aligned} \tag{12}$$

3. določitev največje velikosti amplitude nihanja napetosti S_a v izbrani materialni točki kot polovica razlike med dvema ekstremoma časovno se spreminjajoče absolutne razlike glavnih napetosti.

$$S_a = 0{,}5\cdot\left[\max\left(S_{ij}(t)\right)-\min\left(S_{ij}(t)\right)\right] \text{ oziroma} \tag{13}$$

$$S_a = 0{,}5\cdot\sigma_p^{Tr}\,. \tag{14}$$

Opisana definicija amplitude nihanja napetosti S_a velja v primerih, v katerih so smeri glavnih napetosti nespremenjene ves čas trajanja prehodnega pojava oz. napetostnega cikla. Kadar se smeri glavnih napetosti med ciklom spreminjajo, ASME B&PV Code predvideva uporabo

postopka, opisanega v NB-3216.2 [4]. Bistvo tega postopka je obdelava napetostnega tenzorja še preden določimo glavne napetosti. Amplitudo nihanja napetosti pa iz obdelanega tenzorja določimo po postopku, ki je opisan zgoraj.

4.3.5 Delni faktor izrabe

Faktor izrabe u_i je definiran kot razmerje med številom ponovitev obremenitvenega cikla n_i in dopustnim številom obremenitvenih ciklov N_i. ki ga pri znani amplitudi nihanja napetosti izbranega cikla S_{ai} določimo iz Wöhlerjeve krivulje (Slika 6):

$$u_i = \frac{n_i}{N_i}. \tag{15}$$

Postopek je potrebno ponoviti za vsak obremenitveni cikel posebej.

5 OCENA CIKLIČNIH NAPETOSTI

Kot je razvidno iz poglavja 4, je za določitev faktorja izrabe potrebno poznati napetostni tenzor v vseh materialnih točkah obravnavane komponente. V nadaljevanju so zbrane osnovne enačbe in najbolj pogosti načini njihovega reševanja.

5.1 Osnovne enačbe

Deformacije in napetosti v elastičnem telesu je mogoče popisati s tremi skupinami enačb: ravnovesnimi, kinematičnimi in konstitutivnimi. Skupen zapis vseh treh skupin enačb navadno imenujemo Navier-Laméjeve enačbe. Zapišemo jih v komponentni obliki:

$$\begin{aligned}
&\mu\left(\nabla^2 u + \frac{1}{1-2\nu}\frac{\partial \varepsilon_V}{\partial x}\right) - \frac{\alpha E}{1-2\nu}\frac{\partial T}{\partial x} + f_x = 0 \\
&\mu\left(\nabla^2 v + \frac{1}{1-2\nu}\frac{\partial \varepsilon_V}{\partial y}\right) - \frac{\alpha E}{1-2\nu}\frac{\partial T}{\partial y} + f_y = 0\ , \\
&\mu\left(\nabla^2 w + \frac{1}{1-2\nu}\frac{\partial \varepsilon_V}{\partial z}\right) - \frac{\alpha E}{1-2\nu}\frac{\partial T}{\partial z} + f_z = 0
\end{aligned} \tag{16}$$

kjer predstavlja E elastični modul, u, v in w komponente vektorja pomika, f_x, f_y in f_z komponente vektorja zunanjih sil ter ν Poissonovo število. Volumska specifična deformacija ε_V je definirana kot prva invarianta tenzorja deformacij:

$$\varepsilon_V = \varepsilon_x + \varepsilon_y + \varepsilon_z . \tag{17}$$

Strižni modul μ v izrazu (16) je določena z enačbo:

$$\mu = \frac{E}{2(1+\nu)} . \tag{18}$$

5.2 Analitično reševanje

Analitične rešitve enačb, predstavljenih v tem poglavju, so omejene na razmeroma enostavne geometrije, med katere sodi tudi dolg votli valj. Njihova praktična uporabnost je žal razmeroma omejena, so pa lahko v veliko pomoč pri preverjanju natančnosti in zanesljivosti numeričnih rešitev, ki jih opisujemo v poglavju 5.3.

5.2.1 Omejitve in predpostavke

Omejimo se na linearno-elastično obnašanje materiala. V tem primeru lahko napetosti, ki so posledica toplotnih in tlačnih obremenitev, obravnavamo ločeno, rezultate pa superponiramo. Pri reševanju se omejimo tudi na obliko votlega valja. Večina komponent, ki tvorijo tlačne meje hladil v jedrskih elektrarnah, ima namreč valjasto obliko.

5.2.2 Napetosti zaradi temperaturnih sprememb

Če prihaja do temperaturnih sprememb v telesu, se le to raztegne (povečevanje temperatur) ali skrči (zniževanje temperature). Če ni mogoče prosto krčenje oz. raztezanje telesa, se pojavijo napetosti.

Časovno spremembo temperature (dT/dt) v trdnini z gostoto ρ, prostornino V in specifično toploto c_p je mogoče zapisati kot:

$$\rho V c_p \frac{\mathrm{d}T}{\mathrm{d}t} = \frac{\mathrm{d}Q}{\mathrm{d}t} + \frac{\mathrm{d}Q_V}{\mathrm{d}t}, \tag{19}$$

pri čemer je v izrazu (19) upoštevana vsota toplotnih tokov v obravnavano telo dQ/dt ter generacija toplote v telesu dQ_V/dt. Porazdelitev temperature v (izotropnem) telesu lahko izračunamo s pomočjo Fourierovega zakona prevodnosti:

$$q = -k \nabla T = -k\left(\frac{\delta T}{\delta x}, \frac{\delta T}{\delta y}, \frac{\delta T}{\delta z}\right). \tag{20}$$

V izrazu (20) za toplotni tok q predstavlja k toplotno prevodnost, ki je snovska lastnost. Za večino komponent v primarnem krogu elektrarne lahko predpostavimo, da ni generacije toplote v steni. Z združitvijo enačb (19) in (20) potem dobimo:

$$\rho c_p \frac{\delta T}{\delta t} = \nabla\left(-k \nabla T\right) = k \nabla^2 T = k\left(\frac{\delta^2 T}{\delta x^2} + \frac{\delta^2 T}{\delta y^2} + \frac{\delta^2 T}{\delta z^2}\right). \tag{21}$$

V valjastih koordinatah pa velja

$$\rho c_p \frac{\delta T}{\delta t} = k \nabla^2 T = k\left(\frac{1}{r}\frac{\delta}{\delta r}\left(r\frac{\delta T}{\delta r}\right) + \frac{1}{r^2}\frac{\delta^2 T}{\delta \phi^2} + \frac{\delta^2 T}{\delta z^2}\right). \tag{22}$$

Zgoraj napisani izrazi predstavljajo porazdelitev temperature v trdnini. Za njeno enolično določitev je potrebno opredeliti še začetne in robne pogoje.

Dober približek dogajanja v cevovodih predstavlja idealna izolacija na zunanji površini cevi in predpisana temperatura na notranji površini cevi. Če se temperatura na notranji površini cevi s časom spreminja, imamo opraviti z nehomogenim robnim pogojem. Predpisana temperatura na notranji površini cevi je konservativni mejni primer prestopa toplote s tekočine na cev pri neskončnem prestopnostnim koeficientom.

Izrazi, ki opisujejo mehanizem prevoda toplote in robne pogoje so v nadaljevanju predstavljeni kot brezdimenzijske veličine:

$$\begin{aligned}
&\frac{\mathrm{d}\overline{T}}{dt} = \left(\frac{\partial^2 \overline{T}}{\partial \bar{r}^2} + \frac{1}{\bar{r}} \frac{\partial \overline{T}}{\partial \bar{r}} \right) \\
&\overline{T}\left(\bar{r}, \bar{t} = 0\right) = T_S\left(r\right) - T_R\left(R_1, t = \infty\right) \\
&\overline{T}\left(\bar{r} = \frac{R_1}{R_2}, \bar{t} \right) = T_R\left(R_1, t\right) - T_R\left(R_1, t = \infty\right) \\
&\frac{\partial \overline{T}}{\partial \bar{r}}\left(\bar{r} = 1, \bar{t}\right) = 0
\end{aligned} \quad . \tag{23}$$

$T_s(r)$ predstavlja začetno temperaturo, $T_R(R_1, t)$ je temperaturni robni pogoj na notranjem polmeru cevi, R_1 in R_2 sta notranji in zunanji polmer cevi. V enačbi (23) so brezdimenzijski polmer, temperatura in čas definirani kot

$$\bar{r} = \frac{r}{R_2},$$

$$\overline{T} = T - T_R\left(\infty\right) \text{ in} \tag{24}$$

$$\bar{t} = \frac{t}{t_0} = \frac{t}{\rho\, c_p R_2^2 / \lambda} = t \frac{\chi}{R_2^2}.$$

t predstavlja čas, λ temperaturno prevodnost, T temperaturo, r radij, ρ gostoto, c_p specifično toploto in $\chi = \lambda / \rho\ c_p$ toplotno difuzivnost.

Enačbo (23) lahko rešimo z metodo ločenih spremenljivk v cilindričnem koordinatnem sistemu. Diferencialna enačba se razcepi v časovno in krajevno odvisni diferencialni enačbi. Časovno odvisna diferencialna enačba je linearna homogena enačba prvega reda. Krajevno odvisna enačba predstavlja Besselovo diferencialno enačbo.

V primeru časovno odvisnih robnih pogojev je smiselna uporaba Duchamelovega teorema [22], [23]. Temperaturna porazdelitev za časovno odvisne robne pogoje je v primeru konstantnih začetnih pogojev (ki so lahko izraženi kot ničelni začetni pogoji v normalizirani obliki) enaka

$$\overline{T}\left(\bar{r}, \bar{t}\right) = \int_{\tau=0}^{\bar{t}} f\left(\bar{r}, \bar{t} - \tau\right) \frac{\mathrm{d}\overline{T}_R\left(\tau\right)}{\mathrm{d}\,\tau} \mathrm{d}\,\tau, \tag{25}$$

kjer predstavlja $f\left(\bar{r}, \bar{t} - \tau\right)$ brezdimenzijsko rešitev enačbe (23) s trenutno spremembo robnega pogoja (temperatura površine cevi) iz 0 na 1. Uporabljen je ničelni začetni pogoj. Spremenljivka τ je integracijska spremenljivka, ki poteka preko vseh preteklih časov, pri čemer je temperaturni odziv seštet za neskončno majhne stopničaste spremembe. Tako dobimo:

$$\overline{T}\left(\bar{r},\bar{t}\right)=\overline{T}_R\left(\bar{t}\right)-\sum_{n=1}^{\infty}A_{nCONST}C_n(k_n\bar{r})e^{-k_n^2\bar{t}}F\left(k_n^2,\bar{t}\right), \tag{26}$$

kjer koeficient A_{nCONST} izračunamo kot:

$$A_{nCONST}=\int_a^1 C_n\left(k_n\bar{r}\right)\bar{r}\,\mathrm{d}\,\bar{r}\,/\int_a^1 C_n^2\left(k_n\bar{r}\right)\bar{r}\,\mathrm{d}\,\bar{r}\,. \tag{27}$$

a je razmerje notranjega in zunanjega radija (R_1/R_2) in k_n rešitev enačbe

$$0=Y_1\left(k_n\right)J_0\left(k_n a\right)-Y_0\left(k_n a\right)J_1\left(k_n\right), \tag{28}$$

kjer predstavljata J_n in Y_n Besselove in Neumannove funkcije reda $n = 0$ in $n = 1$. Valjne funkcije C_n določimo kot:

$$C_n=J_0\left(k_n r\right)-\frac{J_0\left(k_n a\right)}{Y_0\left(k_n a\right)}Y_0\left(k_n r\right). \tag{29}$$

Funkcija $F\left(\beta,\bar{t}\right)$ je definirana kot:

$$F\left(\beta,\bar{t}\right)=\int_0^t\frac{\delta T_R(\tau)}{\delta\tau}e^{(\beta\tau)}d\,\tau\,. \tag{30}$$

V dolgem valju z notranjim polmerom R_1 in zunanjim polmerom R_2, kjer je temperaturna porazdelitev $T(r)$ znana in odvisna le od polmera r, znašajo radialna, obročna in osna komponenta termičnih napetosti [24]:

$$\begin{aligned}
\sigma_r&=\frac{\alpha\,E}{1-\nu}\frac{1}{\bar{r}^2}\left(\frac{\bar{r}^2-a^2}{1-a^2}\int_a^1\overline{T}\left(\bar{r}\right)\bar{r}\,\mathrm{d}\,\bar{r}-\int_a^{\bar{r}}\overline{T}\left(\bar{r}\right)\bar{r}\,\mathrm{d}\,\bar{r}\right)\\
\sigma_\theta&=\frac{\alpha\,E}{1-\nu}\frac{1}{\bar{r}^2}\left(\frac{\bar{r}^2+a^2}{1-a^2}\int_a^1\overline{T}\left(\bar{r}\right)\bar{r}\,\mathrm{d}\,\bar{r}+\int_a^{\bar{r}}\overline{T}\left(\bar{r}\right)\bar{r}\,\mathrm{d}\,\bar{r}-\overline{T}\left(\bar{r}\right)\bar{r}^2\right),\\
\sigma_z&=\frac{\alpha\,E}{1-\nu}\left(\frac{2\,\nu}{1-a^2}\int_a^1\overline{T}\left(\bar{r}\right)\bar{r}\,\mathrm{d}\,\bar{r}-\overline{T}\left(\bar{r}\right)\right)+\alpha\,E\left(T_{ref}-T_R(\infty)\right)
\end{aligned} \tag{31}$$

kjer predstavlja α linearni temperaturni razteznostni koeficient, E modul elastičnosti, $\bar{r}$ je brezdimenzijski polmer skladno z izrazom (24). T_ref je temperatura, pri kateri je $\sigma_z = 0$.

V izrazu (31) je bilo upoštevano

$$\int_{R_1}^{R_2}\left(T(r)-T_R(\infty)\right)r\,\mathrm{d}\,r=R_2^2\int_a^1\overline{T}(\bar{r})\,\bar{r}\,\mathrm{d}\,\bar{r}\,. \tag{32}$$

V primeru cevi proste na obeh koncih je potrebno k σ_z dodati σ_z^0:

$$\sigma_z^0 = \alpha\, E\left(\overline{T_A} - T_{ref}\right) = \alpha\, E\left(\frac{\int_a^1 \overline{T}(\bar{r})\, 2\pi\, \bar{r}\, \mathrm{d}\bar{r}}{\pi\,(1-a^2)} - \left(T_{ref} - T_R(\infty)\right) \right). \tag{33}$$

Povprečna temperatura v steni cevi je definirana kot:

$$\overline{T_A} = \frac{2}{1-a^2} \int_a^1 \overline{T}(\bar{r})\, \bar{r}\, \mathrm{d}\bar{r}\,. \tag{34}$$

Spremembe temperature na notranji površini cevi torej povzročajo spremembe temperature in s tem napetosti skozi debelino stene cevi. Najbolj konservativna oblika temperaturne spremembe na notranji površini cevi je stopničasta sprememba (Slika 7), ki predstavlja ovojnico vsem drugim oblikam temperaturnih sprememb (linearna, sinusna,…).

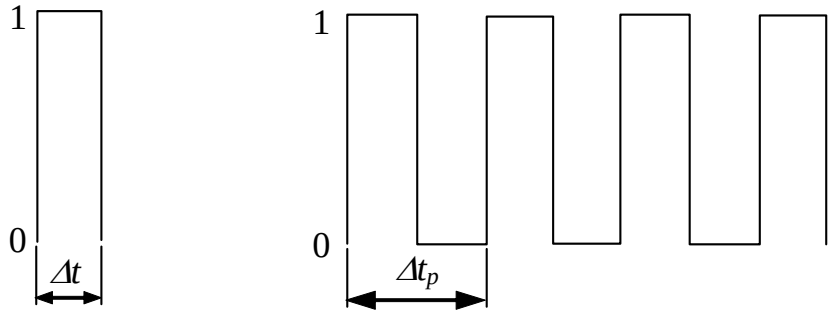

a) enotna stopnica b) periodična sprememba

Slika 7 Stopničaste spremembe temperature iz 0 na 1 in nazaj na 0

Vpliv stopničaste spremembe temperature na amplitudo nihanja napetosti je prikazan na primeru cevi iz primarnega kroga jedrske elektrarne. Debeline cevi značilno znašajo 5-15% polmera cevi. Iz tega sledi razmerje med notranjim in zunanjim polmerom a = 0.85 in a = 0.95. Rezultati so predstavljeni za tri značilna razmerja a: 0.85, 0.9 in 0.95. Materialni parametri, uporabljeni v analizi so značilni za avstenitna nerjavna jekla, ki se uporabljajo v jedrski tehniki: toplotna prevodnost λ = 20 W/mK, gostota ρ = 7880 kg/m^3, specifična toplota c_p = 502 J/kgK, modul elastičnosti E = 206842 MPa, linearni toplotni razteznostni koeficient α = $1.87 \cdot 10^{-5}$ K^{-1}. Čas t_0 je v skladu z enačbo (24) izražen z R_2^2 / χ, kjer je vrednost toplotne difuzivnosti χ = $5.056\ 10^{-6}$ m^2/s. Za prelivni vod tlačnika z zunanjim radijem R_2.= 0,1619 m torej velja t_0 = 5184 s.

Spreminjajoča se napetost je za enojno stopničasto spremembo (Slika 7a) neodvisna od časa trajanja Δt, ker se največja razlika napetosti pojavi v času t = 0 na notranji površini stene cevi, ko pride do spremembe temperature (npr. iz 0 na 1 - Slika 7a). Analiziran je bil vpliv debeline stene cevi pri enojni stopničasti spremembi temperature na amplitudo nihanja napetosti. Iz

rezultatov (Tabela 1) je mogoče razbrati, da se največja S_a pojavi za debele cevi. Iz rezultatov je prav tako mogoče razbrati, da debeline stene cevi v območju 5-15% polmera cevi nimajo pomembnega vpliva na S_a.

R_1 / R_2	S_a [MPa]
0.85	2.74565
0.9	2.74515
0.95	2.74465

Tabela 1 Vpliv stopničaste spremembe (Slika 7a) na amplitudo nihanja napetosti S_a za različne debeline stene cevi

Pri periodični spremembi temperature (Slika 7b) na notranji površini cevi pa povečanje debeline stene cevi povzroča manjšo napetost S_a (Slika 8). Višje frekvence povzročajo manjše povprečne temperature v steni cevi, kar vodi k nižjim napetostim in posledično k nižjim S_a.

Slika 8 prikazuje frekvence v brezdimenzijskem času. Pri njihovi interpretaciji je potrebno upoštevati vrednost t_0, ki je odvisna od konfiguracije cevovoda. Za prelivni vod tlačnika velja t_0 = 5184 s. Frekvenca 100 [1/ t_0] torej znaša pribl. 0,02 Hz.

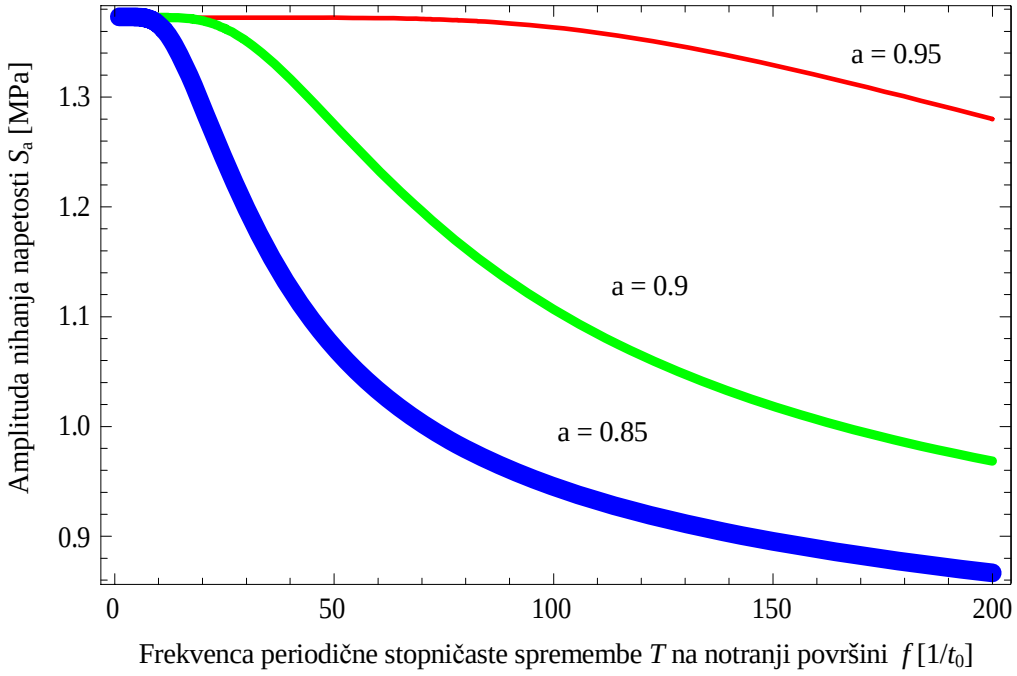

Slika 8 Vpliv frekvence *f* stopničaste spremembe temperature na notranji površini stene cevi na amplitudo nihanja napetosti S_a

5.2.3 Napetosti zaradi notranjega tlaka

Radialna komponenta napetosti v cevi, obremenjeni z notranjim tlakom p_N, znaša:

$$\sigma_r = p_N \frac{R_1^2}{R_2^2 - R_1^2}\left(1 - \frac{R_2^2}{r^2}\right). \tag{35}$$

Obročna komponenta napetost v cevi, obremenjeni z notranjim tlakom p_N, znaša:

$$\sigma_\phi = p_N \frac{R_1^2}{R_2^2 - R_1^2}\left(1 + \frac{R_2^2}{r^2}\right). \tag{36}$$

Če sta oba konca valja togo vpeta ($\varepsilon_z = 0$), nastane hkrati v osni smeri napetost:

$$\sigma_z = 2\nu\, p_N \frac{R_1^2}{R_2^2 - R_1^2} = konst. \tag{37}$$

Kadar pa je valj na obeh konceh zaprt, notranji tlak v osni smeri povzroči napetost:

$$\sigma_z = p_N \frac{R_1^2}{R_2^2 - R_1^2} = konst. \tag{38}$$

V izrazih (35) do (38) je $R_{1,2}$ notranji oz. zunanji polmer cevi, r je polmer cevi na katerem računamo napetost ($R_1 \leq r \leq R_2$) in ν Poissonovo število.

Obročna napetost (izraz (36)) ima maksimum pri $r = R_1$. Pri tem pogoju lahko z limitnim procesom $R_2/R_1 \rightarrow 1$, torej za tankostenske cevi, dobimo t. i. kotlovsko enačbo, ki je osnova za dimenzioniranje valjastih lupin po ASME III [4]. Napetost v obročni smeri v tankostenski cevi dobimo kot [21]:

$$\sigma_\phi = p_N \frac{R_1}{R_2 - R_1}. \tag{39}$$

Napetost v osni smeri je približno polovico manjša ($R_2/R_1 \rightarrow 1$):

$$\sigma_z = p_N \frac{R_1^2}{R_2^2 - R_1^2} = \sigma_\phi \frac{R_1}{R_2 + R_1} \approx \frac{1}{2}\sigma_\phi. \tag{40}$$

V votlem valju oz. cevi obremenjeni z notranjim tlakom največja napetost nastane v obročni smeri.

V primeru, ko je cev obremenjena z notranjim tlakom p_N, je največja razlika napetosti odvisna od obročne in radialne komponente napetosti. Vpliv debeline stene cevi na amplitudo nihanja napetosti S_a pokaže, da se le-ta povečuje, ko se debelina stene cevi zmanjšuje (Slika 9).

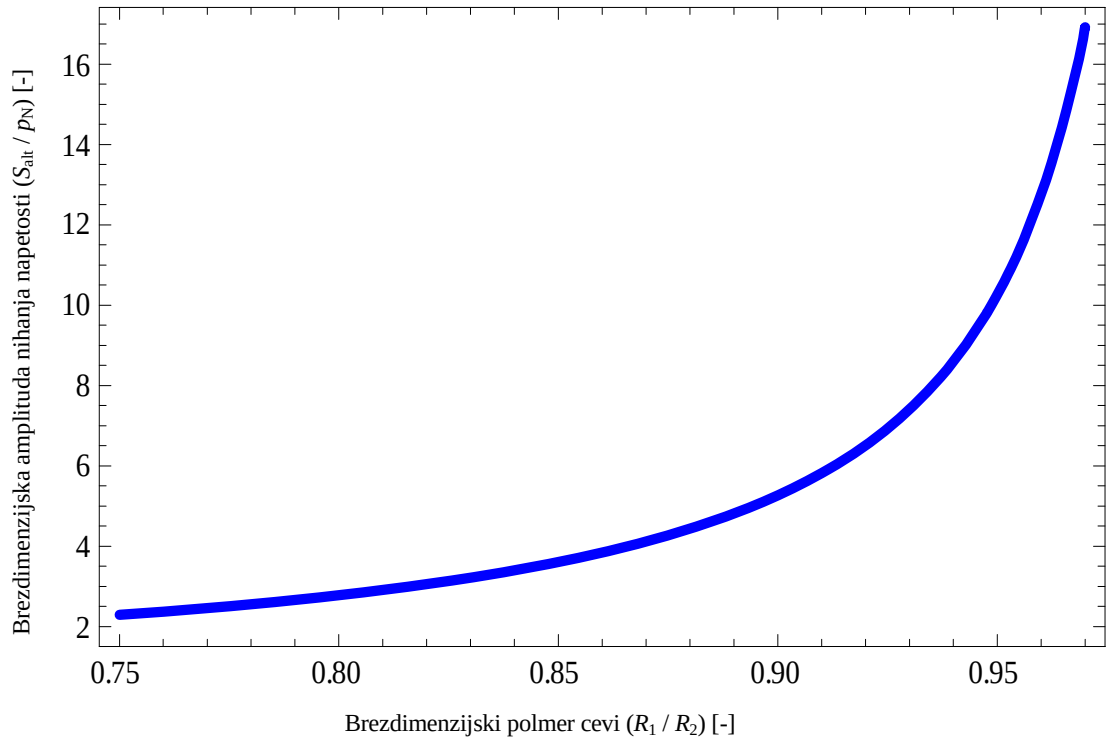

Slika 9 Vpliv brezdimenzijskega polmera R_1/R_2 na brezdimenzijsko amplitudo napetosti S_a

5.3 Numerično reševanje

Kadar ne znamo matematičnega modela rešiti analitično, ga rešujemo numerično. Pri numeričnem reševanju se trudimo čimbolj natančno rešiti nalogo pri danih vrednostih podatkov. Numerične metode so zelo močno orodje za reševanje matematičnih modelov, ki izhajajo iz inženirske prakse. Eno od takšnih orodij je metoda končnih elementov (MKE), ki omogoča reševanje zelo širokega spektra linearnih in nelinearnih inženirskih problemov.

5.3.1 Metoda končnih elementov

Metoda končnih elementov je dosegla izreden razvoj, omogoča široko področje uporabe in je praktično nepogrešljiva metoda za reševanje praktičnih primerov v jedrski stroki. Najbolj splošen tip končnih elementov, ki je na razpolago za trdnostne analize, je družina tridimenzionalnih končnih elementov, saj so vse strukture, ki so predmet numeričnih analiz, v svoji izvirni obliki tridimenzionalne. Numerične modele pa lahko tudi poenostavimo in sicer v odvisnosti od oblik obravnavanih komponent, pričakovane natančnosti izračunov in predlogov standardov. Tako lahko poleg tridimenzionalnih volumskih elementov uporabimo še linijske (npr. nosilci, cevi), dvodimenzionalne (npr. plošče) in tridimenzionalne lupinske elemente.

5.3.2 Osnovne omejitve, predpostavke in značilna uporaba modelov

V standardu ASME [4] ni navodil za uporabo MKE pri projektiranju komponent. Nekaj smernic pa lahko najdemo v literaturi MKE [5]. Tako je navedeno, da bi se naj glavne napetosti in ekvivalentne napetosti, ki jih potrebujemo za izračun amplitude nihanja napetosti, računale na osnovi linearizacije napetosti. Pri tem pa je potrebno razvrstiti izračunane napetosti v eno ali več skupin: glavna membranska napetost P_m, lokalna membranska napetost P_L, glavna

upogibna napetost P_b, napetost zaradi ekspanzije P_e, sekundarna napetost Q, najvišja napetost F. Razdelitev napetosti po kategorijah ni enolična, kljub pojasnjevanju v tabeli NB-3217-1 [4]. Poleg tega pa računalniški programi za analizo po MKE praviloma izračunajo napetosti v obliki celotnih napetostnih tenzorjev in jih ne razdelijo v prej naštete kategorije, kar je omenjeno tudi v opombi pri sliki NB-3222-1 [4]. Dodatna težava lahko nastopi pri izbiri poti za linearizacijo in izbiri števila točk [2], predvsem na mestih diskuntinuitet komponent, kjer lahko slabo izbrana pot za linearizacijo vodi k napačnim rezultatom. Zaradi tega smo intenziteto napetosti določili direktno iz rezultatov analize kot polovico napetosti po Tresca kriteriju, saj so v njej zajete vse uporabljene obremenitve in diskontinuitete komponent in materiala.

Pri uporabi prostorskih modelov, diskretiziranih z volumskimi elementi in pri uporabi dvodimenzionalnih elementov morajo biti izpolnjeni trije bistveni pogoji:

1. zagotovljena mora biti dovolj gosta mreža na vseh mestih, kjer se pričakuje velike temperaturne oz. napetostne gradiente.
2. razmerje robov osnovnega gradnika (končni element v obliki prizme pri prostorskih modelih in pravokotnika pri ravninskih modelih) mora ostati v predpisanih mejah [25], sicer lahko pričakujemo numerične nestabilnosti in s tem povezane netočnosti pri rezultatih. Glede na priporočila [5] se naj ne bi uporabljali nepravokotni elementi.
3. končni model mora imeti čim manj elementov, tako, da računski časi niso predolgi. Optimalno mrežo oziroma število končnih elementov vzdolž debeline stene komponente določimo na osnovi primerjave rezultatov analitične rešitve enačb (poglavje 5.2) in numeričnih rezultatov.

Numerični model je potrebno verificirati z rezultati dobljenimi po standardu ASME. Predvsem je to pomembno na mestih diskuntinuitet. V ta namen so lahko v pomoč tudi analize v literaturi, npr. [26].

Pri analizah utrujanja lahko kombiniramo različne tipe elementov, s čemer lahko dobimo manjše računske modele ob ne bistveno zmanjšanji natančnosti rezultatov. Tako lahko npr. za problem toplotnega razslojevanja [27] uporabimo kombinacijo tridimenzionalnih volumskih elementov (področje spreminjajočih se temperatur po prerezu) in linijskih elementov (področje konstantnih temperatur po prerezu).

Glavni rezultat linijskih modelov so pomiki, katerih vrednosti so podane v vozliščih. Reakcijske sile in momenti ustrezajo predpisanim robnim pogojem. Iz rezultatov lahko uporabimo notranje sile in momente, s katerimi lahko s postopki po ASME izvršimo kontrolo napetosti v obravnavanih prerezih ali pa izračunavamo komponente tenzorja napetosti glede na podane obremenitve.

Dvodimenzionalne elemente lahko uporabimo za določevanje možnih temperaturnih sprememb na notranji strani cevi, če poznamo meritve temperature na zunanjem robu cevi. Tako določene temperaturne spremembe na notranji strani lahko potem uporabimo v analizi za določitev izrabe komponent.

Tako lahko glede na vhodne podatke potrebne za utrujenostne analize z MKE v linijskih modelih uporabimo podatke dobljene na osnovi meritev iz procesno informacijskega sistema, v ravninskih modelih podatke dobljene na osnovi lokalnih meritev po obodu cevi, v prostorskih modelih pa lahko poleg omenjenih podatkov uporabimo še podatke dobljene na osnovi simulacij s programi za modeliranje dinamike tekočin.

6 ZAKLJUČKI

Med pomembnejše aktivnosti pri obvladovanju staranja pasivnih komponent (npr. cevovodi in tlačne posode) v jedrskih elektrarnah sodi tudi sprotno spremljanje utrujenostne izrabe komponent. Pri tem si lahko obratovalno osebje elektrarne v veliki meri pomaga z izmerjenimi parametri obratovalnih dogodkov in prehodnih pojavov. Praviloma so spremembe tlakov, temperatur in pretokov manjše, kot je bilo konzervativno ocenjeno v projektu. Zato je tudi njihov vpliv na trajnostno dobo dostikrat manjši.

Za zanesljivo oceno dejanske izrabe komponent poleg projektnih in dejansko izmerjenih podatkov o obratovalnih dogodkih in prehodnih pojavih potrebujemo še računske modele, s katerimi lahko ocenimo prispevke posameznega prehodnega pojava k skupni izrabi komponent. Ključni viri podatkov v ta namen so projektna dokumentacija, procesni informacijski sitem, neposredne meritve, simulacije s programi za računalniško dinamiko tekočin in tuje izkušnje. Dostopnost in podrobnost podatkov seveda bistveno vplivata na natančnost ocene izrabe.

V poročilu smo zasnovali metodo za spremljanje izrabe komponent jedrskih elektrarn, ki jo označujeta primerno uravnotežena dostopnost podatkov in kompleksnost uporabljenih računskih modelov. Nakazujemo tudi nekatere možne poti za rekonstrukcijo manjkajočih podatkov. Metoda je zasnovana v skladu s standardom ASME, po katerem je projektirana in grajena jedrska elektrarna v Krškem. Zato omogoča tudi primerjave z originalnimi projekti.

Metoda je namenjena predvsem podpori pri načrtovanju zamenjave komponent in preventivnega vzdrževanja jedrskih elektrarn. Zelo uporabna bi lahko bila tudi pri neodvisni presoji projektnih izračunov. Zasnova pa omogoča tudi morebitno dodelavo in razširitev za izvajanje projektnih izračunov v prihodnosti.

7 VIRI

[1] Zafošnik, B., Cizelj, L.: Baza prehodnih pojavov v jedrski elektrarni Krško, IJS delovno poročilo, IJS-DP-10077, 2009.

[2] Zafošnik, B., Cizelj, L.: Pilotni primeri izračuna faktorja utrujenostne izrabe, IJS delovno poročilo, IJS-DP-10076, 2009.

[3] Zakon o varstvu pred ionizirajočimi sevanji in jedrski varnosti (ZVISJV-UPB2), Ur.l. RS 102/04, 12360.

[4] ASME Boiler and Pressure Vessel Code, 1986.

[5] Rao, K. R.: Companion Guide to the ASME Boiler & pressure Vessel Code, Volume 1, ASME PRESS, New York, 2002.

[6] 10 CFR 54 – Requirements For Renewal Of Operating Licenses For Nuclear Power Plants (Revised as of January 1, 2006; http://www.gpoaccess.gov/cfr/retrieve.html).

[7] Mukhopadhyay, N. K., Dutta, B. K., Swami Prasad, P., Kuswaha, H. S., Kakodkar, A.: Implementation of finite element based fatigue monitoring system at Heavy water Plant Kota, Nucl. Eng. Des., 187, 1999, str. 153-163.

[8] Kleinöder, W., Golembiewski, H.-J.: Monitoring for fatigue – examples for unexpected component loading, SMiRT 16, Washington DC, August 2001.

[9] Sakai, K., Hojo, K., Kato A., Umehara, R.: On-line fatigue-monitoring system for nuclear power plant, Nucl. Eng. Des., 153, 1994, str. 19-25.

[10] Maekawa, O., Kanazawa, Y., Takahashi, Y., Tani, M.: Operating data monitoring and fatigue evaluation systems and findings for boiling water reactors in Japan, Nucl. Eng. Des., 153, 1995, str. 135-143.

[11] Botto, D., Zucca, S. Gola, M.M.: A methodology for on-line calculation of temperature and thermal stress under non-linear boundary conditions, Int. J. Press. Vess. Pip., 80, 2003, str. 21-29.

[12] Samal, M. K., Dutta, B. K., Guin, S., Kushawa, H. S.: A finite element program for on-line life assessment of critical plant components, Eng. Fail. Analy., 16, 2009, str. 85-111.

[13] Duda, P., Taler, J., Roos E.: Inverse method for temperature and stress monitoring in complex-shaped bodies, Nucl. Eng. Des., 227(3), 2004, str. 331-347.

[14] Bartonicek, J., Schoeckle, F.: Monitoring of unspecified loads as a tool for ageing management, ASME PVP Conference, Seattle, 2000.

[15] Suresh, S.: Fatigue of Materials, second edition, Cambridge University press, 2004.

[16] Vojvodič – Tuma, J.: Mehanske lastnosti kovin, Fakulteta za gradbeništvo in geodezijo, Univerza v Ljubljani, 2002.

[17] US NRC Bulletin No. 88-11: Pressurizer Surge Line Thermal Stratification, Dec. 20, 1988.

[18] US NRC Information Notice No. 88-80: Unexpected Piping Movement Attributed To Thermal Stratification, Oct. 7, 1988.

[19] ANS N-18.2: Nuclear Safety Criteria for the Design of Stationary Pressurized Water Reactor Plants, 1973.

[20] Frank, T., Adlakha M., Adlakha, C., Lifante, H.-M., Prasser, F. Menter: Simulation of Turbulent and Thermal Mixing in T-Junctions Using URANS and Scale-Resolving Turbulenc Models in ANSYS CFX, XCFD4NRS - Experiments and CFD Codes Application to Nuclear Reactor Safety, OECD/NEA & International Atomic Agency (IAEA) Workshop, 10.-12. September 2008, Grenoble, France, str. 23.

[21] Alujevič, A.: Elasto-plastomehanika, Univerza v Mariboru, Tehniška fakulteta 1991.

[22] Özişik, M. N.: Heat conduction, John Wiley & Sons, inc., New York, 1993

[23] Myers, G. E.: Analytical Methods in Conduction Heat Transfer, McGraw-Hill, New York, 1971.

[24] Timoshenko, S., Goodier J. N.: Theory of elasticity, Kogakusha Company LtD, Tokyo, 1951.

[25] ABAQUS 6.6-1, 2006.

[26] WENX 98/01 –Rev. 2: Structural Analysis of Reactor Coolant Loop for the KRŠKO Nuclear Power Plant, Volume 1, Piping Analysis of the Reactor Coolant Loop, SSR-NEK-11.5: revison 2, May 2000, Final.

[27] Boros, I., Aszodi, A.: Analysis of thermal stratification in the primary circuit of a VVER-440 reactor with the CFX code, Nucl. Eng. Des., 238, 2008, str. 453-459.

International Conference
Nuclear Energy for New Europe 2009
Bled / Slovenia / September 14-17

Fatigue relevance of stratified flows in pipes: a parametric study

Leon Cizelj, Igor Simonovski
Jožef Stefan Institute, Reactor Engineering Division
Jamova 39, 1000 Ljubljana, Slovenia
Leon.Cizelj@ijs.si, Igor.Simonovski@ijs.si

ABSTRACT

Stratified flows may form in pipelines under certain conditions and could lead to increased fatigue loading that was only marginally accounted for during the design phase of the second generation of nuclear power plants. Extension of operational license would require explicit account for fatigue loads imposed by stratified flows. This further requires rather complex state-of-the-art computational technology combined with measurements of the temperatures at the outside surfaces of pipes, which comprise pressure boundary of the reactor coolant.

A parametric study using detailed finite element analysis has been performed to quantify the possible range of fatigue loads and fatigue usage factors. The example taken was a typical pressurized water reactor pressurizer surge line containing stratified flow of cold and hot water. The investigated parameters include the film coefficients governing the heat transfer from fluid to the pipe wall and the velocity of the interface between then cold and hot water.

Results of the paper include the expected ranges of fatigue loading and usage given the range of investigated parameters. It is shown that the estimation of the film coefficients is essential to arrive at reliable fatigue estimate. Additionally, predictions of readings provided by hypothetical thermocouples at the pipe outer surface are provided.

1 INTRODUCTION

Stratified flows that may form in pipelines under certain conditions could lead to increased fatigue loading that was only marginally accounted for during the design phase of the second generation of nuclear power plants [1, 2] designed in accordance to the ASME Boiler and Pressure Vessel Code [3]. Extension of operational license would in most countries require explicit account for fatigue loads imposed by stratified flows. This further requires rather complex state-of-the-art computational technology combined with measurements of the temperatures at the outside surfaces of pipes, which comprise pressure boundary of the reactor coolant [4, 5].

There is a wide consensus that within the reactor coolant systems of the pressurized water reactors (PWR) the stratified flows are most likely to occur in surge lines. The rather slow flows caused by the pressure controlling activities of the pressurizer could result in the stratified flow of cold and hot water. The typically reported velocity of such flows is in the order of cm/s [6]. The typical temperature difference between the hot and cold water is reported to be in the range of 120-150 °C. Such temperature differences are believed to be the cause of rather significant thermal stresses resulting in accelerated fatigue usage and in some cases also in observed fatigue damage [6-9].

An impressive body of open literature already exists. Some recent contributions include, among others, an attempt to simulate stratified flows using the computational fluid mechanics tools [6], proposal [9] to update the fatigue analysis procedures in the ASME Boiler and Pressure Vessel Code [3] and example of surge line fatigue analysis [7].

The published fatigue analyses are however to a large extent based on assumption that the temperatures at the pipe surface are known. In practice however, we may be aware of the temperatures and velocities of stratified fluids. Then, the temperature of the pipe surface would depend on the heat transfer or film coefficient.

The intention of this paper is to investigate the consequences of different assumptions on the heat transfer coefficient and the velocity of the fluid-fluid interface on the thermal stress ranges and therefore also on fatigue usage of the pipe. A typical 12 inch pressurized water reactor pressurizer surge line made of austenitic stainless steel has been chosen as the numerical example.

2 MODEL

The finite element model is reported in detail in [10, 11] together with some best estimate assessments of the fatigue loading. The model (Figure 1) contains 39049 finite elements with parabolic interpolation. Element types DC3D20 and C3D20 have been used for thermal and stress analyses using the ABAQUS/standard finite element code [12], respectively.

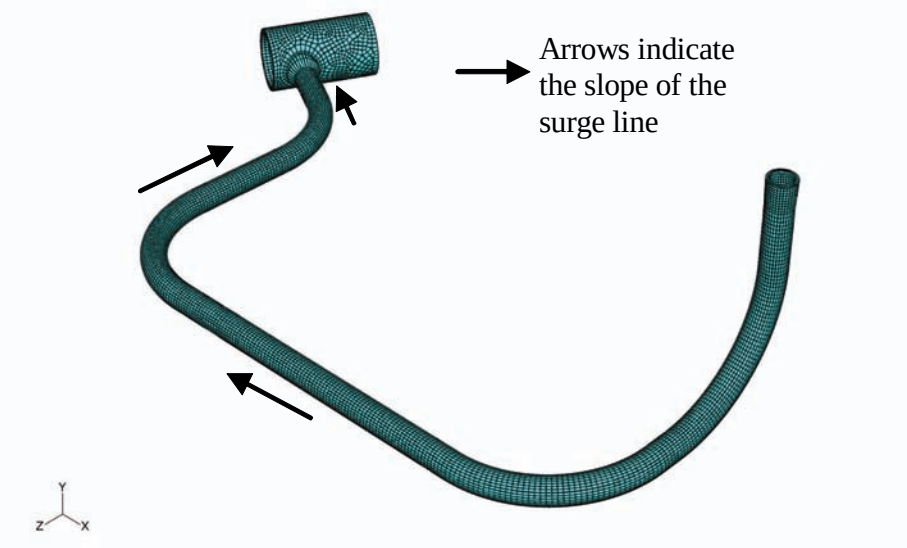

Figure 1**:** Outline and the finite element mesh of the surge line

The goal of this paper is to give a range of possible fatigue loads. The data on the pipe loads and results may therefore differ significantly from those reported in [10, 11].

The density of the finite element mesh has been evaluated against closed form solutions outlined in [13] and has been found sufficient for the range of loads considered here.

The temperature dependent material properties defined in [3] were consistently used.

2.1 Thermal analysis

In the first step, a transient heat transfer analysis has been performed. The temperature of the cold fluid entering the pressurizer surge line from the reactor coolant system was assumed at 96°C. The hot fluid entering the pressurizer surge line from the pressurizer was

assumed at 223°C. The temperature difference between both fluids of 127°C is consistent with data published elsewhere [6-9].

The assumed transient started from a steady state with already developed stratification: the interface between both fluids has been assumed at the lower surface of the surge line close to the nozzle attached to the primary piping (Figure 2, up). The interface was then assumed to move in the vertical direction with the velocity consistent with the typical capacity of the pressurizer sprays. After reaching the top of the pipe (Figure 2, down), the interface started to travel back down with the same velocity.

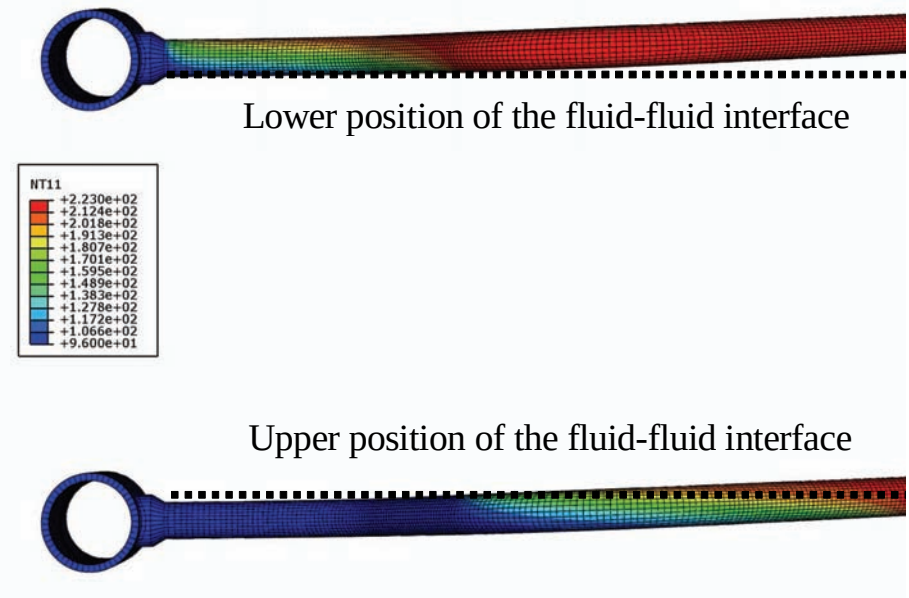

Figure 2**:** Lower and upper positions of fluid-fluid interface with respective steady state temperature distributions (°C, film coefficient of 50 W/m^{2}K)

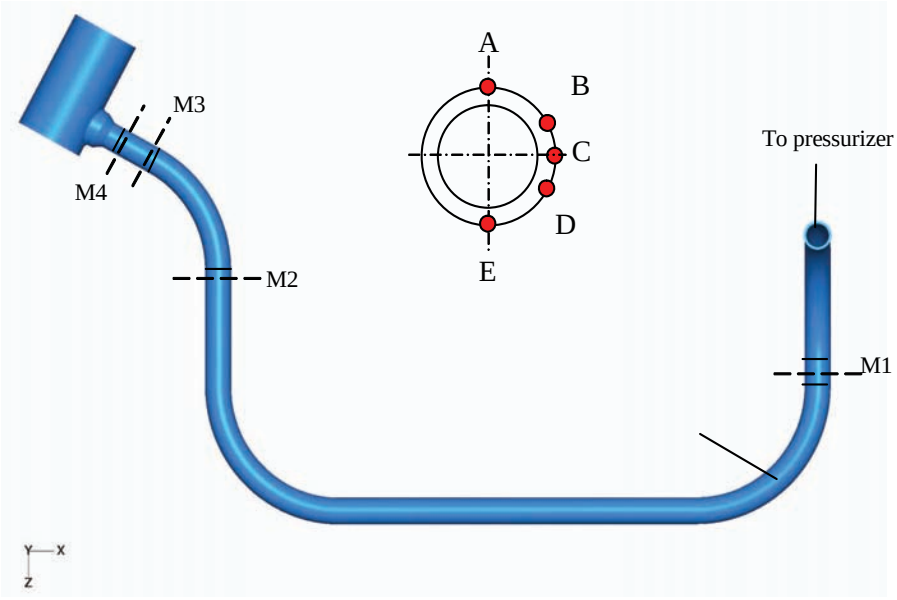

Figure 3**:** Assumed locations of thermocouples mounted on the outside pipe surface

The interface between the fluids was modelled as a horizontal plane with a step change in fluid temperatures in the vertical direction. The film coefficient was assumed constant for both cold and hot fluids with estimated value of 50 W/m^{2}K, which was deemed consistent

with the observed fluid velocities in the order of mm/s [10, 11]. In addition, film coefficients of 100, 500, 1.000 and 100.000 W/m^{2}K have been analyzed in the sensitivity analysis. Outer pipe surface was assumed perfectly insulated in all analyzed cases.

The vertical velocity of the interface was estimated at 2 mm/s [10, 11]. In addition, values of 5, 10, 50 and 100 mm/s have been analyzed in the sensitivity analysis.

The main results were transient temperature fields in the pipe. Additionally, temperature histories were recorded at inner and outer pipe surface at hypothetical positions of fatigue monitoring system thermocouples as indicated in Figure 3.

2.2 Stress analysis

The temperature fields were used to assess the transient stress fields in the second step. In addition, a constant internal pressure of 2,5 MPa was assumed.

2.3 Fatigue analysis

The fatigue analysis followed the ASME Boiler and Pressure Vessel rules [3]. The transient principal stresses $\sigma_1 > \sigma_2 > \sigma_3$ were used to define the stress amplitude:

$$S_a = 0{,}5 \cdot \left[\max\left(S_{ij}(t)\right) - \min\left(S_{ij}(t)\right)\right], \quad (1)$$

with:

$$\begin{aligned} S_{12}(t) &= \left|\sigma_1(t) - \sigma_2(t)\right| \\ S_{23}(t) &= \left|\sigma_2(t) - \sigma_3(t)\right| \\ S_{31}(t) &= \left|\sigma_3(t) - \sigma_1(t)\right|. \end{aligned} \quad (2)$$

The value of the stress amplitude S_a is then compared with the fatigue properties defined in [3] to obtain the allowable number of load cycles. It is useful to note here that for S_a below 93 MPa, 10^{11} or more of the loading cycles are considered acceptable, given a typical stainless steel used to manufacture the surge line. In other words, load cycles exceeding S_a of 93 MPa should be considered as fatigue relevant.

3 RESULTS

The simulated temperature fields are in the first step investigated through the readings of potential thermocouples (for assumed locations see Figure 3). Figure 4 depicts two examples detected at location M3-C. The cold water enters the surge line and pushes the interface between cold and hot water from the lower towards the upper surface of the pipe. When the tops surface is reached, the interface starts the downward motion with the same velocity.

As a consequence, the temperature at the pipe inside surface starts to decrease at about 30 s and decreases until about 200 s (dotted lines). Then the downward motion of the interface is noted and the temperatures of the inside surface start to increase. The temperature difference is, as expected, governed by the film coefficient. Different steady state temperatures at the beginning an the end of the transient are attributed to rather low film coefficients giving rise to the competition between heat conduction within the pipe wall and heat transfer from the water to the pipe. This is to some extent illustrated by the temperature field in Figure 6 indicating notable circumferential heat fluxes at the pipe inner surface.

The outside surface temperature readings (bold lines, Figure 4) clearly show delays and significantly underestimate the temperature transients at the pipe inner surface. While larger film coefficient clearly improves the sensitivity of the outside surface thermocouple, Figure 5 shows that faster movement of the fluid interface would tend to decrease both the maximum

temperature difference experienced by any material point of the pipe and the indication given by a potential thermocouple. We may also argue that the thermocouples may be able to detect the vertical motion of the stratification interface with velocities in the order of mm/s and are at the same time rather insensitive to motions with velocities exceeding some cm/s. It is therefore clear that a reliable interpretation of the thermocouple signals requires a significant amount of reverse engineering.

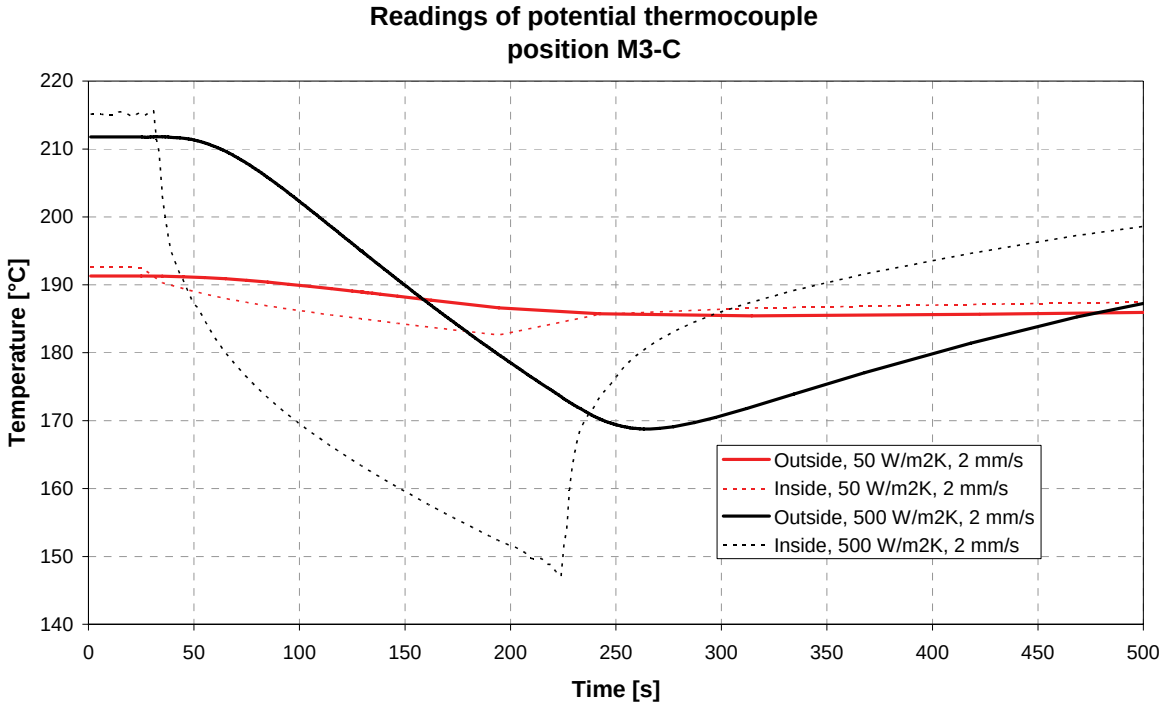

Figure 4**:** Example readings of potential thermocouple at position M3-C (Figure 3) with inside surface temperatures

A snapshot of a Tresca stress field is shown in Figure 7 and indicates rather high local variations. The results obtained as maxima of eq. (1) applied to the entire transient stress field are summarized in Table 1. It is shown that the velocity of the fluid interface (assuming fixed film coefficient value!) has negligible influence on the resulting stress amplitudes and that the increasing film coefficient increases the stress amplitude. Assuming that fatigue relevance requires stress amplitudes exceeding 93 MPa, it may be concluded that the transient studied is marginally fatigue relevant. It shall be noted here that it is only theoretically possible to decouple film coefficient and fluid velocities: it is well known that increasing fluid velocities increase the film coefficient. A detailed computational fluid dynamic study on the fluid to pipe wall heat transfer would certainly contribute to the more refined assessment of the fatigue relevance.

Table 1: Maximum stress amplitude S_a in the model [MPa]

Velocity of the fluid interface [mm/s]	**Film Coefficient [W/m^{2}K]**				
	50	**100**	**500**	**1.000**	**100.000**
2	68,6	84,4	105,1	114,1	228,9
100	68,7	84,5	105,4		

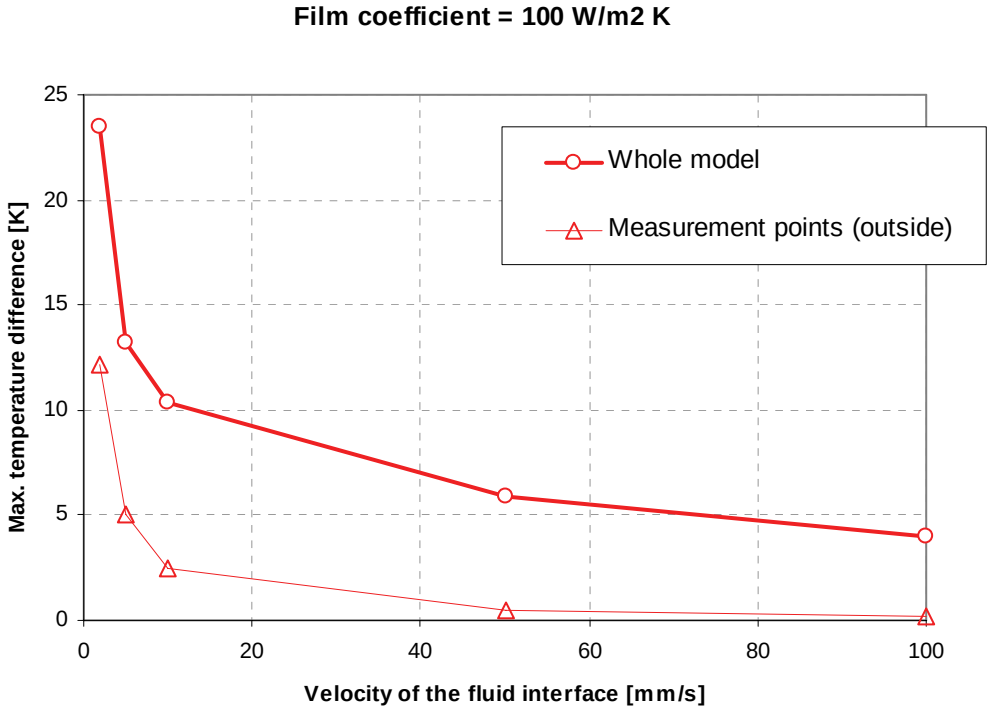

Figure 5**:** Maximal temperature difference in the model: calculated and indicated by potential thermocouple

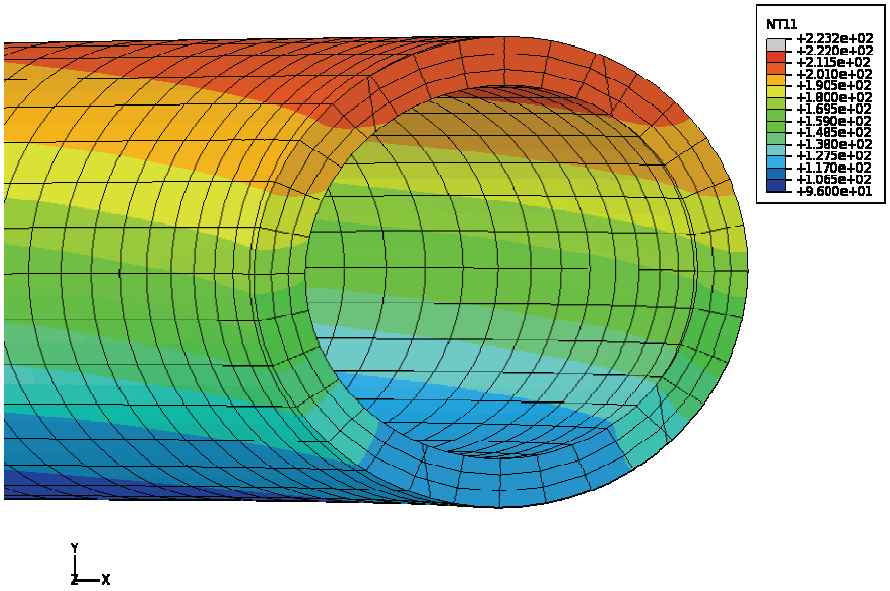

Figure 6**:** Example of the temperature distribution through a pipe wall in the middle of the assumed transient (°C)

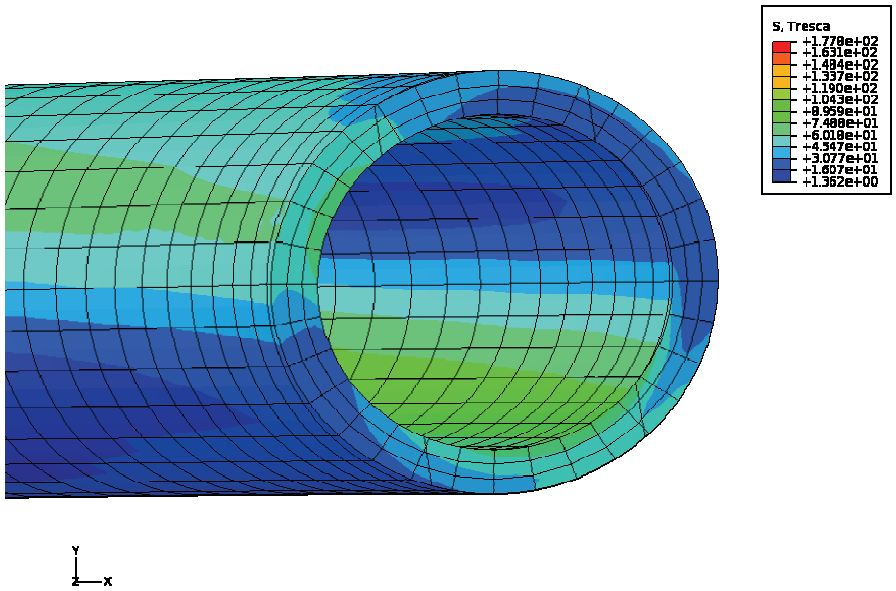

Figure 7**:** Example of the Tresca stress distribution through a pipe wall in the middle of the assumed transient (MPa)

4 CONCLUSIONS

A parametric study using detailed finite element analysis has been performed to quantify the possible range of fatigue loads and fatigue usage factors. The example taken was a typical pressurized water reactor pressurizer surge line containing stratified flow of cold and hot water. The investigated parameters include the film coefficients governing the heat transfer from fluid to the pipe wall and the velocity of the interface between then cold and hot water.

It has been shown that the velocity of the fluid interface, assuming fixed film coefficient value, has negligible influence on the resulting stress amplitudes and that the increasing film coefficient increases the stress amplitude. The results indicated marginal fatigue relevance. It shall be noted here that it is only theoretically possible to decouple film coefficient and fluid velocities: it is well known that increasing fluid velocities increase the film coefficient. A detailed computational fluid dynamic study on the fluid to pipe wall heat transfer would certainly contribute to the more refined assessment of the fatigue relevance.

It has been also shown that the potential thermocouples on the outside pipe surface may be able to detect the vertical motion of the stratification interface with velocities in the order of mm/s and are at the same time rather insensitive to motions with velocities exceeding some cm/s. It is therefore clear that a reliable interpretation of the thermocouple signals requires a significant amount of reverse engineering.

ACKNOWLEDGMENTS

The authors gratefully acknowledge the financial support from Slovenian research agency (grants Z2-9488(B), V2-0553 (C) and P2-0026 (C)), Krško Nuclear Power Plant (grant Z2-9488(B)) and Slovene Nuclear Safety Administration (grant V2-0553 (C)).

REFERENCES

[1] Pressurizer surge line thermal stratification. Bulletin 88-11: U.S. Nuclear Regulatory Commission; 20.12.1988.

[2] Unexpected piping movement attributed to thermal stratification. Information notice 88-80: U.S. Nuclear Regulatory Commission; 7.10.1988.

[3] ASME. Boiler and pressure vessel code. III Rules for construction of nuclear power plant components: ASME; 1989.

[4] Bartonicek J, Zaiss W, Hienstorfer W, Kocklemann H, Schöckle F. Monitoring systems and determination of actual fatigue usage. Nucl Eng Des. 1995;153(2-3):127-133.

[5] Pöckl C, Kleinöder W. Developing and implementing of a fatigue monitoring system for the new European pressurized water reactor EPR. In: Jenčič I, Lenošek M, editors. International conference Nuclear energy for new Europe. Portorož, Slovenia: Nuclear Society of Slovenia; 2007.

[6] Boros I, Aszódi A. Analysis of thermal stratification in the primary circuit of a VVER-440 reactor with the CFX code. Nucl Eng Des. 2008;238(3):453-459.

[7] Jhung MJ, Choi YH. Surge line stress due to thermal stratification. Nuclear Engineering and Technology. 2008;40(3):239-250.

[8] Kim KC, Lim JH, Yoon JK. Thermal fatigue estimation due to thermal stratification in the RCS branch line using one-way FSI scheme. Journal of Mechanical Science and Technology. 2008;22(11):2218-2227.

[9] Kweon HD, Kim JS, Lee KY. Fatigue design of nuclear class 1 piping considering thermal stratification. Nucl Eng Des. 2008;238(6):1265-1274.

[10] Zafošnik B, Cizelj L. Data base of transients in nuclear power plant Krško (in Slovene). "Jožef Stefan" Institute; 2009.

[11] Zafošnik B, Cizelj L. Design of a method for monitoring the usage of nuclear power plant components (in Slovene). "Jožef Stefan" Institute; 2009.

[12] ABAQUS. ABAQUS User's Manual 6.6-1. Providence, RI, USA: Dassault Systèmes Simulia Corp; 2006.

[13] Zafošnik B, Cizelj L. Safe fatigue life of nuclear piping exposed to temperature and pressure fluctuations. In: Rožman S, Žagar T, Žefran B, editors. International conference Nuclear energy for new Europe. Portorož, Slovenia: Nuclear Society of Slovenia; 2008.

Proceedings of the 18th International Conference on Nuclear Engineering
ICONE18
May 17-21, 2010, Xi'an, China

ICONE18-30122

STRATIFIED FLOWS IN PIPES
A PARAMETRIC STUDY TOWARDS FATIGUE RELEVANCE

Leon Cizelj, Igor Simonovski
Jožef Stefan Institute, Reactor Engineering Division
Jamova cesta 39, SI-1000 Ljubljana, Slovenia
Leon.Cizelj@ijs.si, Igor.Simonovski@ijs.si

ABSTRACT

Stratified flows may form in pipelines under certain conditions and could lead to increased fatigue loading that was only marginally accounted for during the design phase of the second generation of nuclear power plants designed in accordance with the ASME Boiler and Pressure Vessel Code. Extension of operational license would require explicit account for fatigue loads imposed by stratified flows. This typically involves rather complex state-of-the-art computational technology, which may in some cases be combined with measurements of the temperatures at the outside surfaces of pipes, which comprise pressure boundary of the reactor coolant.

A parametric study using detailed finite element analysis of the entire span of the pipe has been performed to quantify the possible range of fatigue loads and fatigue usage factors. The example taken was a typical pressurized water reactor pressurizer surge line containing stratified flow of cold and hot water. The investigated parameters include the film coefficients governing the heat transfer from the both fluids to the pipe wall and the velocity of the interface between the cold and hot water.

The main results include the expected ranges of fatigue loading given the range of investigated parameters. It is clearly shown that the choice of the film coefficients is essential to arrive at reliable fatigue estimate.

Additionally, predictions of readings provided by hypothetical thermocouples at the pipe outer surface are provided. Some of their limitations are identified and discussed.

NOMENCLATURE

A	Area of heat transfer
c_p	Specific heat capacity
DT	Temperature difference
h	Film coefficient
k	Thermal conductivity
Q	Heat flux
S_a	Stress amplitude
S_{ij}	Difference between principal stresses i and j
t	Time
T	Temperature
T_f	Temperature of the fluid far from the surface
T_p	Temperature of the pipe surface
ρ	Density
σ_1	Principal stress 1
σ_2	Principal stress 2
σ_3	Principal stress 3

INTRODUCTION

Stratified flows that may form in pipelines under certain conditions could lead to increased fatigue loading that was only marginally accounted for during the design phase of the second generation of nuclear power plants [1, 2] designed in accordance with the ASME Boiler and Pressure Vessel Code [3]. Extension of operational license would in most countries require explicit account for fatigue loads imposed by stratified flows. This typically involves rather complex state-of-the-art computational technology, which may in some cases be combined with measurements of the temperatures at the outside surfaces of pipes, which comprise pressure boundary of the reactor coolant [4, 5].

There is a wide consensus that within the reactor coolant systems of the pressurized water reactors (PWR) the stratified flows are most likely to occur in pressurizer surge lines.

These rather slow flows caused by the pressure controlling activities of the pressurizer could result in the stratified flow of cold and hot water. The typically reported velocity of such flows is in the order of cm/s [6]. The typical temperature difference between the hot and cold water is reported to be in the range of 120-150 °C. Such temperature differences are

believed to be the cause of rather significant thermal stresses resulting in accelerated fatigue usage and in some cases also in observed fatigue damage [6-9].

An impressive body of open literature already exists. Some recent contributions include, among others, an attempt to simulate stratified flows using the computational fluid mechanics tools [6], proposal [9] to update the fatigue analysis procedures in the ASME Boiler and Pressure Vessel Code [3] and example of surge line fatigue analysis [7].

In typical practical situations, the histories of the temperatures and velocities of stratified fluids inside the pipe, and, possibly, the temperatures at selected points along the outside pipe surface, may be known. The published fatigue analyses are to a large extent based on an assumption equating the temperatures at the pipe surface with the temperatures of the fluid. The conservatism of such approach is widely accepted, especially while dealing with rather large fluid velocities causing rather large transfer of heat between the fluid and the pipe. The stratified flows on the other hand are expected to remain stable only at lower fluid velocities. It is therefore deemed essential that the heat transfer from the fluid to the pipe wall is also taken into account in the analysis.

The purpose of this paper is to investigate the consequences of different assumptions on the heat transfer from the fluid to the pipe wall. In particular, a sensitivity analysis is performed to investigate the effects of the film coefficient and the velocity of the fluid-fluid interface on the thermal stress ranges and on the fatigue usage of the pipe.

A typical 12 inch pressurized water reactor pressurizer surge line made of austenitic stainless steel has been chosen as numerical example.

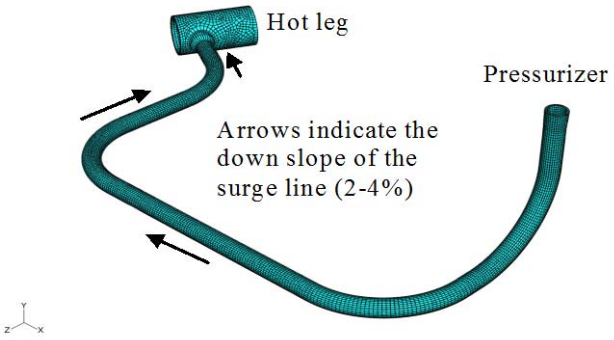

Figure 1. OUTLINE AND THE FINITE ELEMENT MESH OF THE SURGE LINE

MODEL

Figure 1 shows the spatial finite element model of the surge line. On one side, the connection with the hot leg pipe is modeled in detail. On the other end of the pipe a rigid junction to the pressurizer has been assumed. The finite element model contains 39049 3D elements with parabolic interpolation and is reported in considerable detail in [10, 11]. Element types DC3D20 and C3D20 have been used for thermal and stress analyses using the ABAQUS/standard finite element code [12], respectively.

The goal of this paper is to give a wide range of possible fatigue loads, possibly beyond those expected in the plant operation. The data on the pipe loads and results may therefore differ significantly from those reported in [10, 11].

The density of the finite element mesh has been evaluated against closed form solutions outlined in [13]. Very good agreement has been recorded for film coefficient below approximately 1000 W/m^{2}K. At higher film coefficients, the mesh used in the analysis tends to overestimate the temperature gradients and therefore gives conservative results.

The temperature dependent material properties defined in [3] were consistently used in the one-way coupled transient thermal and stress analyses, which are described in some detail below.

Thermal analysis

In the first step, a transient heat transfer analysis has been performed by numerically solving the well known heat transfer, Eqn. (1).

$$\frac{\partial T}{\partial t} = \frac{k}{c_p \rho}\left(\frac{\partial^2 T}{\partial x^2} + \frac{\partial^2 T}{\partial y^2} + \frac{\partial^2 T}{\partial z^2}\right) \tag{1}$$

The tube is assumed to be perfectly insulated at the outside surface. This is a conservative assumption which leads to overestimated temperature gradients and therefore also overestimates stresses. Convective heat transfer, Eqn. (2), is assumed at the inner surface in contact with both stratified fluids.

$$q = h \cdot A \cdot \left(T_p - T_f\right) \tag{2}$$

The temperature of the cold fluid (T_f) entering the pressurizer surge line from the reactor coolant system was assumed at 73 and 96°C, respectively. The hot fluid entering the pressurizer surge line from the pressurizer was assumed at temperature (T_f) of 223°C. The temperature differences between both fluids of 127 and 150°C are consistent with data published elsewhere [6-9].

Fluid-Fluid Interface

The interface between cold and hot fluids was modeled in two different ways, in order to take in account two possibilities of stratification.

Horizontal interface between fluids. In the first case, interface between the fluids was modeled as a horizontal plane with a step change in fluid temperatures in the vertical direction. Identical film coefficient was assumed for both cold and hot fluid. The estimated value of h = 50 W/m^{2}K was deemed consistent with the observed fluid velocities in the order of mm/s [10, 11]. In addition, film coefficients (h) of 100, 500, 1000 and 100000 W/m^{2}K have been analyzed in the sensitivity analysis.

The assumed transient started from a steady state with already developed stratification. The interface between both fluids has been assumed at the lower surface of the surge line close to the nozzle attached to the primary piping (Fig.2, up). The interface was then assumed to move in the vertical direction with the constant velocity consistent with the typical capacity of the pressurizer sprays. After reaching the top of the pipe (Fig.2, down), the interface started to travel back down with the same velocity.

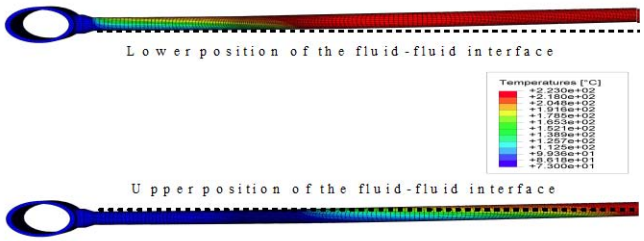

Figure 2. LOWER AND UPPER POSITIONS OF FLUID-FLUID INTERFACE (°C, FILM COEFFICIENT 50 W/m^{2}K).

The vertical velocity of the interface was estimated at 2 mm/s [10, 11]. In addition, values of 5, 10, 50 and 100 mm/s have been analyzed in the sensitivity analysis.

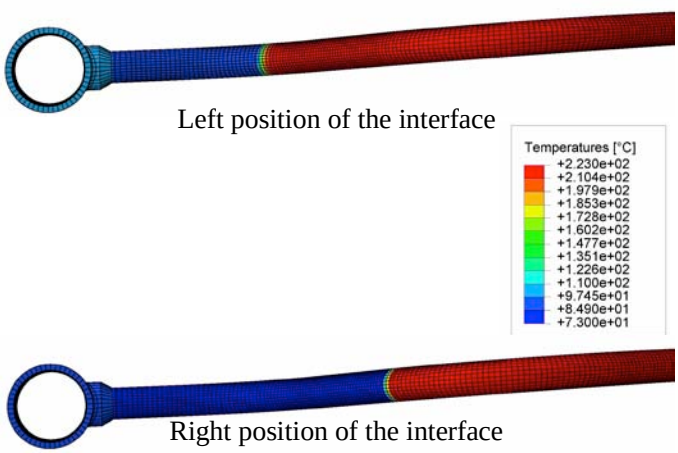

Figure 3. LEFT AND RIGHT POSITIONS OF FLUID-FLUID INTERFACE (°C, FILM COEFFICIENT 2000 W/m^{2}K).

Vertical interface between fluids. In the second case, interface between the fluids was modeled as a vertical plane with a step change in fluid temperatures in the horizontal direction. Identical film coefficient was assumed for both cold and hot fluid. The estimated value of h = 2000 W/m^{2}K was deemed consistent with the observed fluid velocities in the order of m/s [10, 11].

In addition, film coefficients (h) of 1000 and 4000 W/m^{2}K have been analyzed in the sensitivity analysis.

The assumed transient started from a steady state with already developed stratification. The interface between both fluids has been assumed at the left position of the surge line close to the nozzle attached to the primary piping (Fig. 3, up). The interface was then assumed to move in the axial direction with the constant velocity consistent with the typical capacity of the pressurizer sprays. After reaching the right position (Fig. 3, down), the interface started to travel back down with the same velocity.

The axial velocity of the interface was estimated at 400 mm/s [10, 11]. In addition, values of 200 and 800 mm/s have been analyzed in the sensitivity analysis.

The main results in both interface cases are transient temperature fields in the pipe. Additionally, temperature histories were recorded at inner and outer pipe surfaces at hypothetical positions of fatigue monitoring system thermocouples as indicated in Fig. 4.

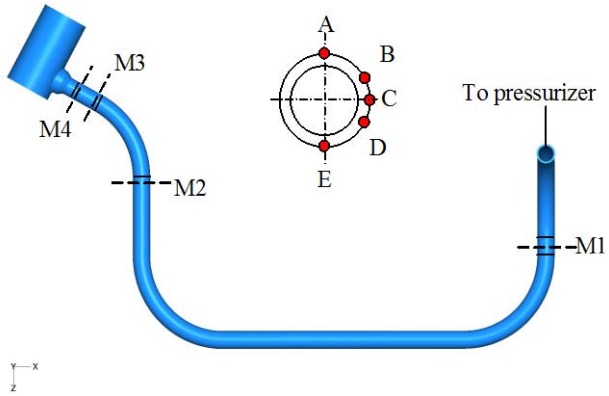

Figure 4. ASSUMED LOCATIONS OF THERMOCOUPLES MOUNTED ON THE OUTSIDE PIPE SURFACE.

Stress analysis

The temperature fields were used to assess the transient stress fields in the second step. In addition, a constant internal pressure of 2.5 MPa was assumed.

Fatigue analysis

The fatigue analysis followed the ASME Boiler and Pressure Vessel rules [3].

The transient principal stresses $\sigma_1 > \sigma_2 > \sigma_3$ were used to define the stress amplitude, Eqn. (3):

$$S_a = 0.5 \cdot \left[\max\left(S_{ij}(t)\right) - \min\left(S_{ij}(t)\right)\right] \quad (3)$$

With $S_{ij}(t)$ defined in set of Eqn. (4)

$$\begin{aligned} S_{12}(t) &= \left|\sigma_1(t) - \sigma_2(t)\right| \\ S_{23}(t) &= \left|\sigma_2(t) - \sigma_3(t)\right| \\ S_{31}(t) &= \left|\sigma_3(t) - \sigma_1(t)\right|. \end{aligned} \quad (4)$$

The value of the stress amplitude S_a is then compared with the fatigue properties defined in [3] to obtain the allowable number of load cycles. It is useful to note here that for S_a below 93 MPa, 10^{11} or more of the loading cycles are considered acceptable, given a typical stainless steel used to manufacture the surge line. In other words, only load cycles exceeding S_a of 93 MPa should be considered as fatigue relevant.

RESULTS

The simulated temperature fields are in the first step investigated through the readings of potential thermocouples (for assumed locations see Fig. 4).

As a second step, simulated Tresca stress fields are evaluated regarding values of maximum stress amplitudes results during the whole model simulation.

Horizontal interface between fluids

Figure 5 depicts two examples of temperature histories detected at location M3-C, for DT=127K. The cold water enters the surge line and pushes the interface between cold and hot water from the lower towards the upper surface of the pipe. When the top surface is reached, the interface starts the downward motion with the same velocity.

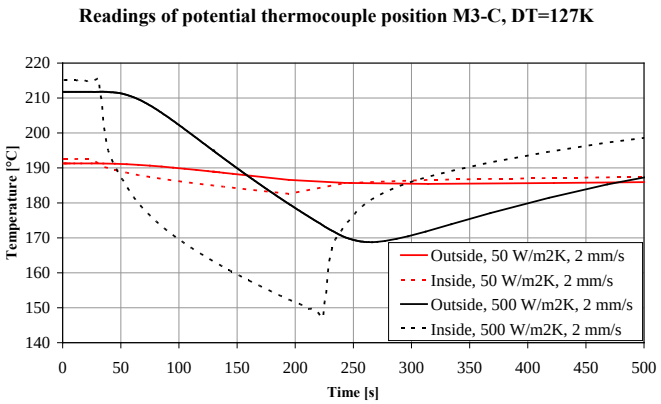

Figure 5. READINGS OF POTENCIAL THERMOCOUPLE AT POSITION M3-C (Fig. 4) WITH INSIDE SURFACE TEMPERATURES. DT=127K.

As a consequence, the temperature at the pipe inside surface starts to decrease at about 30 s and decreases until about 200 s (dotted lines). Then the downward motion of the interface is noted and the temperatures of the inside surface start to increase. The temperature difference is, as expected, governed by the film coefficient. Different steady state temperatures at the beginning and the end of the transient are attributed to rather low film coefficients giving rise to the competition between heat conduction within the pipe wall and heat transfer from the water to the pipe. This is to some extent illustrated by the temperature field in Fig. 6 indicating notable circumferential heat fluxes at the pipe inner surface.

The outside surface temperature readings (bold lines, Fig. 5) clearly show delays and significantly underestimate the temperature transients at the pipe inner surface. While larger film coefficient clearly improves the sensitivity of the outside surface thermocouple, Fig. 7 shows that faster movement of the fluid interface would tend to decrease both the maximum temperature difference experienced by any material point of the pipe and the indication given by a potential thermocouple. We may also argue that the thermocouples may be able to detect the vertical motion of the stratification interface with velocities in the order of mm/s and are at the same time rather insensitive to motions with velocities exceeding some cm/s. It is therefore clear that a reliable interpretation of the thermocouple signals requires a significant amount of reverse engineering.

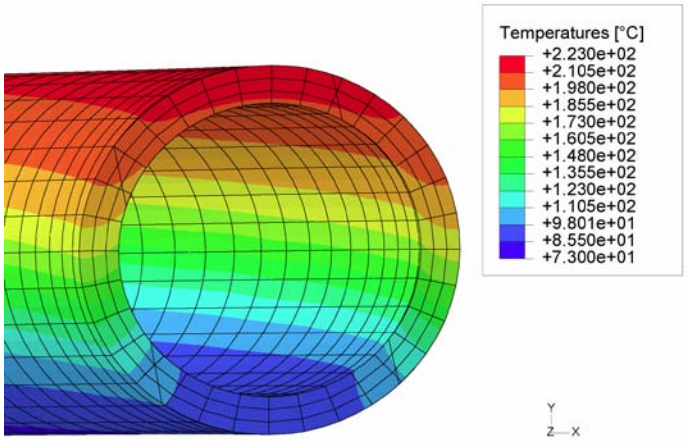

Figure 6: RADIAL TEMPERATURE DISTRIBUTION IN THE MIDDLE OF ASSUMED TRANSIENT (°C)

A snapshot of a Tresca stress field is shown in Fig. 8 and indicates rather high local variations. The results obtained as maxima of Eqn. (3) applied to the entire transient stress field are summarized in Tab. 1, for both temperature differences between hot and cold water. It is shown that the velocity of the fluid interface (assuming fixed film coefficient value!) has negligible influence on the resulting stress amplitudes and that the increasing film coefficient increases the stress amplitude.

Assuming that fatigue relevance requires stress amplitudes exceeding 93 MPa, it may be concluded that the transient studied is only marginally fatigue relevant for film coefficient values below approximately 100 W/m^{2}K.

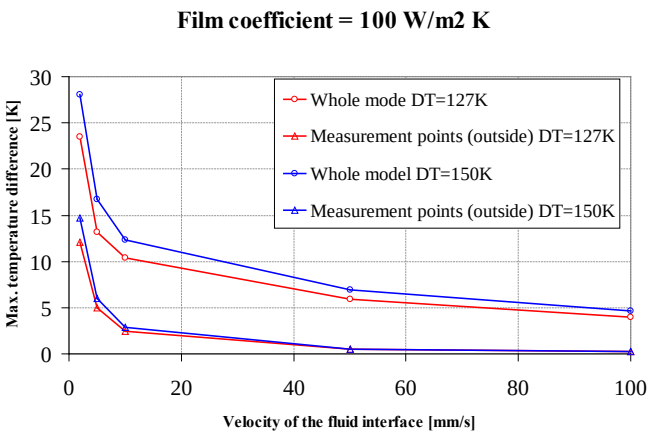

Figure 7. MAXIMAL TEMPERATURE DIFFERENCE IN THE MODEL: CALCULATED AND INDICATED BY POTENCIAL THERMOCOUPLE.

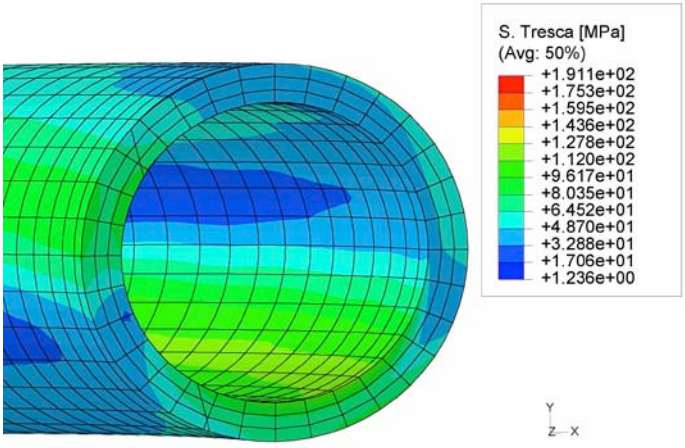

Figure 8. TRESCA STRESS DISTRIBUTION IN THE MIDDLE OF ASSUMED TRANSIENT (MPa)

Table 1. MAXIMUM STRESS AMPLITUDE S_a [MPa]

Temperature difference between hot and cold water [K]	Fluid interface velocity [mm/s]	Film Coefficient [W/m^{2}K]					
		50	100	500	1000	2000	100000
127	2	68.6	84.4	105.1	114.1	135.6	228.9
	100	68.7	84.5	105.4	114.1	135.6	
150	2	72.7	90.8	114.1	134.9	159.6	265.8
	100	72.8	90.9	114.4			

Vertical interface between fluids

Figure 9 depicts two examples detected at location M3-C, for DT=150K. The cold water enters the surge line and pushes the interface between cold and hot water from the left position towards the right position of the pipe (Fig. 3). When the right position is reached, the interface starts the motion in the opposite direction with the same velocity.

As a consequence, the temperature at the pipe inside surface starts to decrease at about 5 s and decreases until about 2000 s (dotted lines, Fig. 9), followed by the temperature at the pipe outside surface (bold lines, Fig. 9). It takes around 3000s to achieve the steady state and initiate the motion of the interface between fluids in the opposite direction. At 5000s in the time line for higher film coefficient and 6500s for lower value of film coefficient. Then the temperatures of the inside surface start to increase again, followed by the outside surface temperatures. The temperature difference in time is, as expected, governed by the film coefficient.

This is to some extent illustrated by the temperature field in Fig. 10 indicating notable axial heat fluxes at the pipe inner surface. Figure 10 shows the temperature distribution in the middle of the assumed transient (°C) in an axial section of the pipe.

The outside surface temperatures readings (bold lines, Fig. 9) clearly show some delays with the inner surface temperatures readings. Figure 9 indicates that larger film coefficient clearly improves the sensitivity of the outside surface thermocouple.

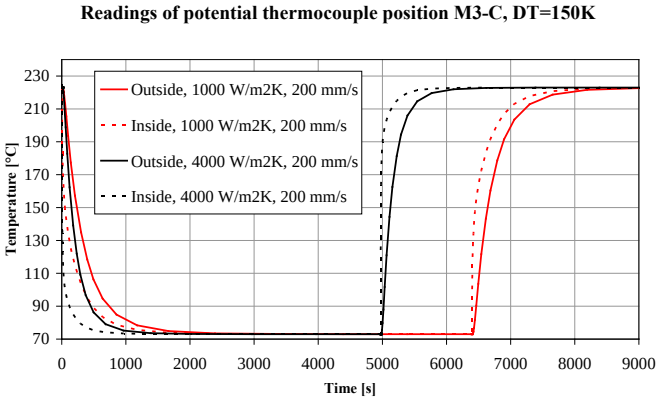

Figure 9. EXAMPLE READINGS OF POTENTIAL THERMOCOUPLE AT POSITION M3-C (SEE FIG. 3) WITH INSIDE SURFACE TEMPERATURES.

The rather scarce mesh density may give rise to overestimated temperature differences with higher values of film coefficients (e.g., over approximately 1000 W/m^2 K) [13]. This is considered conservative with respect to the fatigue loading and is not further pursued in this paper. Use of more detailed mesh is however recommended for the future analyses.

The resulting stress amplitudes obtained as maxima of Eqn. (3) applied to the entire transient stress field are summarized in Tab. 2. It is shown that the velocity of the fluid interface (assuming fixed film coefficient value!) has negligible influence on the resulting stress amplitudes and that the increasing film coefficient increases the stress amplitude. Assuming that fatigue relevance requires stress amplitudes

exceeding 93 MPa, it may be concluded that the transient studied is fatigue relevant.

It shall be noted here that it is only theoretically possible to decouple film coefficient and fluid velocities; it is well known that increasing fluid velocities increase the film coefficient.

A detailed computational fluid dynamic study on the fluid to pipe wall heat transfer would certainly contribute to the more refined assessment of the fatigue relevance.

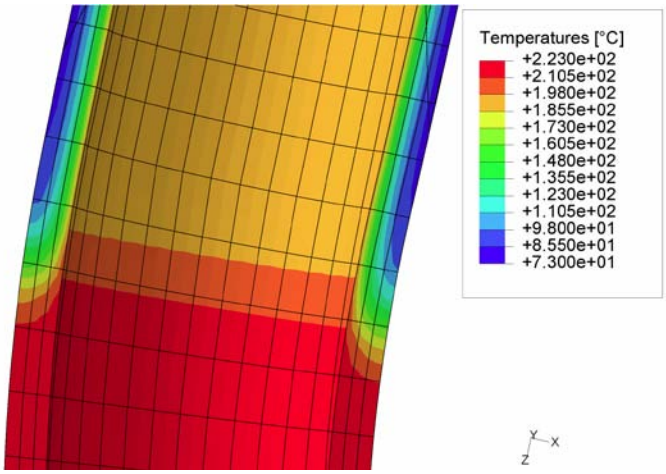

Figure 10. AXIAL TEMPERATURE DISTRIBUTION IN THE MIDDLE OF ASSUMED TRANSIENT (°C)

Table 2. MAXIMUM STRESS AMPLITUDE S_a [MPa]

Temperature difference between hot and cold water [K]	Fluid interface velocity [mm/s]	Film Coefficient [W/m^{2}K]		
		1000	2000	4000
127	200	96.5	129.1	159.8
	400	96.7	129.9	160.6
	800	97.2	130.0	160.3
150	200	112.6	152.0	187.4
	400	113.1	151.8	187.0
	800	113.45	152.6	187.6

CONCLUSIONS

A parametric study using detailed finite element analysis has been performed to quantify the possible range of fatigue loads. The example taken was a typical pressurized water reactor pressurizer surge line containing stratified flow of cold and hot water. The investigated parameters include the film coefficients governing the heat transfer from fluid to the pipe wall and the velocity of the interface between cold and hot water.

Two cases for the fluid-fluid interface have been modeled. In first case, the interface has been modeled as a horizontal plane with a step change in fluid temperatures in the vertical direction and, in the second case the interface is a vertical plane with a step change in fluid temperatures in the horizontal direction.

In both cases, it has been shown that the velocity of the fluid interface, assuming fixed film coefficient value, has negligible influence on the resulting stress amplitudes and that the increasing film coefficient increases the stress amplitude. It shall be noted here that it is only theoretically possible to decouple film coefficient and fluid velocities; it is well known that increasing fluid velocities increase the film coefficient.

Results in the first case with horizontal interface between fluids indicated marginal fatigue relevance for films coefficients below only approximately 100 W/m^{2}K. As well, it has been shown that the potential thermocouples on the outside pipe surface may be able to detect the vertical motion of the stratification interface with velocities in the order of mm/s and are at the same time rather insensitive to motions with velocities exceeding some cm/s. It is therefore clear that a reliable interpretation of the thermocouple signals requires a significant amount of reverse engineering.

Results in the second case with vertical interface between fluids indicated fatigue relevance of the analyzed transient. The potential of the thermocouples on the outside pipe surface to accurately capture the transient inside of the pipe is substantial on this case.

A detailed computational fluid dynamic study on the fluid to pipe wall heat transfer and more detailed finite element mesh in the analyses involving film coefficients over 1000 W/m^{2}K could contribute to the more refined assessment of the fatigue relevance in the future.

ACKNOWLEDGMENTS

The authors gratefully acknowledge the financial support from Slovenian research agency (grants Z2-9488(B), V2-0553 (C) and P2-0026 (C)), Krško Nuclear Power Plant (grant Z2-9488(B)) and Slovene Nuclear Safety Administration (grant V2-0553 (C)). The authors are also indebted to Mr. Oriol Costa Garrido, who helped immensely in running the simulations and compiling the results.

REFERENCES

[1] Pressurizer surge line thermal stratification. Bulletin 88-11: U.S. Nuclear Regulatory Commission; 20.12.1988.

[2] Unexpected piping movement attributed to thermal stratification. Information notice 88-80: U.S. Nuclear Regulatory Commission; 7.10.1988.

[3] ASME. Boiler and pressure vessel code. III Rules for construction of nuclear power plant components: ASME; 1989.

[4] Bartonicek J, Zaiss W, Hienstorfer W, Kocklemann H, Schöckle F. Monitoring systems and determination of

actual fatigue usage. Nucl Eng Des. 1995;153(2-3):127-133.

[5] Pöckl C, Kleinöder W. Developing and implementing of a fatigue monitoring system for the new European pressurized water reactor EPR. In: Jenčič I, Lenošek M, editors. International conference Nuclear energy for new Europe. Portorož, Slovenia: Nuclear Society of Slovenia; 2007.

[6] Boros I, Aszódi A. Analysis of thermal stratification in the primary circuit of a VVER-440 reactor with the CFX code. Nucl Eng Des. 2008;238(3):453-459.

[7] Jhung MJ, Choi YH. Surge line stress due to thermal stratification. Nuclear Engineering and Technology. 2008;40(3):239-250.

[8] Kim KC, Lim JH, Yoon JK. Thermal fatigue estimation due to thermal stratification in the RCS branch line using one-way FSI scheme. Journal of Mechanical Science and Technology. 2008;22(11):2218-2227.

[9] Kweon HD, Kim JS, Lee KY. Fatigue design of nuclear class 1 piping considering thermal stratification. Nucl Eng Des. 2008;238(6):1265-1274.

[10] Zafošnik B, Cizelj L. Data base of transients in nuclear power plant Krško (in Slovene). "Jožef Stefan" Institute; 2009.

[11] Zafošnik B, Cizelj L. Design of a method for monitoring the usage of nuclear power plant components (in Slovene). "Jožef Stefan" Institute; 2009.

[12] ABAQUS. ABAQUS User's Manual 6.6-1. Providence, RI, USA: Dassault Systèmes Simulia Corp; 2006.

[13] Zafošnik B, Cizelj L. Safe fatigue life of nuclear piping exposed to temperature and pressure fluctuations. In: Rožman S, Žagar T, Žefran B, editors. International conference Nuclear energy for new Europe. Portorož, Slovenia: Nuclear Society of Slovenia; 2008.

Nuclear Engineering and Design xxx (2010) xxx–xxx

Contents lists available at ScienceDirect

Nuclear Engineering and Design

journal homepage: www.elsevier.com/locate/nucengdes

Fatigue relevance of stratified flows in pipes: A parametric study

Leon Cizelj*, Igor Simonovski

Jožef Stefan Institute, Reactor Engineering Division, Jamova Cesta 39, SI-1000 Ljubljana, Slovenia

ARTICLE INFO

Article history:
Received 25 January 2010
Received in revised form 19 March 2010
Accepted 24 March 2010
Available online xxx

ABSTRACT

Stratified flows may form in pipelines under certain conditions and could lead to increased fatigue loading that was only marginally accounted for during the design phase of the second generation of nuclear power plants designed in accordance with the ASME Boiler and Pressure Vessel Code. Extension of operational license would require explicit account for fatigue loads imposed by stratified flows. This typically involves rather complex state-of-the-art computational technology, which may in some cases be combined with measurements of the temperatures at the outside surfaces of pipes, which comprise pressure boundary of the reactor coolant.

A parametric study using detailed finite element analysis of the entire span of the pipe has been performed to quantify the possible range of fatigue loads and fatigue usage factors. The example taken was a typical pressurized water reactor pressurizer surge line containing stratified flow of cold and hot water. The investigated parameters include the film coefficients governing the heat transfer from the both fluids to the pipe wall and the velocity of the interface between then cold and hot water.

The main results include the expected ranges of fatigue loading and usage factors given the range of investigated parameters. It is clearly shown that the choice of the film coefficients is essential to arrive at reliable fatigue estimate.

Additionally, predictions of readings provided by hypothetical thermocouples at the pipe outer surface are provided. Some of their limitations are identified and discussed.

1. Introduction

Stratified flows that may form in pipelines under certain conditions could lead to increased fatigue loading that was only marginally accounted for during the design phase of the second generation of nuclear power plants (USNRC, 1988a,b) designed in accordance with the ASME Boiler and Pressure Vessel Code (ASME, 1989). Extension of operational license would in most countries require explicit account for fatigue loads imposed by stratified flows.

This typically involves rather complex state-of-the-art computational technology, which may in some cases be combined with measurements of the temperatures at the outside surfaces of pipes, which comprise pressure boundary of the reactor coolant (Bartonicek et al., 1995; Pöckl and Kleinöder, 2007).

There is a wide consensus that within the reactor coolant systems of the pressurized water reactors (PWR) the stratified flows are most likely to occur in pressurizer surge lines. The rather slow flows caused by the pressure controlling activities of the pressurizer could result in the stratified flow of cold and hot water. The typically reported velocity of such flows is in the order of cm/s (Boros and Aszódi, 2008). The typical temperature difference between the hot and cold water is reported to be in the range of 120–150 °C. Such temperature differences are believed to be the cause of rather significant thermal stresses resulting in accelerated fatigue usage and in some cases also in observed fatigue damage (Boros and Aszódi, 2008; Jhung and Choi, 2008; Kim et al., 2008; Kweon et al., 2008). The possible safety consequences of the material ageing are studied elsewhere (e.g., Čepin and Volkanovski, 2009; Leskovar and Uršič, 2009; Prošek and Mavko, 1999).

An impressive body of open literature already exists. Some recent contributions include, among others, an attempt to simulate stratified flows using the computational fluid mechanics tools (Boros and Aszódi, 2008; Štrubelj et al., 2010), proposal (Kweon et al., 2008) to update the fatigue analysis procedures in the ASME Boiler and Pressure Vessel Code (ASME, 1989) and example of surge line fatigue analysis (Jhung and Choi, 2008).

In typical practical situations, the histories of the temperatures and velocities of stratified fluids inside the pipe, and, possibly, the temperatures at selected points along the outside pipe surface, may be known. The published fatigue analyses are to a large extent based on the assumption equating the temperatures at the pipe surface with the temperatures of the fluid. The conservativity of such approach is widely accepted, especially while dealing with rather large fluid velocities causing rather large transfer of heat between

* Corresponding author. Tel.: +386 1 5885 215; fax: +386 1 5885 377.
E-mail addresses: Leon.Cizelj@ijs.si (L. Cizelj), Igor.Simonovski@ijs.si (I. Simonovski).

0029-5493/$ – see front matter © 2010 Elsevier B.V. All rights reserved.
doi:10.1016/j.nucengdes.2010.03.030

Nomenclature

A	area (of heat transfer)
c_p	specific heat capacity
h	film coefficient
k	thermal conductivity
q	heat flux
S_a	stress amplitude
S_{ij}	difference between principal stresses σ_i and σ_j
t	time
T	temperature
T_f	temperature of the fluid far from the surface
T_p	temperature of the pipe surface

Greek symbols

ρ	density
$\sigma_1, \sigma_2, \sigma_3$	principal stresses

the fluid and the pipe. The stratified flows on the other hand are expected to remain stable only at lower fluid velocities. It is therefore deemed essential that the heat transfer from the fluid to the pipe wall is also taken into account in the analysis.

The purpose of this paper is to investigate the consequences of different assumptions on the heat transfer from the fluid to the pipe wall. In particular, a sensitivity analysis is performed to investigate the effects of the film coefficient and the velocity of the fluid–fluid interface on the thermal stress ranges and on the fatigue usage of the pipe. A typical 12 in. pressurized water reactor pressurizer surge line made of austenitic stainless steel has been chosen as numerical example.

2. Model

The spatial finite element model (Fig. 1) of the surge line has been developed. On one side, the connection with the hot leg pipe is modeled in detail. On the other end of the pipe a rigid junction to the pressurizer has been assumed, allowing for the unrestricted thermal expansion of the tube in the radial direction. The finite element model contains 39049 3D elements with parabolic interpolation and is reported in considerable detail in Zafošnik and Cizelj (2009a,b). Element types DC3D20 and C3D20 have been used for thermal and stress analyses using the ABAQUS/standard finite element code (ABAQUS, 2006), respectively.

The goal of this paper is to explore the range of possible fatigue loads, possibly beyond those expected in the plant operation. The data on the pipe loads and results may therefore differ significantly from those reported in Zafošnik and Cizelj (2009a,b).

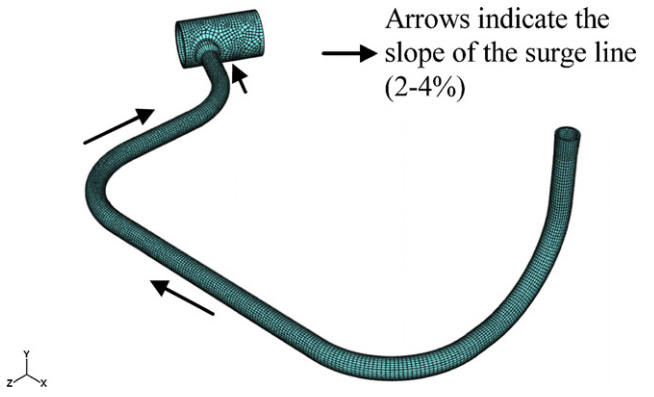

Fig. 1. Outline and the finite element mesh of the surge line.

The density of the finite element mesh has been evaluated against closed form solutions outlined in Zafošnik and Cizelj (2008) and has been found sufficient for the range of loads considered here. It is however acknowledged that the mesh density in the radial tube direction may be the weakest point of the model, especially in situations with rather efficient transfer of heat from the fluid to the pipe wall.

The temperature dependent material properties defined in ASME (1989) were consistently used in the one-way coupled transient thermal and stress analyses, which are described in some detail below.

2.1. Thermal analysis

In the first step, a transient heat transfer analysis has been performed by numerically solving the well known heat transfer equation (Myers, 1971):

$$\frac{\partial T}{\partial t} = \frac{k}{c_p \rho}\left(\frac{\partial^2 T}{\partial x^2} + \frac{\partial^2 T}{\partial y^2} + \frac{\partial^2 T}{\partial z^2}\right).$$

The tube is assumed to be perfectly insulated at the outside surface. Convective heat transfer is assumed at the inner surface in contact with both stratified fluids (Myers, 1971): $q = hA(T_p - T_f)$

The temperature of the cold fluid (T_f) entering the pressurizer surge line from the reactor coolant system was assumed at 73 and 96 °C, respectively. The hot fluid entering the pressurizer surge line from the pressurizer was assumed at temperature (T_f) of 223 °C. The temperature differences between both fluids of 127 and 150 °C are therefore consistent with data published elsewhere (Boros and Aszódi, 2008; Jhung and Choi, 2008; Kim et al., 2008; Kweon et al., 2008).

The interface between the fluids was modeled as a horizontal plane with a step change in fluid temperatures in the vertical direction. Identical film coefficient was assumed for both cold and hot fluid. The estimated value of $h = 50\ \mathrm{W/m^2\ K}$ was deemed consistent with the observed fluid velocities in the order of mm/s (Zafošnik and Cizelj, 2009a,b). In addition, film coefficients (h) of 100, 500, 1.000 and 100.000 $\mathrm{W/m^2\ K}$ have been analyzed in the sensitivity analysis.

The value of 100.000 $\mathrm{W/m^2\ K}$ was used to mimic the very efficient transfer of heat from the fluid to the pipe wall. This is a limiting case, which is only used to illustrate the upper limit of the temperature gradients, stresses and fatigue usage.

The assumed transient started from a steady state with already developed stratification. The interface between both fluids has been assumed at the lower surface of the surge line close to the nozzle attached to the primary piping (Fig. 2, up). The interface was then assumed to move in the vertical direction with the constant velocity consistent with the typical capacity of the pressurizer sprays. After reaching the top of the pipe (Fig. 2, down), the interface started to travel back down with the same velocity.

The vertical velocity of the interface was estimated at 2 mm/s (Zafošnik and Cizelj, 2009a,b). In addition, values of 5, 10, 50 and 100 mm/s have been analyzed in the sensitivity analysis.

The main results were transient temperature fields in the pipe. Additionally, temperature histories were recorded at inner and outer pipe surface at hypothetical positions of fatigue monitoring system thermocouples as indicated in Fig. 3.

2.2. Stress analysis

The temperature fields were used to assess the transient stress fields in the second step. In addition, a constant internal pressure of 2.5 MPa was assumed.

Please cite this article in press as: Cizelj, L., Simonovski, I., Fatigue relevance of stratified flows in pipes: A parametric study. Nucl. Eng. Des. (2010), doi:10.1016/j.nucengdes.2010.03.030

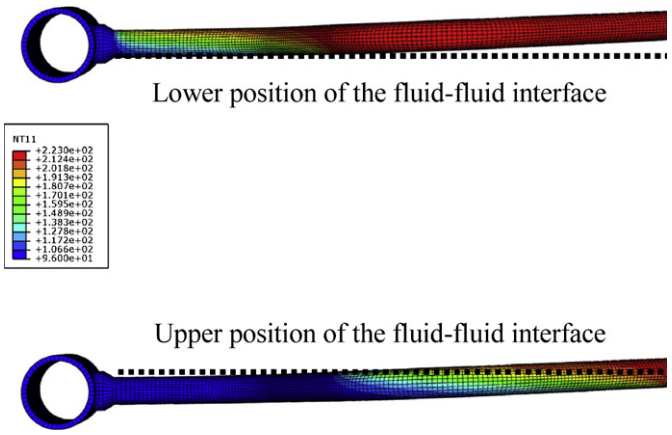

Fig. 2. Lower and upper positions of fluid–fluid interface with respective steady state temperature distributions (°C, $\Delta T = 127$K, film coefficient of 50 W/m^2 K).

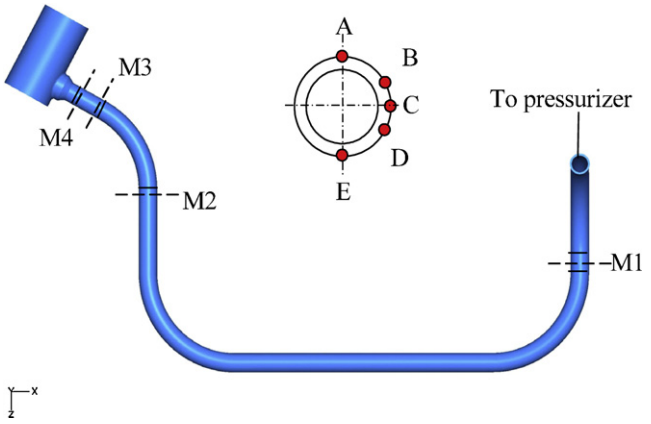

Fig. 3. Assumed locations of thermocouples mounted on the outside pipe surface.

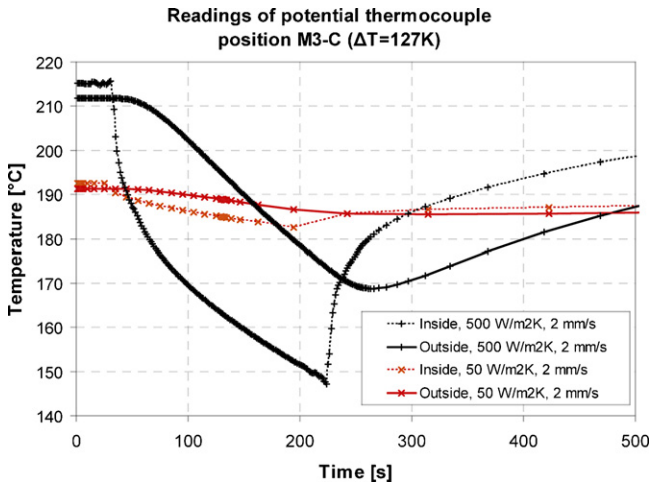

Fig. 4. Example readings of potential thermocouple at position M3-C (see Fig. 3) with inside surface temperatures.

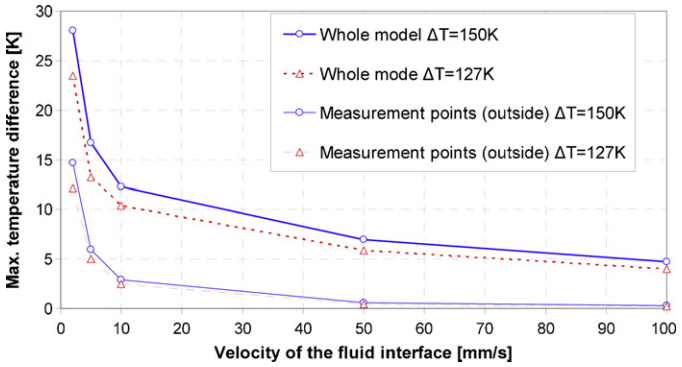

Fig. 5. Maximal calculated temperature differences in the model compared to the maximal indication of all thermocouples ($h = 100$ W/m^2 K).

2.3. Fatigue analysis

The fatigue analysis followed the ASME Boiler and Pressure Vessel rules (ASME, 1989). The transient principal stresses $\sigma_1 > \sigma_2 > \sigma_3$ were used to define the stress amplitude:

$$S_a = 0.5 \left| \max(S_{ij}(t) - \min(S_{ij}(t)) \right|, \quad (1)$$

with:

$$\begin{aligned} S_{12}(t) &= |\sigma_1(t) - \sigma_2(t)| \\ S_{23}(t) &= |\sigma_2(t) - \sigma_3(t)| \\ S_{31}(t) &= |\sigma_3(t) - \sigma_1(t)| \end{aligned}. \quad (2)$$

The value of the stress amplitude S_a is then compared with the fatigue properties defined in ASME (1989) to obtain the allowable number of load cycles.

For the purpose of this paper it is sufficient to note that for S_a below 93 MPa, 10^{11} or more of the loading cycles are considered acceptable, given a typical stainless steel used to manufacture the surge line. In other words, load cycles exceeding S_a of 93 MPa should be considered as fatigue relevant.

3. Results

3.1. Temperatures

The simulated temperature fields are in the first step investigated through the readings of potential thermocouples. Fig. 4 depicts two examples detected at location M3-C (see Fig. 3) for two different values of the film coefficient. Please note that in the assumed thermal cycle the cold water enters the surge line and pushes the interface between cold and hot water from the lower towards the upper surface of the pipe. When the top surface is reached, the interface starts the downward motion with the same velocity.

As a consequence, the temperature at the pipe inside surface starts to decrease at about 30 s and decreases until about 200 s. Then the downward motion of the interface is noted and the temperatures of the inside surface start to increase. The temperature difference between the temperatures at the wetted inside and monitored outside surface is, as expected, strongly related to the film coefficient.

Different steady state temperatures at the beginning and the end of the transients with film coefficients of 50 and 500 W/m^2 K are also attributed to rather low film coefficients giving rise to the competition between heat conduction within the pipe wall and heat transfer from the water to the pipe. This is to some extent illustrated by the temperature field in Fig. 6, which clearly shows notable circumferential heat fluxes at the pipe inner surface.

The outside surface temperature readings (Fig. 4) clearly show delays in the temperature changes. Also, the temperature histories measured at the outside surface are shown to significantly underestimate the temperature transients at the pipe inner surface. Larger film coefficient clearly improves the relative sensitivity of the outside surface thermocouple.

Faster movement of the fluid interface tends to decrease both the maximum temperature difference experienced by any material

Please cite this article in press as: Cizelj, L., Simonovski, I., Fatigue relevance of stratified flows in pipes: A parametric study. Nucl. Eng. Des. (2010), doi:10.1016/j.nucengdes.2010.03.030

Table 1
Maximum stress amplitude S_a in the model [MPa].

Temperature difference between hot and cold water [K]	Velocity of the fluid interface [mm/s]	Film coefficient [W/m² K]					
		50	100	500	1.000	2.000	100.000
127	2	68.6	84.4	105.1	114.1	135.6	228.9
	100	68.7	84.5	105.4	114.1	135.6	
150	2	72.7	90.8	114.1	134.9	159.6	265.8
	100	72.8	90.9	114.4			

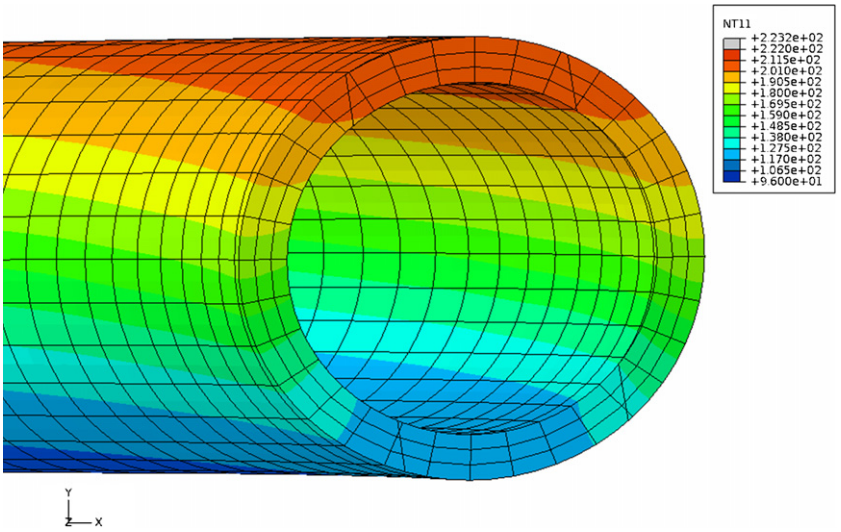

Fig. 6. Example of the temperature distribution through a pipe wall in the middle of the assumed transient (°C).

point of the pipe and the indication given by a potential thermocouple (Fig. 5). It is also clearly shown that the thermocouples may be able to detect the vertical motion of the stratification interface of fluids with temperature differences of 127 or 150 K with velocities in the order of mm/s and are at the same time rather insensitive to motions with velocities exceeding some cm/s (Fig. 5).

It is therefore clear that a reliable interpretation of the thermocouple signals requires a significant amount of reverse engineering.

3.2. Stress amplitudes

A snapshot of a Tresca stress field is shown in Fig. 7 and indicates rather high local variations. The stress amplitudes (Eq. (1)) were therefore obtained for the entire transient stress field in the analyzed pipe. The maximal values are summarized in Table 1.

The velocity of the fluid interface (assuming fixed film coefficient value!) is shown to have only minor influence on the

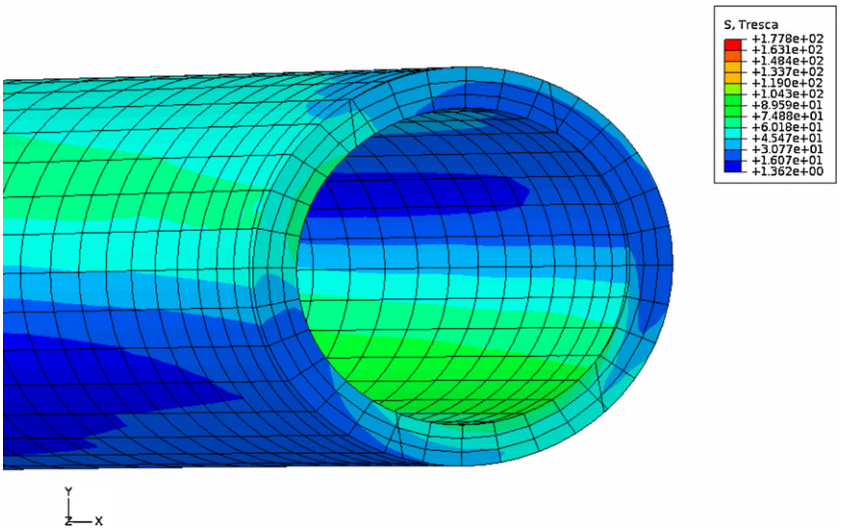

Fig. 7. Example of the Tresca stress distribution through a pipe wall in the middle of the assumed transient (MPa).

Please cite this article in press as: Cizelj, L., Simonovski, I., Fatigue relevance of stratified flows in pipes: A parametric study. Nucl. Eng. Des. (2010), doi:10.1016/j.nucengdes.2010.03.030

resulting stress amplitudes. As expected, increasing the film coefficient would increase the thermal gradients and therefore also increases the stress amplitude. It is also clearly shown that the conservativity of the traditional conservative approach with very large film coefficient might in certain cases overestimate the stress amplitudes by a factor of two or even more.

Assuming that fatigue relevance requires stress amplitudes exceeding 93 MPa, it may be concluded that the transient studied is marginally fatigue relevant. It shall be noted here that it is only theoretically possible to decouple film coefficient and fluid velocities: it is namely well known that increasing fluid velocities increases the film coefficient. A detailed computational fluid dynamic study on the fluid to pipe wall heat transfer would certainly contribute to the more refined assessment of the fatigue relevance in the future.

4. Conclusions

A parametric study using detailed finite element analysis has been performed to quantify the possible range of fatigue loads and fatigue usage factors. The example taken was a typical pressurized water reactor pressurizer surge line containing stratified flow of cold and hot water. The investigated parameters include the film coefficients governing the heat transfer from fluid to the pipe wall and the velocity of the interface between then cold and hot water.

It has been shown that the increasing film coefficient increases the stress amplitude and that the velocity of the fluid interface (assuming fixed film coefficient value) has only minor influence on the resulting stress amplitudes. The results also indicated marginal fatigue relevance of the investigated transient. It shall be noted here that it is only theoretically possible to decouple film coefficient and fluid velocities: it is well known that increasing fluid velocities increase the film coefficient. A detailed computational fluid dynamic study on the fluid to pipe wall heat transfer would certainly contribute to the more refined and reliable assessment of the fatigue relevance.

For the transient studied, the potential thermocouples on the outside pipe surface may be able to detect the vertical motion of the stratification interface with velocities in the order of mm/s and are at the same time rather insensitive to the motions with velocities exceeding some cm/s. It is therefore clear that a reliable interpretation of the thermocouple signals requires a significant amount of reverse engineering.

Acknowledgements

The authors gratefully acknowledge the financial support from Slovenian research agency (grants Z2-9488(B), V2-0553 (C) and P2-0026 (C)), Krško Nuclear Power Plant (grant Z2-9488(B)) and Slovene Nuclear Safety Administration (grant V2-0553 (C)).

References

ABAQUS, 2006. ABAQUS User's Manual 6.6-1. Dassault Systèmes Simulia Corp, Providence, RI, USA.
ASME, 1989. Boiler and pressure vessel code. III. Rules for Construction of Nuclear Power Plant Components. ASME.
Bartonicek, J., Zaiss, W., et al., 1995. Monitoring systems and determination of actual fatigue usage. Nuclear Engineering and Design 153 (2–3), 127–133.
Boros, I, Aszódi, A., 2008. Analysis of thermal stratification in the primary circuit of a VVER-440 reactor with the CFX code. Nuclear Engineering and Design 238 (3), 453–459.
Čepin, M, Volkanovski, A., 2009. Consideration of ageing within probabilistic safety assessment models and results. Kerntechnik 74 (3), 140–149.
Jhung, M.J., Choi, Y.H., 2008. Surge line stress due to thermal stratification. Nuclear Engineering and Technology 40 (3), 239–250.
Kim, K.C, Lim, J.H., et al., 2008. Thermal fatigue estimation due to thermal stratification in the RCS branch line using one-way FSI scheme. Journal of Mechanical Science and Technology 22 (11), 2218–2227.
Kweon, H.D, Kim, J.S., et al., 2008. Fatigue design of nuclear class 1 piping considering thermal stratification. Nuclear Engineering and Design 238 (6), 1265–1274.
Leskovar, M, Uršič, M., 2009. Estimation of ex-vessel steam explosion pressure loads. Nuclear Engineering and Design 239 (11), 2444–2458.
Myers, G.E., 1971. Analytical Methods in Conduction Heat Transfer. McGraw-Hill, New York.
Pöckl, C., Kleinöder, W., 2007. Developing and implementing of a fatigue monitoring system for the new European pressurized water reactor EPR. In: Jenčič, I., Lenošek, M., International Conference Nuclear Energy for New Europe. Nuclear Society of Slovenia, Portorož, Slovenia.
Prošek, A., Mavko, B., 1999. Evaluating code uncertainty. I. Using the CSAU method for uncertainty analysis of a two-loop PWR SBLOCA. Nuclear Technology 126, 170–185.
Štrubelj, L., Ézsöl, G., et al., 2010. Direct contact condensation induced transition from stratified to slug flow. Nuclear Engineering and Design 240 (2), 266–274.
USNRC, 1988a. Pressurizer surge line thermal stratification. Bulletin 88-11. U.S. Nuclear Regulatory Commission.
USNRC, 1988b. Unexpected piping movement attributed to thermal stratification. Information notice 88-80. U.S. Nuclear Regulatory Commission.
Zafošnik, B., Cizelj, L., 2008. Safe fatigue life of nuclear piping exposed to temperature and pressure fluctuations. In: Rožman, S., Žagar, T., Žefran, B. International Conference Nuclear energy for New Europe. Nuclear Society of Slovenia, Portorož, Slovenia.
Zafošnik, B., Cizelj, L., 2009a. Data base of transients in nuclear power plant Krško (in Slovene). "Jožef Stefan" Institute.
Zafošnik, B., Cizelj, L., 2009b. Design of a method for monitoring the usage of nuclear power plant components (in Slovene). "Jožef Stefan" Institute.

Please cite this article in press as: Cizelj, L., Simonovski, I., Fatigue relevance of stratified flows in pipes: A parametric study. Nucl. Eng. Des. (2010), doi:10.1016/j.nucengdes.2010.03.030

Safety, Reliability and Risk Analysis: Theory, Methods and Applications – Martorell et al. (eds)
© 2009 Taylor & Francis Group, London, ISBN 978-0-415-48513-5

Probabilistic safety assessment for other modes than power operation

Marko Čepin
"Jožef Stefan" Institute, Jamova cesta 39, SI-1000 Ljubljana, Slovenia

Rudolf Prosen
Nuclear Power Plant Krško, Vrbina 12, SI- 8270 Krško, Slovenia

ABSTRACT: Probabilistic safety assessment is a standardized method for assessment and improvement of nuclear power plant safety. The paper presents the probabilistic safety assessment of 4 modes of operation of the nuclear power plant: 1) normal power operation, 2) plant startup, 3) hot standby and 4) hot shutdown. The modeling features are presented and the differences between the models are highlighted with the emphasis on comparison between hot standby and normal power operation. The results are shown and the findings are discussed. The considered probabilistic safety assessment model includes internal and external events, but the comparison is made considering internal events only. The considered probabilistic safety assessment model is a model of a nuclear power plant with pressurized water reactor, with two loops and with more than 20 years of successful plant operation. The results of probabilistic safety assessment for other modes than plant normal power operation show certain differences in risk measures for each considered mode. In spite of the fact that the time duration of plant being in other modes is short comparing to the power operation, some conservatism in modeling and consequently in the results is reduced, which lead to our higher confidence in better models and results.

1 INTRODUCTION

Probabilistic safety assessment (PSA) is a standardized method for assessment and improvement of nuclear power plant safety, which is widely applied (Čepin & Mavko 2002, Cepin 2005).

Normally, it is performed for plant power operation, although it can be used for other plant modes (Kiper 2002).

Consideration of the plant shutdown is in practice usually a separate issue and a probabilistic safety assessment of a nuclear power plant at shutdown states is therefore separated from analyses of plant power operation.

The objective of the paper is to show how can probabilistic safety assessment model for normal power operation be used for development of probabilistic safety assessment models for other modes of plant operation such as start-up, hot standby and hot shutdown.

The paper presents the probabilistic safety assessment of 4 modes of operation of the nuclear power plant: 1) power operation, 2) plant startup, 3) hot standby and 4) hot shutdown.

The modeling features are presented and the differences between the models are highlighted. The procedure for preparation of new models is described. The results are shown and the findings are discussed.

2 METHOD

The procedure for development of PSA models for selected plant states is developed (section 2.1).

The method for integration of the results of specific models is defined to assess the overall risk (section 2.2).

2.1 *Procedure*

The respective probabilistic safety assessment documents and the computerized probabilistic safety assessment model are both analyzed.

For each of the selected plant states:

– plant operation in plant startup (mode 2),
– plant operation in hot standby (mode 3) and
– plant operation in hot shutdown (mode 4),

its respective PSA model was prepared based on the PSA model for normal plant operation.

Initiating events and their frequencies are reviewed and changed, if needed for a specific mode of operation.

E.g. the frequencies of Loss of Coolant Accidents are lower for plant in hot shutdown than for plant in normal operation and are changed to lower frequencies in the PSA model for plant operation in hot shutdown.

Table 1. Link between PSA models and plant parameters.

Name and description of PSA model	Definition of plant operation	Plant mode	Plant state	Comments about description of the main plant parameters
Basic PSA model	steady state full power operation	MODE 1	–	Plant operation at full power
Basic PSA model is assumed to be representative	Not steady state operation	MODE 1	–	Plant operation at reduced power
Changed PSA model: POS1C-preliminary	Not steady state operation	MODE 2	POS1C	Plant operation at reducing power
			POS15A	Increasing power
Changed PSA model: POS2A-preliminary	Hot standby	MODE 3	POS2A	Cool-down with Steam Generators, core is sub-critical
			POS14	Reactor coolant system heat up with steam generators
Changed PSA model: POS3A-preliminary	Hot shutdown	MODE 4	POS3A	AFW and RHR are in operation, plant cooling is assured by AFW, core is sub-critical
			POS13	Reactor coolant system heat up

The functional events and the branches of the event tree are reviewed and changed, if needed for a specific mode of operation. E.g. functional event: reactor trip is not needed and it is deleted from the respective event trees in the PSA model for plant operation in hot shutdown.

The fault trees linked to the respective functional events of the event trees are reviewed and changed if needed for a specific mode of operation. Those potential changes include:

- the change of logic of the fault tree (e.g. a branch or a gate is removed, if it is not needed in the model),
- change of basic events of the fault tree (e.g. basic event is deleted, if it is not needed in the model),
- changes of parameters of the basic events (e.g. change of failure probability of certain equipment or change of human error probability, if it is needed in the model).

Definition of plant operating states (POS) is selected similarly as in document NUREG/CR-6144, which defines 15 plant operating states (POS1, POS2, . . . POS15). Some of the sub-states are defined in addition for certain states, which in more details represent the connection between specific operational mode and the operating state: e.g. POS1A, POS1B, POS1C, POS2A, POS2B, POS3A, POS3B, POS15A, POS15B, POS15C.

There is no exact mach between definition of specific POS and definition of specific operational mode. Definition of plant operational modes is written in technical specifications (6 modes) of the plant safety analysis report.

The following assumptions are stated for determining the plant conditions for analyzed PSA models, which are summarized in Table 1:

- For normal steady state operation of NPP, the existing PSA for normal operation applies.
- For power operation at reduced power in mode 1 and not in a steady state operation, PSA for normal operation is assumed to be representative. As the power level is lower than the nominal, the initial decay heat after reactor trip is lower. Operators have more time for respond to transients, so their respective human error probabilities are the same as for power operation or lower. Initiating event frequency for loss of main feedwater could be slightly higher.
- For power operation at reduced power in mode 2, a slightly changed PSA model named POS1C-preliminary is developed.
- For hot standby, a slightly changed PSA model named POS2A-preliminary is developed.
- For hot shutdown, a slightly changed PSA model named POS3A-preliminary is developed.

Normally, the plant conditions are in certain operating state not identical for both possibilities: if the plant goes in the direction of shutting it down or if the plant goes in the direction of starting it up.

2.2 *Method for assessing the overall risk*

The results of probabilistic safety assessment of specific modes can be used to assess the overall risk of the plant. The method is simple and it bases on determining the mean value of the considered results of considered modes of operation taking into account

the time duration of each of considered modes. The expression for determining the overall risk is the following:

$$R = \frac{\sum_{i=1}^{I} RiTi}{\sum_{i=1}^{I} Ti} \quad (1)$$

where R = overall risk measure (either core damage frequency on the plant or event tree or sequence level, or the system unavailability at the system or subsystem level); R_i = risk measure of i—th mode of operation; T_i = the time duration for the plant being in i—th mode of operation; I = the number of considered modes of operation.

3 MODELS

The considered probabilistic safety assessment model includes internal and external events. It is a model of a nuclear power plant with pressurized water reactor, with two loops and with more than 20 years of successful plant operation.

The probabilistic safety assessment model for normal operation is a detailed model consisting of thousands of basic events and gates, hundredths of system and subsystem fault trees and tenths of event trees.

The model integrates the internal and external events, but only the portion for internal events is selected for comparison purposes in this paper.

3.1 *PSA model for Mode 2 - Plant operation at reducing power*

Plant operating state POS1C covers the following plant conditions, which apply to Mode 2 (less than 5% of nominal plant power):

- Turbine is shutdown.
- Main feedwater pumps are shutdown, feedwater system is not needed, but it may serve as a backup for auxiliary feedwater system operation, if it fails.
- Motor driven pumps of auxiliary feedwater system are running.
- The power is between 0 and 5% of nominal power.

The key similarities between POS1C, which is represented by POS1C-preliminary model, and power operation are the following:

- RCS temperatures and pressures are essentially the same.
- The secondary side temperatures and pressures are essentially the same.
- The same types of initiating events are applicable.

The key differences between POS1C, which is represented by POS1C-preliminary model, and power operation are the following:

- The plant is not operating in a stable steady state.
- The reactor power level is significantly decreased.
- The decay heat is lower.
- Plant transients are developing slower than at full power.
- The control rods are nearly fully inserted into the core.
- Engineered safety features actuation system and reactor trip system setpoints and interlocks may be changed or may be blocked.

3.2 *PSA model for Mode 3 - Hot standby*

Plant operating state POS2A covers the following plant conditions, which apply to hot standby (Mode 3):

- Turbine is shutdown.
- Main feedwater pumps are shutdown, feedwater system is not needed, but it may serve as a backup for auxiliary feedwater system operation, if it fails.
- Motor driven pumps of auxiliary feedwater system are running.

The key similarities between POS2A, which is represented by POS2A-preliminary model, and power operation are the following:

- RCS temperatures and pressures are essentially the same.
- The secondary side temperatures and pressures are essentially the same.

The key differences between POS2A, which is represented by POS2A-preliminary model, and power operation are the following:

- The decay heat is lower in hot standby than in power operation.
- All control rods and shutdown rods are fully inserted into the core.
- Initiating event anticipated transient without scram—ATWS is not needed.
- As the power conversion system is shutdown, the respective initiating events are not applicable (transients with main feedwater, transients without main feedwater, large steam/feedline break).
- Initiating event frequencies for loss of coolant accidents (LOCA), steam generator tube rupture (SGTR) are significantly lower.
- Human error probabilities are lower in general due to slower transients and due to more time to respond.

Table 2 shows the selected 6 changes from out of more than 50 changes applicable for the internal events for hot standby PSA model versus normal operation PSA model.

Table 2. Changes for hot standby PSA model versus normal operation PSA model.

Affected issue in NEK PSA model	Description of the change	Justification for the change
Medium loss of coolant accident, event tree, sequence no. 8	Sequence no. 8 is deleted	Medium loss of coolant accident, event tree, consequence: anticipated transient without scram is not applicable, because the control rods are fully inserted
Medium loss of coolant accident, event tree, functional event: reactor trip 1	Functional event: reactor trip 1 is deleted	
Basic event HFE-OP1-751, probability parameter	probability parameter OP1-751 is changed to 1,3E-3	Human error probability HFE-OP1-751 is for a factor of 8.1E-2 smaller due to longer time for action
Parameter, frequency initiating event small loss of coolant accident	frequency changed from 2,7E-3/ry to 1,62E-3/ry	initiating event frequency is significantly lower in hot standby
Event tree steam line break	Event tree steam line break is deleted	As the power conversion system is shutdown, the respective initiating event is not applicable
Fault tree auxiliary feedwater system	Basic events BE-11020, BE-11000, BE-11044 are deleted	AFW is already running (motor driven pumps)

3.3 *PSA model for Mode 4 - Hot shutdown*

Plant operating state POS3A covers the following plant conditions, which apply to hot shutdown (Mode 4):

- Turbine is shutdown.
- Main feedwater pumps are shutdown, feedwater system is not needed, but it may serve as a backup for auxiliary feedwater system operation, if it fails.
- Motor driven pumps of auxiliary feedwater system are running.
- Reactor coolant temperature is decreasing.

The key differences between POS3A, which is represented by POS3A-preliminary model, and power operation are the following:

- The decay heat is lower in hot shutdown than in power operation.
- All control rods and shutdown rods are fully inserted into the core.
- Initiating event anticipated transient without scram - ATWS is not needed.
- As the power conversion system is shutdown, the respective initiating events are not applicable (transients with main feedwater, transients without main feedwater, large steam/feedline break).
- Initiating event frequencies for loss of coolant accidents (LOCA) are significantly lower.
- Initiating event steam generator tube rupture (SGTR) is not needed in hot shutdown.
- Human error probabilities are lower in general due to slower transients and due to more time to respond.
- Reactor coolant temperature is decreasing.
- Component cooling water system (CCW), service water system (ESW) and instrument air system (IA) logic are limited to branches connected to operating systems (e.g. AFW).

4 ANALYSIS AND RESULTS

The results of probabilistic safety assessment include:

- lists of minimal cut sets for all and for individual event trees and sequences,
- lists of minimal cut sets for fault trees of safety systems, subsystems and support systems,
- core damage frequency,
- risk measures for components and human failure events and for their groups at all levels of analyses from fault tree analysis to sequence analysis and all event trees analysis.

Figure 1 shows part of the results of the probabilistic safety assessment for normal operation: contribution to core damage frequency for all defined initiating events, which represent the internal events probabilistic safety assessment.

Table 3 shows descriptions of initiating events presented on Figure 1.

The results of the PSA model for internal initiating events for hot standby shows that the number of gates and basic events in the fault trees and event trees is notably lower, which is expected due to the fact that some event trees and some event tree sequences have been deleted, some fault tree branches and some events have been removed.

The core damage frequency decreases for 30% and distribution of contributions from initiating events changes slightly, which is presented on Figure 2.

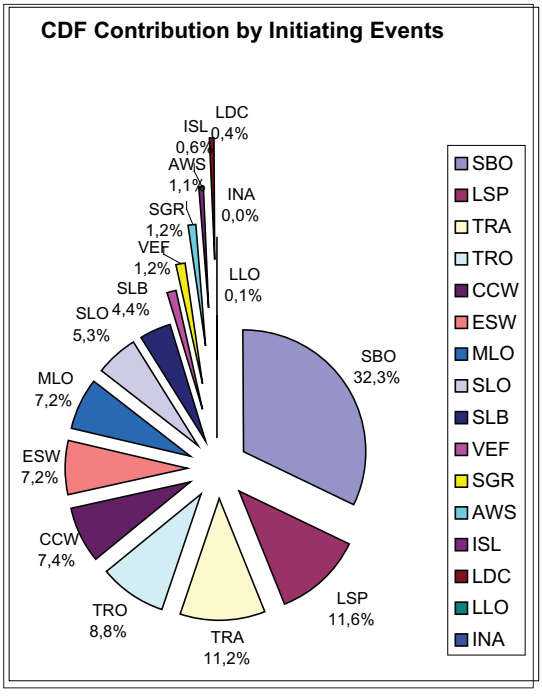

Figure 1. Contribution to core damage frequency for internal events for normal operation.

Figure 3 shows the fractional contribution of selected human failure events for normal operation and for hot standby. The figure shows that the fractional contribution for selected human failure events is lower in hot standby and for some it is higher in hot standby.

Fractional contribution (FC) is calculated based on expression:

$$FCi = \frac{R - R(Qi = 0)}{R} \qquad (2)$$

where R = risk measure, which can be either core damage frequency on the plant or event tree or sequence level, or the system unavailability on the system or subsystem level; Qi = unavailability of component i; FCi = fractional contribution of component i.

The events for which fractional contribution is lower at hot standby are connected with establishing power to instrumentation, if the normal power supply fails.

Figure 4 shows the fractional contribution of selected groups of components for normal operation and for hot standby.

Table 4 shows the definitions of the groups of events shown on Figure 4.

Table 3. Initiating events.

INITIATING EVENT	IE
ANTICIPATED TRANSIENT WITHOUT SCRAM	AWS
INTERFACING SYSTEMS LOCA	ISL
LARGE LOCA	LLO
LOSS OF 125V DC VITAL BUS	LDC
LOSS OF COMPONENT COOLING WATER SYSTEM	CCW
LOSS OF ESSENTIAL SERVICE WATER SYSTEM	ESW
LOSS OF INSTRUMENT AIR	INA
LOSS OF OFFSITE POWER	LSP
MEDIUM LOCA	MLO
SMALL LOCA	SLO
STATION BLACKOUT	SBO
STEAM GENERATOR TUBE RUPTURE	SGR
STEAM LINE BREAK	SLB
TRANSIENT WITH MFW AVAILABLE	TRA
TRANSIENT WITH MFW UNAVAILABLE	TRO
VESSEL FAILURE	VEF

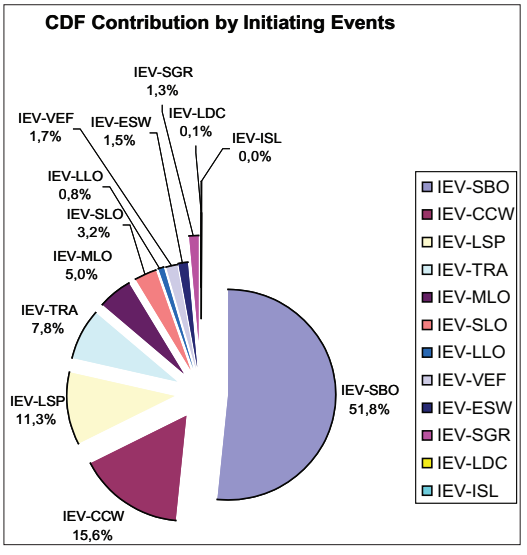

Figure 2. Contribution to core damage frequency for internal events for hot standby.

The fractional contribution for a group named human-errors, which comprise all human failure events, is lower in hot standby.

All human error probabilities of all human failure events have either remained the same or have been reduced due to larger amount of time for operators.

The fractional contribution of auxiliary feedwater pumps is higher in hot standby in spite of the fact

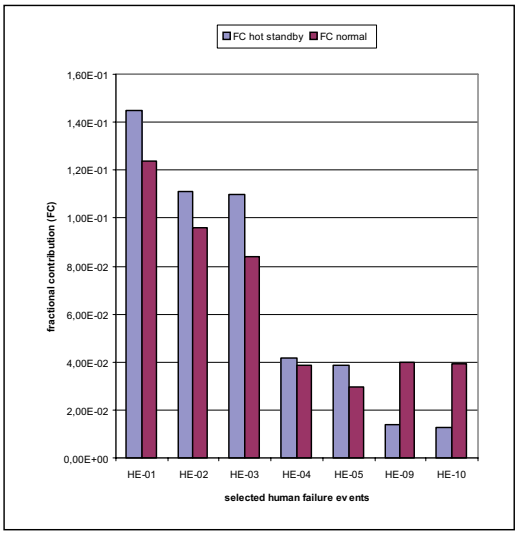

Figure 3. Fractional contribution of selected human failure events.

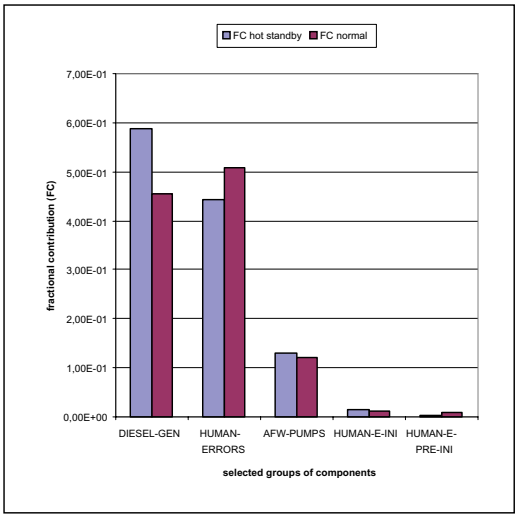

Figure 4. Fractional contribution of selected groups of components.

that all changes related to auxiliary feedwater system were only connected with removal of respective basic events (e.g. removal of pump fails to start, as the pumps are already running) and removal of branches of the fault trees (e.g. contribution of test and maintenance activities).

The reason for this lays in a fact that the contribution of removed part connected with auxiliary feedwater

Table 4. Definition of groups of events.

BASIC EVENT GROUP NAME	BASIC EVENT GROUP DESCRIPTION
DIESEL-GEN	All basic events corresponding to diesel generators
HUMAN-ERRORS	All basic events corresponding to human failure events
AFW-PUMPS	All basic events corresponding to auxiliary feedwater pumps
HUMAN-E-INI	All basic events corresponding to initiator human failure events
HUMAN-E-PRE-INI	All basic events corresponding to pre-initiator human failure events

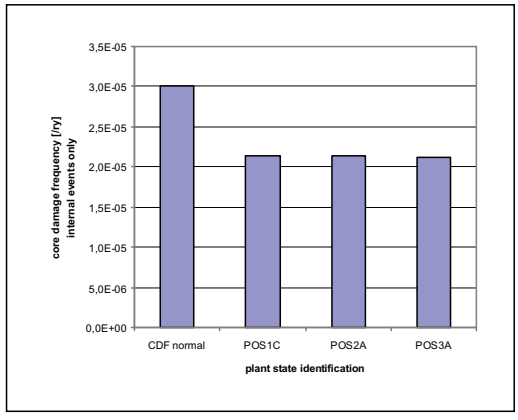

Figure 5. Core damage frequency comparison for the selected plant states.

is relatively lower than the contribution of removal of other items that are not connected to auxiliary feedwater.

Figure 5 shows the preliminary core damage frequency comparison for the selected plant states.

5 CONCLUSIONS

The results of probabilistic safety assessment for other modes than plant power operation show certain differences in risk measures for each considered mode. Although, the time duration of plant being in other modes is short comparing to the power operation, some conservatism in modeling and consequently in the results is reduced, which lead to our higher confidence in better models and results.

In addition, the results contribute to the overall goal to complete the probabilistic safety assessment of different plant operating states with the same concept as it is used for the normal operation. This will give a

comparison to shutdown PSA, which was performed for the plant under investigation well ago.

REFERENCES

Čepin M. & B. Mavko. 2002. A Dynamic Fault Tree. Reliability Engineering and System Safety 75 (1): 83–91.

Čepin M. 2005. Analysis of Truncation Limit in Probabilistic Safety Assessment. Reliability Engineering and System Safety 87 (3): 395–403.

Čepin, M. & Prosen, R. 2006. Update of human reliability analysis for nuclear power plant. In Glumac, Bogdan (ed.), Lengar, Igor (ed.), International Conference Nuclear Energy for New Europe, Portorož, 2006. Proceedings. Nuclear Society of Slovenia.

Kiper K.L. 2002. Insights from an All-Modes PSA at Seabrook Station. International Topical Meeting on Probabilistic Safety Assessment. Detroit 2002. Proceedings. 429–434. ANS.

NUREG/CR-6144, Evaluation of Potential Severe Accident During Low Power and Shutdown Operations at Surry, Unit 1, NRC, 1995.

Risk Comparison of Methods for Dependency Determination within Human Reliability Analysis

Marko Čepin
Institut Jožef Stefan, Ljubljana, Slovenia

Abstract: Dependency between human failure events is an issue, which include subjectivity in the models and consequently in the results of human reliability analysis and thus in probabilistic safety assessment. Many methods connected with human reliability analysis were developed in the last decades, which mostly include determination of dependency between human failure events: e.g. Standardized Plant Analysis Risk HRA - SPAR-H and Institute Jožef Stefan - Human Reliability Analysis - IJS-HRA. A comparison of dependency as it is applied within the selected methods is performed on an example probabilistic safety assessment model of a selected nuclear power plant. Pre-initiators and post-initiators are considered. It is investigated how the contribution of consideration of dependency of pre-initiators and dependency of post-initiators and dependency of both impacts the human error probabilities, which are then used within probabilistic safety assessment. The results of comparison show that selection of the method for determining dependency between human failure events may largely impact the results of human reliability analysis and consequently the probabilistic safety assessment. The subjectivity can be reduced by development of more detailed guidelines for human reliability analysis with many detailed practical examples for all steps of the process of evaluation of human performance.

Keywords: Probabilistic Safety Assessment, Human Reliability, Dependency, Human Error Probability.

1. INTRODUCTION

Dependency between Human Failure Events (HFE) is an issue, which include subjectivity in the models and consequently in the results of Human Reliability Analysis (HRA) and thus in Probabilistic Safety Assessment (PSA). The human reliability analysis is a systematic framework, which includes the process of evaluation of human performance and associated impacts on structures, systems and components for a complex facility.

1.1. Objectives

The objective of the paper is to show that subjectivism can largely impact the results of human reliability analysis and consequently the results and applications of probabilistic safety assessment in a Nuclear Power Plant (NPP). The objective is to identify the key features, which may decrease the subjectivity of human reliability analysis. In this sense, two human reliability analysis methods are compared with emphasis on the comparison of dependency consideration: Institute Jožef Stefan - Human Reliability Analysis (IJS-HRA) [1, 2, 3, 4] and Standardized Plant Analysis Risk HRA (SPAR-H) [5]. They are selected from a large set of existing methods, because they are relatively new.

1.2. Overview of Current Developments

A number of developed methods for assessment of human reliability were published in last decades in addition to the mentioned two methods. Those include: Technique for Human Error Rate Prediction - THERP [6], Systematic Human Action Reliability Procedure - SHARP [7], Accident Sequence Evaluation Program - ASEP [8], A Technique for Human Event Analysis - ATHEANA [9, 10], Cognitive Reliability and Error Analysis Method - CREAM [11], Human Cognitive Reliability - HCR [12], Electric Power research Institute HRA – EPRI HRA [13], Commission Errors Search and Assessment - CESA [14]. In addition, good practices about HRA were published [15].

2. COMPARISON OF IJS–HRA AND SPAR-H

2.1. IJS-HRA

The human reliability analysis (IJS-HRA) is a method for evaluation of human failure events in sense to determine the reliability of the respective human actions [1, 2, 3, 4]. Human action is a specific action required by human operator. If it is not performed or it is not performed in time and correctly, it is referred to as a human failure event.

Figure 1 shows the schematic representation of the IJS-HRA method. The main inputs for IJS-HRA method include (left part of the Figure 1):

- Probabilistic Safety Assessment (PSA) model, which is interconnected with the human reliability analysis,
- plant information, which is the source of information which supports the evaluation and
- state-of-the-art in the respective field: standards, guides, good features of existing methods and good practice.

The method is developed including consideration about dependencies between human failure events [1, 4, 6]. The success criteria for human failure events include information about their time window, i.e. information about the time, in which operators have to perform the action. This information about the available time comes from safety analyses, where scenarios about operating safety systems are evaluated. This is the reason for appearance of text box of safety analysis on Figure 1 and its connection with text box: evaluation. Results of the human reliability analysis are inserted into the probabilistic safety assessment, which is shown by upper feedback on the Figure 1.

Figure 1 shows that identification of HFE distinguishes pre-initiator events (i.e. pre-initiators), initiator events (i.e. initiators) and post-initiator events (i.e. post-initiators). Pre-initiators are the events that may cause the equipment to be unavailable before the initiating event has occurred. Initiators are the events that may contribute to the occurrence of initiating events. Post-initiators are the events, which are connected with human actions to prevent accident or mitigate its consequences after initiating event has occurred. Evaluation of HFE including evaluation of dependencies integrates assessment of human error probabilities (HEP) with plant information, operator interview, simulator experience and plant data base.

Figure 1: Scheme of IJS-HRA method

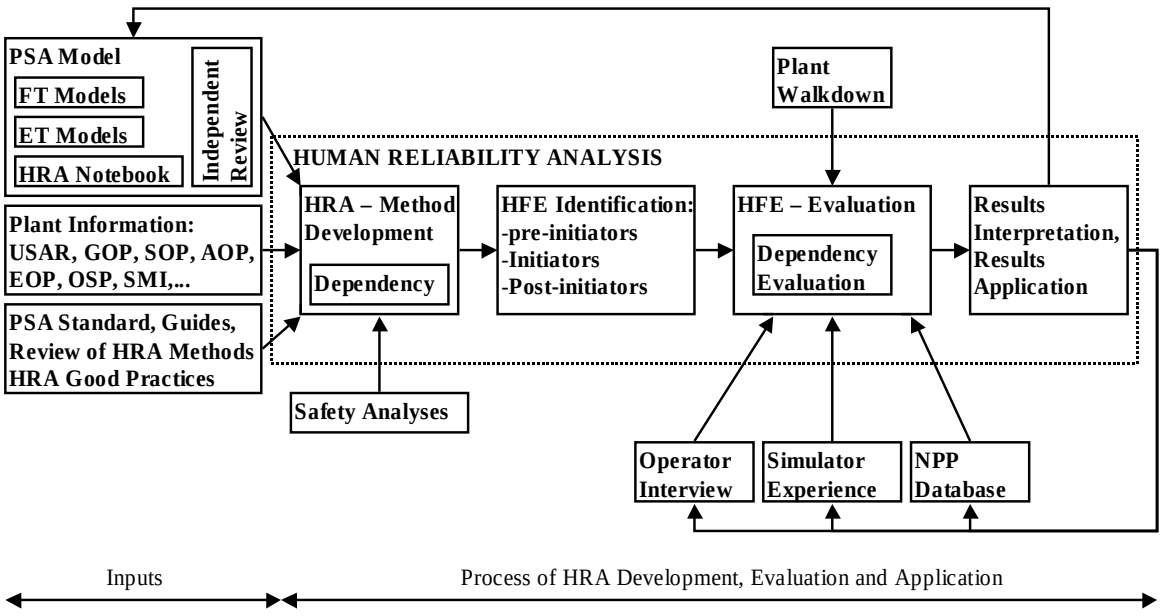

The five levels of dependency are determined in the same way as they are considered in THERP: Zero Dependency (ZD), Low dependency (LD), Moderate dependency (MD), High dependency (HD), Complete dependency (CD) [2]. Human error probability (HEP) of dependent HFE A and B is determined according to equation: PXD(PB|PA)=PA*(1+K·PB)/(K+1); where: K=0, 1, 6, 19, ∞, for dependency levels ZD, LD, MD, HD, CD, where X=Z, L, M, H, C, respectively [6].

Figure 2: IJS-HRA Dependency – Pre-Initiator HFE

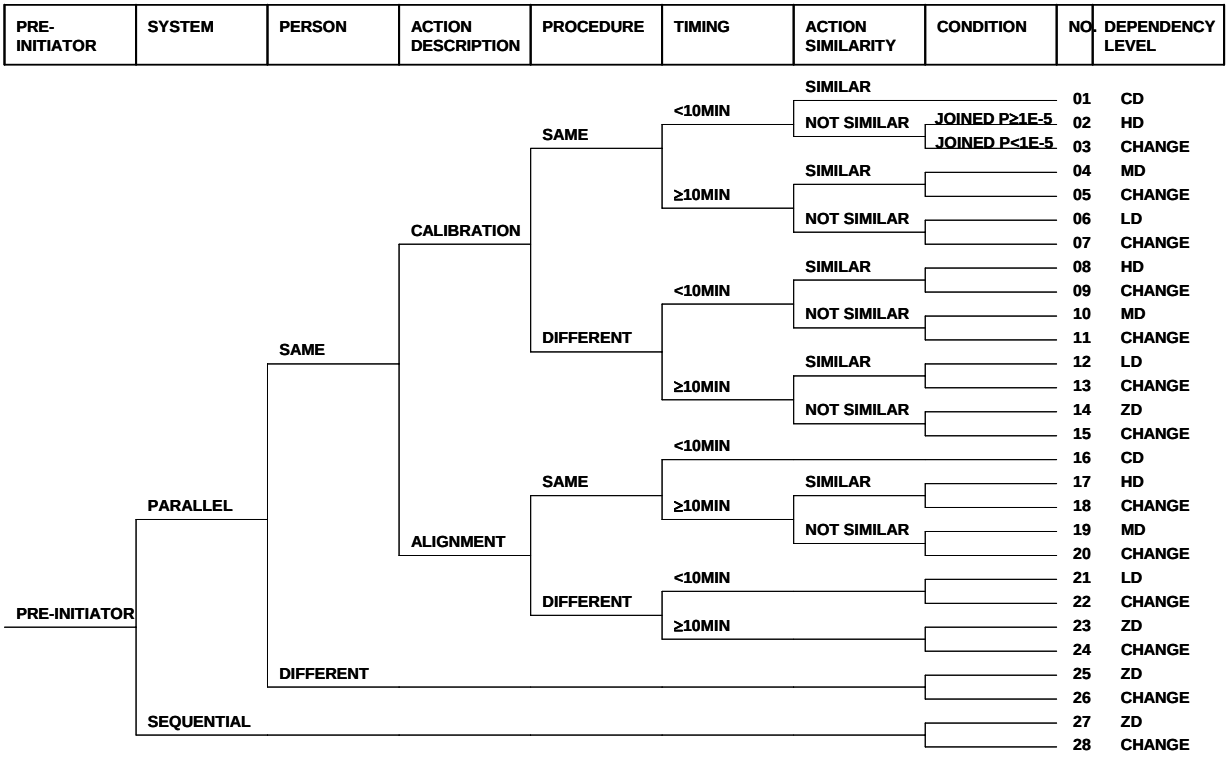

Figure 3: IJS-HRA Dependency – Post-Initiator HFE

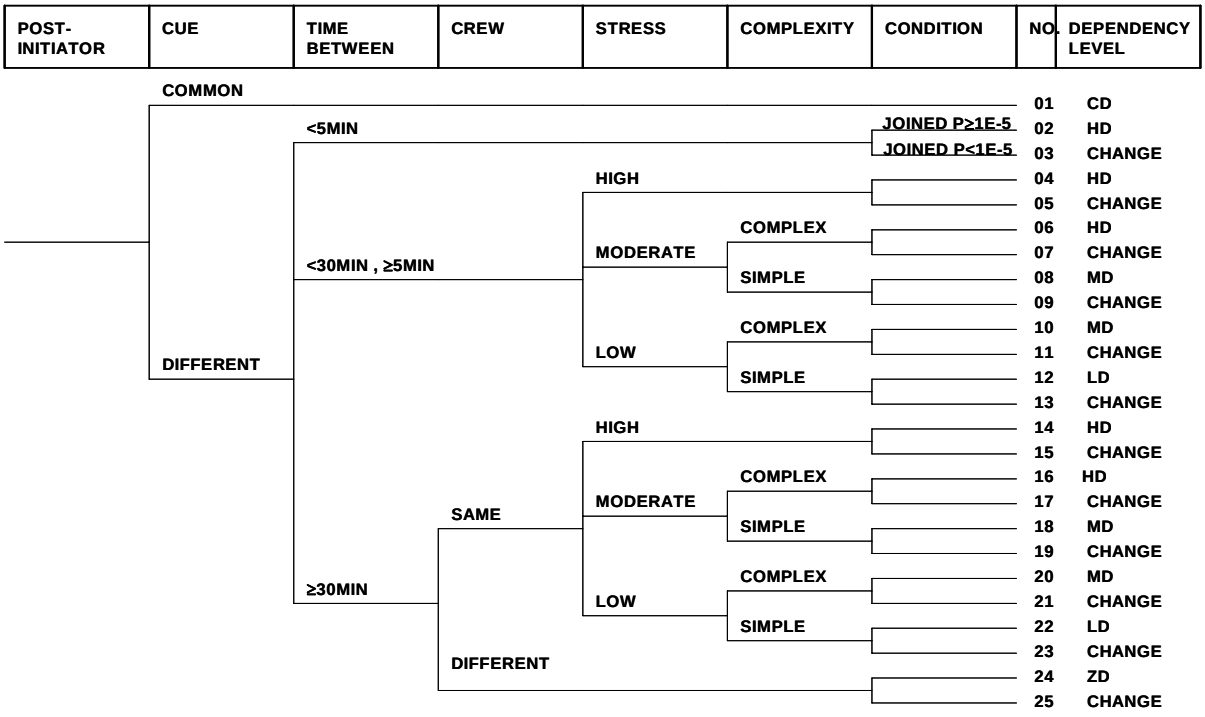

Figure 2 for pre-initiators and Figure 3 for post-initiators show that the dependency evaluation code is identified (e.g. LD12) based on the parameters, which are connected with their representative human failure events. Dependency evaluation code consists of first two characters identifying the level of dependency (e.g. ZD, LD, MD, HD, CD). The next numbers in the code represents the scenario number of the corresponding scenario from dependency method presented in its respective figure and identify parameters that are important for determining the level of dependency: e.g. cue, time between, crew, stress, complexity, location, system, action description, procedure, timing, person, action similarity [1, 4].

E.g. for 2 dependent post-initiators, a dependency level LD is determined on Figure 3 (LD12), which shows: different cue, 5-30 min between the events, low stress, simple action and no change of probability needed as joined HEP>1E-5. Additionally, an algorithm based on geometry average is used for pre-initiators for calculation of HEP [1, 4], which determines the same HEP for similar actions on both trains and prevents that associated HEP of HFE on one train and HEP of HFE on another train would differ significantly, if both HFE represent similar actions.

2.2. SPAR-H

Standardized Plant Analysis Risk HRA (SPAR-H) is a method for estimating the human error probabilities (HEP) associated with operator actions and decisions in nuclear power plants [5].

Table 1 shows how dependency between HFE is determined within SPAR-H. Five levels of dependency are determined, similarly to THERP and IJS-HRA. The parameters for determining the level of dependency differ from THERP and from IJS-HRA.

Table 1: SPAR-H Dependency [5]

Condition Number	Crew (same or different)	Time (close in time or not close in time)	Location (same or different)	Cues (additional or no additional)	Dependency	
1	S	C	S	NA	COMPLETE	When considering recovery in a series: e.g., 2nd, 3rd, or 4th checker: if this error is the **3rd error in the sequence**, then the dependency is at least **moderate;** if this error is the **4th error in the sequence**, then the dependency is at least **high.**
2				A	COMPLETE	
3			D	NA	HIGH	
4				A	HIGH	
5		NC	S	NA	HIGH	
6				A	MODERATE	
7			D	NA	MODERATE	
8				A	LOW	
9	D	C	S	NA	MODERATE	
10				A	MODERATE	
11			D	NA	MODERATE	
12				A	MODERATE	
13		NC	S	NA	LOW	
14				A	LOW	
15			D	NA	LOW	
16				A	LOW	
17					ZERO	

SPAR-H dependency table is applicable to both: pre-initiators and post-initiators.

3. ANALYSIS AND RESULTS

3.1. Qualitative Comparison

Table 2 shows a theoretical comparison of both dependency methods in sense to compare the dependency determined by IJS-HRA method and by SPAR-H method.

Table 3 is the subset of Table 2. Table 3 focuses only to those scenarios (specific scenario suit specific set of parameters), which suit real HFE considered in the specific HRA (practical comparison of both dependency methods based on specific PSA model). Both tables show, that for specific HFE, their respective HEP may be evaluated as a different value, if it is determined with one or the other method.

More dependencies in columns at SPAR-H means that among all HFE, for which a certain dependency level was determined by IJS-HRA, application of SPAR-H required certain dependency level for some HFE and certain dependency level for some other HFE.

Table 2: Comparison of dependency levels – theory

Pre-Initiators		**Post-Initiators**		
IJS-HRA	**SPAR-H**	**IJS-HRA**	**SPAR-H**	
CD1	CD1, HD3	CD1	CD1, HD3, HD5, MD7, MD9, MD11, LD13, LD15	Increase of initially determined dependency due to larger number of consecutive actions in a sequence
HD2	CD2, HD4	HD2	CD2, HD4, MD10, MD12	
MD4	HD5, MD7	HD4	CD2, HD4, MD6, LD8, MD10, MD12, LD14, LD16	
LD6	MD6, LD8	HD6	CD2, HD4, MD6, LD8, MD10, MD12, LD14, LD16	
HD8	CD1, HD3	MD8	CD2, HD4, MD6, LD8, MD10, MD12, LD14, LD16	
MD10	CD2, HD4	MD10	CD2, HD4, MD6, LD8, MD10, MD12, LD14, LD16	
LD12	HD5, MD7	LD12	CD2, HD4, MD6, LD8, MD10, MD12, LD14, LD16	
ZD14	MD6, LD8	HD14	MD6, LD8	
CD16	CD1, CD2, HD3, HD4	HD16	MD6, LD8	
HD17	HD5, MD7	MD18	MD6, LD8	
MD19	MD6, LD8	MD20	MD6, LD8	
LD21	CD1, CD2, HD3, HD4	LD22	MD6, LD8	
ZD23	HD5, MD6, MD7, LD8	ZD24	LD14, LD16	
ZD25	MD9, MD10, MD11, MD12, LD13, LD14, LD15, LD16			
ZD27	CD1, CD2, HD3, HD4, HD5, MD6, MD7, LD8, MD9, MD10, MD11, MD12, LD13, LD14, LD15, LD16			

Table 3: Comparison of dependency levels – practice for dependencies of the specific PSA model

Pre-Initiators		**Post-Initiators**		
IJS-HRA	**SPAR-H**	**IJS-HRA**	**SPAR-H**	
LD12+calculation [1,4]	HD5	CD1	CD1	
HD17+calculation [1,4]	HD5	HD2	CD2, MD12	
		MD8	HD4, LD8	
		MD18	LD8	
		MD20	LD8	
		LD12	LD8	MD-3th-in-sequence
Example row->		LD22	MD6, LD8	MD-3th-in-sequence, HD-4th-in-sequence
		ZD24	LD14, LD16	MD-3th-in-sequence, HD-4th-in-sequence

In the example row in Table 3: among 13 post-initiators, for which the dependency level LD22 was determined by IJS-HRA, for 6 of them low dependency LD8 is determined by SPAR-H, for one of them moderate dependency MD6 is determined and for others moderate dependency MD (for 3 of them: MD-3th-in-sequence) and high dependency HD (for 3 of them: HD-4th-in-sequence) is determined due to SPAR-H rule (see the right column of table 1: for more events in a sequence, it is possible that the dependency level is required to be increased from the initially determined one).

3.2. Quantitative Comparison

PSA model, which was used for the evaluation purposes, includes 64 HFE, which HEP are changed if HRA dependency method changes.

Table 4 shows a selected part of those HFE with identified dependency levels and calculated the respective HEP for both methods IJS-HRA and SPAR-H. The terms CALC and IND marked at pre-initiators represent the calculation of final HEP as the geometry average between the independent value of HEP for action at one train and the respective dependent HEP assessed as low dependency (LD12) for similar action at the other train.

Table 4: Selected HFE with quantified HEP (for IJS-HRA and for SPAR-H)

BASIC EVENT ID	DEPENDENCY LEVEL IJS-HRA	FINAL HEP IJS-HRA	DEPENDENCY LEVEL SPAR-H	FINAL HEP SPAR-H
PRE_INI_01	CALC, IND, LD12	1,91E-03	HD5	5,00E-01
PRE_INI_02	CALC, IND, LD12	1,91E-03	HD5	5,00E-01
POST_INI_34	ZD24	4,52E-03	LD16	5,43E-02
POST_INI_42	MD8	1,71E-01	LD8	8,08E-02
POST_INI_53	ZD24	1,58E-02	LD14	6,50E-02
POST_INI_63	LD22	5,07E-02	HD-4th-in-seq	5,00E-01
POST_INI_66	HD2	5,16E-01	MD12	1,70E-01
POST_INI_69	ZD24	1,04E-03	LD14	5,10E-02
POST_INI_79	ZD24	1,96E-04	MD-3th-in-seq	1,43E-01

Table 5 shows the results of importance factors, i.e. Risk Increase Factor (RIF) and Risk Decrease Factor (RDF) of selected HFE, which are calculated based on analysis runs with PSA model evaluated based on IJS-HRA dependency and same PSA model evaluated based on SPAR-H dependency considered. Selected HFE in the table are those with RDF>1,05 and RIF>2, according to criteria for identification of risk significant events. The differences between identification of importance factors in PSA model evaluated using IJS-HRA and in PSA model evaluated using SPAR-H are significant.

Table 5 shows that identification of important HFE shows only one HFE, which is identified as important in both analyses (POST_INI_04, which deals with operator establishing Auxiliary Feedwater Pumps).

Table 5: Results of Importance of HFE

PSA MODEL BASED ON HEP OF HFE DETERMINED BY IJS-HRA			
HFE	RDF	HFE	RIF
POST_INI_42	1,13E+00	POST_INI_04	2,26E+02
POST_INI_63	1,09E+00	POST_INI_12	7,46E+01
POST_INI_88	1,09E+00	POST_INI_100	4,49E+01
		POST_INI_95	3,66E+01
		INI_01	2,34E+01
		INI_02	2,34E+01
		POST_INI_102	2,23E+01
		POST_INI_02	1,75E+01
		POST_INI_34	6,73E+00
		POST_INI_35	3,19E+00
		POST_INI_69	2,68E+00
		POST_INI_63	2,62E+00
		POST_INI_60	2,01E+00

PSA MODEL BASED ON HEP OF HFE DETERMINED BY SPAR-H			
HFE	RDF	HFE	RIF
PRE_INI_06	1,01E+01	POST_INI_53	5,76E+00
PRE_INI_05	8,18E+00	POST_INI_04	5,63E+00
POST_INI_102	2,07E+00		
POST_INI_53	1,55E+00		
PRE_INI_09	1,51E+00		
PRE_INI_10	1,51E+00		
PRE_INI_04	1,40E+00		
PRE_INI_01	1,40E+00		
PRE_INI_02	1,38E+00		
PRE_INI_03	1,38E+00		
POST_INI_79	1,06E+00		

Figure 4: Comparison of Fractional Contribution of HFE

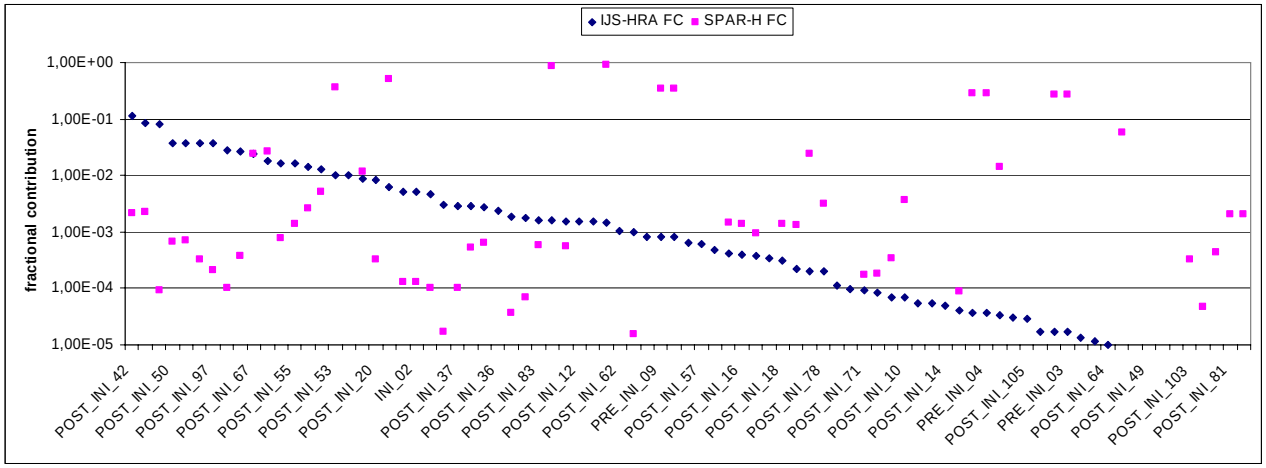

Figure 5: Comparison of Risk Increase Factor of HFE

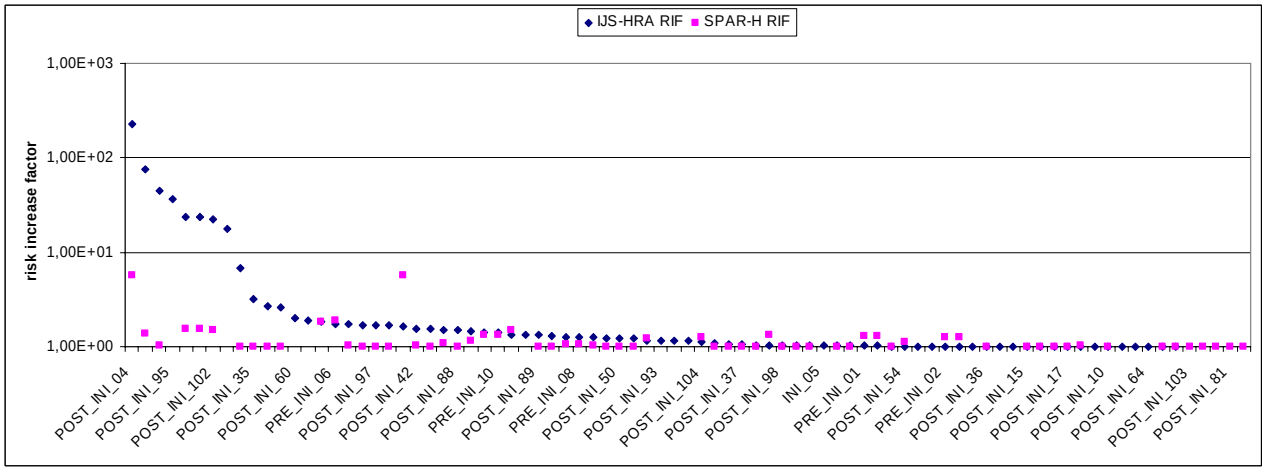

The difference between core damage frequency obtained by PSA model evaluated using IJS-HRA and the PSA model evaluated using SPAR-H is significant (an order of magnitude).

Figure 4 shows a comparison of fractional contribution of HFE for both analyses. Figure shows that there are no comparable results: events, which contribute significantly, if IJS-HRA dependency is considered, can be insignificant, if SPAR-H dependency is considered and vice versa.

Figure 5 shows that no comparable results exist also at evaluation of risk increase factor of HFE for both analyses.

If instead of five levels of dependency, less dependency levels are determined with different equations for evaluation of dependency, which would suit the number of selected dependency levels, another dimension of large differences is identified.

4. CONCLUSION

Several methods for dependency determination between human failure events within human reliability analysis have been examined and two methods have been compared in details. Consideration of human error probability of the first human failure event in a sequence as it is and an increase of independent human error probability of the next human failure event in a sequence is common to most of the HRA methods, except IJS-HRA, which for relatively similar actions determines identical failure probability based on geometry average.

The methods differ mostly in definition of a set of parameters, which impact the dependency, in the application of the parameters and in the defined dependency level, which applies to specific states of the contributed parameters. All those distinctions are subjective. The subjectivism can lead to a difference of several orders of magnitude, considering either the results of HRA or the overall PSA results, which include the results of HRA. Those distinctions can cause identification of different key human failure events, which are subjected to their prioritization of simulator training. Those distinctions can cause different calculation of core damage frequency and its sensitivity to changes, which can impact the risk-informed decision-making.

The reduction of these distinctions can be done by preparation of more detailed guidelines for HRA application. The detailed guidelines should be highlighted with many practical examples for evaluation of human error probability for all possible situations, which can be found in the models. More detailed procedures for all steps of HRA are needed with emphasis on dependency determination steps, together with clear and useful practical examples.

The nuclear power plant probabilistic safety assessment data base should be extended by specific experience obtained from plant simulator considering human failure events and their dependencies.

Acknowledgements

The Slovenian Research Agency partly supported this research (partly research program P2-0026, partly research project V2-0376 supported together with Slovenian Nuclear Safety Administration).

References

[1] M. Čepin, DEPEND-HRA - A method for consideration of dependency in human reliability analysis, Reliability Engineering & System Safety, in press, 2008.
[2] A. Prošek and M. Čepin, Success criteria time windows of operator actions using RELAP5/MOD3.3 within human reliability analysis, Journal of Loss Prevention in the Process Industries, in press, 2008.
[3] M. Čepin, Importance of human contribution within the human reliability analysis (IJS-HRA), Journal of Loss Prevention in the Process Industries, in press, 2008.
[4] M. Čepin and X. He, Development of a Method for Consideration of Dependence between Human Failure Events. ESREL2006, (2006).
[5] NUREG/CR-6883. The SPAR-H Human Reliability Analysis Method. US NRC, (2005).
[6] NUREG/CR-1278. Handbook for Human Reliability Analysis with Emphasis on Nuclear Power Plants Application. US NRC, (1983).
[7] SHARP. Systematic Human Action Reliability Procedure. EPRI. NP-3583, (1984).
[8] NUREG/CR-4772. Accident Sequence Evaluation Program: Human Reliability Analysis Procedure. US NRC, (1987).
[9] NUREG-1624. Technical Basis and Implementation Guidelines for A Technique for Human Event Analysis (ATHEANA). US NRC, (1999).
[10] J. Forester, D. Bley, S. Cooper, E. Lois, N. Siu, A. Kolaczkowski and J. Wrethall, Expert elicitation Approach for Performing ATHEANA Quantification. Reliability Engineering & System Safety, Vol. 83, pp.207-220, (2004).
[11] E. Hollnagel, Cognitive Reliability and Error Analysis Method, CREAM. Elsevier Science Ltd, (1988).
[12] A. Spurgin, Another view of the state of human reliability analysis (HRA). Reliability Engineering & System Safety, Volume 29 (3), pp. 365-370, (1990).
[13] J. F. Grobbelaar, J. A. Julius and F. Rahn, Analysis of Dependent Human Failure Events Using the EPRI HRA Calculator. PSA05. Proceedings, (2005).
[14] B. Reer, V. N. Dang, and S. Hirschberg, The CESA Method and its Applications in a Plant-Specific Pilot Study on Errors of Commission. Reliability Engineering & System Safety, Vol. 83, pp.187-205, (2004).
[15] NUREG-1792. Good Practices for Implementing Human Reliability Analysis. US NRC, (2005).

ANS PSA 2008 Topical Meeting - Challenges to PSA during the nuclear renaissance
Knoxville, Tennessee, September 7–11, 2008, on CD-ROM, American Nuclear Society, LaGrange Park, IL (2008)

HUMAN RELIABILITY ANALYSIS WITHIN PROBABILISTIC SAFETY ASSESSMENT FOR OTHER MODES THAN POWER OPERATION

Čepin M
Jožef Stefan Institute
Jamova cesta 39, 1000 Ljubljana, Slovenia
marko.cepin@ijs.si

ABSTRACT

Probabilistic safety assessment (PSA) is normally performed for nuclear power plant power operation, although it can be used for other plant modes. The objective of the paper is to show how can probabilistic safety assessment model for normal power operation be used for development of probabilistic safety assessment models for other modes of plant operation such as start-up, hot standby and hot shutdown. The analysis of all three models is performed. The results of the analysis include the most important risk measures for all three analyzed states. The results show that the risk of the plant is lower for any of the considered states, if it is compared to the risk of the plant during normal operation. The results of human reliability analysis comparison show that part of the human error probabilities change notable in other modes of plant operation and some of their importance measures change significantly.

Key Words: human reliability analysis, probabilistic safety assessment

1 INTRODUCTION

Probabilistic safety assessment (PSA) is a standardized method for assessment and improvement of nuclear power plant safety, which is normally performed for nuclear power plant power operation, although it can be used for other plant modes [1,2].

The objective of the paper is to show how can probabilistic safety assessment model for normal power operation be used for development of probabilistic safety assessment models for other modes of plant operation such as startup, hot standby and hot shutdown. The focus of the work is placed to the adjustment of the human reliability analysis, which largely depends on the time parameters. The time parameters of concern for each human action, which is considered in the probabilistic safety assessment and which can turn into human failure event, if it is not performed or if it is performed wrongly, are:

- the time window of the action,
- the actual time needed for performing the action and
- the additional available time for action.

The time window of the human action actually represents the success criteria for the action. It represents the time interval, in which operators have to perform the action in order that the plant is operating according to the technical specifications and operating procedures. The actual time needed for performing the action is the realistic time in which operators perform the action and it can be obtained from the simulator experience. The additional available time for action is

defined as the difference between the time window of the action and the actual time needed for performing the action, which is assessed based on the real simulator scenarios.

It is assumed that other modes, such as cold shutdown, are considered in a separate study, i.e. in the shutdown probabilistic safety assessment.

2 RELATED LITERATURE

The related literature includes the references about IJS-HRA method, which was developed for the purpose of updating the human reliability analysis for the probabilistic safety assessment of the nuclear power plant in normal power operation [3, 4, 5, 6, 7]. IJS-HRA method is developed to consider three groups of human failure events: pre-initiators, initiators and post-initiators.

Pre-initiators are events that may cause the equipment to be unavailable before the initiation of undesired scenario, which may lead to accident. Initiators are events that may contribute to initiation of undesired scenario, which may lead to accident. Post-initiators are events, which are connected with human actions to prevent accident or mitigate its consequences after initiation of undesired scenario, which may lead to accident, has occurred.

The method identifies dependencies based on scenarios, where consecutive human actions are modeled, and based on a list of minimal cut sets, which is obtained by running the minimal cut sets analysis considering high values of human error probabilities in the evaluation [3].

A large example study, which consisted of a large number of human failure events, has demonstrated the applicability of the method. Comparative analyses, which were performed, show that both: selection of dependency method and selection of dependency levels within the method largely impacts the results of probabilistic safety assessment. If the core damage frequency is not impacted much, the listings of important basic events in terms of risk increase and risk decrease factors may change considerably [3].

The results of sensitivity analyses show that only few parameters from human reliability database contribute significantly to the risk. Identification of dominating human failure events and identification of the significant parameters are a valuable input for determining the priorities of simulator training [4].

The comparison of applying different human reliability analysis methods to the same problems shows large differences in the results [7]. Subjectivism can be avoided by placing additional efforts to the field of human reliability analysis.

3 METHOD AND DEVELOPMENT OF MODELS

Consideration of probabilistic safety assessment in several modes of operation is straightforward. The results of probabilistic safety assessment of specific modes can be used to assess the overall risk of the plant by determining the mean value of the considered results of considered modes of operation taking into account the time duration for each of the considered modes. The expression for determining the overall risk is the following:

$$R = \frac{\sum_{i=1}^{I} R_i T_i}{\sum_{i=1}^{I} T_i} \quad (1)$$

where R = overall risk measure (either core damage frequency on the plant or event tree or sequence level, or the system unavailability at the system or subsystem level); R_i = risk measure of i – th mode of operation; T_i = the time duration for the plant being in i – th mode of operation; I = the number of considered modes of operation.

The approach is not suitable for the risk importance measures. The experience shows that certain equipment or human actions can be important in some of the modes of operation and not important in others. Their averaging would lead to the loss of information rather to some improvement.

3.1 Probabilistic Safety Assessment Models for Other Modes than Power Operation

The respective probabilistic safety assessment documents and the computerized probabilistic safety assessment model are both analyzed.

For each of the selected plant states:

- plant operation in plant startup (mode 2),
- plant operation in hot standby (mode 3) and
- plant operation in hot shutdown (mode 4),

its respective PSA model was prepared based on the PSA model for normal plant operation.

Initiating events and their frequencies are reviewed and changed, if needed for a specific mode of operation. E.g. the frequencies of Loss of Coolant Accidents are lower for plant in hot shutdown than for plant in normal operation and are changed to lower frequencies in the PSA model for plant operation in hot shutdown.

The functional events and the branches of the event tree are reviewed and changed, if needed for a specific mode of operation. E.g. functional event: reactor trip is not needed and it is deleted from the respective event trees in the PSA model for plant operation in hot shutdown.

The fault trees linked to the respective functional events of the event trees are reviewed and changed if needed for a specific mode of operation. Those potential changes include:

- the change of logic of the fault tree (e.g. a branch or a gate is removed, if it is not needed in the model),
- change of basic events of the fault tree (e.g. basic event is deleted, if it is not needed in the model),
- changes of parameters of the basic events (e.g. change of failure probability of certain equipment or change of human error probability, if it is needed in the model).

3.1.1 Consideration of changes related to human reliability

Human error probabilities are determined by using IJS-HRA method [3, 4]. The method and its features are presented in previous papers [3, 4, 5, 6]. Only the feature important for the

contents of this paper is mentioned here: quantification of human error probability is performed with consideration or without consideration of recovery.

Additional available time for action (Ta) is defined as the difference between the time window of the action (Tw) and the actual time needed for performing the action (Tp), which is assessed based on real simulator scenarios:

$$Ta=Tw-Tp \quad (2)$$

If additional available time for action is larger than determined time interval (e.g. 10 minutes), than recovery as independent mode of verification is considered. If additional available time for action is shorter than determined time interval, recovery is not considered.

Consideration of recovery causes lower human error probability and may cause a different impact of human error to the overall probabilistic safety assessment results.

Determination of the time window, in which operators have to perform the action, is obtained from deterministic safety analysis [6].

3.2 Models

The models of probabilistic safety assessment include the human reliability analysis models and their subsequent human error probabilities. Models of deterministic safety analysis serve for determination of success criteria within probabilistic safety assessment and separately for determination of time windows of specific human actions modeled in probabilistic safety assessment.

3.2.1 Models of probabilistic safety assessment

The models of probabilistic safety assessment include the model for normal plant operation and subsequent separate models adopted for startup, for hot standby and for hot shutdown modes of operation.

The models are large including thousands of basic events and gates, hundredths of fault trees, which represent system models, and tenths of initiating events and their respective event trees, which together include hundredths of accident sequences.

3.2.2 Human reliability analysis models

Human reliability analysis models are divided to models for pre-initiators, for initiators and for post-initiators.

The dependency between different human failure events is specially considered as an important issue, which impact significantly the evaluated human error probabilities.

4 RESULTS

Selected results of the analyses are presented. Figure 1 shows that the core damage frequency decreases for plant startup (POS1C - on the figure), hot standby (POS2A - on the figure) and hot shutdown (POS3A - on the figure) compared to the core damage frequency at power operation (power - on the figure).

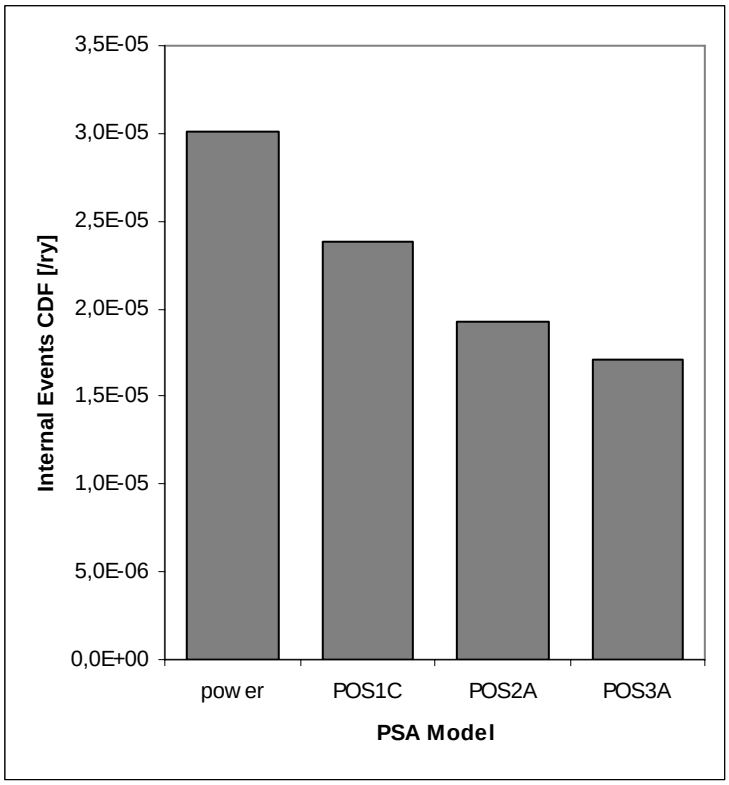

Figure 1. Core damage frequency for 4 plant operating states.

Figure 2 shows the change of fractional contribution of selected human failure events in plant startup, hot standby and hot shutdown versus plant power operation. The changes in risk importance measures are significant for selected equipment, which is more true for risk increase factor and fractional contribution than for risk decrease factor in the case of the investigated PSA model.

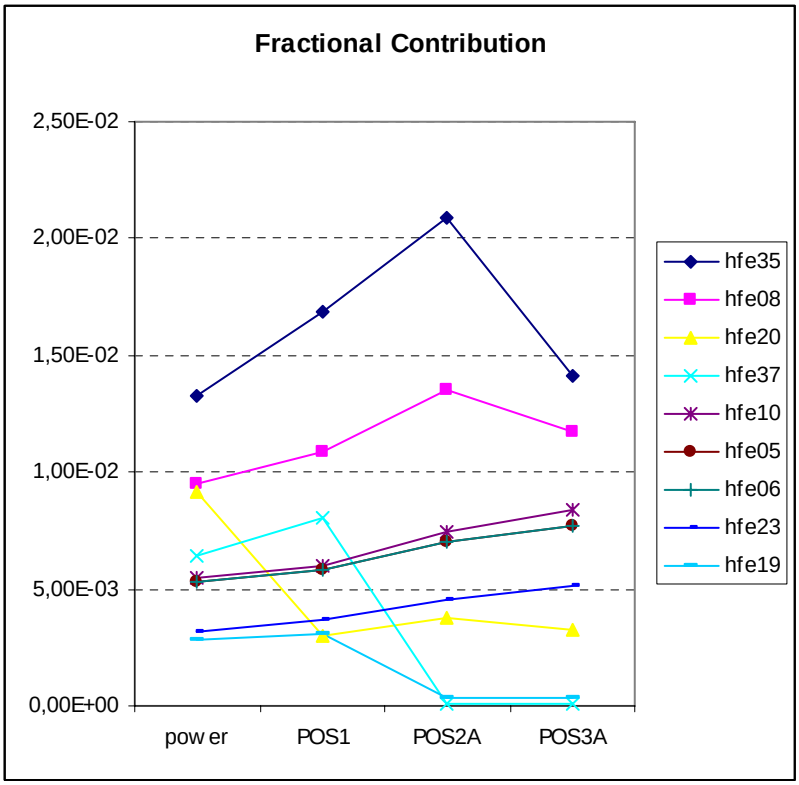

Figure 2. Fractional contribution of selected human failure events.

Figure 3 shows the risk importance measures for selected groups of components for the compared probabilistic safety assessment models: PSA model in power operation versus PSA models in startup, hot standby and hot shutdown. Table I shows description of the selected groups. The results show that human actions are more important in other considered states than in power operation (see fractional contribution of group HUMAN-ERRORS). The results show that risk increase factor for human actions is much larger in power operation than in other states.

Table I. Definition of groups of events.

BASIC EVENT GROUP NAME	BASIC EVENT GROUP DESCRIPTION
DIESEL-GEN	All basic events corresponding to diesel generators
HUMAN-ERRORS	All basic events corresponding to human failure events
AFW-PUMPS	All basic events corresponding to auxiliary feedwater pumps
HUMAN-E-INI	All basic events corresponding to initiator human failure events
HUMAN-E-PRE-INI	All basic events corresponding to pre-initiator human failure events

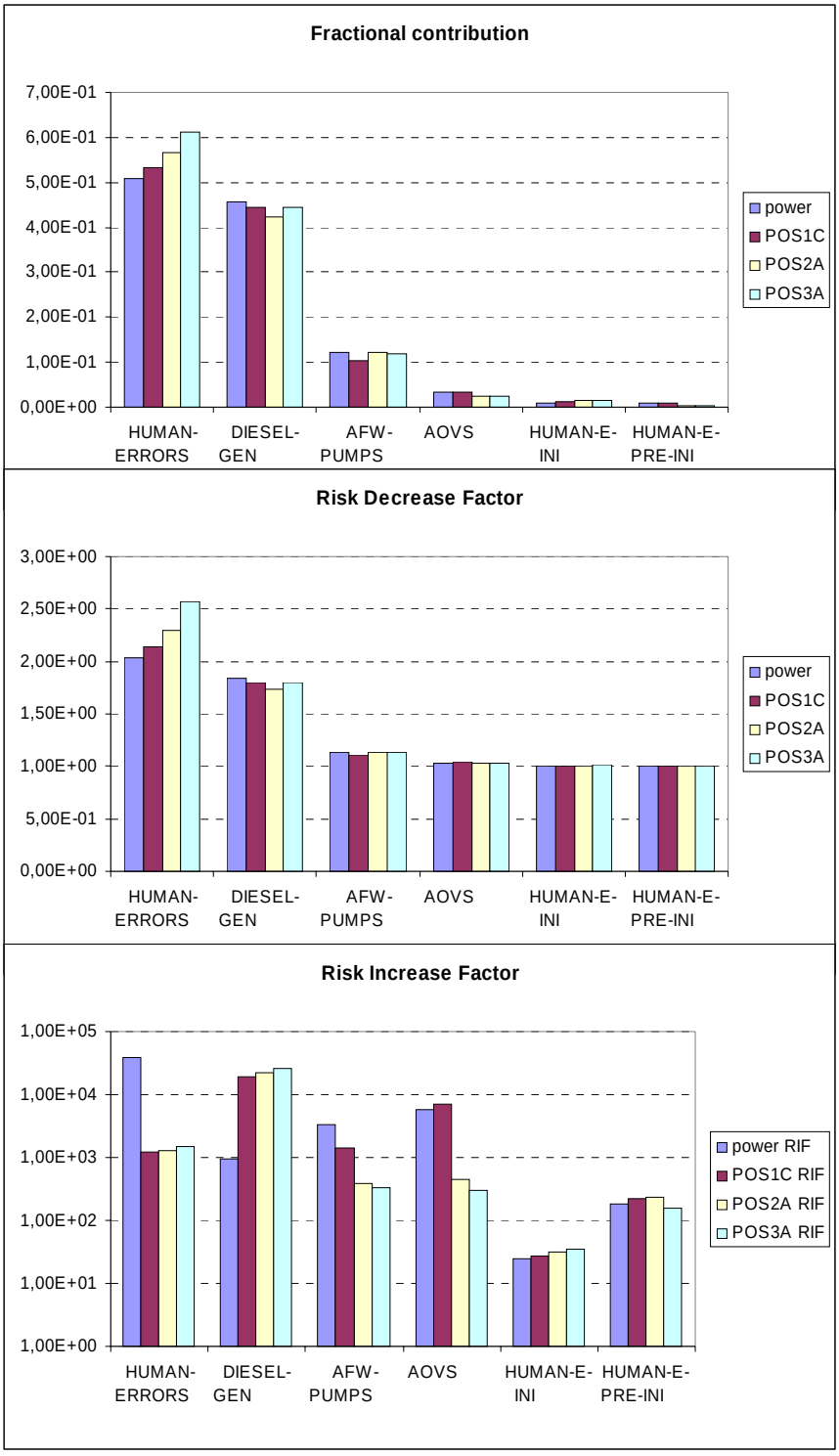

Figure 3. Comparison of risk measures for selected groups of components (note: logarithmic scale at RIF).

5 CONCLUSIONS

The objective of the paper is to show how can probabilistic safety assessment model for normal power operation be used for development of probabilistic safety assessment models for other modes of plant operation such as startup, hot standby and hot shutdown.

The analysis of all three models in addition to the analysis of power operation is performed. The results of the analysis include the most important risk measures for all three analyzed states. The results show that the risk of the plant is lower for any of the considered states, if it is compared to the risk of the plant during normal operation. The comparison of human reliability analyses results show that a part of the human error probabilities change notable in other modes of plant operation and some of their importance measures change significantly.

6 ACKNOWLEDGMENTS

The Slovenian Research Agency supported this research (partly research program P2-0026, partly research project V2-0376 supported together with Slovenian Nuclear Safety Administration).

7 REFERENCES

1. K. L. Kiper, Insights from an All-Modes PSA at Seabrook Station, International Topical Meeting on Probabilistic Safety Assessment, Detroit, Oct 6-9, Proceedings, pp. 429-434 (2002).
2. M. Čepin & B. Mavko, A Dynamic Fault Tree, Reliability Engineering and System Safety **Vol. 75,** no 1, pp. 83-91 (2002).
3. M. Čepin, DEPEND-HRA-A method for consideration of dependency in human reliability analysis, Reliability Engineering and System Safety, **Vol. 93**, no. 10, pp. 1452-1460 (2008).
4. M. Čepin, Importance of human contribution within the human reliability analysis (IJS-HRA), Journal of Loss Prevention in the Process Industries, **Vol. 21**, no. 3, pp. 268-276 (2008).
5. M. Čepin & R. Prosen, Update of human reliability analysis for nuclear power plant. In Glumac, Bogdan (ed.), Lengar, Igor (ed.), International Conference Nuclear Energy for New Europe, Portorož, 2006. Proceedings. Nuclear Society of Slovenia.
6. A. Prošek, M. Čepin, Success criteria time windows of operator actions using RELAP5/MOD3.3 within human reliability analysis, Journal of Loss Prevention in the Process Industries, **Vol. 21**, no. 3, 260-267 (2008).
7. M . Čepin, Risk comparison of methods for dependency determination within human reliability analysis, KAO, Tsu-Mu (ed.), ZIO, Enrico (ed.), HO, Vincent (ed.), PSAM 9, 8-23 May 2008, Hong Kong, China. Proceedings, Edge Publication Group Limited, 8 pages (2008).

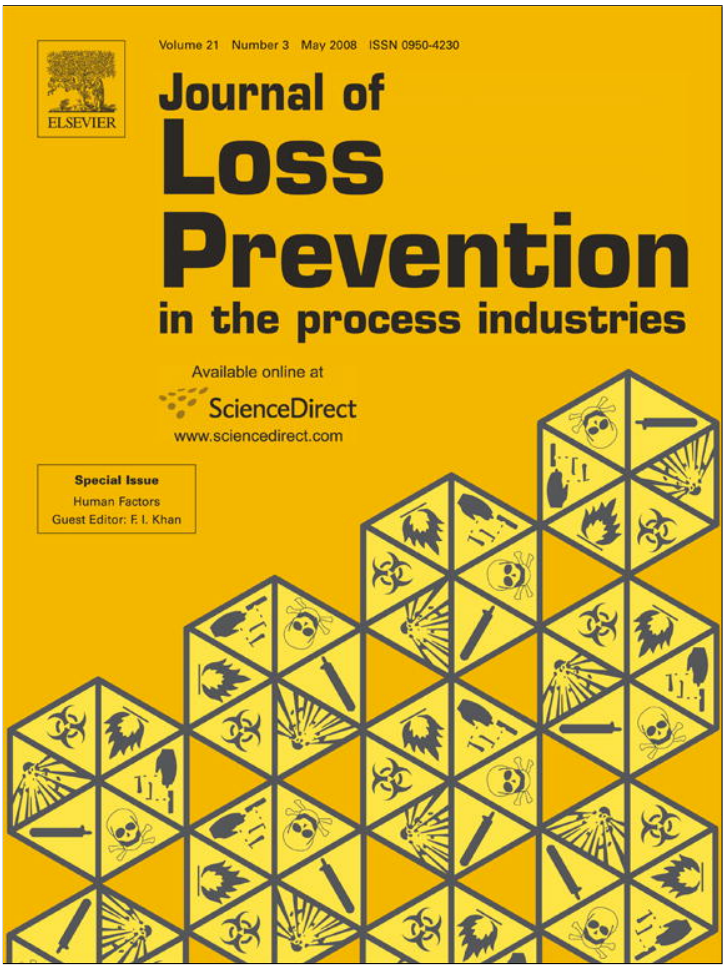

Available online at www.sciencedirect.com
ScienceDirect
Journal of Loss Prevention in the Process Industries 21 (2008) 268–276
Journal of Loss Prevention in the process industries
www.elsevier.com/locate/jlp

Importance of human contribution within the human reliability analysis (IJS-HRA)

Marko Čepin*

Jožef Stefan Institute, Ljubljana, Slovenia

Received 13 February 2007; received in revised form 19 April 2007; accepted 19 April 2007

Abstract

The human reliability analysis (HRA) was investigated intensively in the last decades and many methods have been developed. The most important feature of HRA is a good data, which can be obtained from full scope plant simulators. The objective of this study is to investigate how importance factors of human failure events obtained from results of probabilistic safety assessment (PSA) can be used in sense to improve human reliability. The study considers recently developed method: Institute Jožef Stefan (IJS)-HRA, which integrates some features of existing methods and some new features, and its application in a large PSA model. Two ways for quantification and application of importance factors are presented. The results show that only few human failure events dominate in the HRA analysis. The results show that only few parameters from human reliability database contribute significantly to the risk. Identification of dominating human failure events and identification of the significant parameters are a valuable input for determining the priorities of simulator training.

Keywords: Human reliability analysis; Success criteria; Probabilistic safety assessment

1. Introduction

The contribution of human factor to safety of complex facilities is large in spite of intensive automation of systems and processes. The field was investigated intensively in the last decades, which is specially the case for chemical industry (Khan, Amyotte, & DiMattia, 2006), for aviation (Harris et al., 2005) and for nuclear power plants (Grobbelaar, Julius, & Rahn, 2005; Kennedy, Siemieniuch, Sinclair, Kirwan, & Gibson, 2007; Reer, Dang, & Hirschberg, 2004). Probabilistic safety assessment (PSA) applications are source of many interactions with human reliability analysis (HRA) (ASME-RA-S-2002, 2002; Čepin & Mavko, 1997; Čepin, 2002; Čepin & Mavko, 2002; Čepin, 2005b; Holy, 2004; Mosleh & Chang, 2004).

Many methods connected with HRA were developed in this period, e.g. technique for human error rate prediction (THERP, NUREG/CR-1278, 1983), systematic human action reliability procedure (SHARP, 1984), accident sequence evaluation program (ASEP, NUREG/CR-4772, 1987), a technique for human event analysis (ATHEANA; Forester et al., 2004; NUREG-1624, 1999), cognitive reliability and error analysis method (CREAM, Hollnagel, 1988), human cognitive reliability (HCR, Spurgin, 1990), standardized plant analysis risk HRA (SPAR-H, NUREG/CR-6883, 2005).

In addition, Institute Jožef Stefan (IJS)-HRA was developed recently (Čepin, 2005a; Čepin & He, 2006). It integrates some features of existing methods and some new features such as contribution of the simulator experience in order to consider the newest requirements and recommendations in the field and in order to be integrated in a modern computerised PSA, which offers a number of options for analyses from several points of view (NUREG-1792, 2005).

The most important feature of HRA is a good collection, interpretation and application of human failure data. Full scope plant simulators are a good support as they represent a source of valuable data.

*Tel.: +386 1 5885 263; fax: +386 1 5885 377.
E-mail address: marko.cepin@ijs.si

0950-4230/$ - see front matter © 2007 Elsevier Ltd. All rights reserved.
doi:10.1016/j.jlp.2007.04.012

The objective of this study is to investigate how importance factors of human failure events obtained from results of PSA can be used in sense to improve human reliability. The human failure events are firstly considered as indivisible entities with their respective human error probability. Secondly, human failure events are split to specific standardised tasks, which are all quantified as items in the human reliability database and the importance of the respective items from human reliability database is evaluated.

Section 2 briefly summarizes the IJS-HRA method. Section 3 gives the basic information about the PSA model, which was analysed. Section 4 gives an example evaluation of selected human failure model from selected model. Section 5 presents the procedure, analysis and results of importance analyses that were performed together with discussion of implications of the results. Conclusions bring the most important findings and future work.

2. IJS-HRA

The IJS-HRA is a method for evaluation of human failure events in sense to determine the reliability of the respective human actions (Čepin, 2005a). Human action is a specific action required by human operator. If it is not performed or it is not performed in time and correctly, it is referred to as a human failure event.

Fig. 1 shows the schematic representation of the IJS-HRA method. The main inputs for IJS-HRA method include (left part of the Fig. 1):

- PSA model, which is interconnected with the HRA,
- plant information, which is the source of information which supports the evaluation, and
- state-of-the-art in the respective field: standards, guides, good features of existing methods and good practice.

The method is developed including consideration about dependencies between human failure events (Čepin & He, 2006).

The success criteria for human failure events include information about their time window, i.e. information about the time, in which operators have to perform the action. This information about the available time comes from safety analyses, where scenarios about operating safety systems are evaluated. This is the reason for appearance of text box of safety analysis in Fig. 1 and its connection with text box: evaluation. Results of the HRA are inserted into the PSA, which is shown by upper feedback in Fig. 1.

The method consists of the following steps that are presented in Fig. 2:

1. *Statements on objectives, definition of the work and scope of the analysis:* the main objective is to evaluate human failure events and to assess their respective human error probabilities for their insertion to the PSA of a specific nuclear power plant.
2. *Identification of human failure events:* pre-initiator events (i.e. pre-initiators), initiator events (i.e. initiators) and post-initiator events (i.e. post-initiators) are considered. Pre-initiators are the events that may cause the equipment to be unavailable before the initiation of undesired scenario, which may lead to accident. Initiators are the events that may contribute to initiation of undesired scenario, which may lead to accident. Post-initiators are the events, which are connected with human actions to prevent accident or mitigate its consequences after

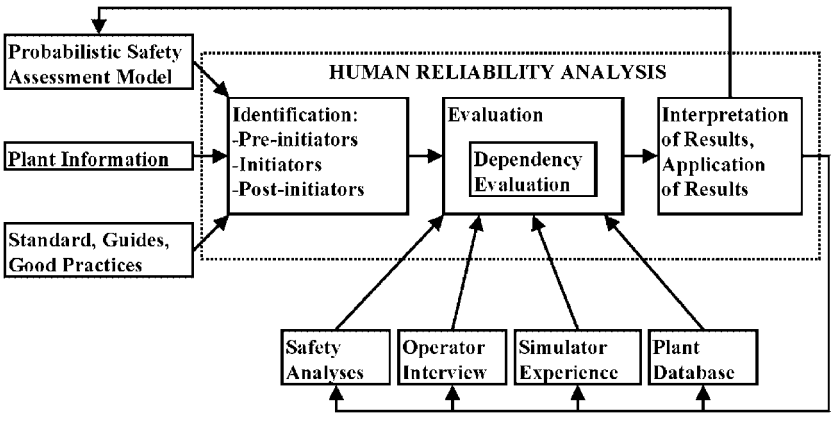

Fig. 1. Schematic representation of human reliability analysis (IJS-HRA).

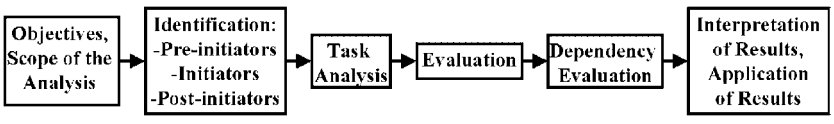

Fig. 2. Flowchart of steps of human reliability analysis (IJS-HRA).

initiation of undesired scenario, which may lead to accident, has occurred.

3. *Task analysis of human failure events:* information about human failure events is collected, which includes review of plant documents (e.g. safety analysis report, plant procedures), plant databases, PSA (with emphasis on all its parts that are connected with HRA).

Preparation and analysis of interview with the plant operators is performed, which identify information about tasks, about the time needed for performing human actions, about performance shaping factors connected with their respective human failure events.

Tasks, which compose the respective human failure event, are identified and analysed, separately for diagnosis and for action tasks.

4. *Evaluation of human failure events:* measurement of time needed for performing human actions is performed through real simulator scenarios.

Assessment of simulator experience with human actions that are included in human failure events is done, which increases or reduces the human failure probabilities obtained from generic sources. Simulator experience is collected and evaluated in order to expand the database with the plant specific information.

Failure model table is prepared, which based on analysis of diagnosis and subtask analysis identifies human errors and specifies their general evaluation procedure: i.e. consideration or no consideration of recovery. If additional available time for action is more than determined time interval, e.g. 10 min, than recovery as independent mode of verification is considered. Additional available time for action is defined as the difference between the time window of the action (obtained from success criteria for the action: the time in which operators have to perform the action), i.e. the time in which action has to be performed in order that it meets the success criteria, and the actual time needed for performing the action.

Data table is prepared, which connect human errors with database about human error probabilities.

Quantification table is prepared, which contains human error probabilities of tasks within human failure event and overall failure probability of respective human failure event.

5. *Consideration of dependencies between human failure events:* the dependencies between tasks of human actions within one human failure event can be considered and the dependencies between separate human failure events can be considered. The five levels of dependency are determined.

Zero dependency (ZD) means that human failure events are independent one from another. The probability of failure of both human failure events (A and B) equals to the product of their respective human error probabilities (P_A and P_B): $P_{ZD}(P_B|P_A) = P_A P_B$.

Low dependency (LD) means: that the human error probability of dependent event is increased and the probability of failure of both human failure events in one sequence equals to the product: $P_{LD}(P_B|P_A) = P_A(1 + 19P_B)/20$.

Moderate dependency (MD) means: that the human error probability of dependent event is increased and the probability of failure of both human failure events in one sequence equals to the product: $P_{MD}(P_B|P_A) = P_A(1 + 6P_B)/7$.

High dependency (HD) means: that the human error probability of dependent event is increased and the probability of failure of both human failure events in one sequence equals to the product: $P_{HD}(P_B|P_A) = P_A(1 + P_B)/2$.

Complete dependency (CD) means: that the human error probability of dependent event is increased to 1 and the probability of failure of both human failure events in one sequence equals to the human error probability of the first event: $P_{CD}(P_B|P_A) = P_A$.

In general: $P_{XD}(P_B|P_A) = P_A(1 + K \cdots P_B)/(K+1)$; where: $K = 0,\ 1,\ 6,\ 19,\ \infty$, for dependency levels ZD, LD, MD, HD, CD, where $X = Z, L, M, H, C$, respectively. The equations for determining the dependency levels uses set of factors K for their respective dependency levels, which are based on judgment or on previous references (Čepin & He, 2006; NUREG/CR-1278, 1983).

Separately for pre-initiators, initiators and post-initiators the parameters are determined, which influence determination of level of dependency and for combinations of those parameters the levels of dependencies are defined (Čepin & He, 2006). The following parameters are identified as important for determining the level of dependency for pre-initiators:

- calibration or alignment for the event under investigation,
- the same (or very similar) or different procedure for the event compared to the previous event,
- the amount of time between the events (less or more than 10 min between event and previous event),
- the same or different person is performing the event,
- similar or not similar event; in the case of alignment this is related to the same or different visual frame of the event; in the case of calibration this is related to same or different calibration tool used for the event.

The following parameters are identified as important for determining the level of dependency for initiators and post-initiators:

- diagnosis part of the event compared to the previous event (or task) is common or different,
- the time between the events: less than 5 min; or as more than 5 but less than 30 min; or more than 30 min. E.g. if the consecutive actions are placed immediately one after another (i.e. within 5 min), their dependency is assumed to be high,
- the same or different crew is performing the event compared to the previous event,
- three levels of stress: high, medium and low,
- complex or simple event (e.g. more or less then couple of tasks within the event, e.g. more or less than eight simple actions).

The method for consideration of dependencies is widely described in reference (Čepin & He, 2006), where equations for dependency determination are widely elaborated and where diagrams are presented, which show, how dependency levels are determined based on the sets of parameters mentioned above (Čepin & He, 2006).

6. *Inclusion of HRA to PSA, interpretation of results:* human failure events with their respective human error probabilities are inserted into PSA. The quantification of PSA is performed considering human error probabilities as quantified with the described method. The results of PSA include: combinations of component failures and human failure events that may contribute to the plant risk, the lists of the most important component failures and human failure events according to the defined importance factors.

The most important human failure events are identified, i.e. human failure events with the largest risk factors (e.g. fractional contribution, e.g. risk increase factor, e.g. risk reduction factor).

The human failure events with the largest risk factors are reported to simulator training management for prioritisation of simulator training.

More detailed description of the method can be found in reference (Čepin, 2005a). More detailed description of consideration of the dependency within the method can be found in reference (Čepin & He, 2006).

2.1. Application of HRA within PSA

The human failure events together with their calculated human error probabilities are used in the PSA in two main ways.

- Human failure event is represented by a functional event in the event tree: this means that human failure event is modelled as an event with its description and its failure probability and it is linked to a functional event (i.e. event tree heading) within the respective event tree according to the analysed scenarios (i.e. accident sequences) of the event tree.
- Human failure event is represented by a basic event in the fault tree: this means that human failure event is modelled as a basic event with its description and its failure probability and it is part of the respective fault tree. In general, basic event is the smallest entity of the fault tree it represents component or equipment failure or human failure.

Actually, the features of the PSA computer code, that we use, allow also exchange events, which are another way of using the human error probabilities in the PSA. Exchange event allows exchange of one basic event, which is applicable in certain conditions, with another basic event, which is applicable in different conditions. But, the use of exchange events can be replaced by adding additional fault trees with changed basic events, so the use of exchange events is not treated as unique feature of the method.

2.2. Consideration of simulator experience into HRA

The training of plant operators on a full scope simulator is a complex process. One of the features of this process is that simulator personnel collect and analyse responses of operators on real scenarios and real events.

The consideration of simulator experience into HRA is as follows:

- Human failure events, which are part of PSA, are identified and their descriptions are provided to simulator personnel.
- Simulator personnel recognise and assess experience of operators with each particular human failure event in a way that the events, which are better or worse than the average, are identified. The events with average success of response of operators are marked with N. The events, for which more difficulties in success of response of operators than average are identified, are marked with N+. The events, for which less difficulties in success of response of operators than average are identified, are marked with N−. Such expert opinion of simulator personnel is performed separately for diagnosis phase of the event and separately for action phase of the event.
- Human reliability assessment is modified as follows. The human error probabilities of human failure events marked with N+ (either diagnosis phase or action phase or both) increase their probability for 10%. The human error probabilities of human failure events marked with N− (either diagnosis phase or action phase or both) reduce their probability for 10%. If both: N+ and N− exist for the same human failure event: one for diagnosis phase and the other for action phase, HEP is not changed.

2.3. Consideration of HRA for simulator activities

The ranking of importance factors of human failure events is one of inputs for selection of plant conditions that are the subject of the simulator training. If the schedule of simulator training does not include scenarios, which include the most important human failure events as determined in PSA, those scenarios are added to the schedule of simulator activities.

Consideration of HRA for simulator activities combined with a consideration of simulator experience into HRA represents an iterative procedure for improvement of human reliability.

With more training of identified human failure events, the operator experience increases and more human error probabilities are reduced due to operator experience. More human failure events with reduced human error probability means better average success of operators and risk reduction. Better average success of operators gives new lists of importance factors and thus identifies the most

important human failure events. With more training of identified human failure events, the operator experience increases and the next iteration continues.

3. Example model

The PSA model of a nuclear power plant is used for quantification. The characteristics of the model show that it is a large and detailed model, which includes: 4748 gates, 1810 basic events, 16 initiating events and main event trees, 738 fault trees, which include 125 human failure fault trees, 57 parameters (failure rate), 418 parameters (probability), which include 55 parameters connected with human error probability (those 55 parameters are obtained from 18 different basic human error probability parameters, which are expanded to 55 parameters considering different performance shaping factors for basic human error probability parameters), 18 groups for parameters of human errors, 117 groups for human error basic events.

4. Application of the method on an example event

Example event represents manual actuation of auxiliary feedwater in case of transients (MAAFT). The identifier for this event in Fig. 4, where the results of human failure events are compared, is HFE_028.

4.1. Context description

In the case of transients in a nuclear power plant, one of the means to cool the reactor is through the functioning of the auxiliary feedwater system, which is automatically put into operation. The system is made of two motor driven pumps and one turbine driven pump and the operation of one out of three pumps is enough to maintain the auxiliary feedwater flow, which keeps the plant in a safe state. If the pumps would not start automatically, operators should intervene.

4.2. Event description

The operators need to recognize that the pumps have not been automatically started. The operators need to start the pumps. The detailed procedures for all operator actions exist and are in use by the operators. Success criteria defined based on the safety analyses require operation of one of three pumps to maintain the flow and require that the pumps are started in 30 min.

4.3. Task analysis identifies two tasks

1. Recognize that pumps are not running (diagnosis phase: omission of diagnosis is assumed possible, commission is assumed possible); 2. Start pumps (action phase: omission is assumed possible, commission is assumed possible).

4.4. Evaluation

The experience of operators with plant simulator shows that the actual time for performing the event is 1–10 min. So, additional time for performing the event is 20–29 min (i.e. success criteria time minus actual time for performing the event), which gives enough time for possible recovery action. Low stress is assumed, very good labelling of controls is observed, diagnosis and action are assumed as very simple, which gives performance shaping factor 0.1 for commission errors. Table 1 shows relation to database and evaluation of the event. The left column shows the description of specific task within human failure event. The middle column shows human error probability of the respective task as defined in the database. The right column shows short name of respected parameter, which is used in quantifications and in figures (e.g. Fig. 5). Quantification of human error probability for complete example event (HEP_{HFE_028}) shows human error probability as 2.31E-4 (data from Table 1 is considered):

$$\begin{aligned} HEP_{HFE\text{-}028} &= (\text{“PAR\_14”} + \text{“PAR\_56”}) \cdot \text{“PAR\_58”} \\ &\quad + (\text{“PAR\_14”} + \text{“PAR\_21”}) \cdot \text{“PAR\_58”} \\ &= 2.31\text{E-}4. \end{aligned}$$

4.5. Dependency

As the pump status indicators are very close together, diagnosis of one or diagnosis of more pumps not running is treated as one task. As the start of pumps is made closely one after another, as controls are similar, as diagnosis is nearly the same, the complete dependency is assumed for tasks of starting the pumps. As only one human failure event is investigated in this example, its dependency with other human failure events is not mentioned here.

Reduction of calculated HEP is possible due to assessed simulator experience with this event, which is better than the average (i.e. reduction of 10% can be allowed for this HEP, which is marked with N−).

Table 1
A part of human reliability data base related to example event

Human error short description	HEP	Parameter ID.
Error of omission: omission, if procedure is available	1.30E-03	PAR_14
Error of commission: select wrong control	1.30E-04	PAR_21
Error of commission: observing wrong indication on the indicator lamps	1.20E-04	PAR_56
Error of recovery: engineering judgment: control room checking/recovery	8.10E-02	PAR_58

5. Importance of human contribution

Importance of human contribution can be assessed in two general ways:

- Assessment of importance of individual human failure events (this is widely known procedure and is regularly used for assessing and ranking of contributions of human failure events).
- Assessment of importance of items from human reliability database, which direct human error probabilities of human failure events (this procedure is not widely known and it is described in continuation).

Both ways can deal with individual events/items or with groups of events/items. Fig. 3 shows the relation between human error probabilities of the complete human failure events on the left part of the figure and human error probabilities of their specific tasks on the right part of the figure. Specific tasks of human failure events may be included in a number of human failure events.

Assessment of importance of items from human reliability database, which direct human error probabilities of human failure events is performed by replacing basic events, which model human failure events in the fault trees or which are linked to functional events in the event trees, with human error fault trees.

This means that basic event, which represents a human failure event within the fault tree, is replaced with its respective sub-fault tree, i.e. human error fault tree.

Similarly, it is with basic event that is linked to a functional event in the event tree. Instead the link to a human failure event, which represents a functional event in the event tree, the link to its respective sub-fault tree (i.e. human error fault tree) is made.

Such representation of human failure event results in more detailed information about HRA to be inserted into the PSA. In addition to parameters of human error probabilities of human failure events, also the parameters of human error probabilities of diagnosis phases and parameters of human error probabilities of sub-tasks of specific actions are inserted into the fault trees and thus to the PSA.

More detailed models allow more options in the evaluation of importance factors: e.g. fractional contribution (FC), e.g. risk increase factor (RIF) and e.g. risk decrease factor (RDF). Importance factors can be evaluated for specified basic events, for specified groups of basic events, for specified reliability parameters and for groups of reliability parameters.

The list of equipment with larger fractional contribution identifies equipment, which contributes largely to the risk of the system.

$$\mathrm{FC}_i = \frac{Q_s(Q_i) - Q_s(Q_i = 0)}{Q_s(Q_i)} \tag{1}$$

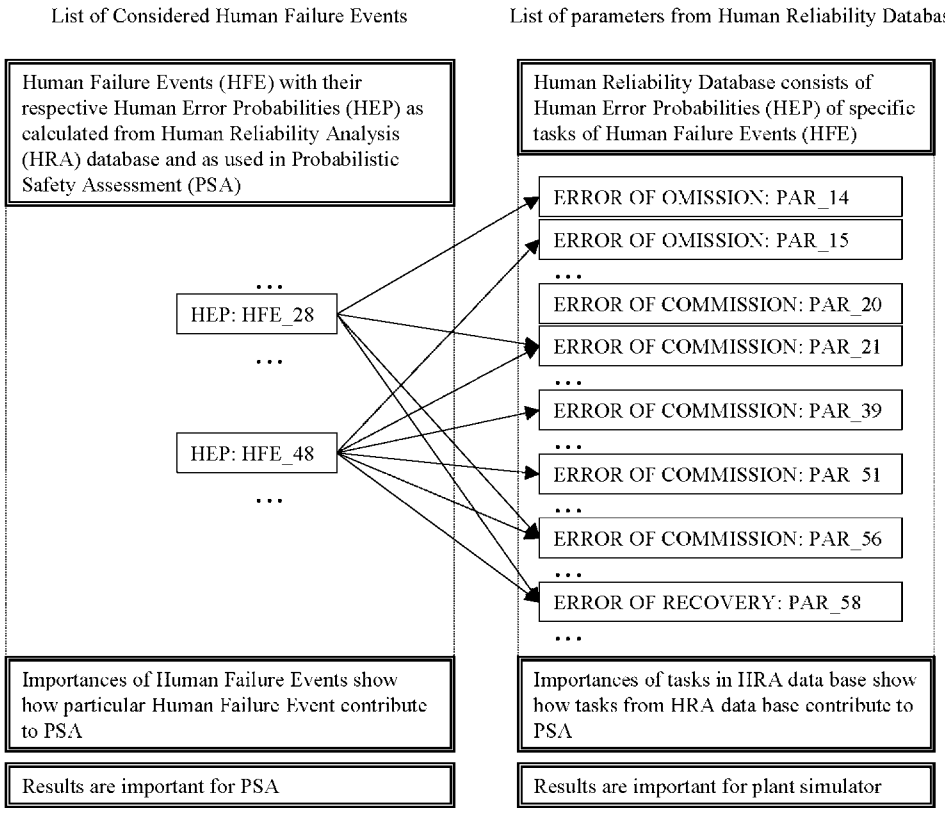

Fig. 3. Representation of relation between HEPs of HFEs and human reliability database items.

where FC_i is the fractional contribution of component i (or equipment i or human failure event i), Q_s the system unavailability, and Q_i is the unavailability of component i (or equipment i or human failure event i).

The list of equipment with larger risk increase factor identifies equipment, which is worthy candidate for monitoring and maintenance, in order that the risk is not increased.

$$RIF_i = \frac{Q_s(Q_i = 1)}{Q_s(Q_i)}. \quad (2)$$

where RIF_i is the risk increase factor of component i (or equipment i or human failure event i).

The list of equipment with larger risk decrease factor identifies equipment, which is worthy candidate for improvement, in order that the risk is decreased.

$$RDFi = \frac{Qs(Qi)}{Qs(Qi = 0)}. \quad (3)$$

where RDF_i is the risk decrease factor of component i (or equipment i or human failure event i).

5.1. Results

Importance results of the example model are presented on the following figures. Fig. 4 shows importance factors (FV, RIF and RDF) for individual human failure events. For each human failure event all its subsequent human reliability parameters are grouped and evaluated as one item. The most important human failure events (21 events) are extracted from the complete list of events (72 events).

According to the importance criteria for the risk important components: $RDF_i > 1{,}05$, $RIF_i > 2$, there are two human failure events with $RDF_i > 1.05$ and 12 human failure events with $RIF_i > 2$. No event exists, which would not be identified by RIF or RDF lists and would appear at fractional contribution of more than 1% to the overall result, so fractional contribution does not reveal any additional human failure events.

Events HFE_048 (i.e. operator is aligning high pressure recirculation) and HFE_028 (example event described in Section 4) are candidates for HEP reduction, as the HEP reduction would decrease risk. For both events an independent verification or other means may be added to the procedure, which may result in justification of lower human error probability of recovery. For the event HFE_048 many subtasks are modelled, each is considered little conservatively as omission of steps represents a generic HEP from human reliability database. And, no favourable performance shaping factors are considered for omissions, although the procedure steps exists and are well written, operators are well trained and experienced and low stress is assessed. The modelling should be reviewed in details and the links of tasks to appropriate human error probabilities should be checked.

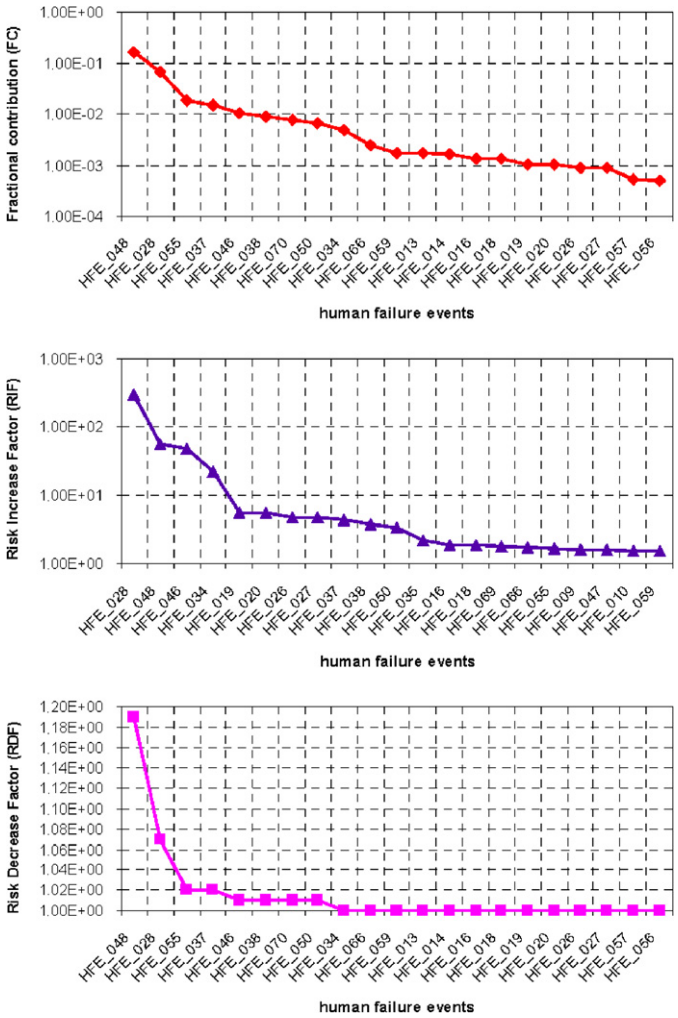

Fig. 4. Importance factors for individual human failure events (example PSA model).

12 human failure events (including example event) with $RIF_i > 2$ are candidates for simulator training (Fig. 4), because their occurrence may significantly increase the risk.

5.2. Results of example event

Results show that risk contribution of the example event (manual actuation of auxiliary feedwater in case of transients: HFE_028) to the plant risk is significant (Fig. 4). The event is contributing to the core damage frequency for approximately 10%, which ranks it to the 2nd place among the most important risk contributors. The event is the most important among the events ranked by RIF and has a high RIF, which means the simulator training on this event should be performed. The event is 2nd among the events ranked by RDF, but has a low RDF, so improvement of procedures is possible but it may not significantly reduce the risk connected with the event.

5.3. Results connected with importance of parameters

Fig. 5 shows importance factors for parameters from human reliability database (part of database is in Table 1). Each parameter contributes to one or more human failure events depending on the nature of the parameter. It can be more universal, which means that it contributes to several (or even more tenths) human failure events. Or, it can be more specific, which means that it may contribute to few or to only one human failure event.

According to the importance criteria for the risk important components: $RDF_i > 1.05$, $RIF_i > 2$, there are three parameters with $RDF_i > 1.05$ and 8 parameters with $RIF_i > 2$. Those three parameters with $RDF_i > 1.05$ (PAR_58, PAR_15, PAR_14) contribute to many human failure events: PAR_58 contributes to 50 HFE, PAR_15 contributes to 73 HFE and PAR_14 contributes to 40 HFE.

Those identified parameters are candidates for human reliability database improvement. Namely, from history of simulator training it is needed to specify more specific human tasks for the human reliability database and increase their number from only 17 to more. At the same time the human error probabilities of those added tasks should be estimated and the human reliability database is updated with plant specific information.

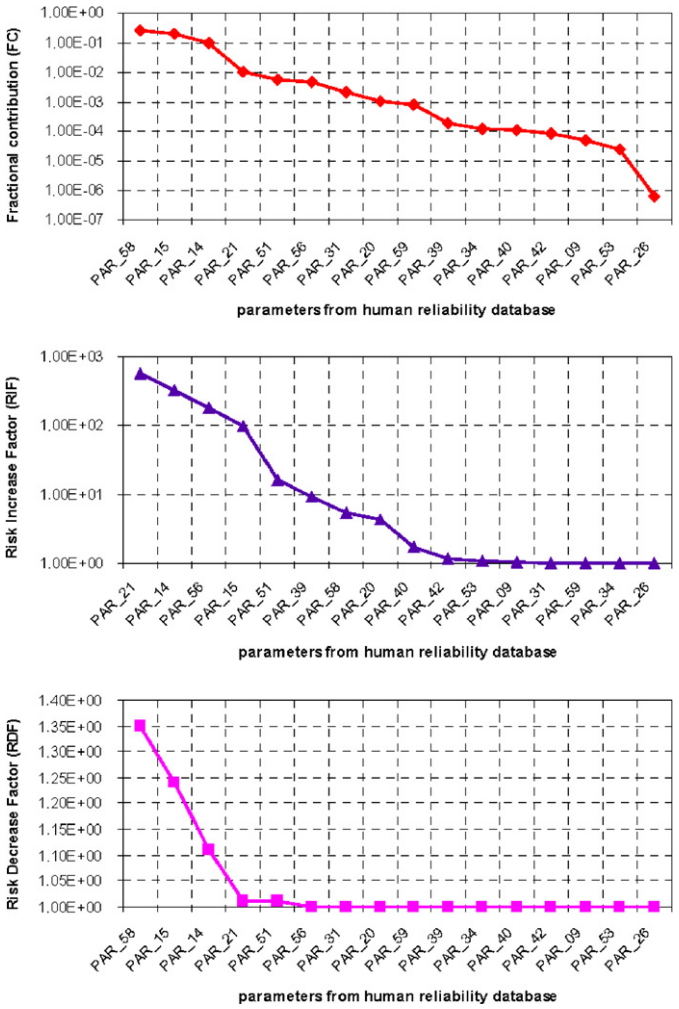

Fig. 5. Importance factors for HRA parameters (example PSA model).

5.4. Implications of the results

The analysis of importance of parameters from human reliability database showed that only 13 parameters from human reliability database, which consists of 66 generic parameters, are actually modeled in the HRA. Eight of those 13 parameters are identified as important parameters. As each of those parameters relates to a relatively large number of human failure events, which may differ significantly one from another by the nature of the tasks, it is recommended to make new specific parameters, which will replace the generic ones. A larger number of more specific parameters in the human reliability database will allow evaluation of the human failure events and their respective tasks in more detailed manner using more convenient and specific human error probabilities obtained from the experience of simulator training.

The replacement of human failure events, which are modeled in PSA with their respective human error probability (one HFE is represented with one basic event with its respective human error probability), with human error fault trees, which contain several basic events with their respective parameters from human reliability database, causes the difference in results due to truncation (Čepin, 2005b). Truncation is a term, which means that contribution of contributors to risk is neglected, if the contribution to risk is lower than the specified limit (i.e. truncation limit). This replacement means that more events with lower probabilities are consisting the model. At the same truncation limit, larger portion of the risk results may be cut off. This may cause more difficulties for direct comparison of the effects of replacement. A selection of lower truncation limit reduces the difference.

6. Conclusions

The IJS-HRA is a method for evaluation of human failure events in sense to determine the reliability of the respective human actions. This method:

- integrates features of several methods known from the field of HRA,
- includes some specific features:
  - inclusion of parameters from plant specific full scope simulator: timing of human actions under investigation in the real scenarios,
  - experience of simulator training for adjustment of generic human error probabilities in the first phase (this is done) and parameters from simulator training for determining plant specific human error probabilities in the second phase (this is planned) and
- includes the newest recommendations and good practice in the field.

The method is applicable for HRA of complex facilities including nuclear power plants.

The method can be used as an on-line tool for sensitivity analysis within PSA with a wide number of options for evaluation of the model and its physical and conceptual parts. These evaluations from different points of view gives new knowledge about the observed plant, which may be used for the improvement of HRA and thus plant safety.

The results of importance analysis show that only few human failure events dominate in the HRA. The results show that only few parameters from human reliability database contribute significantly to the risk. Identification of dominating human failure events and identification of the significant parameters are a valuable input for determining the priorities of simulator training.

Future work includes the more detailed analysis of simulator experience, which will result in more detailed and plant specific human reliability database.

Acknowledgements

The Slovenian Research Agency supported this research (partly research program P2-0026, partly research projects J2-6556 and V2-0376 supported together with Slovenian Nuclear Safety Administration).

References

ASME RA-S-2002. (2002). Standard for probabilistic risk assessment for nuclear power plant applications. The American Society of Mechanical Engineers.

Čepin, M. (2002). Optimization of safety equipment outages improves safety. *Reliability Engineering and System Safety*, *77*, 71–80.

Čepin, M. (2005a). Human reliability analysis—Methods and applications, problems and solutions. Internal Report, IJS.

Čepin, M. (2005b). Analysis of truncation limit in probabilistic safety assessment. *Reliability Engineering and System Safety*, *87*(3), 395–403.

Čepin, M. & He, X. (2006). Development of a method for consideration of dependence between human failure events. ESREL2006.

Čepin, M., & Mavko, B. (1997). Probabilistic safety assessment improves surveillance requirements in technical specifications. *Reliability Engineering and Systems Safety*, *56*, 69–77.

Čepin, M., & Mavko, B. (2002). A dynamic fault tree. *Reliability Engineering and System Safety*, *75*(1), 83–91.

Forester, J., Bley, D., Cooper, S., Lois, E., Siu, N., Kolaczkowski, A., et al. (2004). Expert elicitation approach for performing ATHEANA quantification. *Reliability Engineering & System Safety*, *83*, 207–220.

Grobbelaar, J. F., Julius, J. A. & Rahn, F. (2005). Analysis of de-pendent human failure events Using the EPRI HRA calculator. In PSA05. Proceedings.

Harris, D., Stanton, N. A., Marshall, A., Young, M. S., Demagalski, J., & Salmon, P. (2005). Using SHERPA to predict design-induced error on the flight deck. *Aerospace Science and Technology*, *9*, 525–532.

Hollnagel, E. (1988). *Cognitive reliability and error analysis method, CREAM*. Elsevier Science Ltd.

Holy, J. (2004). Some insights from recent applications of HRA methods in PSA effort and plant operation feedback in Czech Republic. *Reliability Engineering & System Safety*, *83*(2), 169–177.

Kennedy, G. A. L., Siemieniuch, C. E., Sinclair, M. A., Kirwan, B. A., & Gibson, W. H. (2007). Proposal for a sustainable framework process for the generation, validation, and application of human reliability assessment within the engineering design lifecycle. *Reliability Engineering & System Safety*, *92*(6), 755–770.

Khan, F., Amyotte, P. R., & DiMattia, D. G. (2006). HEPI: A new tool for human error probability calculation for offshore operation. *Safety Science*, *44*(4), 313–334.

Mosleh, A., & Chang, Y. H. (2004). Model-based human reliability analysis: Prospects and requirements. *Reliability Engineering & System Safety*, *83*, 241–253.

NUREG-1624. (1999). Technical basis and implementation guidelines for a technique for human event analysis (ATHEANA). US NRC.

NUREG-1792. (2005). Good Practices for implementing human reliability analysis (HRA). US NRC.

NUREG/CR-1278. (1983). Handbook for human reliability analysis with emphasis on nuclear power plants application. US NRC.

NUREG/CR-4772. (1987). Accident sequence evaluation program: Human reliability analysis procedure. US NRC.

NUREG/CR-6883. (2005). The SPAR— human reliability analysis method. US NRC.

Reer, B., Dang, V. N., & Hirschberg, S. (2004). The CESA method and its applications in a plant-specific pilot study on errors of commission. *Reliability Engineering & System Safety*, *83*, 187–205.

SHARP. (1984). Systematic human action reliability procedure. EPRI. NP-3583.

Spurgin, A. (1990). Another view of the state of human reliability analysis (HRA). *Reliability Engineering & System Safety*, *29*(3), 365–370.

M. Čepin and A. Volkanovski

Consideration of ageing within probabilistic safety assessment models and results

Ageing is a process, where the properties of systems and processes may degrade through the time and age. The objective of the paper is to analyze the possibilities of introduction of ageing directly into the probabilistic safety assessment. Theoretical models of ageing and examples of their application are investigated, which show, how the current models can be upgraded in sense to directly include the effects of ageing into the models of probabilistic safety assessment. This paper shows that consideration of ageing is theoretically a straightforward issue, which can be dealt with in several ways, which are demonstrated in the paper. The most important problem is the lack of data about the effects of ageing, which would suit to the detailed models of ageing. The results, which are obtained, do not show significantly different results compared to the initial models without direct consideration of ageing. The majority of risk measures change slightly or notably, but no major break through has been found. Contribution of ageing may be smaller then contribution of changes due to other parameters.

Berücksichtigung der Alterung in Modellen und Ergebnissen der probabilistischen Sicherheitsanalyse. Alterung ist ein Prozess, bei dem die Eigenschaften der Systeme und Prozesse sich im Laufe der Zeit verschlechtern. Ziel dieses Papiers ist die Analyse der Möglichkeiten, Alterung direkt in probabilistischen Sicherheitsanalysen (PSA) zu berücksichtigen. Theoretische Alterungsmodelle und Beispiele ihrer Anwendung werden dahingehend untersucht, wie die gegenwärtigen Modelle erweitert werden können, um direkt die Alterungseffekte in die PSA-Modelle einzufügen. Das Papier zeigt, dass die Betrachtung der Alterung auf verschiedene Weise behandelt werden kann, wie hier näher ausgeführt wird. Das größte Problem ist aber die ungenügende Datenbasis über Alterungseffekte, die sich für eine detaillierte Modellierung der Alterung eignet Die erzielten Ergebnisse zeigen keine signifikant unterschiedlichen Ergebnisse im Vergleich mit dem ursprünglichen Modell ohne direkte Betrachtung der Alterung. Die Mehrzahl der Risikomaße ändern sich wenig oder auch deutlich, aber ein großer Durchbruch wurde nicht gefunden. Eventuell sind die Beiträge aufgrund der Alterung kleiner als die Beiträge aufgrund von Änderungen anderer Parameter.

1 Introduction

Ageing is a process, where the properties of systems and processes may degrade through the time and age. A large number of ongoing activities connected with evaluation of ageing can be generally divided to those, which study the properties of materials and their degradation [1, 2], to those, which investigate the mathematical models of ageing [3–5], to those, which assess the degradation and ageing effects of actual equipment [6–9] and to those, which include a part or most of these.

1.1 State-of-the-art

Several studies include the effects of the ageing of the specific nuclear power plant (NPP) components, systems and structures [10–14] including the reactor pressure vessel and primary coolant system [15, 16]. The application of the two parametric Weibull distribution and Bayesian models for ageing modelling was proposed [17, 18] including the statistical approach for estimation of age of the degraded system [19]. The implication of maintenance, test strategies and working conditions on ageing of the components was analysed [20, 21] including the optimization of maintenance activities accounting the ageing of the components [22, 23]. The approaches for managing the effects of ageing in the NPP and inclusion of passive components ageing into probabilistic safety assessment (PSA) were proposed [24, 25]. Activities connected with probabilistic safety assessment of NPP include: collected and evaluated data for age-related degradation of US NPP [26], modelling ageing of passive systems, structures and components (SSC) by incorporating a flow accelerated corrosion model into PSA [27], a procedure for transformation of PSA to age-depended evaluation [28], a quantification of the ageing induced risk using PSA and component ageing models [29, 30], a derivation of the linear ageing model and extension to nonlinear and depended ageing phenomena [31], ageing-related failure analysis of the nuclear power plant operational data [32, 33] and the impact of the component ageing on the selected support systems reliability and NPP safety [34].

The application of the methods is more theoretical than practical due to lack of real data for the support of the parameters in mathematical formulations.

1.2 Objectives

Probabilistic safety assessment is a standardized tool for assessment of safety of nuclear power plants [35–38]. The guidelines are developed and the risk criteria are established [39–41]. Existence of guidelines and criteria enable that the results of probabilistic safety assessment are more and more included in the risk-informed decision-making, which is proven with an increasing number of its applications [42–44].

The issues connected with degradation and ageing are currently included in the models through the constant failure rate approach.

The first objective of the paper is to investigate, if the ageing effects can be considered in probabilistic safety assessment in more details, as it is currently done. The second ob-

jective is to examine the options for direct and separate inclusion of ageing in probabilistic safety assessment to compare the effectiveness of the models and the applicability of the results.

The work is focused to existing nuclear power plants with light water reactors.

2 Methods

Many mathematical methods for consideration of ageing exist. Usually, they include mathematical formulations of parameters, for which it is very difficult to get appropriate data, which could make the methods widely applicable for practical purposes.

Selected methods for consideration of ageing are presented in the following sections, which seem the most suitable for their use for upgrading the existing probabilistic safety assessment models.

2.1 Basic methods for modelling of ageing

The linear method, the exponential method and the Weibull method are presented [28].

2.1.1 Linear method

This method represents the failure rate of equipment with a function, where the failure rate is changed with age of equipment from constant failure rate before the threshold age to linear increasing failure rate after the threshold age [28]. Threshold can be incorporated in the mathematical formulation to represent the beginning of ageing at some nonzero age. The basic mathematical formulation of the method is presented in the equation below.

$$\lambda(w) = \lambda \qquad \forall \quad w \le w_0$$
$$\lambda(w) = \lambda_0 + \alpha(w - w_0) \qquad \forall \quad w > w_0 \tag{1}$$

λ_0 … initial constant failure rate
α … linear ageing rate
w_0 … threshold age after which the failure rate increases

2.1.2 Exponential method

This method represents the failure rate of equipment with a function, where the failure rate is changed with age of equipment from constant failure rate before the threshold age to exponentially increasing failure rate after the threshold age [28]. The basic mathematical formulation of the method is presented in the equation below.

$$\lambda(w) = \lambda_0 \qquad \forall \quad w \le w_0$$
$$\lambda(w) = \lambda_0 \cdot \exp(c(w - w_0)) \qquad \forall \quad w > w_0 \tag{2}$$

λ_0 … initial constant failure rate
c … exponential scale parameter
w_0 … threshold age after which the failure rate increases

2.1.3 Weibull method

This method represents the failure rate of equipment with a function, where the failure rate is changed with age of equipment from constant failure rate before the threshold age to the Weibull increasing failure rate after the threshold age [28]. The basic mathematical formulation of the method is presented in the equation below.

$$\lambda(w) = \lambda_0 \qquad \forall \quad w \le w_0$$
$$\lambda(w) = \lambda_0 \left[\frac{w}{w_0}\right]^b \qquad \forall \quad w > w_0 \tag{3}$$

λ_0 … initial constant failure rate
b … Weibull shape parameter
w_0 … threshold age after which the failure rate increases

2.2 Basic methods for consideration of ageing in probabilistic safety assessment

Two main options exist when the basic methods for consideration of ageing in probabilistic safety assessment are considered.

The first option, which is known as stepwise constant failure rates, includes modification of probabilistic safety assessment models in sense that the ageing contribution is added to the initial models, which consequently causes also the modified results, when evaluation is performed [28]. The failure rates are determined as constant in determined time intervals, but as the time intervals go on, the failure rates increase, if the ageing contribution to the failure rates increase [33].

The second option includes modification of the resulted minimal cut sets in sense that the ageing contribution is added to the resulted minimal cut sets [28, 29].

2.2.1 Method of stepwise constant failure rates

The standpoint for the development of this method lays in a fact that a detailed probabilistic safety assessment of a nuclear power plant exist, which does not directly include consideration of ageing in its probabilistic models. In this sense, it seemed that the extension of the existing probabilistic safety assessment models with addition of ageing as an independent contribution would be the easiest solution. The deficiency of such approach would be the fact that contribution of ageing may not be independent from existing contribution. Fig. 1 shows the difference in modelling, if ageing is considered as independent contribution or not.

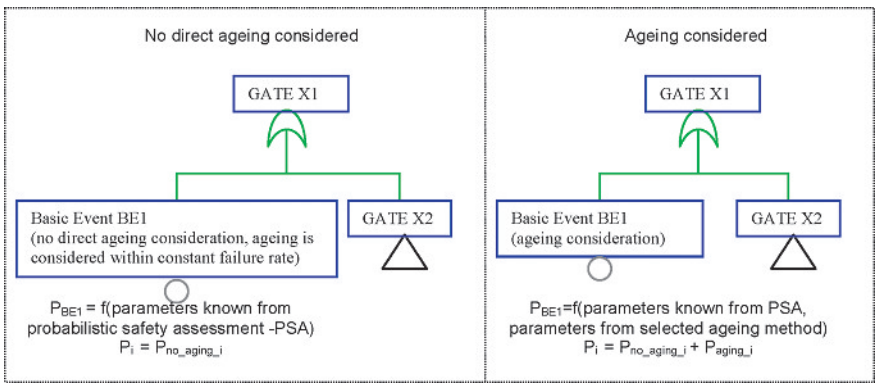

Fig. 1. Schematic modelling for consideration of ageing

Stepwise constant failure rate method assumes the constant failure rates or constant failure probabilities of equipment in the determined time intervals

$\{t_i, t_{i+1}\}$, and hence this failure rates or failure probabilities are determined as their average through the time of the time interval. The failure rates or failure probabilities change through the selected time intervals according to the selected method for evaluation of failure rates or failure probabilities due to ageing.

At each selected time interval the average failure rates or failure probabilities are calculated for the equipment under investigation and the evaluation of the probabilistic safety assessment is performed. An advantage of this method is that it can be used in standard probabilistic safety assessment by standard tools for performing probabilistic safety assessment. Figure 2 shows the basic principle of method. Update of probabilistic safety assessment model for consideration of ageing is done in two directions:

- addition of components to the models and
- changes made to existing models, changes of the probabilistic data.

The focus of the activities can be placed to the most important components or to all components, alternatively. The risk criteria for determining the most important equipment can follow the suggested guidelines [40]. The risk criteria for selection of equipment, for which a consideration about the neighbouring passive components is performed, are presented in Table 1. In the current probabilistic safety assessment it is possible that:

- the failures of certain structures or passive components or other equipment are not considered, because their failure probability is negligibly low, or
- the failures of certain passive components are indirectly considered within the existing models and data connected with the corresponding active components.

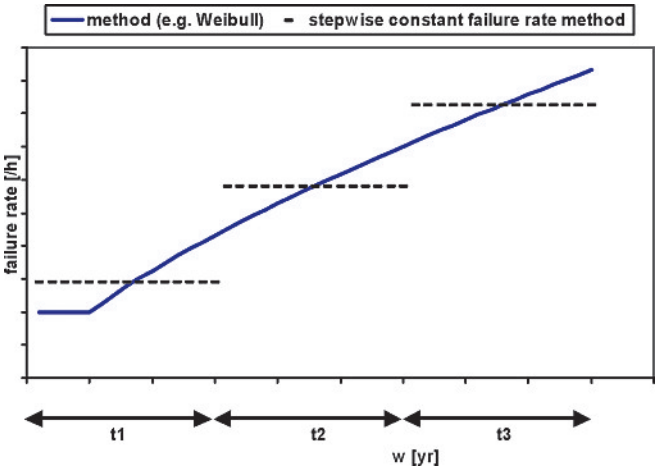

Fig. 2. Method of stepwise constant failure rates

Table 1. Risk criteria for determining important equipment

Risk importance measures	Criteria
RAW – Risk Achievement Worth	>2
RRW – Risk Reduction Worth system level component level	 >1.05 >1.005
FV-Fussell – Vesely Importance system level component level	 >0.05 >0.005

In other words, probabilistic safety assessment models generally does not directly include passive components, which may be susceptible to the ageing issues more than active and tested components. Therefore the models may be updated with inclusion of the passive components.

The method for selection of passive components may consider the importance results of existing probabilistic safety assessment. The equipment with higher risk importance factors may be investigated in sense if the consideration of additional passive components improves the model.

Frequencies of initiating events such as large, medium or small loss of coolant accident, steam generator turbine rupture and steam line break depends on the history of experience with the pipes. The frequencies of failures of newer pipelines may be lower than the frequencies of older ones. Method of stepwise constant initiating event frequency can be used considering linear increase of initiating event frequency.

2.2.2 Method of prioritization of ageing from results of probabilistic safety assessment

The method of assessment of ageing from results of probabilistic safety assessment is presented in reference [28], while the data are analysed also in reference [33]. The mathematical formulation bases on the database about components ageing rates: TIRGALEX database [33], which is presented in Table 2. The mathematical formulation of the method is the following. The change of the failure rate $\Delta\lambda_i$ of component i due to the ageing is given with expression:

$$\Delta\lambda_i = \lambda_i - \lambda_{i0} \tag{4}$$

λ_{i0} … failure rate of equipment *i* (no ageing considered)
λ_i … failure rate of equipment *i* with ageing considered
$\Delta\lambda_i$ … the increase of failure rate of equipment *i* due to ageing

Table 2. TIRGALEX data base for ageing rates of equipment [per hour per year]

Component	Ageing rate
AC bus	1.0E-09/h/y
Air operated valve	4.0E-07/h/y
Battery	3.0E-07/h/y
Check valve	4.0E-09/h/y
Circuit breaker	2.0E-08/h/y
DC bus	1.0E-09/h/y
Diesel generator	3.6E-06/h/y
Motor driven pump	2.0E-07/h/y
Motor operated valve	3.6E-06/h/y
Relay	3.0E-07/h/y
Safety/relief valve	7.0E-07/h/y
Transformer	2.0E-09/h/y
Turbine driven pump	3.0E-06/h/y
Solenoid operated valve	6.7E-07/h/y

The change of the component unavailability Δq_i with consideration of the ageing is given as:

$$\Delta q_i = q_i - q_{i0} \tag{5}$$

q_{i0} … unavailability of equipment i (no ageing considered)
q_i … unavailability of equipment i with ageing considered
Δq_i … the increase of unavailability of equipment i due to ageing

For a linear ageing failure rate, the average unavailability increase [29] due to the ageing for tested equipment is:

$$\Delta q_i = \frac{1}{4} a_i (L_i - T_i) T_i + \frac{1}{6} a_i T_i^2 \tag{6}$$

a_i … ageing rate of equipment i
T_i … test interval of equipment i
L_i … replacement (overhaul) interval of equipment i

The overhaul or replacement interval L is the interval at which the component is replaced with a new one and the age of the component is restored effectively to a value of zero. The surveillance interval T is interval at which the component surveillance is performed, in order to assure operational status with minimal repair being performed. The component is basically in the same condition after the test as before the test. The replacement interval of equipment $i(L_i)$ is obtained [29] as:

$$L_i = \frac{1}{\lambda_{i0}} \tag{7}$$

If there is no surveillance tests expected on the component between replacements, then T is set equal to L. In the case when the mean time to failure of the component is larger than the facility lifetime and there is no surveillance test expected the formula for the unavailability increase [29] with is:

$$\Delta q_i = \frac{1}{2} a_i t_0^2 \tag{8}$$

t_o … facility lifetime

To calculate the core damage frequency change ΔCDF as a function of the component and structure ageing changes Δq_i, a Taylor expansion approach was utilized to express ΔCDF as a function of the Δq_i:

$$\Delta CDF = \sum_i S_i \Delta q_i + \sum_{i>j} S_{ij} \Delta q_i \Delta q_j + \sum_{i>j>k} S_{ijk} \Delta q_i \Delta q_j \Delta q_k + \ldots + S_{12..n} \Delta q_1 \Delta q_2 \ldots \Delta q_n \tag{9}$$

ΔCDF … change in core damage frequency
S_i … standard Taylor expansion coefficients, importance of equipment i
Δq_i … change of the component/system unavailability

The Taylor expansion coefficients are obtained as multi order derivates of the CDF and are termed as a core damage frequency sensitivity coefficients or core damage frequency importance coefficients. If only the first order Taylor coefficients are accounted, the upper equation can be simplified as:

$$\Delta CDF = \sum_i S_i \Delta q_i \tag{10}$$

The importance coefficients S_i of equipment i is obtained from the Fussel-Vesely importance measure for specific component.

$$FV_i = \frac{CDF - CDF\ (q_i = 0)}{CDF} \tag{11}$$

$$S_i = \frac{FV_i * CDF}{q_i} = \frac{CDF - CDF\ (q_i = 0)}{q_i} \tag{12}$$

CDF … core damage frequency
$CDF\ (q_i = 0)$ … core damage frequency when unavailability of equipment i is set to zero
FV_i … Fussel-Vesely importance measures for equipment i
q_i … unavailability of equipment i

It is important to know that the relative error for such expression can be very large, if the values CDF and $CDF\ (q_i = 0)$ are close to each other [37].

Table 3. Data for parameters of containment spray system considering ageing contribution

Identification	b	w_0
BE-PAR-01	1	5y
BE-PAR-02 (CCF)	1,3	7y
BE-PAR-03	3	4y
BE-PAR-04	1	6y
BE-PAR-05	4	5y
BE-PAR-06	1,3	7y
BE-PAR-07 (T&M)	1	2y
BE-PAR-08	0,7	4y
BE-PAR-09	4	5y
BE-PAR-10	0,2	5y
BE-PAR-11	17	10y
w_0 … threshold age *b … Weibull shape parameter*		

3 Analysis and results of selected examples

3.1 Ageing consideration for existing containment spray system

The containment spray system is selected as an example. Table 3 shows data for 11 parameters of the containment spray system considering ageing contribution. Parameters of ageing connected with of common cause failures are the same as the parameters of ageing connected with the respective basic events modelling respective primary failures. Figure 3 shows calculated basic event unavailabilities due to ageing, which

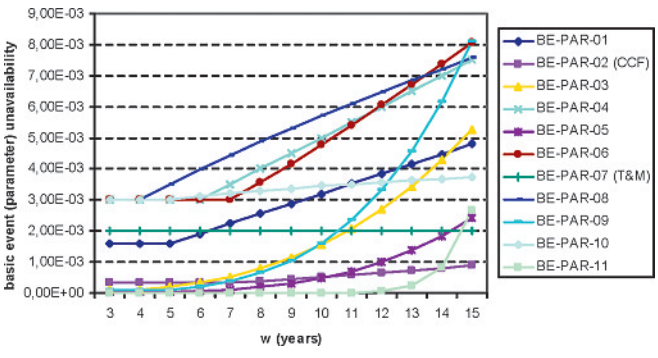

Fig. 3. Basic event unavailability due to ageing

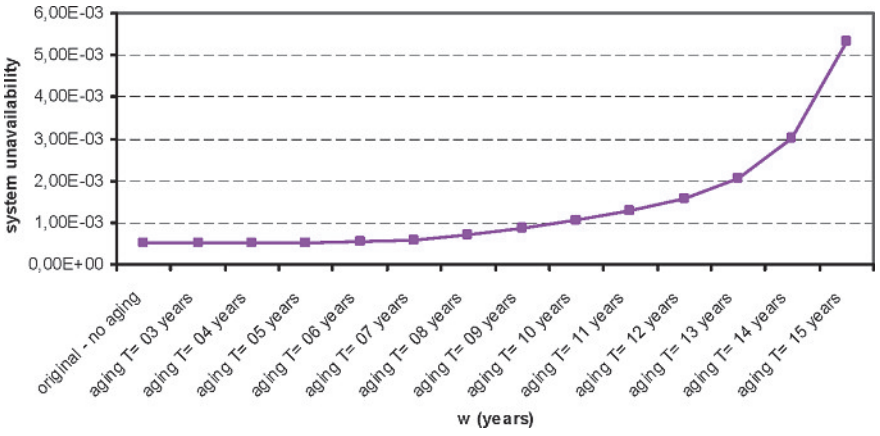

Fig. 4. System unavailability due to ageing

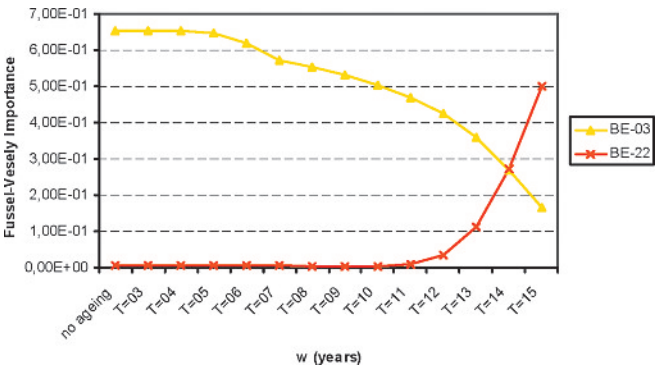

Fig. 5. Fussel-Vesely Importance due to ageing

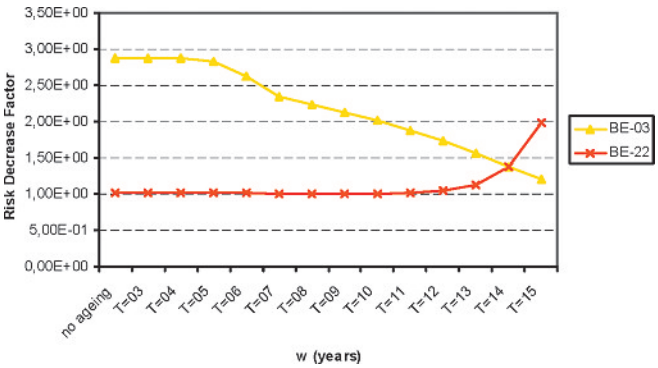

Fig. 6. Risk Decrease Factor due to ageing

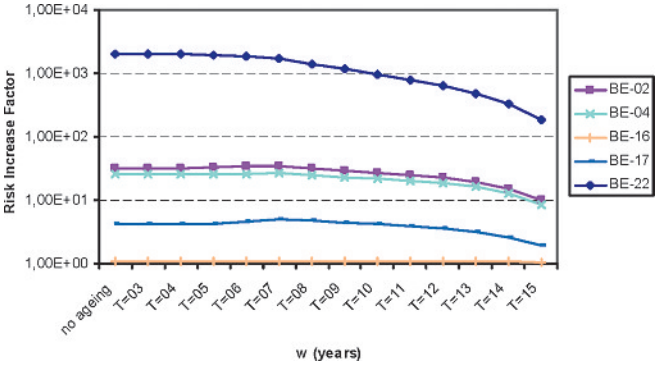

Fig. 7. Risk Increase Factor due to ageing

depend on timely independent unavailability and ageing parameters, such as Weibull parameter b and threshold age. Unavailability of basic events connected to test and maintenance is constant through the age. Figure 4 shows the system unavailability due to ageing, which is obtained through the fault tree evaluations specified for time intervals of 1 year. Results show the increase of system unavailability of one order of magnitude for the considered period of 15 years. Figure 5 shows Fussel-Vesely importance measure for the selected basic events of the fault tree representing selected components of the system. Results show that some equipment can be non-important, if no ageing is considered, and very important if ageing is considered and vice versa. Figure 6 shows the risk decrease factor due to ageing. Figure 7 shows the risk increase factor due to ageing. Results show that risk factors may considerably vary depending on ageing.

3.2 Ageing consideration for passive components in containment spray system

The fault tree of containment spray system has been changed. Basic events representing the piping failures were added to their respective places with small piping failure probability assessed based on piping length, number of elbows and number of welds ($Q_{\text{piping0}} = Q_{\text{piping0\_pipelenght}} + Q_{\text{piping0\_no\_elbow}} + Q_{\text{piping0\_no\_welds}} = 1\text{E-}6$). Factor of ageing is assessed as linear function $k_{\text{piping}}(w) = K_a{*}w$ and $K_a = 8{,}76\text{e-}6$/year is assumed and 15 years of operating time is considered.

The results show that system unavailability slightly changed from 5,059E-4 to 5,092E-4, which can be assumed as neglected. The risk measures connected with piping give no indication of piping importance, except of the risk increase factor ($RIF_{\text{piping}} = 26$), when ageing is 15 years. Experience shows that the most important issue for consideration of piping is that the models of piping are performed on train bases or on appropriate segments basis. If all piping of one system is simplified and considered as one component, the model is not suitable and as such not needed.

3.3 Ageing consideration in complete probabilistic safety assessment

Complete probabilistic safety assessment of a nuclear power plant is selected as another example. The probabilistic safety assessment model is a detailed model with thousandths of gates, thousandths of basic events, hundredths of fault trees and 16 event trees with 16 initiating events.

3.3.1 Adding passive components

Systems and subsystems, which models are changed with added basic events about piping failure probability are the following: auxiliary feedwater system motor driven pump 1, pump 2, turbine driven pump, chemical volume and control system, component cooling system train A, train B, instrument air train A, train B, residual heat removal train A, train B, safety injection to cold leg 1, cold leg 2, safety injection pump 1, pump 2, containment spray injection pump 1, pump 2, service water system train A and train B.

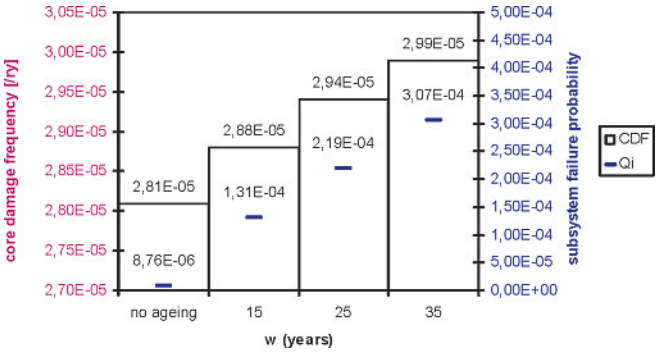

Fig. 8. Sensitivity of core damage frequency due to changes of the piping failure probabilities due to ageing

Added basic events about piping failure probability do not change the core damage frequency and do not impact significantly other probabilistic safety assessment results ($Q_{\text{piping\_i\_0}}$ = 1E-6).

If the ageing of piping is considered, the core damage frequency changes negligibly from 2,81E-5/ry to 2,88E-5/ry: $Q_{\text{piping\_i\_0}}$ = 1,31E-4 for the period between 10 and 20 years of plant operation; $k_{\text{piping}}(w) = K_a{*}w$ is assumed; K_a = 8,76e-6/year; 15 years of ageing is assumed as the average for the period between 10 and 20 years of plant operation. The risk increase factor of the parameter piping becomes significant (RIF_{piping} = 1,74E+4). Significant $\text{RIF}_{\text{piping}}$ means that the core damage frequency and thus risk may increase significantly with the increase of piping failure probability. Fig. 8 shows sensitivity of core damage frequency due to changes of the piping failure probabilities due to ageing.

3.3.2 Changing existing models – initiating events only

Initiating events frequencies were changed for two groups of initiating events. The first group includes initiating events: large loss of coolant accident, medium loss of coolant accident, small loss of coolant accident, steam line break and steam generator tube rupture. The second group includes initiating events: interfacing system loss of coolant accident, loss of essential service water, loss of component cooling water and loss of instrument air. For the initiating events from the first group, the initiating events frequency is changed according to linear method of consideration of ageing. For the initiating events from the second group, only the assessed part of the initiating event frequency due to piping is changed according to linear method of consideration of ageing. For the initiating events from the second group, this means that the impact of ageing is negligible, because a small increase of small part of the initiating event frequency may be lower than the round up.

The resulted core damage frequency increases with increasing initiating event frequencies depending on the percentage contribution of respective initiating events to the core damage frequency. Table 4 shows sensitivity of core damage frequency due to changes of the initiating events frequency due to ageing. Results show that the core damage frequency increases for less than 8 percents, because the contribution of selected basic events to the initial core damage frequency (without consideration of ageing) is approximately only 21 %.

3.3.3 Adding passive components and changing existing models

Both separate considerations from previous sections are joined together and the results are obtained. Results on Figure 9 show that core damage frequency changes up to 14 %. Results show that importance measures change more than

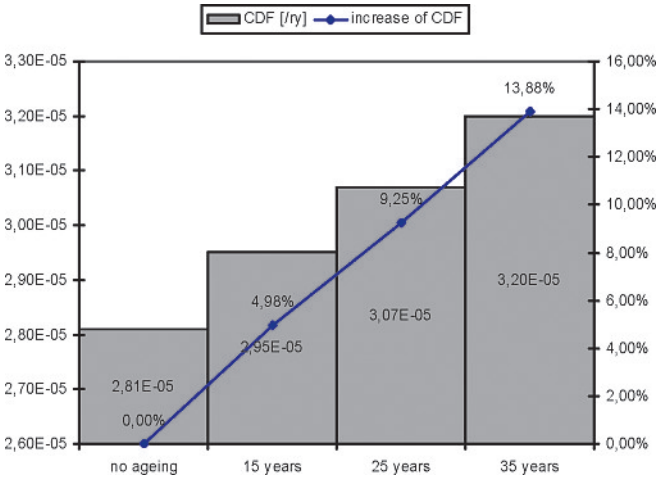

Fig. 9. Sensitivity of core damage frequency due to ageing

Table 4. Sensitivity of core damage frequency due to changes of the initiating events frequency due to ageing

	f_{IE0}	f_{IE}(15y)	f_{IE}(25y)	f_{IE}(35y)
Large LOCA	5,00E-06/ry	5,50E-06/ry	6,05E-06/ry	6,66E-06/ry
Medium LOCA	1,38E-03/ry	1,52E-03/ry	1,67E-03/ry	1,84E-03/ry
Small LOCA	2,70E-03/ry	2,97E-03/ry	3,27E-03/ry	3,59E-03/ry
SLB	1,30E-02/ry	1,43E-02/ry	1,57E-02/ry	1,73E-02/ry
SGTR	1,82E-03/ry	2,00E-03/ry	2,20E-03/ry	2,42E-03/ry
CDF	2,81E-05/ry	2,88E-05/ry	2,94E-05/ry	3,02E-05/ry
IE frequency increases for *K* i. e. for 10 % per ten years.				
LOCA … Loss of Coolant Accident; SLB … Steam Line Break SGTR … Steam Generator Tube Rupture; CDF … Core Damage Frequency				

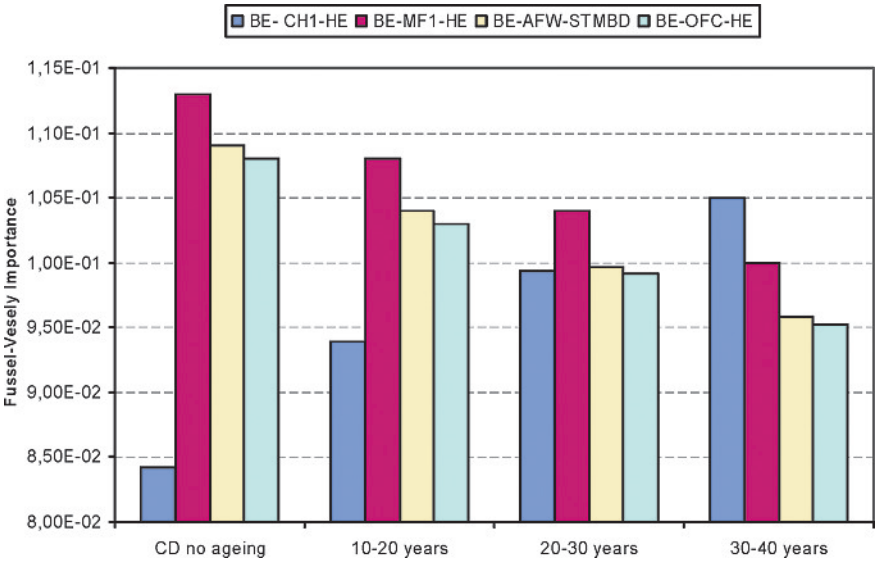

Fig. 10. Fussel-Vesely importance measure for selected basic events

core damage frequency (Fussel-Vesely importance measure may change for more than 30 %). Figure 10 shows Fussel-Vesely importance measure for selected four important components.

The contribution of ageing of tenths of percents of the core damage frequency is smaller than the experienced change of the core damage frequency due to modifications of probabilistic safety assessment model due to plant modifications and due to procedure changes.

3.4 Results of prioritization of ageing from results of probabilistic safety assessment

Results of prioritization of ageing from results of probabilistic safety assessment are presented in Table 5 and Table 6. Results include change of core damage frequency due to ageing for different test intervals (T) and replacement intervals (L), given in months, for a selected probabilistic safety assessment model. Table 7 shows the summary of results from Table 5 and Table 6, which show larger increase of *CDF* at larger test intervals and at larger replacement intervals. Table 5 and Table 6 contain only 10 components, which are the largest contributors to the change of core damage frequency due to ageing. The increases of core damage frequency are relatively large and it is questionable how those large increases of core damage frequency are comparable to changes due to other parameter changes.

4 Problems connected with inclusion of ageing in probabilistic safety assessment

Experience shows that the contribution of ageing into the probabilistic safety assessment is a difficult issue at the current stage of developed models and availability of data. Some facts still prevent inclusion of ageing into the probabilistic safety assessment:

- It is very difficult to distinguish between failures due to other reasons and failures due to ageing.
- Ageing components are mostly made of many subcomponents and possibly the problems with subcomponents may cause failures of components. It is difficult to distinguish ageing of component parts and ageing of the components themselves.
- Conservatism of models and analyses in probabilistic safety assessment may be much larger as the contribution of ageing itself.
- Uncertainty of data is large in probabilistic safety assessment. The uncertainty of the results with inclusion of ageing may be larger.
- Consideration of ageing may require significant efforts and largely more complex models, and the effects to the results may not justify the invested efforts.

Table 5. Results of consideration of ageing

Basic event	q_i	FV_i	α_i	S_i	T = 1 m, L = 18 m	
					Δq_i	ΔCDF_i
BE01 (CCF DG)	2.81E-05	3.05E-03	4.11E-10/h^2	1.09E-03/ry	9.41E-04	1.02E-06/ry
BE02 (ECCS valve)	1.20E-05	7.81E-04	4.11E-10/h^2	6.51E-04/ry	9.41E-04	6.12E-07/ry
BE03 (ECCS valve)	2.40E-06	1.56E-04	4.11E-10/h^2	6.50E-04/ry	9.41E-04	6.12E-07/ry
BE04 (DC bus)	2.40E-05	8.83E-03	3.43E-11/h^2	3.68E-03/ry	7.84E-05	2.88E-07/ry
BE05 (ECCS valve)	2.40E-06	3.73E-05	4.11E-10/h^2	1.55E-04/ry	9.41E-04	1.46E-07/ry
BE06 (ECCS valve)	1.20E-05	1.86E-04	4.11E-10/h^2	1.55E-04/ry	9.41E-04	1.46E-07/ry
BE07 (ECCS valve)	2.40E-06	3.13E-05	4.11E-10/h^2	1.30E-04/ry	9.41E-04	1.23E-07/ry
BE08 (ECCS valve)	1.45E-03	1.89E-02	4.11E-10/h^2	1.30E-04/ry	9.41E-04	1.23E-07/ry
BE09 (ECCS valve)	2.96E-05	2.83E-04	4.11E-10/h^2	9.56E-05/ry	9.41E-04	9.00E-08/ry
BE10 (PCS valve)	1.45E-03	1.29E-02	4.11E-10/h^2	8.90E-05/ry	9.41E-04	8.37E-08/ry

Table 6. Results of consideration of ageing (continued)

Basic event	T = 18 m, L = 18 m		T = 1 m, L = 72 m		T = 6 m, L = 72 m		T = 72 m, L = 72 m	
	Δq_i	ΔCDF_i	Δq_i	ΔCDF_i	Δq_i	ΔCDF_i	Δq_i	ΔCDF_i
BE01	1.15E-02	1.25E-05/ry	3.82E-03	4.14E-06/ry	1.28E-01	1.39E-04/ry	1.84E-01	2.00E-04/ry
BE02	1.15E-02	7.49E-06/ry	3.82E-03	2.48E-06/ry	1.28E-01	8.32E-05/ry	1.84E-01	1.20E-04/ry
BE03	1.15E-02	7.48E-06/ry	3.82E-03	2.48E-06/ry	1.28E-01	8.31E-05/ry	1.84E-01	1.20E-04/ry
BE04	9.59E-04	3.53E-06/ry	3.18E-04	1.17E-06/ry	1.07E-02	3.92E-05/ry	1.53E-02	5.64E-05/ry
BE05	1.15E-02	1.79E-06/ry	3.82E-03	5.93E-07/ry	1.28E-01	1.99E-05/ry	1.84E-01	2.86E-05/ry
BE06	1.15E-02	1.78E-06/ry	3.82E-03	5.92E-07/ry	1.28E-01	1.98E-05/ry	1.84E-01	2.85E-05/ry
BE07	1.15E-02	1.50E-06/ry	3.82E-03	4.98E-07/ry	1.28E-01	1.67E-05/ry	1.84E-01	2.40E-05/ry
BE08	1.15E-02	1.50E-06/ry	3.82E-03	4.98E-07/ry	1.28E-01	1.67E-05/ry	1.84E-01	2.40E-05/ry
BE09	1.15E-02	1.10E-06/ry	3.82E-03	3.65E-07/ry	1.28E-01	1.22E-05/ry	1.84E-01	1.76E-05/ry
BE10	1.15E-02	1.02E-06/ry	3.82E-03	3.40E-07/ry	1.28E-01	1.14E-05/ry	1.84E-01	1.64E-05/ry

Table 7. Summary of results due to consideration of ageing

T	PS_TTIL	ΔCDF
T = 1 m	L = 18 m	4.58E-06/ry
T = 18 m	L = 18 m	5.60E-05/ry
T = 1 m	L = 72 m	1.86E-05/ry
T = 6 m	L = 72 m	6.22E-04/ry
T = 72 m	L = 72 m	8.96E-04/ry

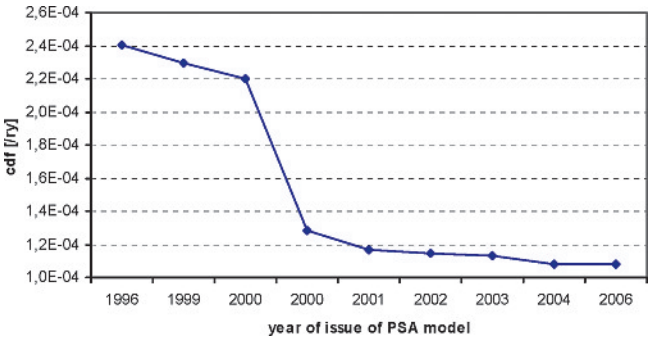

Fig. 11. The history of CDF for a selected PSA model due to changes (plant modifications and procedure changes)

- One can always argue that the consideration of ageing has already been included in the existing models with assumed constant failure rates, because the constant failure rates are determined as the average values, where all failure history is taken into account, no matter if the failures are in the beginning or at the end of the component life time.
- Consideration of ageing does not consider changes of human reliability, which is an important issue in probabilistic safety assessments contributing to the core damage frequency in the order of tenths of percents. Neglecting the changes of human reliability due to simulator experience and due to operators experience about the plant itself may be a larger portion than the contribution of ageing.

Fig. 11 shows an example of history of core damage frequency for a selected probabilistic safety assessment model. Figure shows that the relative decrease of core damage frequency due to updates of the model according to the plant modifications and procedure changes is much larger then the relative increase of core damage frequency due to ageing.

Those findings about consideration of ageing in probabilistic safety assessment:

- may change when considering new nuclear power plant designs, when passive components and systems may be in a larger extent a contributor to safety. As new plants are expected to be safer, which means that lower failure probabilities will be reached, the failure probabilities of the passive components may not be negligible compared to other equipment;
- may not be completely applicable for other than current designs of current light water reactors. Namely, consideration of piping in CANDU (CANada Deuterium Uranium) reactors may be somehow more important than consideration of piping in LWR due to the design features of CANDU reactors, which may impact the results.

5 Conclusions

The paper presents theoretical models of ageing and practical examples, which show, how the current models can be upgraded in sense to directly include the effects of ageing into the models of probabilistic safety assessment. The most important problem is the lack of data about the effects of ageing, which would suit to the well developed and detailed models of ageing. Evaluation of ageing within the probabilistic safety assessment is difficult mostly due to two the most important facts:

- it is difficult to distinguish equipment random failures and equipment failures, which causes are connected with degradation due to ageing,
- it is difficult to define the basic elements of the evaluation, which are the components themselves, as they are mostly made of several parts or subcomponents, which may de-

grade through time and age differently one from another and which can be partly exchanged or renewed or inspected.

One may argue that ageing is already included in the existing models. It only isn't separated from other causes of components and systems faults.

At the moment, it seems that the additional information, which may be extracted from the results of the models, which are developed or upgraded with direct inclusion of ageing into the probabilistic safety assessment, may not justify the costs and efforts for their realization.

Acknowledgement

The Slovenian Research Agency partly supported this research (partly research program P2-0026, partly research project V2-0553 supported together with Slovenian Nuclear Safety Administration).

(Received on 4 February 2009)

References

1 *Yee, R. K.; Sidhu, K. L.*: "Innovative laser heating methodology study for crack growth retardation in aircraft structures", International Journal of Fatigue, 2005, vol. 27, no. 3, p. 245–253
2 *Simonovski, I.; Nilsson K. F.; Cizelj L.*: "Crack tip displacements of microstructurally small cracks in 316L steel and their dependence on crystallographic orientations of grains", Fatigue and Fracture of Engineering Materials and Structures., 2007, vol. 30, no. 6, p. 463–478
3 *Weibull, W.*: "A statistical distribution of wide applicability", Journal of Applied Mechanics, 1951, 18, p. 293–297
4 *Briš R.; Čepin, M.*: "Stochastic ageing models under two kinds of failures", 31st ESReDA Seminar, Smolenice, Slovakia, November 7–8, 2006, p. 124–136
5 *Kolowrocki, K.*: "Reliability, availability and cost analysis of large multi-state systems with ageing components", Proceedings of ESREL2008, Valencia, 2008
"6 *Cizelj, L.; Mavko, B.*: "On the risk-based steam generator lifetime optimization", Theoretical and Applied Fracture Mechanics, 1995, vol. 23, p. 129–137
7 *Tipping, P.*: "Lifetime and ageing management of nuclear power plants: a brief overview of some light water reactor component ageing degradation problems and ways of mitigation", International Journal of Pressure Vessels and Piping, 1996, vol. 66, p. 17–25
8 *Dvoršek, T.; Cizelj, L.; Mavko, B.*: "Safety and availability of steam generator tubes affected by secondary side corrosion", 1998, Nuclear Engineering and Design, vol. 185, p. 11–21
9 *Blom, F. J.*: "Reactor pressure vessel embrittlement of NPP borssele: Design lifetime and lifetime extension", Nuclear Engineering and Design, 2007, vol. 237, p. 2098–2104
10 *Anandakumaran, K.*: "Aging and condition monitoring studies of composite insulation cables used in nuclear power plants", IEEE Transactions on Dielectrics and Electrical Insulation, 2007, 14(1), p. 227–237
11 *Gunther, W.; Sullivan, K.*: "Detecting and mitigating rod drive control system degradation in Westinghouse PWRs", IEEE Transactions on Nuclear Science, 1991, 38(6), p. 1760–1765
12 *Ellingwood; B. R.*: "Issues related to structural aging in probabilistic risk assessment of nuclear power plants", Reliability Engineering and System Safety, 1998, 62(3), p. 171–183
13 *Čepin, M.; Briš, R.*: "Models of aging equipment in the probabilistic safety assessment", 31st ESReDA Seminar, Smolenice, Slovakia, November 7–8,2006. Aging. Slovak Nuclear Forum: Slovak Nuclear Society, 2006, p. 165–172
14 *Banjac, T.; Čepin, M.*: "Consideration of Aging in Probabilistic Safety Assessment", Proceedings of NENE2007, Portoroz, 2007
15 *Ouytsel, K. V.; Batist, R. D.; Schaller, R.*: "An internal friction working model to advance the understanding of effects of radiation and thermal ageing on reactor pressure-vessel steels", International Journal of Pressure Vessels and Piping, 2003, 80(5), p. 275–284
16 *Kataoka, S.; Otsuka T.*: "JAPEIC's activity on aging issue related to neutron irradiation of RPV/RV materials", International Journal of Pressure Vessels and Piping, 2000, 77(10), p. 569–574
17 *Bebbington, M.; Lai, C.; Zitikis, R.*: "A flexible Weibull extension", Reliability Engineering and System Safety, 2007, 92(6), p. 719–726
18 *Pulkkinen, U.; Simola, K.*: "Bayesian models and ageing indicators for analyzing random changes in failure occurrence", Reliability Engineering and System Safety, 2000, 68(3), p. 255–268
19 *Finkelstein, M.*: "On statistical and information-based virtual age of degrading systems", Reliability Engineering and System Safety, 2007, 92(5), p. 676–681
20 *Lu, L.; Jiang, J.*: "Analysis of on-line maintenance strategies for k-out-of-n standby safety systems", Reliability Engineering and System Safety, 2007, 92(2), p. 144–155
21 *Martorell, S.; Sanchez, A.; Serradell, V.*: "Age-dependent reliability model considering effects of maintenance and working conditions", Reliability Engineering and System Safety, 1999, 64(1), p. 19–31
22 *Marseguerra, M.; Zio, E.*: "Optimizing maintenance and repair policies via a combination of genetic algorithms and Monte Carlo simulation", Reliability Engineering and System Safety, 2000, 68(1), p. 69–83
23 *Borgonovo, E.; Marseguerra, M.; Zio, E.*: "A Monte Carlo methodological approach to plant availability modeling with maintenance, aging and obsolescence", Reliability Engineering and System Safety, 2000, 67 (1), p. 61–73
24 *Hall, R.; Gunther, W.; Boccio, J.*: "Managing the effects of aging and reliability improvement", Nuclear Engineering and Design, 1989, Volume 115, p. 201 – 205
25 *Philips, J.; Roesener, W.; Magleby, H.; Geidl, V.*: "Incorporation of passive components aging into PRA's", Nuclear Engineering and Design, 1991, Volume 142, p. 167–177
26 *U.S. Nuclear Regulatory Commission (NRC)*: NUREG/CR-6679, BNL-NUREG-52587, "Assessment of Age-Related Degradation of Structures and Passive Components for U.S. Nuclear Power Plants", August, 2000
27 *U.S. Nuclear Regulatory Commission (NRC)*: NUREG/CR-5632, "Incorporating Aging Effects into Probabilistic Risk Assessment – A Feasibility Study Utilizing Reliability Physics Models", August 2001
28 *U.S. Nuclear Regulatory Commission (NRC)*: NUREG/CR-5587, SAIC-92/1137, "Approaches for Age-Dependent Probabilistic Safety Assessments With Emphasis on Prioritization and Sensitivity Studies", August 1992
29 *U.S. Nuclear Regulatory Commission (NRC)*: NUREG/CR-5510, SAIC49/1744, "Evaluations of Core Melt Frequency Effects Due to Component Aging and Maintenance", June 1990
30 *U.S. Nuclear Regulatory Commission (NRC)*: NUREG/CR-5378, EGG-2567, "Aging Data Analysis and Risk Assessment Development and Demonstration Study", August 1992
31 *U.S. Nuclear Regulatory Commission (NRC)*: NUREG/CR-4769, EGG-2476, "Risk Evaluations of Aging Phenomena: the Linear Aging Reliability Model and Its Extensions", April 1987
32 *U.S. Nuclear Regulatory Commission (NRC)*: NUREG/CR-4747, EGG-2473, "An Aging Failure Survey of Light Water Reactor Safety Systems and Components", Volume 1, July 1987
33 *U.S. Nuclear Regulatory Commission (NRC)*: NUREG/CR-5248, PN L-6701, "Prioritization of TIRGALEX Recommended Components for Further Aging Research", November 1988
34 *U.S. Nuclear Regulatory Commission (NRC)*: NUREG/CR-4747, EGG-2473, "An Aging Failure Survey of Light Water Reactor Safety Systems and Components", Volume 2, July 1988
35 *American Society of Mechanical Engineers (ASME)*: Standard for Probabilistic Risk Assessment for Nuclear Power Plant Applications, ASME RA-S-2002, ASME, 2002; Addendum A to ASME RA-S-2002, dated December 5, 2003; Addendum B to ASME RA-S-2002, dated December 30, 2005
36 *U.S. Nuclear Regulatory Commission (NRC)*: RG 1.200, "An Approach for Determining the Technical Adequacy of Probabilistic Risk Assessment Results for Risk-Informed Activities", Rev. 1, 2007
37 *Čepin, M.*: "Analysis of Truncation Limit in Probabilistic Safety Assessment", Reliability Engineering and System Safety, Vol. 87 (3), p. 395–403
38 *Čepin, M.; Mavko, B.*: "A Dynamic Fault Tree", Reliability Engineering and System Safety, 2002, Vol. 75, No. 1, p. 83–91
39 *U.S. Nuclear Regulatory Commission (NRC)*: RG 1.201, "Guidelines for Categorizing Structures, Systems, and Components in Nu-

clear Power Plants According to their Safety Significance", Rev. 1, 2006

40 *Electric Power Research Institute (EPRI)*: "PSA Applications Guide", TR-105396, 1995

41 *Čepin, M.*: "The Risk Criteria for Assessment of Temporary Changes in a Nuclear Power Plant", Risk Analysis, 2007, vol. 27, no. 4, p. 991–998

42 *Čepin, M.; Mavko, B.*: "Probabilistic Safety Assessment Improves Surveillance Requirements in Technical Specifications", Reliability Engineering and Systems Safety, 1997, Vol. 56, p. 69–77

43 *Čepin, M.*: "Optimization of Safety Equipment Outages Improves Safety", Reliability Engineering and System Safety, 2002, Vol. 77, p.71–80

44 *Čepin, M.; Martorell, S.*: "Evaluation of Allowed Outage Time Considering a Set of Plant Configurations", Reliability Engineering and System Safety, 2002, Vol. 78, No. 3, p. 259–266

The authors of this contribution

Assist. Prof. Dr. *Marko Cepin*, Reactor Engineering Division, "Jožef Stefan" Institute, Jamova 39, 1000, Ljubljana, Slovenia,
E-Mail: marko.cepin@ijs.si;
M. Sc. *Andrija Volkanovski*, Reactor Engineering Division, "Jožef Stefan" Institute, Jamova 39, 1000, Ljubljana, Slovenia,
E-Mail: andrija.volkanovski@ijs.si;

You will find the article and additional material by entering the document number **KT110021** on our website at *www.nuclear-engineering-journal.com*

ARTICLE IN PRESS

Available online at www.sciencedirect.com

ScienceDirect

Journal of Loss Prevention in the Process Industries ▮ (▮▮▮▮) ▮▮▮–▮▮▮

Journal of Loss Prevention in the process industries

www.elsevier.com/locate/jlp

Success criteria time windows of operator actions using RELAP5/MOD3.3 within human reliability analysis

Andrej Prošek*, Marko Čepin

Jožef Stefan Institute, Ljubljana, Slovenia

Received 30 March 2007; received in revised form 21 June 2007; accepted 22 June 2007

Abstract

Human reliability analysis (HRA) contributes to assessment and to reduction of the impact of human operators to the risk of technologies and processes. The objective of this paper is to integrate realistic deterministic safety analysis and probabilistic safety assessment to show how deterministic safety analysis impacts the HRA, which is integrated into the probabilistic safety assessment. The RELAP5/MOD3.3 computer code is used for realistic safety analysis. Parametric safety analysis studies give time parameters for human actions as an input for selected HRA. Calculated human error probabilities are inserted into probabilistic safety assessment and the results are obtained, where the focus goes to the most important risk contributors. The method and the results are shown on selected HRA method through two selected representative human actions. Results show that realistic safety analysis represents an important standpoint for assessment of human error probabilities within HRA.

Keywords: Human reliability analysis; Success criteria; Probabilistic safety assessment; Deterministic safety analysis

1. Introduction

Nuclear safety is assessed and improved through the probabilistic safety assessment, which integrates (ASME RA-S-2002, 2002):

- Probabilistic models of components (Jordan Cizelj, Mavko, & Kljenak, 2001), logic models of safety systems and reliability analysis of operator actions,
- Scenarios and sequences of safety system actuations and operator actions (Čepin, 2005b), and
- Accident physical models (Leskovar & Mavko, 2006).

The experience with the results shows that human contribution to undesired events is still significant in spite of the automation of systems and processes. The importance of human contribution causes that the many methods are developed and many activities are performed in the field of human reliability analysis (HRA). This is not true only in the nuclear industry (Čepin, 2005a, 2007; Grobbelaar, Julius, & Rahn, 2005; Kennedy, Siemieniuch, Sinclair, Kirwan, & Gibson, 2007; NUREG/CR-1278, 1983; NUREG/CR-6883, 2005; Reer, Dang, & Hirschberg, 2004), but also in other fields such as in the chemical industry (Khan, Amyotte, & DiMattia, 2006) and in the air and space industry (Harris et al., 2005) for example.

The objective of this paper is to show how the probability of operator to perform an error depends on parameters obtained from safety analysis and what this means for the safety of the nuclear power plant. Namely, the parameters of safety analysis direct the amount of time in which operator has to perform its action and this amount of time is one of important parameters, which direct the human error probability (HEP), i.e. probability of operator to perform an error. Smaller human error probabilities may cause smaller risk and thus improved safety.

IJS-HRA (Institute Jožef Stefan—human reliability analysis) serves as the example method (Čepin, 2005a; Čepin, 2007) for quantification of human error probabilities of specific human actions. The probabilistic safety

*Corresponding author. Tel.: +386 1 5885 450; fax: +386 1 5885 377.
E-mail addresses: andrej.prosek@ijs.si (A. Prošek), marko.cepin@ijs.si (M. Čepin).

0950-4230/$ - see front matter © 2007 Elsevier Ltd. All rights reserved.
doi:10.1016/j.jlp.2007.06.010

Please cite this article as: Prošek, A., & Čepin, M. Success criteria time windows of operator actions using RELAP5/MOD3.3 within human reliability analysis. *Journal of Loss Prevention in the Process Industries* (2007), doi:10.1016/j.jlp.2007.06.010

assessment model of a specific nuclear power plant serves as an example model, which shows how quantified human error probabilities relate to assessment of risk and thus safety. Probabilistic safety assessment is evaluated to assess and compare the measures of safety of the plant in two cases: if recovery is considered or not for each operator action separately. The decision, if recovery is considered or not, depends on the amount of additional time, which operators have to perform the required action (i.e. additional available time for action). The additional available time for action is determined from inputs from experience of training of operators on the plant simulator and from deterministic safety analysis.

Section 2 gives basic information about the IJS-HRA method, which is integrated with probabilistic safety assessment and with deterministic safety analysis. Section 3 focuses on determining the time parameters, which are important for HRA and which are obtained with deterministic safety analysis. Examples are selected, which demonstrate how the calculations were performed and what the results show. Section 4 shows the results of probabilistic safety assessment with emphasis on selected examples from HRA. Section 5 gives the conclusions and implications of the work.

2. HRA within probabilistic safety assessment

The operator actions are mostly only backup for the automatic actuations of the safety systems, which mitigate the accident if undesired initiating event occurs.

IJS-HRA integrates some features of existing methods and some new features such as contribution of the simulator experience in order to consider the newest requirements and recommendations in the field and in order to be integrated in a modern computerized probabilistic safety assessment (Čepin, 2005a; Čepin & He, 2006; NUREG-1792, 2005). More information about the method is written in another article of this journal issue (Čepin, 2007). Only the feature important for the contents of this paper is mentioned here: quantification of HEP is performed with consideration or without consideration of recovery.

If additional available time for action is larger than determined time interval, e.g. 10 min, than recovery as independent mode of verification is considered. If additional available time for action is shorter than determined time interval, recovery is not considered.

Additional available time for action (T_a) is defined as the difference between the time window of the action (T_w) and the actual time needed for performing the action (T_p), which is assessed based on real simulator scenarios:

$$T_a = T_w - T_p.$$

The time window of the human action actually represents the success criteria for the action. It represents the time interval in which operators have to perform the action in order that the plant is put in a safer state, i.e. the plant is put into a scenario that leads to a safe state and not to an accident state.

The actual time needed for performing the action is the realistic time in which operators perform the action and it can be obtained from the simulator experience.

The specified time windows are important for HRA due to the following reason. The HEP of certain operator action is lower if operators have more time available. In the control room of a nuclear power plant there is a team of operators, which is supervised by a shift supervisor. If operators have 10 or more minutes of additional time for action, it can be expected that colleagues or shift supervisor can observe and correct a possible error of their colleague. IJS-HRA method assumes that if the difference between the time window, in which the action has to be performed, and the actual time needed for performing the action is 10 min or more, a recovery can be modeled for the investigated action. If additional available time for action is shorter than determined time interval, recovery is not considered.

Consideration of recovery causes lower HEP and may cause a different impact of human error to the overall probabilistic safety assessment results.

Determination of the time window, in which operators have to perform the action, is obtained from deterministic safety analysis.

Fig. 1 shows integration of probabilistic safety assessment and deterministic safety assessment for improvement of HRA. Full arrows represent dependencies between the items, which are important for understanding this methodology. Dotted arrows on the figure represent dependencies between the items, which are not important for this methodology, but exist as part of processes of specific deterministic and probabilistic safety analysis in a nuclear power plant.

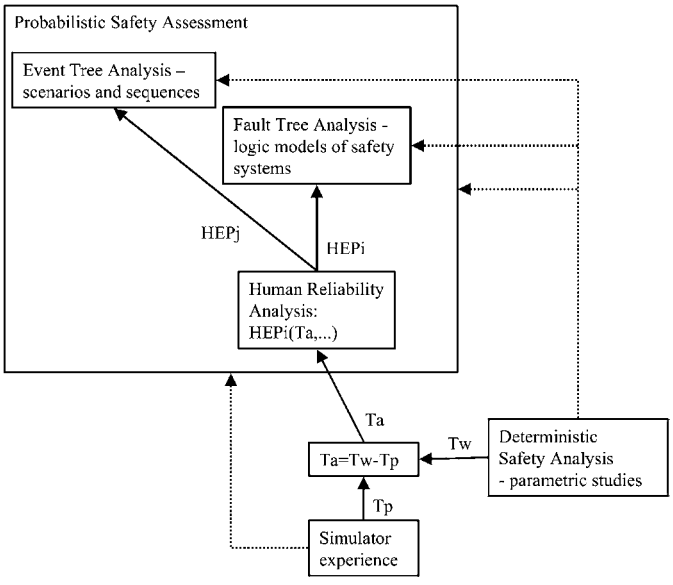

Fig. 1. Integration of probabilistic safety assessment and deterministic safety assessment for improvement of human reliability analysis.

Please cite this article as: Prošek, A., & Čepin, M. Success criteria time windows of operator actions using RELAP5/MOD3.3 within human reliability analysis. *Journal of Loss Prevention in the Process Industries* (2007), doi:10.1016/j.jlp.2007.06.010

3. Determining the time window success criteria

Best-estimate deterministic safety analyses based on their plant specific model serve for determination of the amount of time in which operator has to perform its action (i.e. time window) in order that the safety parameters are not exceeded. Parametric calculations are performed, where the time window is varied and plant response is simulated in order that the safety parameters are not exceeded, and the longest time window for operator actions is obtained, which results in safe conditions of the plant through the complete simulation time.

Deterministic safety analysis represents the time simulation of the most important plant parameters in selected circumstances. Such simulation may include response of the plant to the undesired initiating event, e.g. break of smaller or larger pipe of the most important plant system, e.g. loss of electric power supply, which cause actuation of safety systems to prevent an accident or at least to mitigate its consequences. The simulations of plant behavior after selected undesired initiating events may include a variety of options. Selected safety systems may be assumed operable or inoperable or they may be assumed inoperable for a selected period of time and then be assumed operable.

If the most important plant parameters stay all the time within their acceptable limits, the plant is avoiding accident. If the limits are exceeded, the accident conditions are simulated.

The main objective of these deterministic safety analyses is to show that the plant can be maintained in safe conditions even after a variety of undesired initiating events. Namely, several safety systems are in place to prevent severe accidents in such cases.

The idea of the IJS-HRA method is to use those deterministic safety analyses to perform sensitivity studies of human actions, which are supplement to safety systems actuations. Sensitivity studies include variations of timing of human action. The objective of those sensitivity studies is to determine the latest time, when operators have to perform the needed action in order that the main plant parameters are not exceeded their limits, i.e. in order that the plant is kept in safe conditions and thus avoiding accident.

The definition of accident state in the case of nuclear power plant probabilistic safety assessment is connected with the temperature of the reactor core. It is assumed if the temperature in the reactor core exceeds 923 K for more than 30 min or if temperature of the core exceeds 1348 K, the core damage may occur, which may lead to accident state. The cladding temperature of the hot rod in the core at the hottest vertical location is assumed as the maximum temperature in the core.

Deterministic safety analyses are performed with complex computer codes. The modular accident analysis program (MAAP) has been used in the past in probabilistic safety assessment, where conservative approach was the accepted solution. Wherever, due to lack of information, the models were incomplete, the worst case was examined and considered.

Realistic deterministic safety analyses have been required recently (ASME RA-S-2002, 2002; Han, Lim, & Yang, 2007) for risk-informed applications. So, the realistic i.e. best-estimate RELAP5/MOD3.3 computer code (USNRC, 2001) was used for safety analysis. The RELAP5 computer code has been extensively used in the past for safety analyses (Mavko, Stritar & Prošek, 1993, Prošek & Mavko, 1999). The input model described in reference (Prošek, Parzer, & Krajnc, 2004) was used for calculations.

The new contribution of this study is an evaluation how deterministic safety analysis influences the success criteria time windows, which consequently direct the HEP. The procedure and the results are shown for two selected examples of human actions.

3.1. Example for manual actuation of auxiliary feedwater (AFW) at loss-of-coolant accident

The first example event is a human action: establishing AFW in case of small or medium loss-of-coolant accident, i.e. break of the pipe connected to the reactor coolant system. In the case of small or medium loss-of-coolant accident in a nuclear power plant, and if high pressure safety injection (SI) fails, one of the means to cool the reactor is through the functioning of the AFW, which is automatically put into operation. If the pumps would not start automatically, operators should intervene. Success criterion requires operation of one of three pumps to maintain the flow by which the reactor coolant system is depressurized. The time window is defined based on safety analysis.

Safety analyses were performed for various sizes of equivalent diameter breaks from 1.91 to 7.62 cm (0.75–3 in) and for various cases considering the time of actuation of AFW system. The comparison of the results shows that the latest time that the safety parameters (i.e. rod cladding temperature) are not exceeded is to actuate AFW system is 30 min.

Technical details of determining this time from performed safety analyses are presented below.

Without high pressure SI into the reactor coolant system and the AFW injection into the secondary side there is no additional cooling of the core until the reactor coolant system pressure is depressurized below accumulator injection setpoint at 4.9 MPa. As can be seen from Fig. 2(a) the 5.08 cm (2 in) and larger breaks depressurize (through the break) in any case below accumulator injection setpoint pressure after some time and the AFW is not needed for depressurization. However, AFW is needed for subsequent depressurization for 2.54 cm (1 in) equivalent diameter break and smaller. The reason that 2.54 cm break and smaller cannot depressurize the reactor coolant system is that cooling through the break is not sufficient. Therefore, additional cooling is needed provided by AFW system and

Please cite this article as: Prošek, A., & Čepin, M. Success criteria time windows of operator actions using RELAP5/MOD3.3 within human reliability analysis. *Journal of Loss Prevention in the Process Industries* (2007), doi:10.1016/j.jlp.2007.06.010

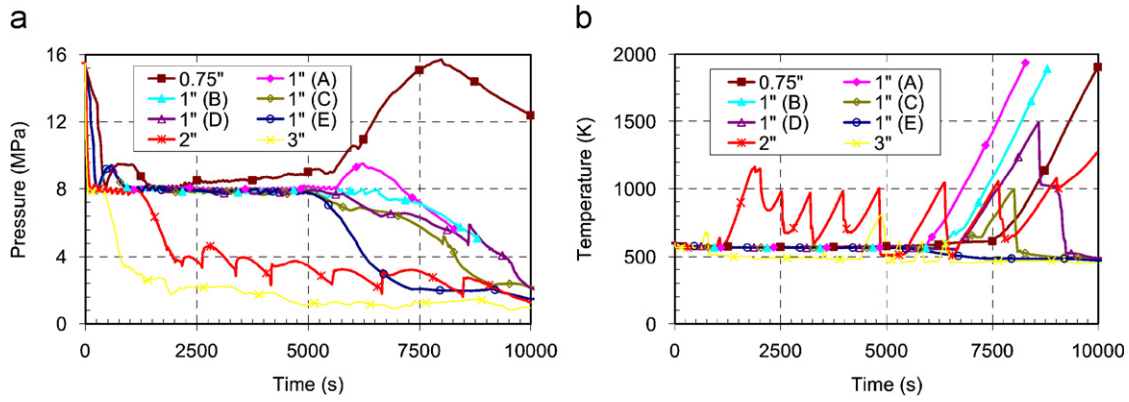

Fig. 2. Calculated trends during loss-of-coolant accident: (a) pressurizer pressure, and (b) rod cladding temperature.

Table 1
Operator actions delays for scenarios with 2.54 cm break

Case	Operator action	
	Auxiliary feedwater start delay	Secondary relief valve full opening delay
A	Action not performed	Action not performed
B	0 min	Action not performed
C	20 min	20 min
D	25 min	25 min
E	30 min	15 min

secondary relief valve, while cooling by high pressure SI is not available by assumption.

As core heatup is earlier for 2.54 cm break than for 1.91 cm break the time window to start AFW was determined for 2.54 cm break. Five different scenarios were analyzed as shown in Table 1. The parameter for indicating depressurization is pressurizer pressure and the parameter for indicating core heatup is rod cladding temperature. The analysis showed (see Fig. 2) that without any AFW (case A) the rod cladding temperature exceeds the criterion 1348 K when core damage may occur. Case B shows that even no delay in the AFW start could not prevent the core heatup. The analysis showed that when the secondary relief valve is operated automatically, it is opened around 25% of the time what is not sufficient to remove all decay heat from the reactor coolant system, resulting in core heatup. This means that another operator action is needed in combination with AFW start—manual full opening of secondary relief valve (cases C, D and E). In the case C, the reactor coolant system is depressurized in time and the core heatup above the core damage criterion is prevented. In the case D, the reactor coolant system is depressurized, but the rod cladding temperature exceeded the criterion. Finally, case E showed that AFW could be delayed 30 min, if secondary relief valve opening delay on AFW start is 15 min.

The experience of operators with plant simulator shows that the actual time for performing the event is 1–10 min. So, additional time for performing the event is 20–29 min (i.e. success criteria time minus actual time for performing the event), which gives enough time for possible recovery action. Low stress is assumed, very good labeling of controls is observed, diagnosis and action are assumed as very simple, which gives performance shaping factor 0.1 for commission errors.

3.2. Example for manual actuation of AFW at transient

The second example event is a human action: establishing AFW in case of transients. This is the same human action as in the previous case, except that it occurs in different circumstances, which means that different plant parameters may require different scenarios of safety systems. The success criterion says that capacity of one train of AFW is adequate to remove decay heat, to prevent overpressurization of reactor coolant system, and to prevent uncovering of the core resulting in core heatup.

Safety analyses were performed for various cases considering the time of actuation of AFW system. The comparison of the results shows that the latest time that the safety parameters (i.e. rod cladding temperature) are not exceeded is to actuate AFW system is 40 min.

Technical details of determining this time from performed safety analyses are presented below.

The pressurizer pressure shows when the reactor coolant system is overpressurized. The core heatup can be prevented by maintaining sufficient reactor coolant system mass inventory and thereby core level, while the core heatup is indicated by rod cladding temperature.

Fig. 3 shows all the relevant parameters: pressurizer pressure, reactor coolant system mass inventory, core collapsed liquid level, and rod cladding temperature. At zero time transient loss of main feedwater was started, followed by reactor trip and SI signal generation starting engineered safety features. At the time when one AFW pump was started to inject into the secondary side, cooling of the secondary side caused the pressurizer pressure to drop below the pressurizer relief valve closure setpoint and then below the maximum pressure capacity of high

Please cite this article as: Prošek, A., & Čepin, M. Success criteria time windows of operator actions using RELAP5/MOD3.3 within human reliability analysis. *Journal of Loss Prevention in the Process Industries* (2007), doi:10.1016/j.jlp.2007.06.010

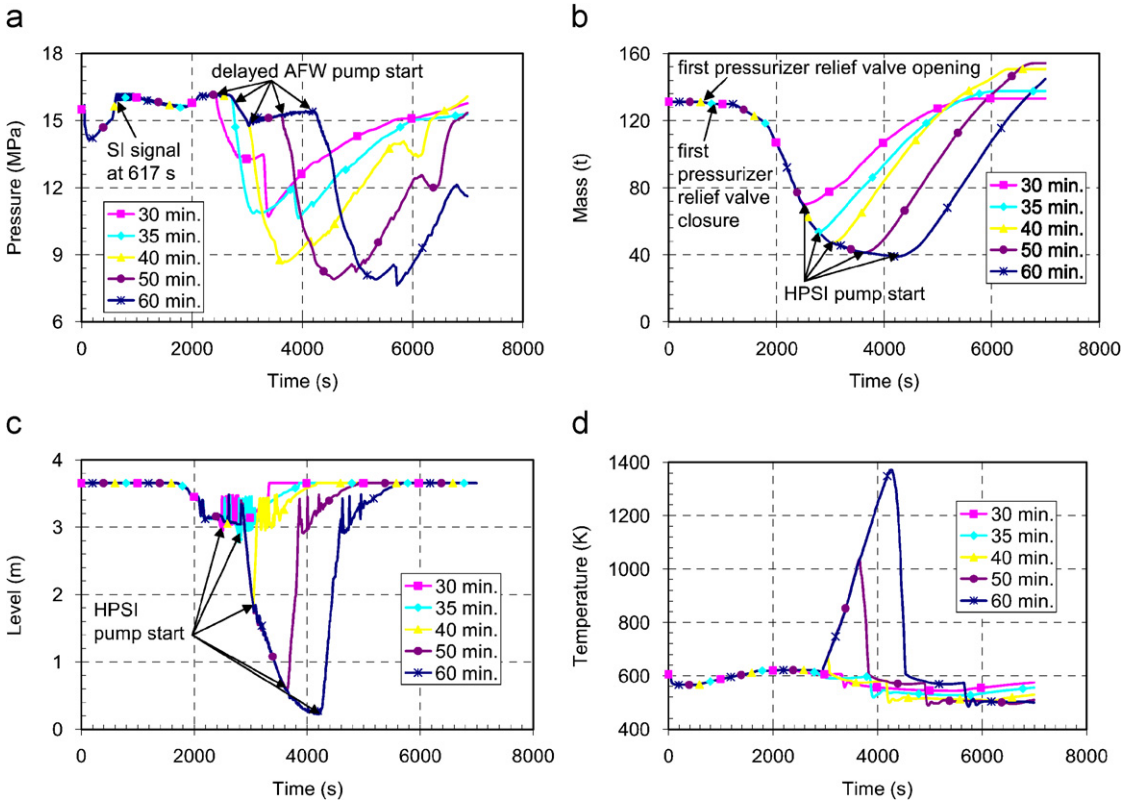

Fig. 3. Calculated trends during transient: (a) pressurizer pressure, (b) reactor coolant system mass inventory, (c) core collapsed liquid level, and (d) rod cladding temperature.

pressure safety injection SI pump (see Fig. 3(a)). There is no overpressurization of the reactor coolant system as the pressurizer pressure remains below 18.95 MPa. The closure of the pressurizer relief valve and coolant injection into reactor coolant system resulted in increasing reactor coolant mass inventory as shown in Fig. 3(b) thus recovering the core level shown in Fig. 3(c) and quenching the core as shown in Fig. 3(d).

From Fig. 3 it can be seen that the core uncovery depends mainly on the delay of one AFW pump start. Unavailability of AFW injection leads to core uncovery. This means that reactor coolant system mass inventory depletion is mostly function of mass released through the pressurizer relief valves. Realistic modeling of the pressurizer relief valve guarantees realistic calculation of the reactor coolant system mass inventory.

The parametric analysis shows that the core uncovers with AFW pump start delayed for 35 min or greater. The case with AFW pump start delayed for 40 min cause small core heatup and with delay of 50 min the core temperature is still below criterion 1348 K for core damage, while in the case with delay of 60 min this value is exceeded. Based on Fig. 3 and considering uncertainties in calculating the rod cladding temperature (Prošek & Mavko, 1999) the time window of 40 min was determined.

The actual time for starting the AFW is 1–10 min. So, additional time for performing the event is 30–39 min (i.e. success criteria time minus actual time for performing the event), which gives enough time for possible recovery action.

4. Probabilistic safety assessment results

4.1. Model description

The probabilistic safety assessment model of a nuclear power plant is named as HRA_IH_1 and is used for quantification. The characteristics of the model HRA_IH_1 show that it is a large and detailed model, which includes: 4748 gates, 1810 basic events, 16 initiating events and main event trees, 738 fault trees, which include 125 human failure fault trees, 57 parameters (failure rate), 418 parameters (probability), which include 55 parameters connected with HEP (those 55 parameters are obtained from 18 different basic HEP parameters, which are expanded to 55 parameters considering different performance shaping factors for basic HEP parameters), 18 groups for parameters of human errors, 117 groups for human error basic events.

Table 2 shows HRA time parameters for selected human actions, which are needed for decision if recovery is considered or no, when quantification of HEP is made.

Please cite this article as: Prošek, A., & Čepin, M. Success criteria time windows of operator actions using RELAP5/MOD3.3 within human reliability analysis. *Journal of Loss Prevention in the Process Industries* (2007), doi:10.1016/j.jlp.2007.06.010

Table 2
Parameters for selected human errors

Human error	T_w (min)	T_p (min)	$T_a = T_w - T_p$ (min)
Manual actuation of auxiliary feedwater at transient	40	1–10	30–39
Manual actuation of auxiliary feedwater at loss-of-coolant accident	30	1–10	20–29

Table 3
Probabilistic safety assessment results

Human error	Basic human error probability	Fractional contribution	Core damage frequency	Main minimal cut set and its contribution	
Manual actuation of auxiliary feedwater at transient	2.31E−4	6.93E−02	2.487E−5 (Ry^{-1})	4	7.136E−7 (Ry^{-1})
Manual actuation of auxiliary feedwater at loss-of-coolant accident	2.31E−4	N/A	2.487E−5 (Ry^{-1})	–	–

4.2. Base case results

The results of the probabilistic safety assessment include many parameters. Only selected results are mentioned below for the analysis with the following features:

- consideration of internal initiating events,
- third order approximation,
- truncation of 2.7E-11 and Ry^{-1},
- recovery is considered for both selected human actions, because additional available time for action (i.e. the difference between the time in which operators have to perform the action in order that it meets the success criteria and the actual time needed for performing the action) is more than determined time interval, e.g. 10 min.

The results include:

- Core damage frequency: 2.487E-5 Ry^{-1}.
- No minimal cut set, which includes event manual actuation of AFW during loss-of-coolant accident. Minimal cut set is a combination of basic events (i.e. component failures, human errors), which may cause undesired state of the system, e.g. accident state. This means that manual actuation of AFW at loss-of-coolant accident is not a safety significant event as it is not involved in any combination of undesired events.
- Minimal cut set no. 4 (ranked by contribution to core damage frequency) contributes to core damage frequency by 7.136E-7 Ry^{-1} and it is the most contributing minimal cut set of those, which include event manual actuation of AFW in case of transients. This means that manual actuation of AFW at transients is a very safety significant event.
- Risk importance factors (i.e. fractional contribution of considered human errors) are provided in Table 3. It is shown that Manual Actuation of AFW at Transient contributes significantly to the core damage frequency, which is observed by high fractional contribution. The manual actuation of AFW in case of loss-of-coolant accident is not listed in the list of minimal cut sets so risk importance factor cannot be calculated (the event is of no safety significance).

4.3. Sensitivity results of selected examples

Sensitivity analysis is performed for each of selected example actions for a case if recovery would not be considered in quantification of HEP, i.e. if additional available time for action would be less than determined time interval. Table 4 shows the results for selected human errors without consideration of recovery.

Results show that consideration of recovery impacts significantly the HEP. This is observed through the comparison of basic human error probabilities in Table 3 (recovery is considered) and Table 4 (recovery is not considered). The change of HEP can significantly impact the core damage frequency and thus the plant risk, if the affected human error is an important contributor to risk, as it is the case with manual actuation of AFW in case of transients. For the important human error it is necessary to determine additional time for action accurately as this may have significant impact to the assessment of risk.

If the conservative analysis would be used instead of the best-estimate analysis, the time window for both actions would be around 15 min, which would not be enough for consideration of recovery. The comparison of results in Tables 3 and 4 shows that selection of best estimate versus conservative analysis leads to significant change in risk

Please cite this article as: Prošek, A., & Čepin, M. Success criteria time windows of operator actions using RELAP5/MOD3.3 within human reliability analysis. *Journal of Loss Prevention in the Process Industries* (2007), doi:10.1016/j.jlp.2007.06.010

Table 4
Results for cases if recovery is not considered at specific human error

Human error	Basic human error probability	Fractional contribution	Core damage frequency	Main minimal cut set and its contribution	
Manual actuation of auxiliary feedwater at transient	2.85E−3	4.80E−01	4.448E−5 (Ry^{-1})	1	8.810E−6 (Ry^{-1})
Manual actuation of auxiliary feedwater at loss-of-coolant accident	2.85E−3	7.71E−04	2.494E−5 (Ry^{-1})	7875	8.424E−11 (Ry^{-1})

results. For manual actuation of AFW in case of loss-of-coolant accident, the change is insignificant, which was expected as the event is not risk important, so its changes does not cause significant changes in the results. For manual actuation of AFW in case of transients, this change is significant, as it nearly doubles the core damage frequency and thus the level of risk.

5. Conclusions

The integration of deterministic safety analysis and probabilistic safety assessment is presented in the field of HRA. Safety analyses served for determination of time parameters, which are inputs for HRA within the probabilistic safety assessment. The propagation of impact of safety analysis through the human reliability to the probabilistic safety assessment is demonstrated. The analysis and results are presented on selected practical examples, which represent typical situations.

Sensitivity studies of safety analysis for scenarios connected with each of selected human errors were performed. The timing of operator intervention was studied using realistic code and the results of safety analysis were examined in sense how late after the required human intervention the operator performs its action that the safety criteria are not exceeded, i.e. the temperature of the reactor core does not exceed the determined limit. This gives available time for operator to act. The less the time available, the more probable the human error of respective action, which is the implication of the HRA that was performed.

The results of HRA and the probabilistic safety assessment results are presented, with focus on the parameters that are connected with impacts of HRA. The results show that consideration of recovery impacts significantly the HEP. The change of HEP can significantly impact the core damage frequency, if the affected human error is an important contributor to risk, as it is the case with one of two example actions. For the important human error it is necessary to determine additional time for action accurately as this may have significant impact to the assessment of risk.

In addition, the results implies that best-estimate deterministic safety analysis removes the unnecessary conservatism compared to conservative deterministic safety analysis and consequently reduce the risk, which is true also for the risk contribution of human actions.

Acknowledgment

The Slovenian Research Agency supported this research (partly research program P2-0026, partly research project V2-0376 supported together with Slovenian Nuclear Safety Administration and partly research project J2-6542).

References

ASME RA-S-2002. (2002). *Standard for probabilistic risk assessment for nuclear power plant applications*. The American Society of Mechanical Engineers.

Čepin, M. (2005a). *Human reliability analysis—methods and applications, problems and solutions*. Internal Report, IJS.

Čepin, M. (2005b). Analysis of truncation limit in probabilistic safety assessment. *Reliability Engineering & System Safety*, *87*(3), 395–403.

Čepin, M. (2007). Importance of human contribution within the human reliability analysis (IJS-HRA). *Journal of Loss Prevention in the Process Industries*. doi:10.1016/j.jlp.2007.04.012.

Čepin, M., & He, X. (2006). Development of a method for consideration of dependence between human failure events. ESREL2006.

Grobbelaar, J. F., Julius, J. A., & Rahn, F. (2005). Analysis of dependent human failure events using the EPRI HRA calculator. PSA05. *Proceedings*.

Han, S. J., Lim, H. G., & Yang, J. E. (2007). An estimation of an operator's action time by using the MARS code in a small break LOCA without a HPSI for a PWR. *Nuclear Engineering and Design*, *237*, 749–760.

Harris, D., Stanton, N. A., Marshall, A., Young, M. S., Demagalski, J., & Salmon, P. (2005). Using SHERPA to predict design-induced error on the flight deck. *Aerospace Science and Technology*, *9*(6), 525–532.

Jordan Cizelj, R., Mavko, B., & Kljenak, I. (2001). Component reliability assessment using quantitative and qualitative data. *Reliability Engineering & System Safety*, *71*, 81–95.

Kennedy, G. A. L., Siemieniuch, C. E., Sinclair, M. A., Kirwan, B. A., & Gibson, W. H. (2007). Proposal for a sustainable framework process for the generation, validation, and application of human reliability assessment within the engineering design lifecycle. *Reliability Engineering & System Safety*, *92*(6), 755–770.

Khan, F., Amyotte, P. R., & DiMattia, D. G. (2006). HEPI: A new tool for human error probability calculation for offshore operation. *Safety Science*, *44*(4), 313–334.

Mavko, B., Stritar, A., & Prošek, A. (1993). Application of code scaling, applicability and uncertainty methodology to large break LOCA analysis of two-loop PWR. *Nuclear Engineering and Design*, *143*, 95–109.

Leskovar, M., & Mavko, B. (2006). Simulation of the Phebus FPT1 severe accident experiment with the MELCOR computer code. *Journal of Mechanical Engineering*, *52*(3), 142–160.

Please cite this article as: Prošek, A., & Čepin, M. Success criteria time windows of operator actions using RELAP5/MOD3.3 within human reliability analysis. *Journal of Loss Prevention in the Process Industries* (2007), doi:10.1016/j.jlp.2007.06.010

NUREG/CR-1278. (1983). *Handbook for human reliability analysis with emphasis on nuclear power plants application*. US NRC.

NUREG/CR-6883. (2005). *The SPAR-H human reliability analysis method*. US NRC.

NUREG-1792. (2005). *Good practices for implementing human reliability analysis* (*HRA*). US NRC.

Prošek, A., & Mavko, B. (1999). Evaluating code uncertainty—I: Using the CSAU method for uncertainty analysis of a two-loop PWR SBLOCA. *Nuclear Technology*, *126*, 186–195.

Prošek, A., Parzer, I., & Krajnc, B. (2004). Simulation of hypothetical small-break loss-of-coolant accident in modernized nuclear power plant. *Electrotechnical Review*, *71*(4), 199–204.

Reer, B., Dang, V. N., & Hirschberg, S. (2004). The CESA method and its applications in a plant-specific pilot study on errors of commission. *Reliability Engineering & System Safety*, *83*, 187–205.

USNRC. (2001). *RELAP5/MOD3.3 code manual* Vols. 1–8. Rockville, MA, Idaho Falls, ID: Information Systems Laboratories, Inc., (prepared for USNRC).

Please cite this article as: Prošek, A., & Čepin, M. Success criteria time windows of operator actions using RELAP5/MOD3.3 within human reliability analysis. *Journal of Loss Prevention in the Process Industries* (2007), doi:10.1016/j.jlp.2007.06.010

ASIGURAREA CALITĂȚII – QUALITY ASSURANCE

CUPRINS – CONTENTS

- **FDI in Multivariate Process with Naive Bayesian Network in the Space of Discriminant Factors** 2
  Teodor Țiplica, Sylvain Verron, Abdessamad Kobi
- **Extending Health Considerations in Generation/Transmission Power System to Include Uncertainty Using Fuzzy Data** 9
  R A.K. Verma, A. Srividya, M.V. Bhatkar
- **Modern Procedures Evaluating MEMS Reliability** 17
  Marius Bâzu, Cătălin Tibeică, Lucian Gălățeanu, Virgil Emil Ilian
- **IJS-HRA – A Method for Human Reliability Analysis** 21
  Marko Cepin
- **How the Paradigm of Management Control enables managers to find new directions in Quality Management** 28
  Jos van Iwaarden, Ton van der Wiele

ASIGURAREA CALITĂȚII – QUALITY ASSURANCE
Ianuarie – Martie 2009 Volumul XV Numărul 57

IJS-HRA – A Method for Human Reliability Analysis

Marko CEPIN

„Jožef Stefan" Institute, Ljubljana, Slovenia

Abstract

The Human Reliability Analysis (HRA) is a systematic framework, which includes the process of evaluation of human performance and associated impacts on structures, systems and components for a complex facility. The objective of the paper is to present the IJS-HRA method and the results of an example study. IJS-HRA is a method, which is a method for evaluation of the human error probabilities of human actions within the probabilistic safety assessment of the nuclear power plants. It is developed based on integration of several important features of previously developed methods. The resulted human error probabilities, which are calculated with application of the method, are used in the example probabilistic safety assessment. A part of the obtained results are presented, which show that the contribution of human factor is still an important contributor to risk in spite of a wide automation, which took place in recent decades. In addition, the most important human failure events are identified, which are candidates for simulator training, which will consequently reduce their human error probability and contribute to improved safety.

Keywords: *Human Reliability Analysis, Risk, Safety, Nuclear.*

1. INTRODUCTION

The experience with the results of probabilistic safety assessment (PSA) and with the contributions of human failure events (HFE) in the models and in the results show that human contribution to the undesired events is still significant in spite of the automation of systems and processes.

The Human Reliability Analysis (HRA) is a systematic framework, which includes the process of evaluation of human performance and associated impacts on structures, systems and components for a complex facility.

1.1. Review of Methods in the Field of Human Reliability Analysis

The contribution of human factor to safety of complex facilities is large in spite of intensive automation of systems and processes. The field was investigated intensively in the last decades, which is specially the case for nuclear power plants (Reer, Dang & Hirschberg, 2004, Grobbelaar, Julius & Rahn, 2005, Kennedy, Siemieniuch, Sinclair, Kirwan & Gibson, 2007).

Probabilistic safety assessment applications are source of many interactions with human reliability analysis (Cepin & Mavko, 1997, ASME-RA-S-2002, Cepin, 2002, Cepin & Mavko, 2002, Holy, 2004, Mosleh & Chang, 2004, Cepin, 2005b).

Many methods connected with human reliability analysis were developed in this period, including Technique for Human Error Rate Prediction (THERP, NUREG/CR-1278, 1983), Systematic Human Action Reliability Procedure (SHARP, 1984), Accident Sequence Evaluation Program (ASEP, NUREG/CR-4772, 1987), A Technique for Human Event Analysis (ATHEANA, NUREG-1624, 1999, Forester et al., 2004), Cognitive Reliability and Error Analysis Method (CREAM, Hollnagel, 1988), Human Cognitive Reliability (HCR, Spurgin, 1990), Standardized Plant Analysis Risk HRA (SPAR-H, NUREG/CR-6883, 2005) and many others.

1.2. Objective

The objective is to present the IJS-HRA method, which is a method for evaluation of the human error probabilities of human actions within the probabilistic

* Correspondence to Assoc. Prof. dr. Marko Cepin, e-mail: **marko.cepin@ijs.si**.

safety assessment of the nuclear power plants. The method integrates specific features of existing methods and specific new features. It includes consideration of dependencies, which is one of the most important features of human reliability analysis.

2. HUMAN RELIABILITY ANALYSIS – METHOD DESCRIPTION

Figure 1 shows the scheme of the method. The main inputs for the human reliability analysis are identified (PSA model, plant information, HRA state-of-the-art), which represent the standpoint for development of the method. The method for evaluation of human failure events is developed including consideration about dependencies between human failure events.

Figure 1 shows that identification of human failure events distinguishes pre-initiator events (i.e. pre-initiators), initiator events (i.e. initiators) and post-initiator events (i.e. post-initiators). Pre-initiators are the events that may cause the equipment to be unavailable before the initiating event has occurred. Initiators are the events that may contribute to the occurrence of initiating events. Post-initiators are the events, which are connected with human actions to prevent accident or mitigate its consequences after initiating event has occurred.

Evaluation of human failure events including evaluation of dependencies integrates assessment of human error probabilities with operator interview, simulator experience and plant data base. Information on time windows of human failure events is obtained from safety analysis.

The information needed for the human reliability analysis come from three main sources, which are the following:

- Information about the plant: information from safety analysis report (information from safety system descriptions), information from plant procedures: e.g. general operating procedures, system operating procedures, abnormal operating procedures, emergency operating procedures, operating surveillance procedure.
- PSA model including fault trees and event trees and the supporting information.
- Standards, requirements, guidelines and good practice for PSA with emphasis on issues, which are applicable for HRA (e.g. ASME standard on PSA: ASME RA-S-2002), and standards, requirements, guidelines and good practice for HRA itself: e.g. HRA methods: e.g. THERP (NUREG/CR-1278, 1983), ASEP (NUREG/CR-4772, 1987), SHARP (SHARP, 1984), ATHEANA

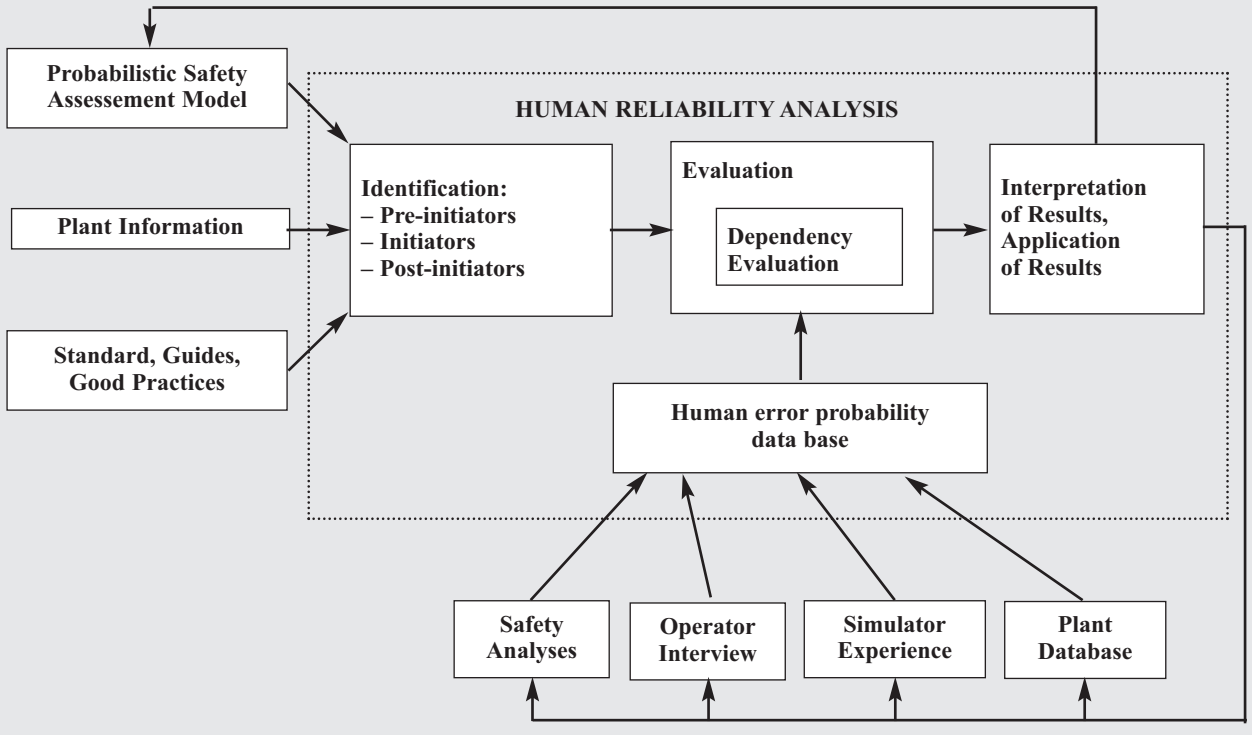

Figure 1. IJS-HRA – A Human Reliability Analysis Method

(NUREG-1624, 1999), CREAM (Hollnagel, 1988), SPAR-H (NUREG/CR-6883, 2005), good practices for implementation of HRA (NUREG-1792, 2005).

The method for analysis of human failure events is developed including consideration about dependencies between human failure events, which are in the PSA model treated as independent. The method for update of human failure events is a method, which include features of several HRA methods, such as THERP (NUREG/CR-1278, 1983), ASEP (NUREG/CR-4772, 1987), ATHEANA (NUREG-1624, 1999), SPAR-H (NUREG/CR-6883, 2005) and features such as dependency method and inclusion of simulator experience.

The method consists of the following steps, which are described in the subsequent subsections:

1. Statements on objectives, definition of the work, scope of the analysis
2. Identification of human failure events
3. Task analysis of human failure events
4. Evaluation of human failure events
5. Consideration of dependencies between human failure events
6. Interpretation of results, inclusion of HRA to PSA

The success criteria for human failure events include information about their time window, i.e. information about the time, in which operators have to perform the action. This information about the available time comes from safety analyses, where scenarios about operating safety systems are evaluated. This is the reason for appearance of text box of safety analysis on Figure 1 and its connection with text box on HRA method.

2.1. Statements on objectives, definition of the work, scope of the analysis

Information on objectives, definition of the work and the scope of the analysis is related with performance of the probabilistic safety assessment of the nuclear power plant.

It is important to emphasise that two terms are widely used in human reliability analysis: human action and human failure event. Human action is a term describing an event or a process, which is performed by the plant operators. Human failure event is a term, which can describe the same event or process from its negative side in sense what can go wrong in order that the human action is not performed or it is not performed correctly.

2.2. Identification of human failure events

HFE identification, which distinguishes pre-initiator events (i.e. pre-initiators), initiator events (i.e. initiators) and post-initiator events (i.e. post-initiators), results in identification of a number of pre-initiators, a number of initiators and a number of post-initiators.

Pre-initiators are the events that may cause the equipment to be unavailable before the initiating event has occurred. Initiators are the events that may contribute to the occurrence of initiating events. Post-initiators are the events, which are connected with human actions to prevent accident or mitigate its consequences after initiating event has occurred.

Pre-initiators are identified with help of the analysis of systems and their relations with operator intervention, with the analysis of sequence of events in the event trees and with consideration of references on good practice on HRA.

Initiators are identified with help of the documents on plant history and with checking the events that may initiate initiating events. The links of fault trees that are linked to the initiating events in the event trees are checked.

Post initiators are identified with help of operator interview, with analysis of event trees and their respective scenarios in a team of operator and PSA HRA analyst.

2.3. Task analysis of human failure events

Task analysis of human failure events includes:

- collection of information about human failure event, which includes review of plant documents (e.g. safety analysis report, plant procedures), plant databases, PSA (with emphasis on all its parts that are connected with HRA),
- preparation and analysis of talk-through with plant operators, which identify information about tasks, about the time needed for performing human actions, about performance shaping factors connected with their respective human failure events,
- identification of the tasks, which compose the respective human failure event,
- identification and analysis of diagnosis activities,
- identification and analysis of action tasks including omission and commission.

2.4. Evaluation of human failure events

Evaluation of human failure events includes:

- measurement of time needed for performing human actions, which is performed through real simulator scenarios,
- assessment of simulator experience with human actions that are included in human failure events,

- preparation of failure model table, which (based on cue table and subtask analysis table) identifies failures and specifies their general evaluation procedure: i.e. consideration or no consideration of recovery. If additional available time for action is determined as one value, e.g. 10 minutes or more, than recovery as independent mode of verification may be considered in such case. Additional available time for action is defined as the difference between the time window of the action (obtained from success criteria for the action: the time in which operators have to perform the action), i.e. the time in which action has to be performed in order that it meets the success criteria, and the actual time needed for performing the action,
- preparation of data table, which connect failures with data base about human error probabilities (HRA data base),
- preparation of quantification table, which contains failure probabilities of tasks within human failure event and overall failure probability of respective human failure event. The quantification table includes the performance shaping factors, which impact the human error probabilities regarding the specific parameters and conditions of the specific action. A specific performance shaping factor equals to one in nominal conditions. In conditions that are worse than nominal, it changes to 2 or to 5 or to 10 according to specific circumstances of the human failure event under investigation. In conditions that are better than nominal, it changes to 0.5 or to 0.2 or to 0.1 according to specific circumstances of the human failure event under investigation. Each human error probability depends on several performance factors. The product of specific performance shaping factors gives the overall performance shaping factor of the investigated human error.

Figure 2 shows an example of calculation of human failure event i.e. operator action, which consists of diagnosis phase and two actions. The diagnosis phase consists of basic diagnosis phase and its recovery phase. Both actions consist of basic action phase and its

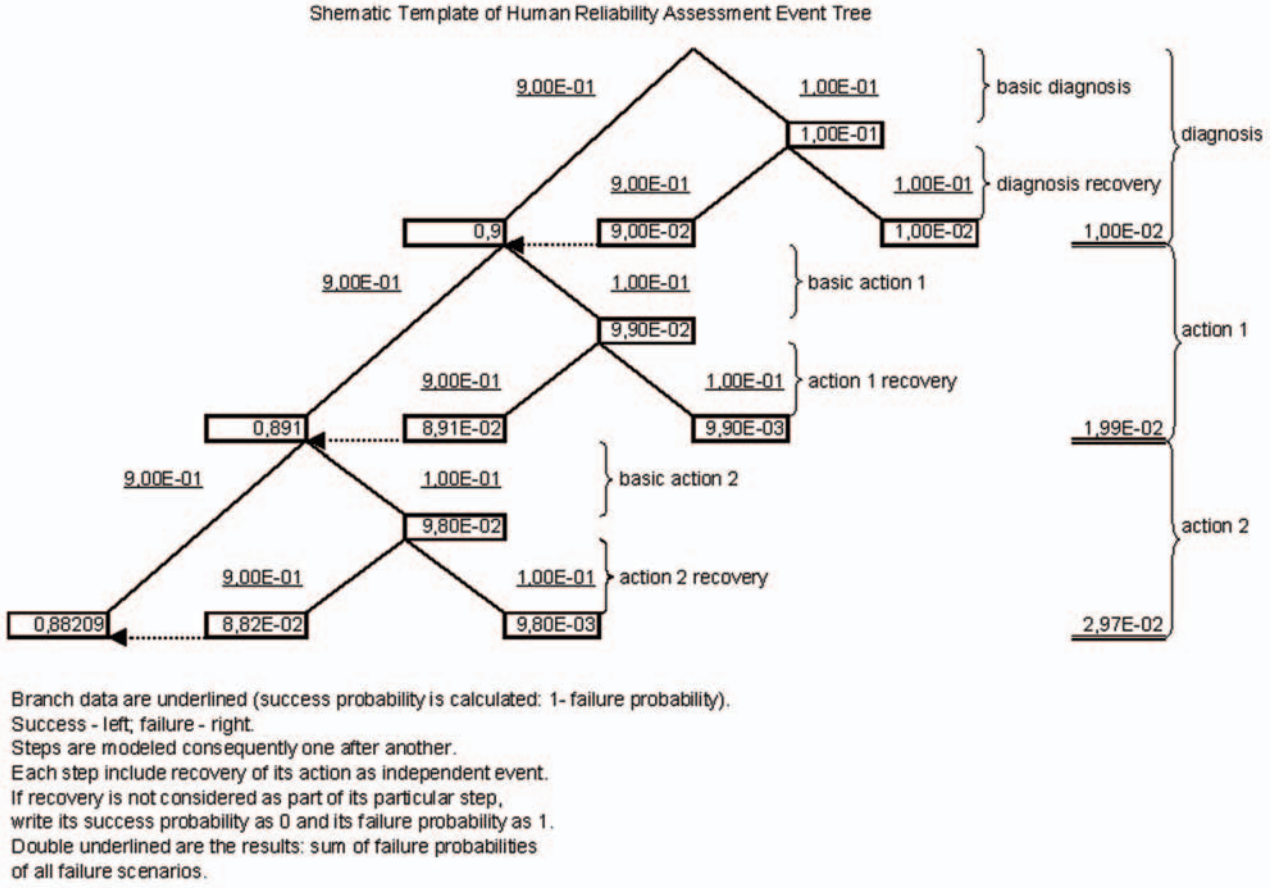

***Figure* 2. HRA Event Tree for Calculation of HEP**

recovery phase. The right branch of each node represents failure probability of the respective phase, while left branch represent its complement.

All failure probabilities: failure probability of diagnosis phase, failure probability of diagnosis recovery, failure probability of basic action 1, failure probability of action 1 recovery, failure probability of basic action 2 and failure probability of action 2 recovery are assessed as 0.1 on this particular example in *Figure* 2. No dependency is assumed in the example. Resulted HEP is written in lower right corner of the figure: 2.97E-2.

2.4.1. Consideration of Simulator Experience into HRA

The training of plant operators on a full scope simulator is a complex process. One of the features of this process is that simulator personnel collect and analyse responses of operators on real scenarios and real events.

The consideration of simulator experience into HRA is proposed as follows:

- Human failure events, which are part of probabilistic safety assessment, are identified and their descriptions are provided to simulator personnel.
- Simulator personnel recognize and assess experience of operators with each particular human failure event in a way that the events, which are better or worse than the average, are identified. The events with average success of response of operators are marked with N. The events, for which more difficulties in success of response of operators than average are identified, are marked with N+. The events, for which less difficulties in success of response of operators than average are identified, are marked with N-. Such expert opinion of simulator personnel is performed separately for diagnosis phase of the event and separately for action phase of the event.

Human reliability assessment is modified as follows. The human error probabilities of human failure events marked with N+ (either diagnosis phase or action phase or both) increase their probability for 10%. The human error probabilities of human failure events marked with N- (either diagnosis phase or action phase or both) reduce their probability for 10%. If both: N+ and N- exist for the same human failure event: one for diagnosis phase and the other for action phase, HEP is not changed.

2.5. Consideration of dependencies between human failure events

Consideration of dependencies between human failure events is an important issue, which is described in more details in reference (Cepin, 2008).

3. MODEL

A full plant specific Probabilistic Safety Assessment (PSA) model of a two loop nuclear power plant is selected for the analysis. The model is developed for the computer code Risk Spectrum PSAP. The probabilistic safety assessment model for normal operation is a detailed model consisting of thousands of basic events and gates, hundredths of system and subsystem fault trees and tenths of event trees. The model integrates the internal and external events, but only the portion for internal events is selected for purposes in this paper.

4. ANALYSIS AND RESULTS

Table 1 shows the selected human failure events with their respective human error probabilities, which are calculated using the IJS-HRA method.

***Table* 1. Part of the calculated human error probabilities**

Description	Human Error Probability	Type
False calibration	1,91E-3	Pre-initiator
Block valve – incorrect position after test	1,07E-2	Pre-initiator
Wrong line up of valve	2,27E-4	Initiator
Wrong line up at cross connection of service water	4,09E-4	Post-initiator
Failure to start the service water pump B	1,15E-2	Post-initiator
Operator fails to align containment spray system recirculation – Train A	1.97E-2	Post-initiator
Operator fails to establish main feedwater	2,2E-2	Post-initiator
Operator fails to check and isolate faulted steam generator	2,76E-2	Post-initiator
Operator fails to manually initiate safety injection	5E-2	Post-initiator

Table 2 and *table* 3 show the importance measures: risk increase factor and risk decrease factor, of the most important human failure events in the nuclear power plant probabilistic safety assessment.

Risk increase factor of specific human failure event shows, how much the risk of the plant increases, if the human error probability of the respective human failure event increases to 1.

Risk decrease factor of specific human failure event shows, how much the risk of the plant decreases, if the human error probability of the respective human failure event decreases to 0.

Those human failure events, which are identified as the most important, are candidates for simulator training, which consequently lead to improvement of sa-

fety. Namely, better trained operators for specific actions perform them more reliably, which means decrease of human error probability.

***Table* 2. Identification of Selected Human Failure Events with the largest Risk Increase Factor**

Basic Event	Risk Increase Factor	Description
HE-POST-INI-004	226	Operator fails to establish auxiliary feedwater & secondary cooling (in transients)
HE-POST-INI-012	75,6	Operator fails to establish auxiliary feedwater & secondary cooling (at loss of offsite power)
HE-POST-INI-105	44,6	Operator fails to align cold leg high pressure recirculation (small loss of coolant accident)
HE-POST-INI-100	36,4	Operator fails to trip the reactor coolant pumps
HE-INI-001	23,3	Wrong lineup of valve
HE-POST-INI-107	22,2E	Operator fails to align cold leg-high pressure recirculation (transients)
HE-POST-INI-033	6,68	Operator fails to start one out of three containment spray pumps within 5 min
HE-POST-INI-034	3,17	Operator fails to start one out of three containment spray pumps within 10 min
HE-POST-INI-074	2,67	Operator fails to initiate cooling and depressurization of reactor coolant system
HE-POST-INI-068	2,61	Operator fails to initiate cooldown of the reactor coolant system

***Table* 3. Identification of Selected Human Failure Events with the largest Risk Decrease Factor**

Basic Event	Risk Increase Factor	Description
HE-POST-INI-047	1,13	Operator fails to initiate reactor coolant pump seal injection
HE-POST-INI-068	1,09	Operator fails to initiate cooldown of the reactor coolant system
HE-POST-INI-093	1,09	Operator fails to action for reactor coolant system inventory restoring

The overall contribution of human failure events to the core damage frequency is large. This means that contribution of human is still an important contributor to risk in spite of a wide automation, which took place in recent decades. Figure 1 shows the risk contributions of selected groups of components based on quantified minimal cut sets.

Group HUMAN-ERRORS includes all basic events corresponding to human failure events, group DIESEL-GEN includes all basic events corresponding to diesel generators, group AFW-PUMPS includes all basic events corresponding to auxiliary feedwater pumps, group HUMAN-E-INI includes all basic events corresponding to initiator human failure events, group HUMAN-E-PRE-INI includes all basic events corresponding to pre-initiator human failure events, group MOVS includes all basic events corresponding to motor operated valves and group AOVS includes all basic events corresponding to air operated valves.

Result on *Figure* 3 show that the risk contribution of all human failure events is similar to the risk contribution of all basic events connected with safety system diesel generators and a little larger that the risk contribution of all basic events connected with auxiliary feedwater system.

CONCLUSIONS

The method for the human reliability analysis is developed with consideration of current requirements and good practice. The selected features of existing methods and selected specific features are introduced into the method.

The method is described and applied. The human error probabilities that are calculated according to the method are applied in the probabilistic safety assessment model and the subsequent analyses were performed. The analysis of the probabilistic safety assessment model shows, that the contribution of human error probabilities is a notable contributor to risk in spite to a large automation in recent years. The results of eva-

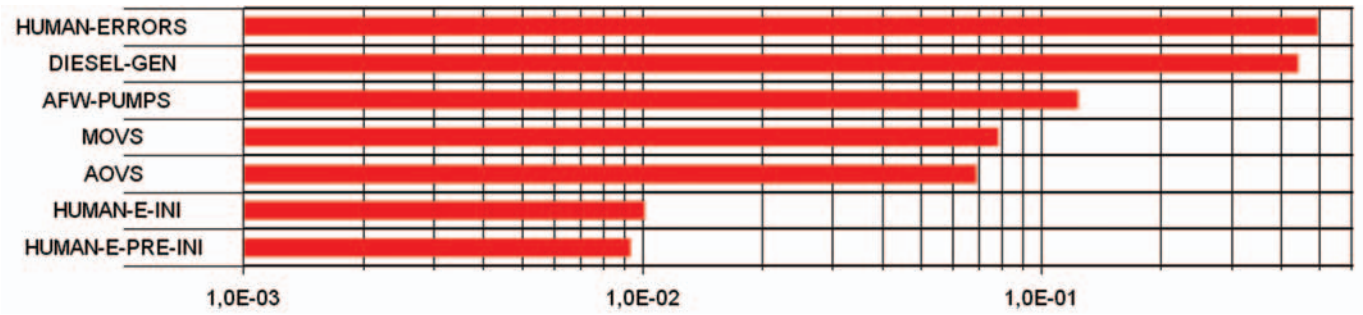

***Figure* 3. Fractional Contribution for Selected Groups of Events**

luating the probabilistic safety assessment model show and quantify the key human failure events, which mainly contribute to risk. Those can be subjected to simulator training, which may subsequently decrease their human error probability, which consequently leads to improved safety.

The problem of human reliability analyses lays in subjectivity of the models and their quantifications. The subjectivity could be decreased with development of more detailed guidelines and procedures for specific detailed examples of human failure events.

The factors, which largely impact the subjectivity of the models and subsequently the uncertainty of the results, are performance shaping factors and the features of dependency. Future activities connected with decreasing the subjectivity of human reliability analysis should be focused to those two fields.

REFERENCES

[1] ASME RA-S-2002 (2002), Standard for Probabilistic Risk Assessment for Nuclear Power Plant Applications, The American Society of Mechanical Engineers.
[2] **Y.H.J. Chang & A. Mosleh** (2007), *Cognitive modeling and dynamic probabilistic simulation of operating crew response to complex system accidents: Part 1: Overview of the IDAC Model*, Reliability Engineering and System Safety, Vol. 93, (11), pp. 1751-1760.
[3] **M. Cepin & X. He** (2006), *Development of a Method for Consideration of Dependence between Human Failure Events*, ESREL2006.
[4] *M. Cepin & B. Mavko* (1997), *Probabilistic Safety Assessment Improves Surveillance Requirements in Technical Specifications*, Reliability Engineering and Systems Safety, Vol. 56, pp. 69-77.
[5] **M. Cepin & B. Mavko** (2002), *A Dynamic Fault Tree. Reliability Engineering and System Safety*, Vol. 75, No. 1, pp. 83-91.
[6] **M. Cepin** (2002), *Optimization of Safety Equipment Outages Improves Safety*, Reliability Engineering and System Safety, Vol. 77, pp.71-80.
[7] **M. Cepin** (2005a), *Human Reliability Analysis – Methods and Applications. Problems and Solutions*, Internal Report, IJS.
[8] **M. Cepin** (2005b), *Analysis of Truncation Limit in Probabilistic Safety Assessment*, Reliability Engineering and System Safety, Vol. 87 (3), pp. 395-403.
[9] **M. Cepin** (2008a), *DEPEND-HRA – A method for consideration of dependency in human reliability analysis*, Reliability Engineering and System Safety, Vol. 93, no. 10, pp. 1452-1460.
[10] **M. Cepin** (2008b), *Importance of human contribution within the human reliability analysis (IJS-HRA)*, Journal of Loss Prevention in Process Industries, Vol. 21, no. 3, pp. 268-276.
[11] **M. Cepin** (2008c), *Comparison of methods for dependency determination between human failure events within human reliability analysis*, Science and technology of nuclear installations, Vol. 2008, pp. 987165/1-987165/7.
[12] **J. Forester, D. Bley, S. Cooper, E. Lois, N. Siu, A. Kolaczkowski & J. Wrethall** (2004), *Expert elicitation Approach for Performing ATHEANA Quantification*, Reliability Engineering & System Safety, Vol. 83, pp. 207-220.
[13] **J. F. Grobbelaar, J. A. Julius & F. Rahn** (2005), *Analysis of De-pendent Human Failure Events Using the EPRI HRA Calculator*, PSA05, Proceedings.
[14] **E. Hollnagel** (1988), *Cognitive Reliability and Error Analysis Method*, CREAM, Elsevier Science Ltd.
[15] **G.A.L. Kennedy, C.E. Siemieniuch, M.A. Sinclair, B.A. Kirwan & W.H. Gibson** (2007), *Proposal for a Sustainable Framework Process for the Generation, Validation, and Application of Human Reliability Assessment within the Engineering Design Lifecycle*, Reliability Engineering & System Safety, Vol. 92 (6), pp. 755-770.
[16] **A. Mosleh & Y.H. Chang** (2004), *Model-based Human Reliability Analysis: Prospects and Requirements*, Reliability Engineering & System Safety, Vol. 83, pp. 241-253.
[17] NUREG/CR-1278 (1983), Handbook for Human Reliability Analysis with Emphasis on Nuclear Power Plants Application, US NRC.
[18] NUREG/CR-4772 (1987), Accident Sequence Evaluation Program: Human Reliability Analysis Procedure, US NRC.
[19] NUREG/CR-6883 (2005), The SPAR-H Human Reliability Analysis Method, US NRC.
[20] NUREG-1624 (1999), Technical Basis and Implementation Guidelines for A Technique for Human Event Analysis (ATHEANA), US NRC.
[21] NUREG-1792 (2005), Good Practices for Implementing Human Reliability Analysis (HRA), US NRC.
[22] **A. Prošek & M. Cepin** (2008), *Success criteria time windows of operator actions using RELAP5/MOD3.3 within human reliability analysis*, Journal of Loss Prevention in Process Industries, Vol. 21, no. 3, pp. 260-267.
[23] **B. Reer, V. N. Dang & S. Hirschberg** (2004), *The CESA Method and its Applications in a Plant-Specific Pilot Study on Errors of Commission*, Reliability Engineering & System Safety, Vol. 83, pp.187-205.
[24] SHARP (1984), Systematic Human Action Reliability Procedure, EPRI, NP-3583.
[25] **A. Spurgin** (1990), *Another view of the state of human reliability analysis (HRA)*, Reliability Engineering & System Safety, Volume 29 (3), pp. 365-370.